SOVIET ASTRONOMY

AJ

VOLUME 1, NUMBER 2 MARCH-APRIL, 1957

# AN INVESTIGATION OF THE PROPERTIES AND ENERGY DISSIPATION OF THE GASEOUS GALACTIC CORONA

S. B. Pikel'ner and I. S. Shklovskii

## ABSTRACT

The distribution of the sources of nonthermal radioemission of the Galaxy is discussed. The division a homogeneous sphere and an "Oort-Westerhout" subsystem is artificial. There is some concentration of emission towards the plane and center of the Galaxy. The strength of the magnetic field in the upper ($H \approx 3 \cdot 10^{-6}$) and lower ($H \approx 6 \cdot 10^{-6}$) layers of the corona is estimated from the distribution of radioemission and two hypotheses: 1) the concentration of cosmic rays is proportional to the field strength and 2) in the upper layers of the corona the magnetic pressure is about the same as the pressure of cosmic rays.

The pressure of the magnetic field and the cosmic rays at the height $z \sim 10$ kps is balanced by the weight of the upper layer. From this condition the density of the layer $n > 0.6 \cdot 10^{-2}$ cm$^{-3}$ is estimated. Evidently the gas pressure does not play an essential role in supporting the corona. To contain the cosmic rays the field of the corona must be irregular. Hence the field is coupled to the gas motions of the same energy. From the difference of H in the upper and lower layers, the mean density of the gas $n \approx 0.01$ cm$^{-3}$ is found.

Spitzer's main objection to high-velocity gas motions in the corona is the strong energy dissipation in supersonic motions. However, the velocity of sound increases in a magnetic field. If the magnetic energy is equal to the kinetic, then the velocity of motion is the same as that of sound. In this case, according to [13], the rate of dissipation decreases 20-30 times and there is also a corresponding decrease in the temperature and ionization of the gas. The energy dissipation cannot be compensated by outbursts of novae or supernovae, nor by the radiation of hot stars.

It is shown that the motions in the corona can evidently be maintained by the waves from the Galactic nucleus, where fast gas motions are observed. The increase in nonthermal radioemission towards the center of the Galaxy is caused by the same motions, which increase the field strength.

Some examples of coronas, with incomplete ionization and in rapid motion, are given. The Large Magellanic Cloud is surrounded by an extended corona, having a neutral hydrogen concentration $n \sim 8 \cdot 10^{-3}$ cm$^{-3}$ on the periphery. High velocities do not lead to a high degree of ionization in the nucleus of our Galaxy, apparently because of the action of the field. Recent radio observations show that the Coma cluster of galaxies is surrounded by a corona with a radial-velocity dispersion ~500 km/sec. The motions are undamped and do not lead to a complete ionization of the gas because of the magnetic field. Radio observations at low frequencies of the Galaxy enabled the estimation of $n_e \sim 0.01$ and $T \sim 10^4$ in the lower layers of the corona.

## 1. Introduction

In 1952, one of the authors [1] showed that the main part of the cosmic radio emission at long wavelengths is due to the Galaxy, and the sources form a spherical system of thickness about 10 kps with increasing concentration towards the Galactic plane and center.

Soon afterward, it was suggested that the rarefied interstellar gas in the Galaxy must form a spherical subsystem [2]. This suggestion was based on the fact that to retain the cosmic rays in the Galaxy a magnetic field with intensity higher than $3 \cdot 10^{-6}$ oersted must be everywhere – in the gas clouds and between them. However, because of the low gas density between the clouds, the gas must have a large velocity spread so that its kinetic energy would be comparable to the magnetic energy. A large velocity spread would have led to a large extension of the gas system along the $\underline{z}$ coordinate. Calculations showed that if the gas concentration was $n \approx 0.1\ \mathrm{cm}^{-3}$, weak, broad lines H and K of Ca$\overline{\mathrm{II}}$ should be observed in the spectra of distant stars. Such lines are, in fact, observed, and this was additional evidence in favor of a spherical gaseous corona. The main experimental evidence was the distribution of the radio emission. The latter, as is well known, is produced during the motion of relativistic electrons in magnetic fields, while the presence of fields requires the existence of gas occupying the same spherical system.

The approximate equality of the kinetic energies in the cloud and outside them was explained by the transfer of energy by hydromagnetic waves.

Since the time of publication of the above work, new and more detailed data on the distribution of radio emission have appeared. In addition, a special investigation [3] showed that, in some cases, the broad lines apparently belong to the star. In some other cases, the unpublished observations of G. Münch* showed that a broad line is resolved into a number of narrower lines, but with a large velocity spread. It must be pointed out that the latter result does not contradict the accepted idea. In fact, in this case, the absorption coefficient is proportional to the square of the density; therefore, the presence of comparatively small fluctuations, which inevitably arise in the moving gas, is enough to produce separate absorption maxima in a line. In any case, the presence of these weak lines confirms the proposition that the more rarefied gas should have a large velocity spread.

Another theoretical objection was made by L. Spitzer [3], who pointed out that at velocities exceeding the velocity of sound the motion of gas will be in the form of shock waves whose energy rapidly goes into heat. L. Spitzer, therefore, while accepting the existence of the corona, considers it to be static and ascribes its extent to a high temperature (about $10^6$ degrees). From the condition of pressure equality in HI gas clouds and in the rarefied gas he finds the concentration to be $n \approx 5 \cdot 10^{-4}$ The aim of the present work is to develop the ideas about the spherical corona, to determine more accurately its properties on the basis of the recent observational data and to investigate the problem of the kinetic-energy dissipation in the corona.

## 2. Analysis of Radio-Emission Data and Estimation of the Field

At the present time, the main observational data from an analysis of which the physical characteristics of the Galactic gaseous corona can be deduced are the radioastronomical observations. The spatial distribution of the sources of nonthermal cosmic radio emission, according to the theoretical ideas widely accepted at the present time, gives the spatial distribution of the electron component of the cosmic rays and of the interstellar magnetic fields. In turn, the latter is definitely connected with the rarefied gaseous medium, forming the corona, and its motions.

Although the idea of an extended spherical corona around the Galaxy, in which the main part of the sources of radio emission are localized, has at the present time received complete confirmation and is widely accepted, individual authors (in particular J. Baldwin [4]) assume that in addition to the spherical distribution there is also another – "Oort-Westerhout" distribution.

The idea of an intermediate system of the distribution of Galactic radio-emission sources ("Oort-Westerhout" distribution) existing together with the spherical system appears to us to be highly artificial. The isophotes of the cosmic radio emission obtained by Baldwin at a wavelength $\lambda = 3.7$ m (which, by the way, differ little from the isophotes obtained by other authors, for example, J. Bolton and K. Westfold [5]) in no way imply the presence of the "Oort-Westerhout" distribution. The latter distribution appears only during the processing of the observational results as a consequence of certain simplifying assumptions (for example, the assumption that volume emissivity is strictly constant for all parts of the spherical Galactic corona).

---

*These results were kindly communicated to us by D. Greenstein during his recent visit to the Crimean observatory.

It is necessary to point out, however, that observations carried out with a high resolving power do not give any indications of the existence of the intermediate "Oort-Westerhout" system. For example, the observations of B. Mills, $\lambda = 3.5$ m, carried out with a "cross" whose angular resolution is about 50' [6] (in Baldwin's case 2° x 15°), give "cross sections" of the sky at constant declination (+2°, −11°, −29.5°). On these sections the sharp, fairly narrow maxima which arise when the galactic equator passes through the given circle of declination are clearly seen. This is the "disc system" of the sources of Galactic radio emission. The intensity falls slowly and smoothly from the Galactic equator to the poles and no signs of the "Oort-Westerhout" system of sources can be discerned.

An analogous situation exists in the distribution of the brightness of Galactic radio emission with Galactic latitude, found by an interferometric method by P. Scheur and M. Ryle [7] ($\lambda = 3.7$ m); for $|b| > 10°$, the theoretical curve based on the "Oort-Westerhout" model falls with increasing $|b|$ considerably faster than the observed curve.

There would be some point in talking about two systems of nonthermal Galactic radio emission (for example, spherical and intermediate) if the physical nature of the radiation sources were different. From the point of view of observation this could lead to differences in the radio spectra of the "spherical" and "intermediate" components. Recently, this question was investigated in detail by R. Adgie and F. Smith [8]. With the help of three fixed antennas with the same orientation, the dependence of the intensity of radio emission on the sidereal time was investigated at 38, 81.5 and 175 Mc. This dependence was found to be the same for all of the three frequencies, consequently, the spectra of the "spherical" and "Oort-Westerhout" components of the Galactic radio emission are the same.

Thus, there is no "intermediate" system of Galactic-radio-emission sources and there is only a concentration towards the center and the Galactic disc of the sources responsible for the spherical component of the nonthermal radio emission of the Galaxy.

It is well known that, being inside the stellar system, it is not easy to form a true picture of the spatial distribution of any of the elements of its population. Interferometric observations of M 31, while proving the existence of a "radio corona" in this galaxy, as yet do not enable the structure of the isophotes near its center and its plane of symmetry to be obtained with sufficient accuracy. However, recent observation of the brightness distribution in the Magellanic Clouds, carried out with a cross-shaped antenna at $\lambda = 3.5$ m [6], indicate without a doubt that the intensity decreases smoothly from the center of these galaxies towards their periphery. No signs of an intermediate component in the radio emission of these galaxies is observed. Two further examples can be given which demonstrate graphically the concentration of the sources of nonthermal radio emission towards the center and the plane of symmetry of the radiogalaxies. These are the radiogalaxies NGC 5128 and 4486. Both of them consist of a bright elliptical nucleus surrounded by an extended spherical corona. For example, in the case of radiogalaxy NGC 5128 (Centaurus-A) the size of the region bounded by the isophote giving half the intensity at the center is 6'.5 x 3', while the diameter of the corona, whose brightness is ~1/100 times as great as that of the central region of the source and falls towards the periphery, reaches 1.5°. In the case of NGC 4486, Smith has recently found an extended (up to 50') corona whose surface brightness is ~1/500 times as great as that of the central part of this radiogalaxy. One could raise the objection that the facts presented concerning the presence of large gradients in the volume emissivity refer to abnormal radio galaxies, while our Galaxy is of the normal type. However, this is not quite the case. The spread in the radio emission of the galaxies is exceptionally large. According to its radio emission, our Galaxy occupies, so to speak, an intermediate position between a normal galaxy, such as M 31, and an abnormal galaxy such as Centaurus-A (NGC 5128), the emission of our Galaxy being only about one order of magnitude less than the emission of the latter. In turn, however, the radio emission of NGC 5128 is one order of magnitude less than that of NGC 4486. Therefore, it can be surmised that the general features of the distribution of the sources of nonthermal radio emission (spherical corona with a concentration towards the center and the plane of symmetry) are common to radiogalaxies with very different radio emission.

In view of the importance of this question, it is desirable to substantiate further, by independent means, the assertion that there should be a gradient of the volume emissivity in the spherical corona towards its center, as well as towards the galactic plane. If the volume density $\epsilon$ of the radiation sources in the corona of radius R were constant, then from simple geometrical considerations it follows that the intensity at $l = 330°$ as a function of the galactic latitude would have the form:

$$. \ I(b) = \frac{\varepsilon}{4\pi} R \left\{ \sqrt{1 - \left(\frac{a}{R}\right)^2 \sin^2 b} + \frac{a}{R} \cos b \right\}, \tag{1}$$

where $a \approx {}^{1}/_{2}R$ is the distance of the sun to the center of the Galaxy. The ratio of intensities at $b = 90°$, $30°$ and $0°$ would be 1.0 : 1.45 : 1.73. On the other hand, according to numerous observations the ratio of the intensity at the pole to the intensity in the region of the center (after subtraction of the disc component of the radio emission) is 1 : 5.5 [9]. It is very significant that at $b = 30°$ and $b = 90°$ the ratio of intensities observed is systematically higher than that predicted from the theoretical model $\epsilon =$ constant. Taking ${}^{1}/_{3}$ of the radiation in the region of the Galactic poles to be of extragalactic origin (see [4], also [10]), we find that according to [10] ($\lambda = 16.4$ m) $T_{b=30} \approx 100{,}000°$, $T_{b=90} \approx 50{,}000°$; consequently, the ratio is 2 : 1. From the data of [5] this ratio is 1.95. According to Baldwin himself [4] this ratio is 2.04. As yet, there are no other measurements of the intensity of cosmic radio emission at $b = 30°$ and $b = 90°$. The systematic deviation of $I_{b=30}/I_{b=90}$, indicated above, from the theoretical value for a homogeneous model can only be explained by the presence of a gradient of the volume emissivity for the radio emission in the galactic corona (the gradient, of course, can be formally introduced by the artificial conception of an "intermediate Oort-Westerhout system"). According to the calculations of one of the authors [11] the volume emissivity of the nonthermal-radiation sources of the Galaxy is 4 times larger in the region of the center than in the vicinity of the sun. At a distance of 10 kps from the galactic plane the volume emissivity can be 5-10 times lower than in the vicinity of the sun, if the disc component of the radio emission is excluded.

Since radio emission is produced by relativistic electrons moving in magnetic fields, it seems completely natural that the volume emissivity should decrease with increase in distance from the galactic plane and center. At such large distances the sources of relativistic electrons (for example, supernovae) are absent. As regards the intensity of the magnetic field, it cannot increase.

In the case of synchrotron radiation by electrons in a magnetic field, the emissivity per unit volume is

$$\varepsilon \propto KH^{(\gamma+1)/2}, \tag{2}$$

where $\gamma$ is the exponent in the differential energy spectrum of the relativistic electrons:

$$aN(E) = KE^{-\gamma}\, dE. \tag{3}$$

If the spectrum of the radiation emitted by relativistic electrons can be represented in the form: $I(\nu)d\nu \propto \nu^{-n}\, d\nu$, than from the theory of synchrotron radiation we have, as is well known,

$$n = \frac{\gamma - 1}{2}. \tag{4}$$

From an analysis of all the pertinent observations it can be concluded that $n = 0.8$ [9], from which $\gamma = 2.6$. On the other hand, the concentration of relativistic particles (especially, electrons) moving along the field lines will be proportional to the magnetic-field intensity H. Consequently $\varepsilon \propto H^{2.8}$.

One of the methods for evaluating the galactic field, proposed by L. Bierman and A. Schluter [12], depends on the fact that the pressure due to the cosmic rays $p_{c.r.}$ cannot be greater than the pressure due to the field.* By this method they estimated the lower limit of the magnetic-field intensity, $H = 5 \cdot 10^{-6}$ oersted. If we consider that in fact $K \propto H$, then the equilibrium in the upper layers of the Galaxy is upset since the magnetic pressure $\propto H^2$. We will assume that for the upper layers of the spherical subsystem, at about $z = 10$ kps,

$$\frac{1}{8\pi} H^2 \approx p_{c.r.}. \tag{5}$$

---

*In Reference [12] the energies of the field and cosmic rays (equal to 3 $p_{c.r.}$) were compared; however, this is apparently less accurate.

Then, in the lower layers $\frac{1}{8\pi}H^2 > p_{c.r.}$, but only slightly. We will assume that the energy density of the cosmic rays in the galactic plane $\sim 1$ ev $= 1.6 \cdot 10^{-12}$ erg/cm$^3$, i.e., $p_{c.r.} = 0.5 \cdot 10^{-12}$ dyne/cm$^3$.* Since the volume emissivity decreases with height (without taking into account the disc component which to a large extent can be due to radiation by ionized gas) by about 5-10 times and $K \infty \cdot \epsilon^{1/2.8}$, the energy density of the cosmic rays in the upper layers can be taken equal to $0.7 \cdot 10^{-12}$-$0.9 \cdot 10^{-12}$ erg/cm$^3$. Using this, from Condition (5) we find that $H \approx 3 \cdot 10^{-6}$ oersted, while near the galactic plane (outside of the disc subsystem) $H \approx 6 \cdot 10^{-6}$, which agrees with other estimates.

Regarding the nature of the disc component of the radio emission, observations at low frequencies carried out in Australia indicate, as was recently communicated to one of the authors by B. Mills, that the bright band of emission which extends along the galactic equator is not of thermal origin. If this is so, then the band can be explained by a somewhat higher value (~10-20%) of the magnetic-field intensity inside the arms than outside them.

The increase of radio emission towards the galactic center, seen clearly from the isophotes, will be discussed below.

## 3. Estimation of the Gas Density in the Spherical System

In Section 2 we came to the conclusion that in the upper layers of the Galaxy, for example, at a distance of the order of 10 kps from the galactic plane, the magnetic-field intensity $H \approx 3 \cdot 10^{-6}$, if the cosmic-ray pressure, $p_{c.r.}$, is comparable to the magnetic-field pressure. The layer of gas lying above the level considered undergoes pressure from below due to the magnetic field and cosmic rays. Since in the intergalactic space, both the magnetic-field intensity and the cosmic-ray energy are considerably lower than in the Galaxy, this pressure can only be compensated by the weight of the layer. If the density is low and the weight of the layer does not compensate for the pressure from below, the upper layers will be ejected into the intergalactic space together with the field and the cosmic rays embedded in them. To explain the presence of radio emission it is necessary, in this case, to assume that there is an equilibrium outflow of gas from the Galaxy. However, if the pressure considerably (for example, by a factor of 2) exceeds the weight so that the effective acceleration, directed upwards, is of the order of g in these layers, then the escape time for the galactic gas will be of the order of, or less than, the half period of oscillations in the Galaxy, i.e., of the order of $10^8$ years – considerably less than the age of the Galaxy. Combining this with the estimate of the density, it can be concluded that a high outflow velocity is not acceptable, i.e., the upper layers must be approximately in equilibrium.

The equilibrium condition for a layer higher than 10 kps can be written in the form

$$\int_{10}^{\infty} g\rho\, dz = \frac{H_{10}^2}{8\pi} + p_{c.r.} + \frac{1}{2}\rho v^2 + p_g, \tag{6}$$

where $p_g$ is the gas pressure.

The contribution of the last two terms is as yet unknown; therefore, we will estimate the lower limit to the density by neglecting them. The weight of a column of gas extending above 10 kps, apparently, is smaller than the weight of a homogeneous layer extending from 10 to 15 kps and having a density $\rho_{10} = n_{10} m_H$:

$$\rho_{10} \int_{10}^{15} g dz > \int_{10}^{\infty} g\rho\, dz > \frac{H_{10}^2}{8\pi} + p_{c.r.} \approx \frac{H_{10}^2}{4\pi}. \tag{7}$$

The function $\psi(z) = \frac{m_{11}}{2k} \int_0^z g(z)\, dz$ has been calculated by J. Oort and is given in Reference [3]. We give some of its values required in the following:

---

*More recent data lead to a somewhat higher energy density because of the soft component. This leads to a corresponding increase in $H^2$ and $\underline{n}_i$ calculated below.

| $z$ | $\psi(z)$ | $2k\psi(z)$ | $\Delta$ |
|---|---|---|---|
| 15 | $20.8 . 10^5$ | $5.7\cdot10^{-10}$ | $1.84\cdot10^{-10}$ |
| 10 | $14 . 10^5$ | $3.86\cdot10^{-10}$ | $3.67\cdot10^{-10}$ |
| 1 | $0.7\cdot10^5$ | $0.19\cdot10^{-10}$ | |

Using (7) and the data of the table, we find

$$n_{10} > \frac{H_{10}^2}{4\pi 2k\,[\psi(15)-\psi(10)]} \approx \frac{0.1\cdot10^{-10}}{4\pi\cdot1.84\cdot10^{-10}} = 0.4\cdot10^{-2}\ \mathrm{cm}^{-3}. \tag{8}$$

Consequently, the gas density of the spherical subsystem, even at a great height, is considerably larger than the value found by L. Spitzer.

Let us now consider the contribution of the terms neglected in (6). In order for gas pressure to contribute significantly to the total pressure supporting the atmosphere, the gas temperature must be of the order of $10^6$ degrees. But then $p_g = nkT \approx 0.5\cdot10^{-12}$, while in the gas clouds, observed also outside the galactic plane, $p_g$ is 1/5-1/10 as large. Consequently, on the gas-cloud boundary the pressure will not be balanced. It is true that the gas pressure, in general, does not play a big part because the magnetic pressure in these layers is $H^2/8\pi \approx 10^{-12}$, i.e., greater than the gas pressure in the clouds. Consequently, inside a gas cloud the most important part is played by the magnetic pressure. The equilibrium of the cloud boundary is determined by the equality of the magnetic pressures inside and outside, while the gas pressure plays only a secondary role. However, in some directions (along the field) the magnetic pressure does not act and $p_g$ inside the cloud must be greater than outside it, since the gas clouds spread out along the field (G.A. Shain). Proceeding from this consideration, and from the consideration that the field itself can support the gas, so that a high temperature is not necessary, we assume for the time being that the gas pressure is less than the magnetic pressure. It is clear that this situation has not been rigorously proved. Below, and in the paper following [13], the temperature will be estimated from other considerations.

Let us now investigate the contribution of the third term on the right-hand side of (6). If we assume that the kinetic-energy density is low compared to the magnetic energy, then we will have a static atmosphere supported by the magnetic field. In such an atmosphere the field must assume a regular nature, in which state its energy is a minimum. Any deformation of the field is associated with magnetic forces which will set a stationary atmosphere into motion, as a result of which the fluctuations will be smoothed out. This is facilitated by the low density of the atmosphere in which the gas pressure is less than the magnetic pressure. Therefore, if the atmosphere is static, the field must be regular, for example, similar to the general field of a star. Such a field, however, will not be able to retain the cosmic-ray particles; they will move away from the Galaxy along the field lines and at large distances will escape from it. A regular field also introduces difficulties in explaining how the atmosphere is maintained – inasmuch as the gas can move freely along the field, it can settle in the galactic plane. Finally, a regular field of intensity $H \approx 5\cdot10^{-6}$ inside a volume of diameter 30 kps has such a high total magnetic flux that very serious difficulties are encountered in explaining its origin. All of this forces us to assume that the gas kinetic energy is of the order of the magnetic energy. The field would then be in equilibrium with the kinetic energy, and all of the difficulties mentioned above will disappear. Assuming that in (6)

$$\frac{1}{2}\rho v^2 \approx \frac{H^2}{8\pi}, \tag{9}$$

we find that $n_{10} \approx 0.6\cdot10^{-2}$ cm$^{-3}$ and from the same Equation (9), using the values of H and $\rho$, we find $v \approx 10^7$ cm/sec.

The gas in the layers below $z = 10$ kps, apparently, is also in equilibrium

$$g\rho\, dz \approx \nabla \frac{H^2}{8\pi} + \nabla p_{\text{c.r.}} + \nabla \frac{1}{2} \rho v^2 \approx 3\nabla \frac{H^2}{8\pi}. \qquad (10)^*$$

From this we can estimate the rate of increase of the gas density towards the galactic plane. Since the details of the variation of the field with height is unknown, we will assume on the basis of Section 2 that near the disc subsystem, but outside it ($z \approx 1$ kps), $H_1 \approx 0.6 \cdot 10^{-5}$. Then the weighted mean value of $\bar{n}$ for the region from 1 to 10 kps is determined by the expression

$$\bar{n} = \frac{3}{8\pi} \frac{H_1^2 - H_{10}^2}{2k\,[\psi(10) - \psi(1)]} = \frac{3}{8\pi} \frac{(0.36 - 0.09) \cdot 10^{-10}}{3.67 \cdot 10^{-10}} = 0.9 \cdot 10^{-2}. \qquad (11)$$

The accuracy of the value obtained is of course low, but the increase of the gas density downwards does, apparently, proceed slowly.

## 4. Energy Dissipation in Shock Waves

L. Spitzer's objection that the magnitude of the dissipation in shock waves is high is based on the fact that a velocity of the order of 100 km/sec is considerably higher than the velocity of sound in the gas, $c_1$. However, it must be taken into account that the galactic gas is in a magnetic field in which small disturbances (sound) travel with a velocity $\sqrt{c_1^2 + V^2 \sin^2\alpha}$, where $V = H/\sqrt{4\pi\rho}$ is the velocity of the hydromagnetic waves and $\alpha$ is the angle between H and the wave normal. If the magnetic energy is in equilibrium with the kinetic energy, then, from (9), we find that $v \approx V \leq \sqrt{c_1^2 + V^2}$. Since, in our case, $c_1 < v$, it can be stated that the velocity of motion is of the order of the velocity of the hydromagnetic waves in directions not too close to H,** i.e., the shock waves are weak and the dissipation of energy in them is not very large. A detailed investigation of dissipation in weak hydromagnetic shock waves has been carried out in [13] and we will only give the results here. If the velocity of the wave is equal to the velocity of sound, then the dissipation will be 1/20-1/30 as large as that in a usual wave with the same velocity but in the absence of a magnetic field. If the wave is produced by the collision of two masses of gas, then the usual wave is damped after traversing a mass of gas comparable to the mass of the incident cloud, while in the presence of a magnetic field the mass traversed by the wave is 20-30 times as large. If the field intensity is higher than that given by (9) (for example, because of the stretching effect due to the differential rotation of the Galaxy), then the dissipation falls sharply as $H^{-4}$.

Let the characteristic length of the motions in the galactic corona be of the order of 100 ps (the order of magnitude of the separation between the gas clouds) and the velocity $v \approx 100$ km/sec. In the usual wave the motion will be strongly dissipated in a characteristic time $t = l/v = 3 \cdot 10^{13}$ sec $= 10^6$ years. In the presence of the magnetic field the dissipation time $\sim 2 \cdot 10^7$ years or more. The energy dissipated goes into heat. Taking into account the various mechanisms which cool the gas, in Reference [13] it has been calculated that in the conditions prevailing in the corona, with the above dissipation, the temperature of the gas will be about 10-15 thousand degrees and the ionization should be appreciable (it depends not on the average temperature, but on the temperature at the wave front which is somewhat higher than the average) but far from complete.

However, the calculation is strongly dependent on changes of the conditions and the results are therefore preliminary.

The dissipation time, $t_0 \sim$ 20-30 million years, is still considerably less than the age of the Galaxy. To estimate the power input into the turbulence mechanism it is necessary to evaluate the total dissipation. It is equal to

$$\frac{1}{t_0} \int \left( \frac{H^2}{8\pi} + \frac{1}{2} \rho v^2 \right) dv \approx 3 \cdot 10^{41} \text{ ergs/sec}, \qquad (12)$$

where the integration is carried out over the total volume of the Galaxy. If the characteristic length of the motions is longer than 100 kps, then the dissipation correspondingly decreases. Let us compare the dissipation obtained with the power input from various possible sources of kinetic energy.

---

*Although $\nabla p_{\text{c.r.}} < \nabla \frac{H^2}{8\pi}$, the error introduced is small.

**In this case a number of arguments can be presented in favor of large values of $\alpha$.

100-200 novae flare up annually in the Galaxy. The mass of the shell of each is $10^{-5}\ M_\odot$-$10^{-4}\ M_\odot$, the velocity $\sim 1000$ km/sec. The total energy-production rate is $\sim 3 \cdot 10^{38}$-$6 \cdot 10^{39}$ ergs/sec, which is considerably less than the dissipation. Assuming that supernovae occur once every 30 years and that the mass of their shells is $\sim 0.1\ M_\odot$, we find that the energy input is $\sim 10^{39}$ ergs/sec, which is also insufficient. According to A.I. Lebedinskii [14] and also J. Oort and L. Spitzer [15], the interstellar gas can receive energy from the radiation of hot stars originating in dense gas and dust clouds. Let us estimate this energy. Direct radiation pressure can impart energy to the gas, the energy being the fraction v/c of the radiation energy, where v is mean velocity of recession of the gas relative to the star. Assuming that there are $N \approx 10^5$ hot stars in the Galaxy, radiating $10^{37}$ ergs/sec, we find that with $v \approx 20$ km/sec the radiation pressure of hot stars will give an energy of $\sim 10^{38}$ ergs/sec, i.e., considerably less than the amount required. In addition to the direct radiation pressure, the gas can be accelerated because of the ionization and heating – the pressure gradient accelerates it to 30-40 km/sec [15]. Assuming that for each star formed there is 200 $M_\odot$ of gas and that a star is formed in the Galaxy, on the average, once in 100 years, we find that the total kinetic energy imparted to the gas by this mechanism is less than $10^{39}$ ergs/sec, i.e., once more insufficient to maintain the motion in the corona. Similarly it can be shown that the stellar-radiation pressure [16], and its fluctuations [17], and the production of turbulence by the gravitational field of moving star clusters are inadequate [18].

There exists a further possible source of the gas kinetic energy of the gas in the corona. Observations in Holland, at a wavelength of 21 cm, showed [19] that in the region of the galactic center, about 3000 ps in diameter and $\sim 240$ ps in thickness, the gas has a high dispersion of velocities (up to 50 km/sec in the line of sight, i.e., $\sim 80$ km/sec in space). The concentration of neutral hydrogen atoms is $\sim 0.4\ \text{cm}^{-3}$. The presence of fast-moving gas in the galactic center explains the considerable increase in the intensity of the nonthermal radio emission at the galactic center (the volume emissivity there is higher than the mean emissivity in the spherical system by 50-100 times). If we use (2), i.e., assuming $\epsilon \propto H^{2.8}$, then the magnitude of H in the nucleus must be higher by a factor of 4-5 than in the spherical system, i.e., H must be near to $2 \cdot 10^{-5}$ oersted. From (9) we find that in the nucleus $H \approx 3 \cdot 10^{-5}$ oersted. Such a good agreement between the values of H obtained by two different methods indicates that Relation (9) and the assumption $K \propto H$ are approximately correct for the conditions of the interstellar gas.* It could be objected, of course, that the total gas density is higher than the figure taken for the ionized hydrogen. However, if $n_e$ were greater than 0.5, the emission measure for the central region would be in excess of 1000. In addition, there would be an appreciable absorption of the long wavelengths in the direction from the center and anticenter. Meanwhile, even at long wavelengths the concentration of the radiation to the center, and to the region of the nucleus is clearly noticeable. Further, according to the private communication by Mills, mentioned above, at a wavelength of about 15 m the absorption by the interstellar gas in the region of the center has the appearance of separate small clouds, i.e., the nucleus does not absorb radiation as a whole. The low degree of hydrogen ionization indicates a comparatively low kinetic temperature of the gas (less than 20,000°). We will use this fact in what follows.

The presence of motion in the central region will lead to the formation of waves coming from the nucleus, i.e., to the production of turbulence in the corona gas. We will estimate how much energy is transferred from the nucleus to the corona. The energy flux through the surface of the nucleus is equal to

$$S\left(\frac{1}{2}\rho_1 v_1^2 + \frac{1}{8\pi} H_1^2\right) V_1 \approx S\rho_1 v_1^3 \approx 2\pi r^2 \rho_1 v_1^3 \approx$$
$$\approx 2\pi\,(4.5 \cdot 10^{21})^2 \cdot 0.8 \cdot 10^{-24}\,(8 \cdot 10^6)^3 = 5 \cdot 10^{41}\ \text{erg/sec}, \tag{13}$$

---

*For regions with a markedly different field the latter relation may not hold since in the motion of a relativistic particle the angle $\vartheta$ between H and v is determined by the condition $\sin^2\vartheta = H$ const, which is only violated when the particles are scattered from inhomogeneities whose dimensions are comparable to the radius of the spiral. For low-energy particles, the radius in the interstellar gas is close to the mean free path; therefore, the presence of such fluctuations is unlikely. Motion in regions of high field intensity is limited by the condition H const. $\leq 1$; therefore, a large part of the particles cannot penetrate into the nucleus from the corona. On the other hand, as was pointed out by V.L. Ginsburg and G.G. Getmantsev, a particle, once it has left the nucleus, moves along a spiral with a large pitch ($\sin\vartheta \ll 1$) and, if it is an electron, the radiation will be small since it is determined by the value of $H_\perp$. However, part of the electrons in the corona can have a secondary origin.

where the subscript denotes quantities referring to the nucleus and $V_1$ is taken to be $\approx v_1$. The flux from the nucleus is found to be comparable to the dissipation. Can this energy flux enter the corona without losses? One of the causes of the losses can be the reflection of the waves back into the nucleus because of the presence of a density gradient. For reflection to be absent, it is necessary that $\lambda < 4\pi\zeta_0$, where $\zeta_0$ is the distance in which the density decreases by a factor e. For all the possible values of the characteristic time for the disordered motion (determining the period of the wave), this condition is satisfied, i.e., the reflection will not be important. A second cause of the losses can be that the wave moving in the direction of decreasing density will be accelerated (when H is constant) as $\rho^{-1/2}$. This can lead to the wave velocity exceeding the velocity of sound and the dissipation will markedly increase. The lower limit for the energy flux will be determined by (13), but with values of $\rho$ and $\underline{v}$ appropriate to the corona. This will decrease the outgoing energy by one order of magnitude. However, it can be assumed that the actual losses will be very much lower. The waves must increase the kinetic energy (and therefore, the field) in the vicinity of the nucleus. This is confirmed by the fact that the nonthermal radio emission near the nucleus is strengthened at a distance greater than 1000 ps from the galactic plane, which is several times greater than the extension of the 21-cm emission. Therefore, we can consider that the conditions near the nucleus (H, $\rho$, $\underline{v}$) vary smoothly with the distance. The additional damping will be negligible if the wave, moving with a velocity equal to the local sound velocity, can transfer all of the energy flux. This reduces to the condition that $S\rho v^2 V$ should not decrease with distance away from the nucleus. A rough estimate shows that this is apparently the case. In any case, the additional dissipation will not be large, and the outgoing flux will be closer to the upper limit than to the lower. A more accurate estimate, as yet, is hard to make because the conditions near the nucleus are not well known. In conclusion, it can be stated that the presence of the nucleus apparently can,in principle, maintain the motions in the corona. The cause that maintains the motion in the nucleus itself is not known at present; however, at this stage of the investigation we can accept this motion as an observed fact.

## 5. Some Immediate Observational Data

The theoretical considerations given above cannot serve as a final argument, since they contain inescapable simplifications and are based on parameters whose values are not sufficiently accurately known. Therefore, it is necessary to confirm the main conclusions by direct observation. These conclusions can be summarized as follows. The corona gas has a relatively high concentration ($n \approx 10^{-2}$ cm$^{-3}$), low temperature ($T \leq 20{,}000°$) which is inadequate for a complete ionization of the hydrogen and is in a state of rapid motion which, together with the magnetic field and the cosmic-ray pressure, leads to a large extension of the corona. The dissipation is low because of the magnetic field – without this, the gas of this density would be strongly heated and ionized (the latter conclusion is based on calculations made in Reference [13]).

The galaxies closest to us – the Magellanic Clouds – show clearly-defined gaseous coronas. From the isophotes, given in Reference [20], for the total intensity of the hydrogen radio emission, it is seen that the regions of this emission are considerably greater than the region of optical emission. From these isophotes we see that the Large and Small Magellanic clouds almost touch. Undoubtedly, if the sensitivity of the apparatus were 2-3 times as high there would be a common isophote enclosing both Clouds. According to [20], the number of hydrogen atoms in a column with unit cross section is related to the total intensity by the expression

$$N = 6.2 \cdot 10^{35} I. \tag{14}$$

On the periphery of the Large Magellanic Cloud the mean value of I is $\approx 5 \cdot 10^{-16}$ W/m$^2$ sterad. The extent of the region with $I \geq 5 \cdot 10^{-16}$ is approximately 15°. Taking the distance to the Clouds to be 65 kps (standard $19^m.1$ [21]), we find that the extent of the corona of the Large Magellanic Cloud is ~17 kps. From this we find the mean concentration of neutral hydrogen atoms on the periphery of this galaxy to be $n_H \sim 8 \cdot 10^{-3}$ cm$^{-3}$. We note that, according to G. de Vaucoulers [22], the Large Cloud shows signs of a spiral structure and, consequently, possesses a plane of symmetry. This clearly shows that this galaxy has a gaseous corona extending to a distance of about 10 kps from the plane of symmetry. According to the same observations, the hydrogen density in the central regions of this galaxy is higher than that in the corona by several orders of magnitude. The clouds cannot be maintained by a high temperature since,in this case, there would be no unionized hydrogen. Therefore, the observed dispersion of radial velocities of about 50 km/sec refers to the macroscopic motions.

A second example is the nucleus of our Galaxy. As was said above the gas there moves with a velocity dispersion of about 80 km/sec, and yet its ionization is far from being complete. A more striking example is given by the radio emission of the cluster of galaxies in Coma Berenices [23]. These measurements have shown that in the cluster there is neutral hydrogen with a mass of $10^{14}$ $M_{\odot}$. It can be shows that this hydrogen is not a constituent of any of the galaxies, but is mainly an intergalactic substratum. This follows, first, from the fact that the half width of the emission region, according to Reference [23], is nearly 5°, while the main part of the optical radiation is emitted by a considerably smaller volume. Second, a mass of $10^{14}$ $M_{\odot}$ is nearly equal to the total mass of the cluster as determined by the virial theorem. At the same time, the mass of the stars in galaxies is usually considerably greater than the mass of gas. Third, in crowded clusters a large number of the galaxies must lose their gas during collisions [24]. According to [23], the radial-velocity dispersion of the gas is of the order of 500 km/sec. Despite such high velocities the gas, to a large extent, is not ionized. This can only occur as the result of the action of a magnetic field which markedly decreases the energy dissipation. In the absence of the field, the gas in waves with these velocities would be completely ionized.

All of these examples show that gas motions with high velocities are possible without giving rise to strong dissipations and for this reason the temperature is insufficient to completely ionize the hydrogen. If we determine the degree of ionization of the hydrogen from observation, then from it we can find the dissipation empirically. It is particularly important to estimate the degree of ionization of the hydrogen in the corona of our Galaxy.

To find the physical conditions prevailing in the gaseous corona of the Galaxy, the analysis of the observations made by G. Reber and G. Ellis [25] at very-low frequencies is of great importance. According to these observations, carried out with the help of directional antennas pointing at the zenith, the intensity of cosmic radio emission at a frequency of 2130 kc shows a marked dependence on the sidereal time. The maximum intensity, observed during the passage of the region near the galactic center through the zenith, was 1.8 times as high as the minimum observed during the passage of the region near the south galactic pole through the zenith. At the same time, the intensity of cosmic radio emission observed at a frequency of 1435 is practically independent of sidereal time. The results of these observations can only be understood by assuming the presence of absorption of the cosmic radio emission by ionized gas situated outside the earth's atmosphere.

According to [26] the optical thickness of the ionized gas for the cosmic radio emission will be given by

$$\tau_{\nu} = \frac{0.98 \cdot 10^{-2}}{T^{3/2}\nu^{2}} \left[19.8 + \ln\left(\frac{T^{3/2}}{\nu}\right)\right] \int n_e^2\, ds. \tag{15}$$

From the results of observations at very low frequencies it follows that at $\nu = 1.435$ Mc, $\tau_{\nu} \approx 1.5$.

Let us assume that the absorption occurs in the gaseous galactic corona. Then, if the kinetic temperature of the corona is $T = 10^{6°}$ (which is the value adopted by Spitzer), $\int n_e{}^2\, ds = 1.1 \cdot 10^{22}$. Taking the extent of the corona as $R \sim 10^4$ ps $= 3 \cdot 10^{22}$ cm, we find that the mean concentration of electrons would be $\sim 0.6$ cm$^{-3}$, which is 1500 times as high as in Spitzer's model and for a number of reasons is completely unacceptable. On the other hand, if $T = 10^4$, then the emission measure becomes very small: ME $\sim 4.5$ and the mean electron concentration near the disc subsystem is $n_e \sim 2 \cdot 10^{-2}$ cm$^{-3}$.

In fact, because of the "shredded" distribution of gas in the corona, which leads to an increase in the emission power, $n_e$ will be even lower by a factor of 2-3, i.e., $\sim 1 \cdot 10^{-2}$ cm$^{-3}$.

In general, however, we cannot exclude the possibility that the absorption of the very low frequencies is due to a cloud near by, or ionized gas within the solar system. Such a cloud, with an emission measure $\sim 5$, will be completely unobservable by optical methods. It must be pointed out, however, that the probability that such a nearby cloud will produce absorption of the observed nature is small. For it is necessary that this cloud be "suspended" in front of the galactic center and, in addition, its absorption has to compensate for the variations of the brightness of the radio emission. But, in general, it could have any orientation. The presence of such a near cloud,in the direction of the center, would have inevitably influenced the results of the observations at the lowest frequencies: $\nu = 900$ kc and $\nu = 520$ kc. Namely, at these frequencies, the radiation from the regions around the center would never be received since it would be completely absorbed by the cloud. There would be no isotropy in the radiation received. As far as can be judged from the published data such effects at these frequencies have not been observed. Regarding absorption by interplanetary plasma, we see that because it is confined to a plane there will be no appreciable absorption. In fact, according to D. Blackwell [27], and also [28], the concentration of electrons in the interplanetary medium at a distance of one astronomical unit from the sun can be taken to be $10^3$ $cm^{-3}$, which gives an emission measure of $\sim 10$ in the plane of the ecliptic. Since the kinetic temperature of the interplanetary gas can be assumed to be $\sim 10^4$, the ecliptic can be observed as a dark band at the frequency $\nu \sim 1.4$ Mc. However, at higher ecliptic latitudes, where according to Reference [27] the electron density is already negligible, there will be no absorption at this frequency.

Therefore, observations at very low frequencies, apparently, indicate that the 1435 kc radiation is absorbed by the gaseous corona of the Galaxy. In this case, the electron concentration in the lower layers of the corona is $n_e \approx 1 \cdot 10^{-2}$ $cm^{-3}$, while the temperature is $\sim 10^4$°K.

There is also another, less direct method for estimating the electron concentration, based on the measurement of the polarization of the nonthermal radio emission [29]. The radiation from a region with a uniform magnetic field must be highly polarized. The plane of polarization is rotated when the radiation traverses interstellar gas with a magnetic field. In traversing a region of length $l$, having a uniform magnetic field, the angle of rotation is proportional to $n_e l H$. Different angles of rotation for radiation coming from different layers of the region will lead to depolarization. For this not to happen, $n_e$ must not be greater than $5 \cdot 10^{-4}$ $cm^{-3}$ if $l \sim 10$ ps and $H \sim 3 \cdot 10^{-6}$. In this case, the statistical addition of polarizations from different regions will give a small residual polarization. Observations carried out at 1.5 m have shown a small (1-2%) polarization. The authors [29] consider that this is evidence for the neutral state of hydrogen in the galactic corona. If this is so, then it would be necessary to assume that the dissipation of kinetic energy is even less than calculated in the present work, perhaps because of the presence of a regular component in the magnetic field. However, it is premature to draw such a conclusion since the magnitude of the polarization is close to the limit of measurement error and the results [29], as pointed out by the authors themselves, are only preliminary. Observations at very low frequencies appear to be more definite. Further measurements of the polarization of the galactic radio emission are very desirable.

## LITERATURE CITED

[1] I.S. Shklovskii, Astron. J. (USSR) 29, 418 (1952).

[2] S.B. Pikel'ner, Izvest. Krymsk. astrofiz. 10, 74 (1953); Doklady Akad. Nauk SSSR 88, 229 (1953).

[3] L. Spitzer, Astrophys. J. 124, 20 (1956).

[4] J. Baldwin, Monthly Notices,Roy. Astron. Soc. 115, 684, 691 (1955).

[5] J. Bolton and K. Westfold, Australian J. Sci. Res. 3A, 19 (1950).

[6] B. Mills, Australian J. Phys. 8, 368 (1955).

[7] P. Scheur and M. Ryle, Monthly Notices,Roy. Astron. Soc. 113, 3 (1953).

[8] R. Adgie and F. Smith, Observatory 76, 181 (1956).

[9] I.S. Shklovskii, Cosmic Radio Emission [in Russian] (Goztekhizdat, Moscow, 1956).

[10] C. Shain and C. Higgins, Australian J. Phys. 7, 130 (1954).

[11] I.S. Shklovskii, Astron. J. (USSR) 29, 418 (1952).

[12] L. Bierman and A. Schluter, Z. Naturforsch. 5a, 2, 237 (1950).

[13] S.B. Pikel'ner, Astron. J. (USSR) 34, 3 (1957).

[14] A.I. Lebedinskii, Doklady Akad. Nauk SSSR 12, 911 (1953).

[15] J. Oort and L. Spitzer, Astrophys. J. 121, 6 (1955).

[16] V.S. Safronov, Doklady Akad. Nauk SSSR 89, 987 (1953).

[17] S.A. Kaplan, Doklady Akad. Nauk SSSR 89, 801 (1953).

[18] A.I. Lebedinskii, Doklady Akad. Nauk SSSR 84, 249 (1952).

[19] K. Kwee, C. Multer and G. Westerhout, Berliner Astronomischer Nachrichten 1954, No. 458.

[20] F. Kerr, J. Hindmann and B. Robinson, Australian J. Phys. 7, 297 (1954).

[21] A. Thackeray and A. Wesselink, Observatory 75, 133 (1955).

[22] G. de Vaucoulers, Observatory 74, 23 (1954).

[23] D. Heeshen, Astrophys.J. 124, 660 (1956).

[24] W. Baade and L. Spitzer, Astrophys. J. 113, 413 (1951).

[25] G. Reber and G. Ellis, J. Geophys. Research 61, 1 (1956).

[26] V.L. Ginsburg, The Theory of Radio Propagation in the Ionosphere [in Russian] (Gostekhizdat, Moscow, 1949).

[27] D. Blackwell, Monthly Notices, Roy. Astron. Soc. 115, 629 (1955).

[28] A. Behr and H. Siedentopf, Z. Astrophys. 32, 19 (1953).

[29] G.G. Getmantsev and V.A. Razin, Proceedings of the Fifth Conference on Cosmogony [in Russian] (Izd. AN SSSR, 1956).

Received December 11, 1956

Crimean Astrophysical Observatory
USSR Academy of Sciences
P.K. Shternberg State Astronomical
Institute

# A NEW CATALOG OF NOVAE RECORDED IN THE CHINESE AND JAPANESE CHRONICLES

Hsi Tse-tsung

On the basis of a study of ancient Chinese, and partly of Japanese, chronicles, the author presents a catalog, with commentary, of novae and supernovae that have flared up in the Galaxy since the year 532 B.C.

Previous catalogs, in particular the well-known catalog of Lundmark, have been corrected and supplemented.

The study of novae is of great significance in cosmogony and radio astronomy. Can the outbursts of novae and supernovae be sources of radio emission? Is there a genetic relation between the planetary nebulae and supernovae or slow novae? Are repeated explosions of novae possible? Do the explosions of novae and supernovae indicate the conversion of ordinary stars to white dwarfs? What is the frequency of supernova outbursts in our Galaxy? To decide all these questions we must have a large quantity of observational data concerning novae and supernovae, ancient as well as modern.

Lundmark has collected early observational data on novae and has compiled a catalog. At present almost all the early data on novae used by astronomers derive from this catalog. But, as Vorontsov-Vel'iaminov has noted, Lundmark's list leaves ample room for all sorts of doubts, in consequence of which it is rather risky to augment our scanty observational material with these data.

Lundmark's catalog includes 60 novae that were observed before or during the 19th century. The data of the catalog were derived chiefly from the Chinese encyclopedia Wen-hsien t'ung-k'ao, published by Ma Tuan-lin. However, in the Chinese chronicles comets and novae are often confused with one another. Moreover, the Wen-hsien t'ung-k'ao does not exhaust all the data recorded in China. Therefore, Lundmark's catalog may not be considered wholly reliable and complete. Recently we examined the Chinese annals, particularly the astronomical entries, the chronicles of various districts, the Wen-hsien t'ung-k'ao and T'ung-chih, and also Japanese astronomical data. As a result, we have ascertained that the following novae in Lundmark's catalog are actually comets.

## The Nova Near $\eta$ Virginis on May 3 A.D. 67

In T'ung-k'ao it is written that "On the 47th cyclical day, 3rd month, 7th year of Yung-p'ing of the reign of the Emperor Ming-ti of the Later Han dynasty a guest star with bright vapor 2 Chinese feet in length was found in the constellation T'ai-wei-yüan, south of the star Tso Chih-fa (Left Military Judge). It shone 75 days in all." It is clear that this was a comet, for it had a tail "2 feet in length." The date given corresponds to April 28 A.D. 67. We shall see later that the nova of September 12 A.D. 684 in Lundmark's catalog was actually Halley's Comet.

## Three Novae, April to July A.D. 837

In T'ung-k'ao it is reported that "On the 21st cyclical day, 3rd month, 2nd year of K'ai-ch'eng of the T'ang dynasty, a guest star appeared beneath the constellation Chien. On the 25th cyclical day a guest star appeared in the constellation Tuan-men, near the star P'ing (Screen). On the 43rd cyclical day it faded away in Tuan-men. On the 19th cyclical day a guest star like a comet was found in the constellation Nan-tou (Southern

[text continued on p. 175]

TABLE

| No. | Original text | Source | Time of observation | Constellation | α | δ | $l$ | b | Remarks |
|---|---|---|---|---|---|---|---|---|---|
| 1 | | Inscriptions on ox bones and tortoise shells. | 15th to 12th century B.C. | | | | | | |
| 2 | | Ditto | Ditto | | | | | | |
| 3 | Spring, 13th year of the reign of Emperor Ching-wang of Chou dynasty, a star appeared in constellation Wu-nü. | Early texts on bamboo tablets | 532 B.C. | | $20^h40^m$ | −10° | 5° | −31° | |
| 4 | 33rd year of Shih-huang-ti of Ch'in dynasty, a bright star appeared in the west. | Ditto | | | | | | | |
| 5 | 7th month, 3rd year of the reign of Emperor Kao-ti of Han dynasty, a comet appeared near Ta-chiao and faded away in 10 days. | Han-shu and Wen-hsien t'ung-k'ao | August 204 B.C. | Near α Boö | $14^h20^m$ | +20° | 346° | +66° | |
| 6 | 6th month, 1st year of Yüan-kuang of Han dynasty, a guest star was seen in the constellation Fang (Room). | Astronomical accounts in Han-shu | 134 B.C. | Sco | $15^h40^m$ | −25° | 313° | +20° | This is the first nova recorded in both Chinese and European literature. |
| 7 | 9th month, 4th year of Yüan-feng of Han dynasty, a guest star was found between the Pole Star and the Northern Dipper in the constellation Tzu-wei-yüan. | Han-shu | 77 B.C. | UMa, near NGC 3587 | $11^h36^m$ | +60° | 103° | +55° | Studied by Williams and Biot |
| 8 | 4th month, 5th year of Yüan-feng of Han dynasty, a bright star was seen between the constellations K'uei and Lou. | Han-shu and T'ung-k'ao | 76 B.C. | Psc | $1^h20^m$ | +25° | 101° | −36° | Williams, Biot and Lundmark |
| 9 | 1st month, 1st year of Ti-chieh of Han dynasty, a comet* was found in the west, 20 feet from Venus. | Han-shu | 69 B.C. | | | | | | |

---

*In the Chinese chronicles, novae are often confused with comets.

| | | | | | | | | | |
|---|---|---|---|---|---|---|---|---|---|
| 10 | 4th month, 1st year of Ch'u-yüan of Han dynasty, a guest star as large as a gourd and blue-white was found in the east at the second star in the constellation Southern Dipper. | Han-shu and T'ung-k'ao | 48 B.C. | Sgr, near NGC 6578 | $18^h$ | −25° | 335° | − 4° | Williams, Biot and Lundmark |
| 11 | 2nd month, 2nd year of Chien-p'ing of Han dynasty, a comet appeared near Ch'ien-niu and was seen for more than 70 days. | Han-shu | 5 B.C. | Near α Aql | $19^h40^m$ | +10° | 16° | − 8° | Possibly a radio point source |
| 12 | 5th year of Chien-wu of Later Han dynasty, a guest star advanced upon the constellation Ti. | "Biography of Yen Kuang" in Hou Han-shu | A.D. 29 | Near α Her | $17^h20^m$ | +15° | 5° | +24° | May be a recurrent nova |
| 13 | 2nd cyclical day, 11th month, 13th year of Yung-yüan of Later Han dynasty, a small guest star, blue-yellow, was visible near the fourth star of the constellation Hsüan-yüan. | Hou Han-shu and T'ung-k'ao | Dec. 30 A.D. 101 | Near 40 Lyn | $9^h20^m$ | +35° | 158° | +47° | Williams and Biot gave the wrong position |
| 14 | 45th cyclical day, 8th month, 1st year of Yung-ch'u of Later Han dynasty, a guest star was southwest of star 15 of the constellation Tung-ching. | T'ung-chih, T'ung-k'ao and Hou Han-shu | Sept. 13 A.D. 107 | Near δ CMa | $7^h$ | −25° | 205° | − 8° | Biot and Lundmark |
| 15 | 11th month, 4th year of Yen-kuang of Later Han dynasty, a guest star was seen in the constellation T'ien-shih (Celestial Market). | T'ung-chih, T'ung-k'ao and Hou Han-shu | Dec. A.D. 125 | Oph | $17^h20^m$ | 0° | 350° | +18° | |
| 16 | 60th cyclical day, 10th month, 2nd year of Chung-p'ing of Later Han dynasty, a guest star appeared in Nan-men, as big as half a mat. It had five colors; thereafter it gradually became fainter and in the following year it faded away. | Hou Han-shu and T'ung-k'ao | Dec. 7 A.D. 185 to March A.D. 186. | Between α and β Cen | $14^h20^m$ | −60° | 282° | 0° | Shklovskii considers this a supernova and radio point source |
| 17 | 41st cyclical day, 9th month, 3rd year of Huang-ch'u of Wei dynasty, a guest star was seen in the constellation T'ai-wei-yüan. | Chin-shu | Nov. 7 A.D. 222 | Between η and β Vir | $12^h$ | + 1° | 248° | +61° | Williams, Biot and Lundmark |

TABLE (continued)

| No. | Original text | Source | Time of observation | Constellation | α | δ | *l* | b | Remarks |
|---|---|---|---|---|---|---|---|---|---|
| 18 | 4th month, 1st year of T'ai-hsi of Chin dynasty, a guest star was found in the constellation Tzu-wei-yüan. | *T'ung-chih* and *T'ung-k'ao* | May A.D. 290 | | | | | | Williams thought that this star might be in Cassiopeia |
| 19 | 3rd month, 1st year of Yung-k'ang of Chin dynasty, an unaccountable star was seen in the south. | *Chin-shu* | Apr. A.D. 300 | | | | | | Williams believed this to be a meteor, but Lundmark considered it a nova |
| 20 | 5th month, 1st year of Yung-hsing of Chin dynasty, a guest star was seen in the constellation Pi. | *Chin-shu*, *T'ung-chih* and *T'ung-k'ao* | June-July A.D. 304 | Tau | $4^h20^m$ | +20° | 144° | −18° | |
| 21 | 8th month, 2nd year of Yung-hsing of Chin dynasty, a comet appeared between the constellations Mao and Pi. | *T'ung-chih* | Sept. A.D. 305 | Tau | $4^h$ | +20° | 141° | −22° | |
| 22 | 24th cyclical day, 5th month, 2nd year of Sheng-p'ing of Chin dynasty, a comet appeared in the constellation T'ien-ch'üan (Celestial Boat). | *T'ung-chih* | June 26 A.D. 358 | Per | $3^h20^m$ | +50° | 114° | − 4° | |
| 23 | 2nd month, 4th year of T'ai-ho of Chin dynasty, a guest star was seen in the western constellation Tzu-wei and it disappeared by the 7th month. | *Chin-shu*, *T'ung-chih* and *T'ung-k'ao* | Mar.-Aug. A.D. 369 | Cas | $0^h \pm$ | +60° ± | 85° | − 2° | Shklovskii and Parenago have noted that a radio point source is observed at this position. Possibly a supernova |
| 24 | 3rd month, 11th year of T'ai-yüan of Chin dynasty, a guest star was in the constellation Southern Dipper. It faded away in the 7th month. | *Chin-shu*, *T'ung-chih* and *T'ung-k'ao* | Apr.-July A.D. 386 | Sgr, near NGC 6644 | $18^h40^m$ | −25° | 338° | −11° | Lundmark |
| 25 | 2nd month, 18th year of T'ai-yüan of Chin dynasty, a guest star was found in the constellation Wei (Queue) and disappeared by the 9th month. | *Chin-shu*, *T'ung-chih* and *T'ung-k'ao* | Mar.-Oct. A.D. 393 | Sco | $17^h$ | −40° | 314° | − 1° | Studied by Williams and Biot, but their results differ. Ours is in agreement with Biot's. This nova is found in the vicinity of NGC II 4637 and a Wolf-Rayet star, −40°10 919. |

| | | | | | | | | | |
|---|---|---|---|---|---|---|---|---|---|
| 26 | 6th month, 1st year of Huang-shih of Wei dynasty, a comet was at the head of Mao. . . At first, a large red star shone between Mao and Pi for more than 50 days. In the 11th month this new star was observed again. It surpassed all other heavenly bodies in brightness. | Wei-shu | Aug. A.D. 396 | Tau | $4^h$ | +20° | 141° | −22° | |
| 27 | 12th month, 5th year of T'ai-ch'ang of Wei dynasty, a guest star was seen in the constellation I (Wing). | Wei-shu | A.D. 421 | | $11^h20^m$ | −20° | 244° | +38° | |
| 28 | 9th cyclical day, 5th month, 2nd year of T'ai-yen of Wei dynasty, a comet was in the constellation Fang (Room). | Wei-shu | June 21 A.D. 436 | Sco | $15^h40^m$ | −25° | 313° | −21° | |
| 29 | 19th cyclical day, 1st month, 3rd year of T'ai-yen of Wei dynasty, a star appeared that was visible even by day. It was near the constellation Ching, was yellow and the size of an orange. | Wei-shu and Sung-shu | Feb. 26 A.D. 437 | Gem | $6^h40^m$ | +20° | 162° | + 9° | |
| 30 | 1st month, 1st year of Yüan-hsiang of Wei dynasty, a guest star appeared in the constellation Tzu-wei-yüan. | Wei-shu | Feb.-Mar. A.D. 538 | | | | | | |
| 31 | 42nd cyclical day, 9th month, 1st year of Pao-ting of Chou dynasty, a guest star was seen in the constellation I (Wing). | Sung-shu and T'ung-chih | Sept. 26 A.D. 561 | | $11^h$ | −20° | 240° | +37° | Williams, Biot and Lundmark. NGC 3242 is nearby |
| 32 | 49th cyclical day, 6th month, 2nd year of Kuang-ta of Ch'en dynasty, a guest star was seen in the east of the constellation Ti. | T'ung-k'ao | July 28 A.D. 567 | | $14^h40^m$ | −15° | 308° | +38° | Biot and Williams have confused the time of observation |
| 33 | 23rd cyclical day, 4th month, 7th year of T'ai-chien of Ch'en dynasty, a comet was near Ta-chiao. | Sui-shu and T'ung-chih | Apr. 27 A.D. 575 | Near α Boō | $14^h20^m$ | +20° | 346° | +66° | |
| 34 | 1st cyclical day, 10th month, 8th year of K'ai-huang of Sui dynasty, a comet was in the vicinity of Ch'ien-niu. | T'ung-chih and T'ung-k'ao | Nov. 22 A.D. 588 | Near α Aql | $19^h40^m$ | +10° | 16° | − 8° | |

TABLE (continued)

| No. | Original text | Source | Time of observation | Constellation | α | δ | l | b | Remarks |
|---|---|---|---|---|---|---|---|---|---|
| 35 | 2nd cyclical day, 3rd month, 13th year of Chen-kuan of T'ang dynasty, a comet was between the constellations Mao and Pi. | Hsin T'ang-shu, Chiu T'ang-shu and T'ung-k'ao | Apr. 30 A.D. 639 | Tau | $4^h$ | +20° | 141° | −22° | |
| 36 | From the 51st to the 59th cyclical day, 7th month, 1st year of Huang-ti, a guest star entered the moon. | Astronomical materials in the Japanese history | Aug. 1-9 A.D. 642 | | | | | | |
| 37 | 53rd cyclical day, 4th month, 2nd year of Ch'ien-feng of T'ang dynasty, a comet was in the northeast among the constellations Wu-ch'e (Five Carts), Pi and Mao. | T'ung-k'ao | May 24 to June 12 A.D. 667 | Tau | $5^h$ | +25° | 145° | − 8° | |
| 38 | 4th month, 1st year of Tsung-chang of T'ang dynasty, a comet was seen in the constellation Wu-ch'e (Five Carts) and shone for 22 days. | T'ang hui-yao, Chiu T'ang-shu, Hsin T'ang-shu, and T'ung-k'ao | May 17 to June 14 A.D. 668 | Aur | $5^h20^m$ | +40° | 136° | + 4° | |
| 39 | 43rd cyclical day, 3rd month, 2nd year of Yung-ch'un of T'ang dynasty, a comet was at the north of the constellation Wu-ch'e. It shone 25 days in all. By the 8th cyclical day it was no longer seen. | Chiu T'ang-shu, Hsin T'ang-shu, and T'ung-k'ao | Apr. 20 to May 15 A.D. 683 | Aur | $5^h$ | +40° | 134° | + 1° | |
| 40 | 18th day, 10th month, 1st year of Ching-lung of T'ang dynasty, a comet was seen in the west. It shone 43 days and disappeared by the 51st cyclical day, 11th month. | T'ang hui-yao, Chiu T'ang-shu, and Hsin T'ang-shu | Nov. 16 to Dec. 28 A.D. 707 | | | | | | |
| 41 | 3rd day, 7th month, 6th year of Yang-lao, a guest star was seen beside the constellation Ko-tao for 5 days in all. | Astronomical materials in the Japanese history | Aug. 19 A.D. 722 | Near δ, ε Cas | $1^h40^m$ | +60° | 97° | − 1° | |
| 42 | 24th day, 1st month, 2nd year of Shen-kuei, a comet was in the constellation Hua-kai. | Astronomical materials in the Japanese history | Feb. 11 A.D. 725 | Near ψ, ω Cas | $1^h20^m$ | +70° | 93° | + 8° | |

|  |  |  |  |  |  |  |  |  |  |
|---|---|---|---|---|---|---|---|---|---|
| 43 | 2nd day, 12th month, 16th year of T'ien-p'ing, a comet was in the constellation Chiang-chūn (General) | Astronomical materials in the Japanese history | Jan. 8 A.D. 745 | Among $\gamma$, $\nu$, $\tau$ And | $1^h40^m$ | +40° | 102° | −21° |  |
| 44 | 58th cyclical day, 1st month, 14th year of Hung-jen, a comet was in the southwest. | Astronomical materials in the Japanese history | Feb. 19 A.D. 823 |  |  |  |  |  |  |
| 45 |  | Geschichte der Astronomie | A.D. 827 | Sco | $17^h\pm$ | −30° ± | 335° ± | −16° ± | Lundmark |
| 46 | 10th month, 3rd year of T'ai-ho of T'ang dynasty, a guest star was seen in Shui-wei (Place of Water) | Hsin T'ang-shu and T'ung-k'ao | Nov. A.D. 829 | CMi | $7^h20^m$ | +10° | 176° | +13° | Williams, Biot and Lundmark |
| 47 | Again in the 1st month, 4th year of K'ai-ch'eng of T'ang dynasty, a comet was found at the northwest of the constellation Chūan-she. On the 52nd cyclical day, 2nd month, it was not observed. | Hsin T'ang-shu | Mar. 12-21 A.D. 839 | Per | $3^h20^m$ | +40° | 120° | −12° |  |
| 48 | 2nd month, 5th year of K'ai-ch'eng of T'ang dynasty, a comet was between the constellations Shih (Room) and Pi (Wall). In 20 days it disappeared. | Hsin T'ang-shu and T'ung-k'ao | Mar. 20 A.D. 840 | Peg | $23^h40^m$ | +20° | 72° | −40° |  |
| 49 | 3rd month, 6th year of Ta-chung, a comet was between the constellations Ts'an and Tsui. | Hsin T'ang-shu | Apr. A.D. 852 | Ori | $5^h40^m$ | +10° | 164° | − 8° |  |
| 50 | 20th hour, 25th day, 1st month, 1st year of Yūan-ch'ing, a guest star was found in the constellation Pi (Wall) (in the west). | Astronomical materials in the Japanese history | Feb. 11 A.D. 877 | Between $\alpha$ And and $\gamma$ Peg | 0 | +20° | 78° | −41° |  |
| 51 | 29th day, 3rd month, 3rd year of K'uan-p'ing, a guest star was 3.2 cm east of the star Tung-hsien. | Ditto | May 11 A.D. 881 | East of stars $\chi$, $\psi$, $\omega$ Oph | $16^h20^m$ | −20° | 324° | +18° |  |
| 52 | 11th month, 1st year of Ching-fu, a comet was between the constellations Tou (Dipper) and Niu (Cow). | Hsin T'ang-shu | Sept. A.D. 892 | Between Sgr and Cap | $19^h40^m$ | −20° | 348° | −22° |  |
| 53 | 1st month, 3rd year of Kuang-hua of T'ang dynasty, near the star Huan-kuan (Courtier) in the central constellation, a guest star appeared that was the size of a peach and brighter than Huan-kuan. | Hsin T'ang-shu and T'ung-k'ao | Feb. A.D. 900 | Her | $17^h$ | +15° | 2° | +29° | Biot and Lundmark |

TABLE (continued)

| No. | Original text | Source | Time of observation | Constellation | α | δ | *l* | b | Remarks |
|---|---|---|---|---|---|---|---|---|---|
| 54 | 1st month, 2nd year of T'ien-fu of T'ang dynasty, a guest star, like a peach, was found beneath the constellation Hua-kai. It was still possible to see it in recent years. | *T'ung-k'ao* | A.D. 902 | Near $\omega$, $\psi$ Cas | $1^h30^m$ | +65° | 97° | − 6° | |
| 55 | 5th month, 1st year of Ch'ien-hua of Liang dynasty, a guest star advanced upon the star Ti. | Ditto | June A.D. 911 | Near $\alpha$ Her | $17^h20^m$ | +15° | 5° | +24° | May be a recurrence of the nova in Hercules in A.D. 29 |
| 56 | From the 5th to the 7th month, 8th year of Yen-ch'ang, a guest star appeared in the constellation Yū-lin. | Astronomical materials in the Japanese history | A.D. 930 | | | | | | |
| 57 | 15th cyclical day, 4th month, 3rd year of Ching-te of Sung dynasty, the star Chou-pe appeared at the south of the constellation Ti, at a distance of 1° from the star Ch'i-kuan (Cavalry Commander). It was as luminous as the half-moon. By the 8th month, because of the revolution of the Earth around the sun, it was approaching the horizon. In the 11th month this star appeared again in the constellation Ti. Since this time in the 11th month it was observed in the morning in the southeast, and in the 8th month at the horizon in the southwest. | *T'ung-k'ao* | May A.D. 1006 | Lup | $15^h$ | −50° | 292° | + 6° | This may be a supernova and source of radio emission* |
| 58 | 14th cyclical day, 1st month, 4th year of Ta-chung-hsiang-fu of Sung dynasty, a guest star was seen before the first four stars in the constellation Nan-tou (Southern Dipper). | *Sung-shih* and *T'ung-k'ao* | | | | | | | |
| 59 | 42nd cyclical day, 6th month, 1st year of Ming-tao of Sung dynasty, | *T'ung-k'ao* | July 15-27 A.D. 1032 | | | | | | |

| | | | | | | | | | |
|---|---|---|---|---|---|---|---|---|---|
| | toward the horizon in the east, a guest star appeared, resembling Jupiter. It shone till the 54th cyclical day and disappeared after 13 days. | | | | | | | | |
| 60 | 2nd cyclical day, 5th month, 1st year of Chih-ho, a guest star appeared southeast of the star T'ien-kuan (Celestial Gate). It shone nearly a year and 10 months, then gradually faded away. | Sung-shih | June 10 A.D. 1054 | Near ζ Tau | $5^h40^m$ | + 20° | 155° | − 3° | The Crab Nebula (NGC 1952, M 1) appears to be a remnant of this outburst** |
| 61 | 33rd cyclical day, 8th month, 1st year of Hsien-yung of Liao dynasty, a guest star invaded the constellation T'ien-miao (Celestial Temple). | "Biography of Tao-tsung" from Liao-shih | Sept. A.D. 1065 | Between Hya and Ant | $10^h20^m$ | −30° | 265° | +32° | |
| 62 | 44th cyclical day, 11th month, 3rd year of Hsi-ning, a guest star appeared in the constellation T'ien-ch'ün (Celestial Barn). | T'ung-k'ao and Sung-shih | Dec. 12 A.D. 1070 | Cet | $2^h40^m$ | + 10° | 132° | −42° | Biot and Lundmark |
| 63 | 43rd cyclical day, 12th month, 5th year of T'ai-k'ang of Liao dynasty, a comet was seen in the constellation Wei. | Liao-shih | Jan. 6 A.D. 1080 | Sco | $17^h$ | −40° | 314° | − 1° | |
| 64 | 5th month, 8th year of Shao-hsing of Sung dynasty, a guest star was found in the constellation Lou. | T'ung-k'ao | June A.D. 1138 | Near β Ari | $1^h50^m$ | + 22° | 112° | −39° | |

---

*The following data also pertain to this supernova: a) Yü-hu ch'ing-hua ("An interesting conversation about a jasper teapot"): "In the 3rd year of Ching-te of the Sung dynasty, a giant star was seen at the west of the constellation Ti, like a gold coin in brightness. No one knew it before this time." b) Astronomical accounts from the Sung-shih: "On the 42nd cyclical day, 3rd month, 3rd year of Ching-te of the Sung dynasty, a guest star appeared in the southeast." c) "Biography of Chen-tsung" from the Sung-shih-hsin-pien: "On the 39th cyclical day, 5th month of Ching-te of the Sung dynasty, the star Chou-pe was observed. On the 39th cyclical day, 11th month, it was observed again." d) Lunar accounts (in Japanese): "On the 2nd day, 4th month, 3rd year of K'uan-hung, at night, near the star Ch'i-kuan was a large guest star, like Mars. For several nights it was seen in the south. It was supposed that this was an explosion of the star 'General of the Cavalry,' during which its brightness increased." e) See also Schönfeld, Astronomischer Nachrichten 127, 153 (1891).

**The following data also pertain to this supernova: a) Lunar accounts: "After the 20th day, 4th month, 2nd year of T'ien-hsi, 2nd hour, a guest star appeared in the constellations Tsui and Ts'an. It was near the star T'ien-kuan. It was as bright as Jupiter." b) "Biography of Chen-tsung" from the Sung-shih-hsin-pien: "On the 8th day, 3rd month, 1st year (corresponds to April 6 A.D. 1056), the Minister of Astronomy reported that, since the 5th month, 1st year of Chih-ho, a guest star was near the star T'ien-kuan and could still be seen up to the present time." c) Duyvendak, Oort and Mayall, "Supernova in Taurus," P.A.S.P. 54, 91 (1942).

TABLE (continued)

| No. | Original text | Source | Time of observation | Constellation | α | δ | *l* | b | Remarks |
|---|---|---|---|---|---|---|---|---|---|
| 65 | 9th cyclical day, 2nd month, 9th year of Shao-hsing of Sung dynasty, a guest star was found in the constellation K'ang (Neck). | Sung-shih and T'ung-k'ao | Mar. 23 A.D. 1139 | Vir | $14^h20^m$ | −10° | 306° | +45° | Biot and Lundmark. |
| 66 | 38th cyclical day, 7th month, 2nd year of Ch'un-hsi of Sung dynasty, a comet was in the west above the star Seven Governors. Its brightness was equal to that of Mars. Until the 43rd cyclical day it grew fainter. | Sung-shih and Sung-shih-hsin-pien | Aug. 10-15 A.D. 1175 | Among Boō, Her and Dra | $16^h$ | +60° | 58° | +44° | |
| 67 | 6th cyclical day, 6th month, 8th year of Ch'un-hsi of Sung dynasty, a guest star was seen in the constellation K'uei and it advanced upon the star Ch'uan-she. On the 10th cyclical day, 6th month of the following year, it faded away. It shone 185 days in all. | Sung-shih and T'ung-k'ao | Aug. 6 A.D. 1181 to Feb. 6 A.D. 1182 | Cas | $1^h40^m$ | +70° | 95° | + 9° | * |
| 68 | 52nd cyclical day, 6th month, 3rd year of Chia-t'ai of Sung dynasty, a guest star appeared at the southeast, in the constellation Wei (Queue) blue-white, of the size of Saturn, and it was still in the constellation on the 1st cyclical day. | Sung-shih | July 28 to Aug. 6 A.D. 1203 | Sco | $17^h$ | −40° | 314° | − 1° | Near NGC 4673. Shklovskii thinks this was a supernova outburst. |
| | 52nd cyclical day, 6th month, 3rd year of Chia-t'ai of Sung dynasty, one star appeared at the southeast, in the constellation Wei. It did not have a point; it was blue-white and as large as Saturn. | T'ung-k'ao | | | | | | | |

|  |  |  |  |  |  |  |  |  |  |
|---|---|---|---|---|---|---|---|---|---|
| 69 | 2nd cyclical day, 6th month, 17th year of Chia-ting of Sung dynasty, a guest star passed through the constellation Wei. | Sung-shih | July 17 A.D. 1224 | Sco | $17^h$ | −40° | 314° | − 1° |  |
| 70 | 34th cyclical day, 11th month, 3rd year of Shao-ting of Sung dynasty, a comet was beneath the star T'u-ssu in the constellation T'ien-shih (Celestial Market); 19th cyclical day, 2nd month of following year, it faded away. | Sung-shih and Sung-shih-hsin-pien | Dec. 15 A.D. 1230 to Mar. 30 A.D. 1231 | Near 109 Her | $18^h20^m$ | + 20° | 16° | + 13° | Biot and Lundmark. In the Japanese historical chronicles there is much material on this nova, but they record it as being in the constellation Cygnus** |
| 71 | 47th cyclical day, again 9th month, 5th year of Shao-ting of Sung dynasty, a comet was visible at the east in the constellation Chiao (Horn). By the 56th cyclical day it had faded away. | Sung-shih, Sung-shih-hsin-pien, Chin-shih, Hsü wen-hsien t'ung-k'ao | Oct. 18 to Nov. 26 A.D. 1232 | Between $\alpha$ and $\zeta$ Vir | $13^h20^m$ | −10° | 286° | + 51° |  |
| 72 | 8th cyclical day, 5th month, 4th year of Chia-hsi of Sung dynasty, a comet was visible in the constellation Shih (Room). By the 3rd month of the following year it had faded away. | Sung-shih | June 5 A.D. 1240 to Apr. 25 A.D. 1241 | Peg | $23^h$ | + 20° | 60° | −36° |  |

---

*The following data also refer to this nova: 1) Chin-shih: "11th cyclical day, 6th month, 21st year of Chin dynasty, a guest star was seen in the constellation Hua-kai. It shone 156 days in all." 2) Wu-ch'i-ching [Azumakagami] ("My Wife's Mirror"– in Japanese): "25th day, 6th month, 1181, at 20 hours a guest star was seen in the northeast, as bright as Jupiter and blue-yellow. It had spicules. From 1006 to the present time there has not been a star to surpass it in brightness." From this we may surmise that it was a supernova. 3) Yū-yeh [Gyokuyo] ("Beautiful Leaf" – in Japanese): "25th-28th day, 6th month, 1181, a guest star appeared near the star Wang-liang." 4) Lunar accounts [Meigetsu-ki]: "25th day, 6th month, 1181, a guest star was visible in the north near the star Wang-liang." 5) Pai-lien-ch'ao [Hyakuren-sho] ("Manuscript of the Finest Temper" – in Japanese): "25th day, 6th month, 1181, a guest star was seen near the north pole."

**1) Pai-lien-ch'ao [Hyakuren-sho]: "On the night of the 29th, 10th month, 2nd year of K'uan-hsi, a guest star appeared. From 1181 to the present time there has not been such a phenomenon." (Dec. 3-4 A.D. 1230). 2) Lunar accounts [Meigetsu-ki]: "On the night of the 3rd, 11th month, 2nd year of K'uan-hsi, an unusual star appeared in the northwest near the constellation Hsi-chung (Cygnus)." 3) Wu-ch'i-ching [Azumakagami]: "From the 28th day, 10th month, to the 5th day, 12th month, a guest star was observed." 4) Pen-kuo-ssu nien-p'u [Hongokuji Nenpu]: "From the 10th to the 11th month a guest star was visible."

TABLE (continued)

| No. | Original text | Source | Time of observation | Constellation | α | δ | *l* | b | Remarks |
|---|---|---|---|---|---|---|---|---|---|
| 73 | 27th cyclical day, 7th month, 4th year of Chia-hsi of Sung dynasty, a guest star appeared in the constellation Wei (Queue). | *Sung-shih* and *Hsü...t'ung-k'ao* | Aug. 17 A.D. 1240 | Sco | $17^h$ | −40° | 314° | − 1° | |
| 74 | 54th cyclical day, 8th month, 1st year of Ta-te of Yüan dynasty, a strange star appeared in the constellation K'uei. On the 58th cyclical day, 9th month, same year, it again appeared in this constellation. | *Yüan-shih* and *Hsü...t'ung-k'ao* | Sept. 9-18 A.D. 1297 | Between Psc and And | $1^h$ | +30° | 95° | −32° | |
| 75 | 11th cyclical day, 12th month, 2nd year of Ta-te of Yüan dynasty, a comet appeared beneath the stars of Tzu-sun (Son and Grandson). | Ditto | Jan. 24 A.D. 1299 | | $6^h$ | −40° | 214° | −25° | |
| 76 | 44th cyclical day, 3rd month, 2nd year of Huang-ch'ing of Yüan dynasty, a comet appeared in the constellation Ching. | *Yüan-shih* | Apr. 13 A.D. 1313 | Gem | $6^h40^m$ | +20° | 162° | + 9° | |
| 77 | 3rd cyclical day, 2nd month, 21st year of Hung-wu of Ming dynasty, a star appeared in the constellation Pi (Wall). | *Ming-shih* | Mar. 29 A.D. 1388 | Between γ Peg and α And | $0^h$ | +20° | 78° | −41° | Position given by Lundmark is incorrect. |
| 78 | 17th cyclical day, 10th month, 2nd year of Yung-lo of Ming dynasty, a star resembling a lamp was southeast of the constellation Nien-tao. It was yellow and did not move. | *Ming-shih* | Nov. 14 A.D. 1404 | Lyr | $19^h$ | +40° | 38° | +14° | |
| 79 | 27th cyclical day, 8th month, 5th year of Hsüan-te of Ming dynasty, a star was seen near the constellation Nan-ho (Southern River), the size of a crossbow bullet, and blue in color. It shone in the sky for 26 days. | *Ming-shih* and *Hsü...t'ung-k'ao* | Sept. 9 A.D. 1430 | CMi | $7^h20^m$ | + 7° | 176° | +13° | Williams and Biot. |

| | | | | | | | | | |
|---|---|---|---|---|---|---|---|---|---|
| 80 | 24th cyclical day, 12th month, 5th year of Hsüan-te of Ming dynasty, a new star was seen near the constellation Chiu-yu (Nine Flags), the size of a crossbow bullet and yellow-white. In 15 days it faded, but it was seen again on the 19th cyclical day, 3rd month, of the following year. | Ming-shih and Hsü...t'ung-k'ao | Jan. 4 to Apr. 29 A.D. 1431 | Near $\mu$, $\omega$, $\psi$ Eri | $5^h$ | −10° | 177° | −27° | Williams and Biot. |
| 81 | 29th cyclical day, 6th month, 5th year of T'ien-shun of Ming dynasty, near the star Tsung-cheng in the constellation T'ien-shih (Celestial Market) was a white star. On the 32nd cyclical day it disappeared. | Ditto | July 30 to Aug. 2 A.D. 1461 | Near $\beta$ Oph | $17^h40^m$ | 0° | 353° | +13° | Lundmark. |
| 82 | 53rd cyclical day, 10th month, 6th year of Lung-ch'ing of Ming dynasty, a comet was seen in the northeast. It shone until the 4th month, 2nd year of Wan-li of Ming dynasty, and then faded away. | "Biography of Shen-tsung" from Ming-shih | Nov. 8 A.D. 1572 to May A.D. 1574 | Near $\gamma$ Cas | $0^h40^m$ | +60° | 90° | − 2° | This is the supernova of Tycho Brahe. In 1952 radio emission was discovered at this position.* |
| 83 | 5th cyclical day, 1st month, 6th year of Wan-li of Ming dynasty, a star like the sun was in the west. | Ming-shih, Ming-shih-k'ao and Hsü...t'ung-k'ao | Feb. 22 A.D. 1578 | | | | | | Williams, Lundmark and Biot have considered this a nova, but in my opinion the probability is not very great. |
| 84 | 46th cyclical day, 6th month, 12th year of Wan-li of Ming dynasty, a star appeared in the constellation Fang (Room) | Ming-shih and Hsü...t'ung-k'ao | July 11 A.D. 1584** | Sco | $15^h40^m$ | −25° | 313° | +21° | Williams, Biot and Lundmark. |

---

*1) Astronomical accounts from Ming-shih: "In the sky there is an unprecedented star, which appeared near the star Ts'e in the 1st year of Wan-li. At first it was bright, but now it is faint." The star Ts'e is $\gamma$ Cas. 2) In Mei Wen-ting's preface to the book "Chinese and European Star Names" it is stated that "near the star Ts'e is a new star which appeared in the 1st year of Wan-li."

**From this time on, European astronomers confused the dates by ten days, because they did not take into account the calendar reform of 1582.

TABLE (continued)

| No. | Original text | Source | Time of observation | Constellation | α | δ | *l* | b | Remarks |
|---|---|---|---|---|---|---|---|---|---|
| 85 | 2nd cyclical day, 9th month, 32nd year of Wan-li of Ming dynasty, at the southwest in the constellation Wei (Queue) was a star as big as a crossbow bullet, reddish-yellow in color. In the 10th month it became faint. On the 58th cyclical day, 12th month, it was seen again at the southeast in the constellation Wei. In the last year, 2nd month, it gradually grew fainter, and on the 4th cyclical day, 8th month, it faded away. | Ming-shih and Hsü...t'ung-k'ao | Oct. 10 A.D. 1604 to Oct. 7 A.D. 1605 | Oph | | | 337° | − 4° | Williams, Biot and Lundmark considered this star a comet. In fact, this is Kepler's supernova. |
| 86 | In the 37th year of Wan-li of Ming dynasty, a large star was seen in the southwest. It had a point. | Ditto | A.D. 1609 | | | | | | Williams, Biot and Lundmark have considered this a nova, but in my opinion it is not very probable. |
| 87 | 10th cyclical day, 4th month, 1st year of T'ien-ch'i of Ming dynasty, a red star was seen in the east. | Ditto | May 22 A.D. 1621 | | | | | | Williams and Lundmark |
| 88 | 25th cyclical day, 1st month, 15th year of K'ang-hsi of Ch'ing dynasty, an unusual star was visible northeast of the constellation T'ien-wan. It was white. | Ch'ing-shih-kao | Feb. 18 A.D. 1676 | Eri | $4^h$ | −10° | 169° | −40° | |
| 89 | 46th cyclical day, 10th month, 27th year of K'ang-hsi, a different star was visible in the constellation K'uei. It was white. | Ch'ing-shih-kao | Nov. 2 A.D. 1688 | And | $1^h$ | +30° | 95° | −32° | |
| 90 | 46th cyclical day, 8th month, 29th year of K'ang-hsi of Ch'ing dynasty, an unusual yellow star was seen in the constellation Ch'i. It shone for 2 nights. | Ditto | Oct. 18 A.D. 1690 | Sgr | $18^h$ | −30° | 331° | −10° | |

Dipper)." In accordance with this text Williams, Biot and Lundmark considered that three novae were observed in 837:

1. From April 29 to May 21, nova in Gemini.
2. From May 3 to June 17, nova near $\upsilon$ Vir.
3. On June 26, nova in the vicinity of $\delta$ and $\lambda$ Sgr.

Recently Shklovskii has expressed the supposition that the nova in Gemini flared up between $\mu$ and $\eta$ Gem, and that the nebula IC 443 may be a remnant of it. A radio point source ($\alpha = 6^h\ 14^m$, $\delta = +22°38'$) was identified with this nova.

However, in the astronomical accounts of the Hsin T'ang-shu, preceding the entry about a nova there is also the following text. "On the 43rd cyclical day, 2nd month, 2nd year of K'ai-ch'eng of the T'ang dynasty, a comet was visible in the constellation Wei (Danger), 7 feet long, and its tail was directed toward the constellation Nan-tou. On the 45th cyclical day it was southwest of Wei and was becoming brighter. On the 50th cyclical day it was visible in the constellation Hsü. On the 58th cyclical day it was more than 10 feet long and moving toward the west while its tail pointed toward the east. On the 59th cyclical day it was in the constellation Wu-nü and was more than 20 feet long and 3 feet wide. On the 60th cyclical day this comet was becoming wider and longer. On the 1st cyclical day, 3rd month, same year, the comet was in the constellation Nan-tou. On the 2nd cyclical day its length was 50 feet and the tail split into two parts, one pointing toward the constellation Ti, the other toward Fang. On the 3rd cyclical day, the comet was in the constellation K'ang (Neck), its tail was 60 feet long, not split, and pointing northward. On the 4th cyclical day it was moving towards the northwest, while its tail was pointed eastward. On the 6th cyclical day the comet was 80 feet long, in the constellation Chang. On the 20th cyclical day the comet faded away, at which time its length was 3 feet." Thus it is clear that this was a comet.

## The Nova on January 31 A.D. 66

Lundmark considered this a nova only because in T'ung-k'ao it is stated: "On the 25th cyclical day, 12th month, 8th year of Yung-p'ing of the Later Han dynasty, a guest star appeared in the east." But, in the collection Tung-han hui-yao it was said that this was a comet. There it was reported: "On the 45th cyclical day, 1st month, 9th year of Yung-p'ing, a guest star appeared in the constellation Ch'ien-niu,8 feet long. It passed through the constellation Chien. When it reached the constellation Fang (Room) it faded out." In the Ku-chin chu of the Tung Han-shu it is also stated that this comet passed through the constellations Tou, Chien, Ch'i, Fang, Chiao and K'ang and finally arrived at the constellation I. It was observed 50 days in all. The tail of this comet was directed eastward. The 45th cyclical day, 1st month of this year corresponds to February 20th, European calendar, i.e., only 20 days after January 31. At this time of year, at 9 p.m., the constellations Tou, Ch'i, Fang, Chiao, K'ang and I are found just in the east. Consequently, the nova observed on the night of January 31st may not be anything but this comet. According to our calculations, Halley's Comet must pass through perihelion on January 26th. On the basis of the computations we may conclude that this was Halley's Comet. Chu Wen-hsin, in his book Historico-Astronomical Investigations, assumed that the comet observed in the 6th month, 8th year of Yung-p'ing (A.D. 65) was Halley's Comet making its appearance. Obviously, this is incorrect, because the comet of the 6th month emerged on the 19th cyclical day and was observed for 56 days. The 19th cyclical day, 6th month, corresponds to July 29th (European reckoning), and 56 days later is September 23rd, while the interval from September 23rd to January 26th of the following year is more than four months.

## The Nova on September 12 A.D. 684

It is recorded in the Japanese annals: "On the 9th cyclical day, 7th month, 12th year of T'ien-wu, a comet appeared in the northwest having a length of more than 10 feet." The date corresponds to September 7 A.D. 684. The perihelion passage of Halley's Comet took place on November 26th of the same year. As is well known, Halley's Comet may often be observed for two or three months before or after the date of its perihelion.

If a comet is seen in the morning, its tail points toward the west; if it is seen in the evening, its tail points toward the east. This is a general rule. However, a comet never points in all four directions, as in this case. On the 21st cyclical day a guest star appeared beneath the constellation Ching.

On the 34th cyclical day, 8th month, a comet again appears in the constellations Hsü and Wei. According to this information, we may conclude that the three novae and these comets are in fact all the same comet, i.e., Halley's Comet. The date of perihelion of Halley's Comet in this year would be March 1st.

## The Nova on January 28 A.D. 962

It is stated in Sung-shih: "On the 46th cyclical day, 12th month, 2nd year of Chien-lung of the Sung dynasty, a guest star appeared in the constellation T'ien-shih (Celestial Market), east of the star Tsung-jen, having a small tail. On the 8th cyclical day, 1st month of the following year, the comet moved to the southwest and entered the constellation Ti. On the 50th cyclical day, 2nd month, it disappeared." It is perfectly obvious that this object was a comet.

In compiling the present catalog we have rejected the erroneous data of Lundmark's catalog and added our own new material. In our catalog there are 90 novae up to A.D. 1700. Of these, 11 may be supernovae (Nos. 17, 27, 30, 45, 57, 60, 67, 68, 70, 82 and 85). We may assume that there have been 7 supernovae in the past thousand years: Lupus A.D. 1006, Taurus A.D. 1054, Cassiopeia A.D. 1181, Scorpio A.D. 1203, Hercules A.D. 1230, Cassiopeia A.D. 1572, and Ophiuchus A.D. 1604. According to this, the frequency of supernova outbursts in the Galaxy must be considerably greater than it was formerly believed to be.

During the compilation of the catalog we have collected some data pertaining to recurrent novae. Vorontsov-Vel'iaminov, in his book Gaseous Nebulae and Novae, improved the formula of P.P. Parenago and B.V. Kukarkin, giving the relation between the period and the amplitude, as follows:

$$\log P = -2.716 + 0.512 \cdot A.$$

If $A = 11^m$ (the average magnitude range of novae), we get $P = 824$ years. In our catalog, No. 12 and No. 15 appeared to be two outbursts of the same nova, and the interval between these two explosions is 882 years. No. 5 and No. 33 may also be two outbursts of a single nova.

We have collected data only up to A.D. 1700 because there are complete European data concerning novae of more recent times.

The table* presents the distribution of 61 novae for which the positions given in the catalog are relatively accurate. The distribution of the novae in galactic latitude is shown.

From the table it is evident that the novae tend to be concentrated toward the galactic plane. Nearly half of the total number lie within the zone of ± 20° in galactic latitude, with not a single nova in the zones ± 70° to ± 90°. This agrees well with modern results. It is also evident from the table that the number of novae found south of the galactic plane is greater than the number found north of it. This may be explained by the fact that the sun is located north of the galactic plane.

As regards the distribution of novae in galactic longitude, the first six groups of novae in the table lie in the celestial hemisphere centered on the galactic center, while the last six groups lie in the other celestial hemisphere. It is apparent from this that the number of novae in the hemisphere centered on the galactic anticenter is greater than the number in the hemisphere centered on the nucleus of the Galaxy. However, we should note that the portion of the Milky Way between 240° and 300° in galactic longitude is not observable from the Yellow River basin in China. Allowing for this, we may conclude that the concentration of observed novae toward the galactic center is small.

The data we have collected concerning outbursts of novae appears to be incomplete. Some of them may be comets, consequently we shall continue the study.

We are publishing this relatively complete catalog only to provide astronomers who are working in the fields of radio astronomy and cosmogony with some reference data.

The author is very grateful to Professors Chu K'o-chen, Yeh Ch'i-sun, Chang Yü-che, Tai Wen-sai and I.S. Shklovskii for help and encouragement during the course of this work.

Received October 25, 1956

Academy of Sciences, Chinese People's Republic
Commission of the History of Chinese Nat. Sciences

---

*The "tables" referred to in this and succeeding paragraphs are the supplementary tables, which were not published in the present paper — Editor's note.

# THE EVOLUTION OF STARS IN THE $\chi$ AND h PERSEI DOUBLE CLUSTER

## A. G. Masevich

Evolutionary tracks for the hottest main sequence stars in the double cluster $\chi$ and h Per and the surrounding association are evaluated. Marked differences between the H−R diagrams of the association and the cluster (according to Johnson and Hiltner [1]) together with the calculated age of these groups lead to the conclusion that the nucleus and the association originated almost simultaneously, but that the process of formation of stars continued for a considerable length of time in the association after it had ceased in the nucleus. This conclusion is in accordance with Oort's theory [11] on the formation of expanding O associations. In connection with this problem, G. Münch's paper on the age of early type supergiants [12] is discussed.

The most interesting fact about the H-R diagrams of the double cluster $\chi$ and h Persei and the surrounding association is the fact that the diagram of the nucleus (cluster) differs greatly from the diagram of the corona (association). These differences have very definite evolutionary significance. Figures 1 and 2 show the H-R diagrams separately for the nucleus and the outer association according to Johnson and Hiltner [1].

The diagram of the nucleus (Figure 1) resembles the usual diagram of a cluster of early spectral type. The main (theoretical) sequence is indicated by a dashed line; the upper part is inclined upwards to the right (broken line). There are a few giants (stars of luminosity classes II and III) indicated by crosses, faint (1b) supergiants (denoted by circles) and bright (1a) supergiants (denoted by squares). The stars of the main sequence (class V) are indicated by heavy dots.

In the diagram of the surrounding association (Figure 2) we also see the main sequence (dashed line) and the deviating uppermost part (broken line). The central line of the deviating part of the main sequence for the association practically coincides with the corresponding broken line for the nucleus (Figure 1). The distinctive difference between these two diagrams is the presence in Figure 2 (association) of main sequence stars of the earliest spectral types (O5-B0) which lie on the undeflected (original) upper portion of the main sequence as well as in the space between the original and deviating branches. Such stars do not appear at all in the diagram of the clusters. The number of giants and supergiants in the association is considerably greater than in the clusters. It is interesting that the arrangement of the supergiants in Figure 2 is very reminiscent of the evolutionary curves of gravitationally contracting stars which were obtained by Henyey, Le Levier and Levee [2]. This similarity is strengthened by the presence, in Figure 2, of a few O stars below the main sequence. For massive stars such as the supergiants which are under consideration here this evolution is very rapid, requiring less than $10^6$ years.

A comparison of the H−R diagrams of the $\chi$ and h Persei clusters and the surrounding association leads to the conclusion that the nucleus and association are of about the same age, but that in the association the formation of stars continued after it had ceased in the nucleus. In support of this conclusion we shall consider the evolutionary interpretation of Figures 1 and 2.

The departure of the brightest stars of the clusters from the central line of the main sequence is usually regarded as the result of evolution of these stars with the production of an inhomogeneous chemical composition in the absence of mixing of matter between the luminous envelope and the convective core [3, 4]. The original or so-called "zero-age" main sequence can be found theoretically in two ways depending on the evolutionary hypothesis which is assumed.

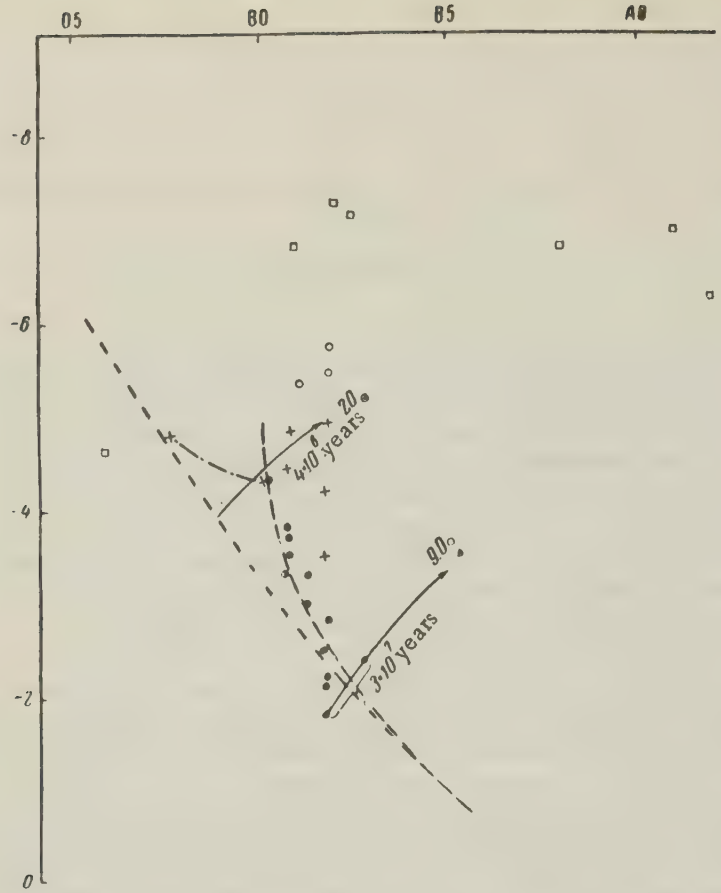

Fig. 1. Color-magnitude diagram of the χ and h Per clusters (nucleus). Dashed line — original (theoretical) main sequence; broken line — deviating upper part of the main sequence; dots and dashes — evolution without mixing; arrows — evolution without and with the formation of an intermediate layer; heavy dots — stars of the main sequence; crosses — giants; open circles — faint supergiants; squares — bright supergiants.

1) If it is assumed that the evolution of all stars proceeds with constant mass and complete absence of mixing, and only as a result of increased difference of chemical composition of the envelope and core as the hydrogen content of the convective core is reduced, it is possible to calculate the position of the "zero-age" main sequence for a definite H–R diagram of a cluster using a star model with constant mass and different values of $\mu_{\text{core}}/\mu_{\text{env}}$. Combining the results for a number of clusters upon the assumption that the differences of chemical composition of stars in different clusters is not important, it is possible to arrive at some general original main sequence for stars whose evolution is just beginning. Thus, Johnson et al. [1, 5] constructed the original sequence for the clusters of the Pleiades, Hyades and Praesepe. This sequence is represented by the dashed line in Figure 3.

2) If it is assumed that the evolution of only a portion of the stars, depending on specific conditions, proceeds without mixing, and we also consider the possibility of stellar evolution with constant or variable mass, using the calculations of a stellar model with constant mass for different $\mu_{\text{core}}/\mu_{\text{env}}$ and the calculations of the same model with variable mass, it is possible to calculate the position of the original sequence on an H–R diagram as was done in our articles, References [3, 6]

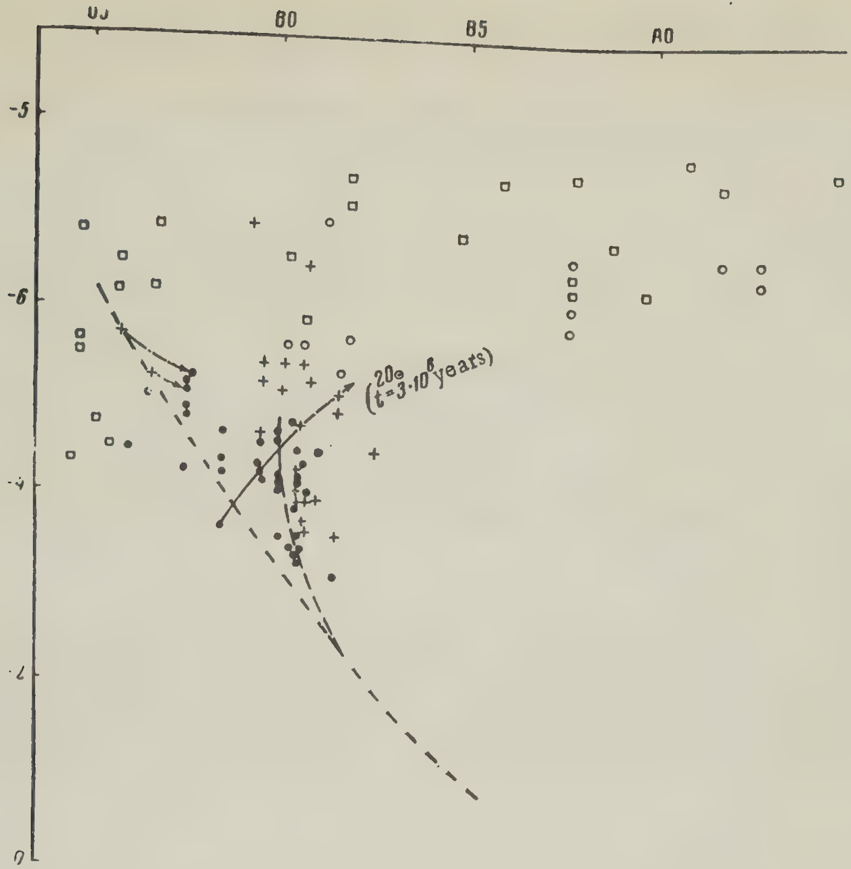

Fig. 2. Color-magnitude diagram of the association around χ and h Persei. The notation is the same as in Figure 1.

The second method differs from the first in that, because of the smaller number of limitations upon the problem, we do not obtain a single general original main sequence (as in the first case). Since, in the formulation of the second problem, the main sequence of the Galaxy is regarded as a set of evolutionary curves for stars formed under different initial conditions and different initial chemical compositions characterized by a mixture of elements heavier than helium, Z (see Ref. [6]), for each value of Z we obtain its "zero-age" sequence, which, however, unlike case 1, extends over a considerable range of spectral types.

Figure 3 shows the zero-age sequence calculated from our model for a chemical composition equivalent to that of the sun (solid curve).

It should be noted that our calculation is based on a model with the absorption law $k = k_0 \rho^{0.875} T^{-3.5}$, while Johnson's calculation is based on Harrison's model [7]. In both instances the source of energy is the carbon-nitrogen cycle. For late spectral types both curves practically coincide. The two curves are generally very close and show only small discrepancies. Our curve extends into the range of earlier spectral types than the Johnson curve; but this is entirely based on the method of calculation. In our case, the upper limit of the theoretical main sequence is bounded only by the value of Z, which, in turn, is determined by the application of the considered stellar model to a star on the undeviating portion of the main sequence of the cluster. In Johnson's case the upper limit of the theoretical sequence is determined by the earliest spectral type in the cluster.

However, the discrepancy between the curves of Figure 3 is not very great, especially in consideration of the indeterminacy that is introduced by imprecise characteristics of the stellar models, especially of the absorption law.

The central line of the main sequence in Figures 1 and 2 (dashed) is the zero-age main sequence which we calculated for χ and h Persei. We now calculate the time required by the brightest main-sequence star which deviates during its evolution to pass from its position in the zero-age main sequence to the position which it occupies at the present time. For the nucleus (see Figure 1) such a star is No. 1268 in list No. 4 of Johnson and Hiltner (B0V): for the association, the two stars HD 17520 (O8V)and BD + 60°470 (O8V).

The evolutionary curves are calculated for the scheme without mixing and with variable mass (see Ref. [8], case IIB). The results are given in the following table.

TABLE

| Star | $M_V$ | Sp | lg $L$ | lg $R$ | lg $\mathfrak{M}$ | lg $L_0$ | lg $R_0$ | lg $\mathfrak{M}_0$ | $Sp_0$ | $M_{V0}$ | $\bar{\mu}/\mu$ | $t$ |
|---|---|---|---|---|---|---|---|---|---|---|---|---|
| Nucleus (Cluster) | | | | | | | | | | | | |
| 1268 | −4.4 | $B0_5$ | 4.70 | 1,06 | 1.20 | 5.13 | 1.01 | 1.31 | 08 | −4.8 | 1.6 | $2 \cdot 10^6$ |
| Association | | | | | | | | | | | | |
| HD 17520 | −5.4 | 08 | 5.32 | 0.94 | 1.36 | 5.59 | 0.93 | 1.43 | 06 | −5.7 | 1.2 | $4 \cdot 10^5$ |
| BD+60°470 | −5.0 | 08 | 5.16 | 0.86 | 1.32 | 5.33 | 0.85 | 1.38 | 07 | −5.3 | 1.1 | $3 \cdot 10^5$ |

The corresponding evolutionary curves are shown in Figures 1 and 2.

Since evolution proceeds more rapidly in more massive and brighter stars the age t in the table is the age of the youngest of the stars in the nucleus and association which depart from the main sequence. The table shows that this age for the association is almost one order of magnitude smaller than for the nucleus. As already indicated above, the arrangement of supergiants in the diagram of the association also denotes an age less than $10^6$ years.

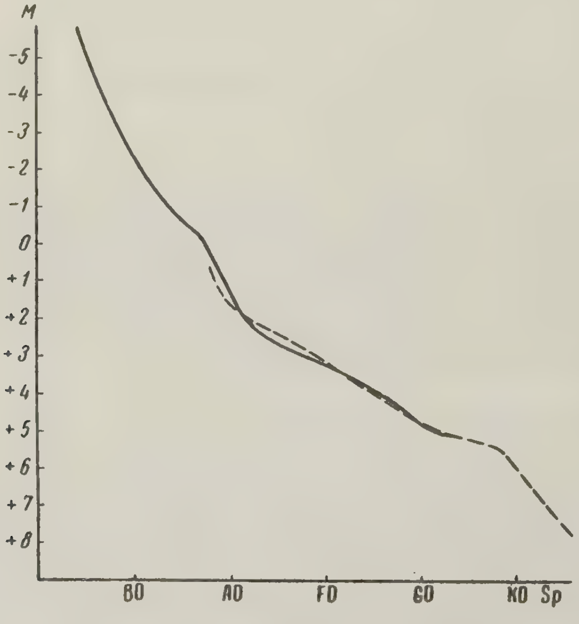

Fig. 3. Theoretical zero-age main sequence: solid line – for our model ($k = k_0\rho^{0.875} \times T^{-3.5}$) and chemical composition of the sun; dashed line – according to Johnson and Hiltner [1].

On the other hand, the giants (stars of classes II and III) which are in both the nucleus and association, also permit us to draw certain conclusions concerning the age characteristics of these groups. Massive stars of early spectral classes of the main sequence can evolve (with constant mass and without mixing) into giants of classes

II and III. As the hydrogen in the convective core is exhausted the size and mass of this core are continuously reduced [9] and the mass of the envelope is continuously increased. Since the chemical composition of the core changes due to the transformation of hydrogen into helium, the average molecular weight of the envelope must also increase somewhat. As was shown in Reference [9], the increase for ordinary stars is generally insignificant. However, in the case of massive stars where evolution is sufficiently rapid so that the matter of the envelope cannot be mixed, as the convective core decreases an intermediate zone can arise at the boundary between the core and envelope with a continuously varying $\mu$. The formation of this zone must effect changes in the external characteristics of the star. Teyler [10] calculated the evolution of a star with $M = 9.9_{\odot}$ and with such an intermediate zone. A series of 10 models was constructed, with the hydrogen content of the intermediate zone varying from 100% to 6%. As a result of such evolution the radius and luminosity of the star are enhanced and it moves to the right from the main sequence into the region of hot giants. Figures 1 and 2 show Teyler's results for $M = 9.9_{\odot}$, which we have converted to the coordinates of the Russell diagrams. We have also shown the evolutionary track of an $M = 20_{\odot}$ star, calculated for the same hypotheses and have given the periods of evolution.

The brightest (and thus the youngest) giant of the association, if it was formed from a star of the main sequence, has an age of $3 \cdot 10^{6}$ years, and the faintest stars are considerably older. The same applies to the nucleus.

Thus, the age of objects which form the nucleus exceeds $2 \cdot 10^{6}$ years and in the surrounding association we encounter stars older than $10^{6}$ years as well as some that are younger by one order of magnitude and some much younger stars of early types in the zero-age main sequence. The nucleus and association were apparently formed as a whole at about the same time ($10^{6}$-$10^{7}$ years ago), but star formation continued for considerable time in the association after it had ceased in the nucleus. This idea, which is based on the color-magnitude diagrams of $\chi$ and h Persei and the surrounding association can be regarded as a confirmation of Oort's hypothesis [11] on the formation of associations. It is Oort's view that the formation of a group of hot stars in a diffusive cloud is accompanied by expansion of the ionization region that forms around these stars and by considerable condensation of the outer cold portions of the cloud, as a result of which favorable conditions are created for star formation in the regions around the original nucleus. Stars formed in such an association receive a portion of the expansion energy of the ionized region. In the example under consideration the double cluster could play the part of the original nucleus and the outer association could be the secondary corona. The youngest stars of the entire group are then the supergiants which by contracting turn into O-type stars of the main sequence of the association (with nuclear reactions as their energy source). After their entrance into the main sequence their evolution follows the path considered above. It is of interest that Oort's estimate of the age of $\zeta$ Per (B1Ib) from the expansion velocity of the association Per II yielded the result $1.5 \cdot 10^{6}$ years, in good agreement with our age for the bright giant with $\mathfrak{M} = 20_{\odot}$, formed from a type-O star of the main sequence: $t = 2 \cdot 10^{6}$ years (see Figure 2). We thus note that Münch's arguments [12] against Oort's age for $\zeta$ Per are faulty. Münch calculated the age of 4 stars of type BI with large $z$ coordinates following the assumption that all of these stars were formed in the galactic plane. The time required by a star to travel from $z = 0$ to its present $z$ is taken to be its age. For all four stars this averages $2 \cdot 10^{7}$ years, which is one order of magnitude greater than the age obtained by Oort for $\zeta$ Per, which star is of an entirely analogous spectral type. Münch also reasons as follows: since the luminosity of this star $L = 10^{5} L_{\odot}$, which corresponds to a rate of transformation of hydrogen into helium $\sim 5 \cdot 10^{19}$ g/sec, its mass can be estimated at $\sim 30_{\odot}$, assuming that in $2 \cdot 10^{7}$ years practically all of the hydrogen will be exhausted. If it is considered that such a star evolved from an O-type star of the main sequence (with lower luminosity) to its present state its mass can be somewhat smaller. Thus, he arrives at the conclusion that the hypothesis which relates the formation of $\zeta$ Per with the start of expansion of the association is unconfirmed, as the age of this star is one order of magnitude greater.

Aside from the question of the reality of age calculated from considerations of stellar dynamics, we note that Münch neglects a very important circumstance. A main sequence star can turn into a bright giant of an early spectral type only if mixing does not occur in it, that is, the hydrogen is consumed only in the convective core which comprises about 0.1 of the stellar mass. A star with mass $20_{\odot}$ reaches this stage in $2 \cdot 10^{6}$ years, as already pointed out above (Figures 1 and 2). After this, the period of peaceful evolution terminates and the star either suffers a catastrophe or if it evolves further with a contracting core, according to Schwarzschild, it turns into a red giant. In neither instance does a supergiant of early type result. If the stars considered by Münch were to possess the age $2 \cdot 10^{7}$ years, their masses would have to be of the order of 200-300 $M_{\odot}$.

If complete mixing occurs in a star, so that during its existence all of its supply of hydrogen can be exhausted, calculations show (see Ref. [8], for example) that it will move downward to the left in a Russell diagram below the main sequence. Thus, even in this case, it cannot become a supergiant unless its original luminosity was greater than its present luminosity by two orders of magnitude (which, again, strongly reduces its life or results in extremely large mass).

We believe that the most likely conclusion to be drawn from Münch's work is the following. The supergiants which he considered have, like the similar stars in associations, a relatively small age of $\sim 10^6$ years, yet they were not formed in the galactic plane, but in high latitudes. This last fact makes the study of these and similar stars extremely urgent.

## LITERATURE CITED

[1] H.L. Johnson and W.A. Hiltner, Astrophys. J. 123, 267 (1956).

[2] L.G. Henyey, R. LeLevier and R.D. Levee, P.A.S.P. 67, 154 (1955).

[3] A.G. Masevich, Astron. J.*32, No. 5 (1955); 33, No. 4 (1956).

[4] H.L. Johnson and A.R. Sandage, Astrophys. J. 121, 616 (1955).

[5] H.L. Johnson and C.F. Knuckles, Astrophys. J. 122, 209 (1955).

[6] A.G. Masevich, Astron. J.* 28, No. 5 (1951).

[7] M.H. Harrison, Astrophys. J. 100, 343 (1944).

[8] A.G. Masevich, Astron. J.* 30, No. 4 (1953); Soobshch. GAISh 99, 1 (1956).

[9] V.S. Sorokin and A.G. Masevich, Astron. J.*28, No. 1 (1951).

[10] R.J. Teyler, Astrophys. J. 120, 332 (1954).

[11] J.H. Oort, Berliner Astron. Nachr. 12, N 455, 177 (1954); Gas Dynamics of Cosmic Clouds (Amsterdam, 1955), p. 147.

[12] G. Münch, P.A.S.P. 68, No. 403, 351 (1956).

Received October 15, 1956

P.K. Shternberg State Astronomical
Institute

---

* USSR.

# SHOCK WAVES IN INTERSTELLAR SPACE

## II. IONIZATION DISCONTINUITIES

S. A. Kaplan

The discontinuities of the parameters of interstellar gas when it flows through the boundary between the H I and H II regions and the velocity of this boundary relative to the un-ionized gas, $v_1$ [Equations (9-12')], have been determined. The automodel problem for the motion of an ionization discontinuity in the interstellar medium has been solved. If the density of the interstellar gas, before the passage of the discontinuity is $\rho_0 > 2 \cdot 10^{-25}$ M g/cm$^2$ (where M is the emission measure of the H II region) then the motion proceeds as follows: a shock wave at which the density increases by several orders of magnitude, accompanied by radiation emission, spreads out in front, with a velocity of ~18 km/sec; following this there is a very narrow (~$10^{-2}$ of the radius) region of compressed un-ionized H I hydrogen also moving with a velocity of ~18 km/sec. A front of rarefaction travels through this H I region, the density of the gas, already ionized, falling on this front to the value ~$4 \cdot 10^{-25}$ M g/cm$^3$. The velocity of the ionization front relative to the H I region is ~0.3 km/sec. Gas begins to flow from the ionization front to the H II region until the gas density becomes equal to ~$2 \cdot 10^{-25}$ M g/cm$^3$. The stability of ionization discontinuities is discussed.

As was already shown by Stromgren [1], the transition zone between regions of ionized (H II) and un-ionized (H I) hydrogen in interstellar space is comparatively narrow (its thickness is of the order of $1/n_1 k_\nu \approx 1.6 \cdot 10^{17}/n_1$ cm, where $n_1$ is the number of neutral hydrogen atoms in a unit volume and $k_\nu$ is the coefficient of absorption from the first level). It is known further, that the gas temperature in H II regions is of the order of 10,000°, while in the H I regions it is less than 1,000° and more likely to be about 100°. From this it follows that the transition zone between H II and H I regions can be stationary with respect to the gas only in the case the pressures on either side of the transition zone are equal, i.e., the densities are inversely proportional to the temperatures. This condition often does not hold, as the result of which the gas must flow through this transition zone. In other words, in this case an ionization discontinuity is formed moving relatively to the interstellar gas. A number of papers have already been devoted to the investigation of these motions (Oort and Spitzer [2], Kahn [3], Savedoff and Greene [4]). In the present work results are presented of an investigation of the motion of ionization discontinuities carried out by the author during 1954-1955. For a number of reasons their publication was delayed. Some of the results obtained by us are already contained in papers [2-4]. However, the different methods of investigation used, and the obtaining of new results and of simpler and more useful equations in the present work, warrants their publication in original form.

### 1. The Ionization of Interstellar Hydrogen

The degree of ionization (in equilibrium conditions) of interstellar hydrogen is determined by the equation:

$$n_p n_e C_{\mathrm{H}} = n_1 \int\limits_{\nu_0}^{\infty} k_\nu \rho_\nu \frac{c d\nu}{h\nu}, \tag{1}$$

where the left-hand side gives the number of recombinations per unit volume per unit time to all of the levels, starting with the second (the recombination to the first level is balanced by ionization due to the diffuse radiation), while the right-hand side gives the number of ionizations per unit volume per unit time due to interstellar radiation with spectral density $\rho_\nu$; $h\nu_0$ is the ionization energy, c the velocity of light, and $n_p$ and $n_e$ are the numbers of protons and electrons per unit volume. Putting the density of the ionizing radiation into the form $\rho_\nu = \rho_\nu^* W e^{-\tau}$, where $d\tau = n_1 k_\nu dr$, W is the dilution coefficient and $\rho_\nu^*$ is the radiation density close to the surface of the ionizing stars, multiplying (1) by $d\tau$ and integrating from 0 to $\infty$, we obtain

$$C_{\mathrm{H}} \int_0^\infty \frac{n_e n_p}{W}\, dr = \int_{\nu_0}^\infty \rho_\nu^* \frac{c\, d\nu}{h\nu}\,. \tag{2}$$

If the H II region is produced by one hot star, then $W = R_*^2/4r^2$, where r is the distance from the star and $R_*$ is its radius. In this case, taking into account that $n_e \approx n_p$ in the H II zone and $n_p \approx 0$ outside it, the well-known Stromgren equation [1] for calculating the radius, $S_0$, of an H II zone (in a somewhat modified form) follows from (2):

$$S_0 n_e^{-2/3} = \left[\frac{3R_*^2}{C_{\mathrm{H}}} \int_{\nu_0}^\infty \rho_\nu^* \frac{c\, d\nu}{h\nu}\right]^{1/2}.$$

In this way it is also easy to obtain the second Stromgren equation, determining the size of an H II region for the case when it is produced by the ionizing radiation of many stars. It is more advantageous, however, to use another equation, which follows directly from (2), and which is applicable in many cases:

$$M = \int n_e n_p\, dr = \frac{\overline{W}}{C_{\mathrm{H}}} \int_{\nu_0}^\infty \rho_\nu^* \frac{c\, d\nu}{h\nu}\,, \tag{3}$$

where M is the emission measure of the H II region, and $\overline{W}$ is the mean value of the dilution coefficient, for this region. Equation (3) is independent of the distribution of $n_e$ and $n_p$ inside the H II region, which is rarely uniform, and is applicable, as well, in the case when the ionization is produced by many stars.

To conclude this section, let us estimate the magnitude of the radiation pressure. Let us first of all consider the pressure of the $L_c$ radiation. It is obvious that it will be small in the H II regions (since the majority of the hydrogen atoms there are ionized), as well as in the H I regions (where the density of the $L_c$ radiation is low) and will reach its maximum value in the transition zone where almost all of the $L_c$ radiation is absorbed. Since at large distances from the star both the radiation flux and the radiation pressure is directed along the radius, taking into account that almost all of the $L_c$ radiation is absorbed in the transition zone, while the energy reradiated in the lines of the Lyman, Balmer and other series is isotropic (consequently, it does not exert a pressure on the transition zone as a whole), we can write the following equation for the radiation pressure on the transition zone:

$$p_{\mathrm{rad}} = W \int_{\nu_0}^\infty \rho_\nu^*\, d\nu = \frac{h\nu_0}{c} M C_{\mathrm{H}}, \tag{4}$$

using (3) and assuming that $h\nu_0 \gg kT$ (so that under the integral sign in Equation (3) $1/\nu_0$ can be substituted for $1/\nu$). The problem of the $L_\alpha$-radiation pressure is of some interest. Unfortunately, it is not yet clear how much greater this pressure is than the $L_c$-radiation pressure. A number of data (Zanstra [5]) indicate that their magnitudes are of the same order. We can neglect the radiation pressure of the $L_\alpha$-radiation so long as we are not considering the structure of the transition zone, inasmuch as the $L_\alpha$-radiation does not exert any pressure (in the first approximation) on the whole zone since this radiation is isotropic.

## 2. The Change of Parameters in the Ionization Discontinuity

To derive the equations determining the change of parameters of the gas during its passage through an ionization discontinuity (i.e., from the condition of un-ionized hydrogen to a condition of complete ionization) we will use, as is always done in similar problems, the conservation conditions for mass and momentum at surfaces taken on either side of the ionization discontinuity:

$$J = \rho_1 v_1 = \rho_2 v_2, \quad \rho_1(v_1^2 + RT_1) = \rho_2(v_2^2 + 2RT_2) + p_{\mathrm{rad}}. \tag{5}$$

Here the subscript 1 denotes parameters referring to the gas in the H I region, the subscript 2, the parameters of the gas in the H II region, $v_1$ and $v_2$ are the normal components of the gas velocities relative to the ionization front and R is the universal gas constant – the factor 2 with the term $RT_2$ is explained by the change of the molecular weight in ionization. The Equation (5) is not complete and in the case of ionization discontinuities it must be supplemented by the following conditions. First, the flow of a mass of gas through the ionization discontinuity is determined by the number of ionizing quanta falling on the discontinuity per unit time:

$$J = m_{\mathrm{H}} \int_{\nu_0}^{\infty} \rho_\nu \frac{c\,d\nu}{h\nu} = m_{\mathrm{H}} C_{\mathrm{H}} M, \tag{6}$$

i.e., it is a given external parameter [3]. Here, $m_H$ is the mass of a hydrogen atom. Second, inasmuch as the cause producing the motion of the ionization front is the change of the degree of ionization and not the external pressure on the region H II, the relative velocity of the gas behind the ionization front must be equal to the local velocity of sound, i.e., $v_2 = \sqrt{2\gamma RT_2}$, where $\gamma$ is the ratio of the specific heats, since the outflow of gas starts immediately behind the ionization front.

It must be pointed out that ionization discontinuities are in many respects analogous to explosion waves. The conditions of flow considered correspond to the Jouguet point, i.e., to the case in which the region of the combustion products is not compressed by the piston.

Substituting (6) and (4) into (5) and taking into account that $v_2 = \sqrt{2\gamma RT_2}$, we find

$$\rho_2 = \frac{m_{\mathrm{H}} C_{\mathrm{H}} M}{\sqrt{2\gamma RT_2}}; \qquad \rho_1 = \frac{m_{\mathrm{H}} C_{\mathrm{H}} M}{v_1};$$
$$\rho_1(v_1^2 + RT_1) = m_{\mathrm{H}} C_{\mathrm{H}} M \left[(\gamma + 1)\sqrt{\frac{2RT_2}{\gamma}} + \frac{h\nu_0}{cm_{\mathrm{H}}}\right]. \tag{7}$$

Here, the parameters $\rho$ and $T_1$ must be considered as known; they are determined by the properties of the medium through which the ionization front spreads. The quantity $m_H C_H M$ must also be considered as a set, external parameter. The magnitude of $T_2$, on the other hand, will vary depending on the density of the gas in the H II region. If, immediately behind the ionization front the density is of the order of $\rho_2 \gtrsim 10^{-23}$ g/cm$^3$, then immediately after the front there is a radiating region in which the temperature $T_2$ reaches a value determined by the condition for thermal equilibrium between the gas and radiation. Usually $T_2 \approx 10{,}000$ (see also [6]). If the density $\rho_2$ is very small, then Equation (7) has to be supplemented by the condition for the conservation of energy flux

$$\frac{\gamma RT_1}{\gamma - 1} + \frac{1}{2} v_1^2 + \frac{1}{\rho_1} \int_{\nu_0}^{\infty} \rho_\nu d\nu = \frac{\gamma + 1}{\gamma - 1} \gamma RT_2, \tag{8}$$

where the third term on the right-hand side determines the energy acquired by the gas during ionization. Equations (7) and (8) then also determine $T_2$. The first case seems to be of greater practical interest. In what follows we will therefore consider that $T_2$ is given and is independent of the state of motion, while $\gamma$ will be set equal to unity. The investigation of the second case is carried out analogously and does not present any difficulties.

Eliminating $\rho_1$ from (7) we obtain a quadratic equation in $v_1$, whose solution has the form ($\gamma = 1$):

$$v_1 = \left[\sqrt{2RT_2} + \frac{1}{2}\frac{h\nu_0}{cm_{\mathrm{H}}}\right] \pm \sqrt{\left[\sqrt{2RT_2} + \frac{1}{2}\frac{h\nu_0}{cm_{\mathrm{H}}}\right]^2 - RT_1}. \tag{9}$$

Ionization discontinuities, both of condensation [plus sign in (9)] and of rarefaction [minus sign in (9)] are possible here. Since very often the inequality $T_2 \gg T_1$ holds, then in the case of ionization condensation discontinuities:

$$v_1 \approx 2\sqrt{2RT_2}\left(1 - \frac{T_1}{8T_2}\right) + \frac{h\nu_0}{cm_{\mathrm{H}}} \approx 2\sqrt{2RT_2},$$

$$\rho_2 \approx 2\rho_1, \quad \rho_1 \approx \frac{m_{\mathrm{H}} C_{\mathrm{H}} M}{2\sqrt{2RT_2}}, \tag{10}$$

while in the case of ionization-rarefaction discontinuities:

$$v_1 \approx \sqrt{2RT_2}\,\frac{T_1}{4T_2}, \qquad \rho_2 \approx \rho_1 \frac{T_1}{4T_2}. \tag{11}$$

If the gas is stationary before the passage of the ionization front, then $v_1$ is numerically equal to the velocity of the ionization front.

Let us give some numerical estimates. The density of the gas behind the wave front at $T_2 = 10{,}000°$ and its relative velocity are:

$$\rho_2 = 4 \cdot 10^{-25}\, M \text{ g/cm}^3; \quad v_2 \approx 13 \text{ km/sec}, \tag{12}$$

where M is expressed in parsecs/cm$^6$. The velocity of the ionization-compression wave and the initial density are:

$$v_1 \approx 26 \text{ km/sec}; \quad \rho_1 \approx 2 \cdot 10^{-25}\, M \text{g/cm}^3. \tag{12'}$$

In the case of an ionization-rarefaction wave at $T_1 = 100°$:

$$v_1 \approx 0.030 \text{ km/sec} \qquad \rho_1 = 400\,\rho_2 \approx 1.6 \cdot 10^{-22} \text{ g/cm}^3. \tag{12"}$$

The quantity $h\nu_0/cm_{\mathrm{H}} \approx 0.004$ km/sec, i.e., we can neglect the effect of the radiation pressure. In the cases where M is small and behind the front of the ionization wave there is not sufficient time for the thermal balance with the radiation to be established, the numerical estimates of $\rho_1$, $v_1$ and $T_2$ are not too different from (12).

Thus, we see that the ionization front can only be propagated in a medium with the definite values of the density given by (12') and (12") which, as a rule, does not happen in real conditions. Therefore, the production of an ionization front must be associated with the simultaneous appearance of either a rarefaction wave or a shock wave, which brings the initial density of the un-ionized hydrogen, $\rho_0$, to the value corresponding to the condition for the propagation of the ionization wave.

If the H I region is isothermal, then the formation of the system rarefaction wave – ionization-condensation front, is not possible for $\rho_0 > \rho_2$. In fact, an isothermal rarefaction wave is propagated with the velocity $\sqrt{RT_0}$ ($T_0$ is the temperature of the stationary gas) and the ionization-condensation wave with the velocity $2\sqrt{2RT_2} > \sqrt{RT_0}$. Therefore, the rarefaction wave will not be able to leave the ionization front. The formation of the system rarefaction wave – ionization-rarefaction wave is possible in practice, but for this it is necessary that the condition $\rho_0 \gg 1.6 \cdot 10^{-22}$ M should hold, which in the actual conditions of the interstellar space, apparently, is hardly possible. It is not hard to convince oneself by comparing velocities that the formation of the system condensation shock wave – isothermal-condensation front (for $\rho_0 < \rho_2$) is also impossible when the gas in the H I region is isothermal.

The most real system of wave motion in interstellar space is condensation shock wave – ionization-rarefaction wave, to the investigation of which we will proceed in the next paragraph.

## 3. The Automodel Problem for the Motion of an Ionization Discontinuity in the Interstellar Medium

Let us consider the following problem. Through a stationary gas consisting of un-ionized hydrogen ($\rho_0$, $T_0$), a shock wave is being propagated which compresses the gas to a density $\rho'_1$ and increases its temperature to the value $T_1$. Then follows a region of compressed isothermal hydrogen, through which propagates an ionization-rarefaction wave ($\rho_1$, the gas density in front of the wave, is, in general, different from $\rho'_1$).

The solutions of such problems can be fairly simply carried out to a numerical result if the motions are automodel ones, i.e., if they are governed by only two parameters with independent dimensions [7, 8]. In our case, such parameters can be the gas density, $\rho_2$, and the gas temperature, $T_2$. ($\rho_0$ and $T_0$ can be chosen as the specifying parameters.) Therefore, in order that the problem considered can be taken as being automodel, we will have to assume that the emission measure of the H II region, M, does not change. The equations of the symmetrical isothermal gas flow have the form

$$\frac{\partial v}{\partial t} + v\frac{\partial v}{\partial r} + RT\frac{\partial \ln \rho}{\partial r} = 0,$$

$$\frac{\partial \ln \rho}{\partial t} + v\frac{\partial \ln \rho}{\partial r} + \frac{\partial v}{\partial r} + (N-1)\frac{v}{r} = 0. \tag{13}$$

where N = 1, 2 and 3 for plane, cylindrical and spherically-symmetrical gas flows, respectively. In view of the automodel nature of the motion all the parameters are a function of the dimensionless quantity:

$$\eta = -\frac{r}{t\sqrt{RT_2}}.$$

From this it immediately follows that both the ionization front and the shock waves propagate with constant velocities:

$$v_i = \eta_i\sqrt{RT_2}; \quad v_s = \eta_s = \sqrt{RT_2}, \tag{14}$$

where the values of $\eta_i$ and $\eta_s$ are to be found. Let us introduce the dimensionless variables:

$$V(\eta) = \frac{v}{\sqrt{RT_2}}, \quad R(\eta) = \frac{\rho}{\rho_2}.$$

Then the System (13) for a region of compressed un-ionized hydrogen can be written in the form:

$$[\eta - V(\eta)]\frac{dV(\eta)}{d\eta} = \frac{T_1}{T_2}\frac{d\ln R(\eta)}{d\eta};$$

$$[\eta - V(\eta)]\frac{d\ln R(\eta)}{d\eta} = \frac{dV(\eta)}{d\eta} + \frac{N-1}{\eta}V(\eta). \tag{15}$$

Let us now obtain the boundary conditions. At the front of the shock wave (see [6]):

$$\eta_s\sqrt{RT_2} = \sqrt{\frac{\rho'_1}{\rho_0}\frac{\rho'_1 RT_1 - \rho_0 RT_0}{\rho'_1 - \rho_0}};$$

$$V(\eta_s)\sqrt{RT_2} = \sqrt{\frac{(\rho'_1 RT_1 - \rho_0 RT_0)(\rho'_1 - \rho_0)}{\rho'_1 \rho_0}}.$$

Introducing the quantities $R(\eta_s) = R_s = \rho'_1/\rho_2$ and $V(\eta_s) = V_s$, we can rewrite these equations in the form:

$$\frac{\eta_s^2}{R_s} = \frac{\rho_2}{\rho_0}\frac{\rho_2 R_s T_1 - \rho_0 T_0}{(\rho_2 R_s - \rho_0)T_2}; \quad V_s^2 = \frac{(\rho_2 R_s T_1 - \rho_0 T_0)(\rho_2 R_s - \rho_0)}{\rho_2 \rho_0 R_s T_2}. \tag{16}$$

The boundary conditions at the ionization-rarefaction front (on the side of the H I region) follow directly from (14), (7) and (9) (neglecting radiation pressure)

$$\begin{aligned} R_i &= R(\eta_i) = \frac{\rho_1}{\rho_2} = \frac{1}{1-\sqrt{1-(T_1/2T_2)}}\,; \\ \eta_i - V_i &= \sqrt{2}\,[1-\sqrt{1-(T_1/2T_2)}]\,. \end{aligned} \tag{17}$$

With the given values of $\rho_0$, $\rho_2$, $T_0$, $T_1$ and $T_2$, the four equations,(16) and (17), connect the six parameters, $\eta_i$, $\eta_s$, $V_i$, $V_s$, $R_i$ and $R_s$. The other two equations, necessary for the complete determination of these parameters, are obtained by solving the System (15).

We were unable to obtain the analytical solution of the System (15) with $N \neq 1$. In the simplest and, at the same time, perhaps the most interesting case $N = 1$ (motion in a plane), the solution is easily found. It is not hard to show that, in the case $N = 1$, the System (15) has two solutions:

$$\text{a) } V = \text{const}, \qquad R = \text{const}, \tag{18}$$

$$\text{b) } V = \eta - \sqrt{T_1/T_2}, \quad R = \text{const}\, e^{\eta\sqrt{T_1/T_2}}. \tag{19}$$

Solution (19) does not satisfy the Boundary Condition (17) with arbitrary values of $T_1$ and $T_2$. Therefore, for the compressed H I region between the shock and ionization waves, we must use Solution (18). Assuming that in the System (16), (17) $R_i = R_s = R$ and $V_i = V_s = V$ in accordance with (18), we find the values of all the parameters which determine the motion.

In the general form the solution of the System (16), (17) and (18) is very unwieldy. Therefore, we will investigate two limiting cases:

a) $T_2 \gg T_1 \geq T_0$, then

$$\begin{gathered} R = 4\frac{T_2}{T_1}, \qquad V = 2\sqrt{\frac{\rho_2}{\rho_0}} - \frac{T_1}{2T_2}\sqrt{\frac{\rho_0}{\rho_2}}, \\ \eta_s = 2\sqrt{\frac{\rho_2}{\rho_0}}, \qquad \eta_i = 2\sqrt{\frac{\rho_2}{\rho_0}} - \frac{T_1}{2T_2}\left(\sqrt{\frac{\rho_0}{\rho_2}} - \frac{1}{\sqrt{2}}\right). \end{gathered} \tag{20}$$

The relative thickness of the region of compressed un-ionized hydrogen is:

$$\frac{\eta_s - \eta_i}{\eta_s} = \frac{T_1}{4T_2}\left[\frac{\rho_0}{\rho_2} - \sqrt{\frac{\rho_0}{2\rho_2}}\right]. \tag{20'}$$

From here it follows that, first, the conditions of the flow considered can only be possible when $\rho_2 < 2\rho_0$ (in the opposite case the velocity of the ionization front will exceed the velocity of the shock wave); second, the compressed layer of un-ionized hydrogen is very thin and dense, therefore, it is probably unstable (with $T_1 \approx 100°$ $T_2 \approx 10{,}000°$ the relative thickness of this layer is of the order of 1/800 and its density is $\rho \approx 400\rho_0$); third, because of such a small thickness of this layer, it is hardly likely that its temperature will have sufficient time to fall to the value $T_0$, the temperature for equilibrium with the radiation.

b) $2T_2 = T_1 \gg T_0$ (from (17) it follows that this value of the temperature, $T_1$, is its upper limit), then

$$\begin{gathered} R = 1, \qquad V = \sqrt{2\frac{\rho_2 - \rho_0}{\rho_0}}\,; \\ \eta_s = \frac{\sqrt{2}\,\rho_2}{\sqrt{\rho_0(\rho_2 - \rho_0)}}\,; \quad \eta_i = \sqrt{2} \pm \sqrt{2\frac{\rho_2 + \rho_0}{\rho_0}}\,. \end{gathered} \tag{21}$$

The relative thickness of the region of compressed un-ionized hydrogen is:

$$\frac{\eta_s - \eta_i}{\eta_s} = \frac{\rho_0}{\rho_2} - \frac{\sqrt{\rho_0(\rho_2 - \rho_0)}}{\rho_2}. \tag{21'}$$

From this it follows that the flow condition is only possible if $\rho_0 < \rho_2 < 2\rho_0$. In this case, the thickness of the layer of compressed un-ionized hydrogen is comparable to the dimensions of the whole region in motion. In this case, however, the gas will radiate and, therefore, the temperature $T_1$ will fall. Thus, the actual state of the motion of the ionization front is intermediate to the two limiting cases; however, it is closer to the first one, but with $T_1 \gg T_0$ (then the Equations (20) and (20') will be somewhat changed).

With $\rho_2 < \rho_0$ the following values of the parameters are probably good approximations. Since, with a small thickness of the compressed-hydrogen layer the temperature in it will not have time to fall, the increase in density should correspond, in the first approximation, to the value obtained from the theory of shock waves without radiation, i.e., $\rho_1 = 4\rho_0$ and $R = 4\rho_0/\rho_2$. Then (17) gives $T_1$

$$T_1 = T_2 \frac{\rho_2}{2\rho_0}\left(2 - \frac{\rho_2}{4\rho_0}\right). \tag{22}$$

In any case, for a complete solution it is necessary to know the rate of radiation by the gas. For a rough estimate we can consider $T_1 \approx 1000°$.

It must be specially emphasized that this picture of the motion of an ionization front, preceded by a shock wave, is possible only in the case when the following condition is satisfied:

$$\rho_0 > \frac{1}{2}\rho_2 = 2 \cdot 10^{-25} M \text{ g/cm}^3.$$

If this condition is not satisfied, i.e., if the density of the un-ionized hydrogen is less than this limit, the ionization front cannot spread into the H I region at all. In this case, the opposite happens – gas from the H II region moves into the H I region since the pressure in the H I region is small. Other flow conditions, however, are also possible, in particular, the automodel nature of the motion can be lost. For this reason, the study of gas motion in ionization fronts with $\rho_0 > \frac{1}{2}\rho_2$ is a complex task and we will not deal with it further.

In actual applications of the theory to the various motions of interstellar gas, the condition $\rho_0 > \frac{1}{2}\rho_2$ is frequently satisfied.

Let us now consider the region of the gas flow behind the front of the ionization wave. Here, the boundary conditions will be:

$$R_1^{(2)} = 1; \quad V_1^{(2)} = \eta_i - \sqrt{2},$$

since $v_2 = v_0 - \sqrt{RT_2V_1^2}$. If we consider that in this region the gas motion is isothermal, then the Equations of Motion (13) and (15) are also applicable here with the necessary substitution of $RT_1$ by $2RT_2$ to take into account the change of the molecular weight. For this region the solution will be given by (19), inasmuch as it satisfies the Boundary Conditions (23),

$$V = \eta - \sqrt{2}, \qquad R = e^{\sqrt{2}(\eta - 2\sqrt{\rho_2/\rho_0})}, \tag{24}$$

i.e., the usual Riemannian isothermal flow. If the H II region is also bounded on the other side, then there exists a region of stationary hydrogen, separated from the region of moving ionized hydrogen by a weak discontinuity, at which $\eta_c = \sqrt{2}$ and the gas velocity is zero, and which is moving with the velocity of sound, $v_c = \sqrt{2RT_2}$. In the stationary H II region the gas density is equal to

$$\rho_c = \rho_2 R_c = \rho_2 e^{2(1 - \sqrt{2\rho_2/\rho_0})}.$$

The motion of the ionized hydrogen described is completely analogous to the motion of gas behind a detonation wave.

Thus, the general picture of the motion of ionization discontinuities is the following. (We will give numerical estimates assuming that $T_2 \approx 10{,}000°$, $T_1 \approx 1000°$, $T_0 \approx 100°$ and $\rho_0 \approx \rho_2$.) The compression shock wave is propagated in front with a velocity $v_s = 2\sqrt{RT_2\rho_2/\rho_0} \approx 18$ km/sec, the density increasing in this region by a factor of 40. Then a narrow region of compressed un-ionized hydrogen follows, moving with the constant velocity $v = 2\sqrt{RT_2\rho_2/\rho_0} \approx 18$ km/sec and with the constant density $\sim 40\rho_0$. Along this region an ionization-rarefaction wave is propagated with a velocity of the order of 0.3 km/sec (relative to the observer this velocity is close to 18 km/sec) in which the hydrogen is ionized and its density again decreases by a factor of 40. Next follows a region of ionized hydrogen, moving with a velocity $v \approx r/t - \sqrt{2RT_2} \approx r/t - 13$ km/sec, where the density falls from the value $\rho_2$ to the value $0.44\rho_2$. Finally, for $r \leq t\sqrt{2RT_2} = (13$ km/sec$)t$ the ionized hydrogen is stationary and its density is constant (and equal to $0.44\rho_2$).

However, it must be emphasized that all of the conclusions given above were obtained with the assumption that M = const. If this condition is not satisfied, the elementary solution obtained by us will not correspond accurately to the true picture of the motion; however, for semiquantitative estimates and for studying the features of the motion of ionization discontinuities, this solution can also be used if M is not a constant.

We have investigated above the one-dimensional planar flow. This solution can be used in those cases where the ionization front is produced by a group of stars situated at comparatively large distances from one another, i.e., at distances comparable to the radius of the ionization wave. This distribution occurs, for example, in associations, spiral arms and similar objects. In the case when the ionization front is produced by a single star, a better approximation would be the spherically symmetrical problem (N = 3). Unfortunately, in this case Equations (15) are not integrable in analytical form. However, because of the very simple form of these equations their numerical integration presents no difficulties. The Boundary Conditions (16) and (17) remain unaltered. Finally, it can be pointed out that the theory of detonation waves [8], in which the spherically symmetric problem is also investigated in detail, can also be extensively used here. If the relative thickness of the layer of compressed un-ionized hydrogen is small, then in the spherically symmetric case, as can be easily shown, it must decrease further by a factor of three.

## 4. Ionization Discontinuities in Interstellar Space

In this way we see that each ionization discontinuity in interstellar space during its motion produces a region of compressed un-ionized hydrogen, whose density is greater than the normal density by a factor of several hundreds. On the ionization discontinuity the pressure again falls to its normal value. The problem of the stability of the compressed-gas regions is of great interest but, as yet, it has not been resolved. Oort and Spitzer [2] and Savedoff and Greene [4] have assumed that this region is unstable, inasmuch as it is accelerated by the less-dense H II region (Rayleigh-Taylor instability). However, irrespective of this reason, the compressed H I region can also be unstable because it moves in a medium with a varying density. For example, if in the space in which the motion investigated occurs, the density changes from values higher than $2 \cdot 10^{-25}$ M to values less than this magnitude, then the conditions for the flow can be markedly disturbed and this must lead to the formation of separate clouds. The surmise of Oort and Spitzer [2], that the formation of stars can also be explained by this, is possible, but, of course, it requires more reliable evidence.

In conclusion, we will make a few remarks about the papers on ionization processes [3, 4] cited above. The formation of a region of compressed un-ionized hydrogen was studied both by Savedoff and Greene and by Kahn. In both papers, also, the theory of isothermic discontinuities was used for describing the front of the shock wave. However, in neither of the papers was the condition for the Jouguet point sufficiently used. The structure of the gas region in motion was investigated in [3, 4] by a primitive method which did not allow the authors to obtain the more general results given in the present work. The statement of this problem as automodel in nature, although it is also limited to a certain extent (for example, it requires that M be constant in the H II region), at the same time enables very simple and useful results to be obtained, which make it possible to calculate all of the parameters of the motion; as a result of this all of the final equations obtained by us are simpler than those of [3, 4]. Finally, it can be pointed out that there are numerous, well-developed methods for the solution of even more general automodel problems [7, 8]. As we have emphasized several times, the theory of detonation waves can be applied, after small modifications, to the investigation of ionization discontinuities.

## LITERATURE CITED

[1] B. Stromgren, Astrophys. J. 89, 526 (1939); 108, 242 (1948).

[2] J.H. Oort and L. Spitzer, Astrophys. J. 121, 6 (1955).

[3] F.D. Kahn, Berliner Astronomischer Nachrichten 12, 456, 187 (1954).

[4] M. Savedoff and J. Greene, Astrophys. J. 122, 477 (1955).

[5] H. Zanstra, Berliner Astronomischer Nachrichten 11, 401 (1949).

[6] S.A. Kaplan, Astron. J. (USSR) 33, 646 (1956).

[7] L.I. Sedov, The Methods of Similarity and Dimensions in Mechanics [in Russian] (Gostekhizdat, Moscow, 1954).

[8] K.P. Staniukovich, Irregular Motions of a Continuous Medium [in Russian] (Gostekhizdat, Moscow, 1955).

Received May 2, 1956

Lvov Astronomical Observatory

# SOME CHARACTERISTICS OF SHELLS OF Be STARS

A. A. Boiarchuk

The quantity log $N_{02}H$ was determined for the shells of 9 Be stars by Unsöld's method [1]. On the basis of the values obtained and Sobolev's theory [2], the optical thickness of a shell was then determined for different frequencies. It was found that the shells of Be stars are opaque in the lines of the Balmer series, at least in its first members, and transparent beyond the limit. The optical thickness of shells of the majority of Be stars beyond the Lyman series limit is not greater than unity. The average mass of the shells of Be stars was determined and was found to be $10^{-10}\,\mathfrak{M}_{\odot}$.

The sizes of the shells were determined on the assumption that their rotation obeys the law vr = const. There is a stratification of radiation in the shells of Be stars. The average size of the emitting part of the shell is 1.7 $R_{st}$, that of the absorbing part, 3.5 $R_{st}$. The dilution coefficient is correspondingly 0.1 and 0.02.

Finally, the motion of the shells was considered. It was found that on the average the shells of Be stars do not show a tendency to expand.

In spite of the fact that much effort is devoted to the study of Be stars, the characteristics of their shells have not been determined with certainty up to the present time. The absence of these data hinders the investigation of the nature of Be stars and their shells.

The present paper attempts to close this gap and considers the problem of the sizes of shells of 11 Be stars and their transparency to different lines.

The observational material was obtained with the large spectrograph (dispersion 23.4 A/mm at Hγ) of the 1200 mm reflector at the Crimean Astrophysical Observatory AN SSSR in the period from November 1953 to August 1956.

## The Transparency of the Shells of Be Stars

This question is of great importance in the solution of problems of radiative transport in the shells of Be stars owing to the fact that in all modern theoretical works concerning these shells some assumption or other is introduced about their transparency in the lines of different series and beyond series limits.

For certain Be stars, namely those having shell absorption lines, it was found possible to determine directly from the observations the optical thickness of the shell in the lines of the Balmer series.

First we shall determine the number of hydrogen atoms in the second energy level above 1 cm² of the shell surface, $N_{02}H$. For this purpose we make use of Unsöld's formula [1]:

$$W_{\lambda} = \frac{\pi^2 e^2 \lambda^2}{mc^2} f \;\; (N_{02}H), \tag{1}$$

where $W_{\lambda}$ is the equivalent width of a sharp shell absorption line, f is the oscillator strength, and the remaining symbols have the usual meaning.

This formula, in the case of an optically thick layer, gives a reduced value of $N_{02}H$. As we go to higher members of the series we shall approach the case of an optically thin layer because of the sharp decrease in the value of f, and the values of $N_{02}H$ determined will be more accurate.

TABLE 1

| Star | $\log N_{02}H$ | $\tau(H_\alpha)$ | $\tau(H_\beta)$ | $\tau(H_\gamma)$ | $\tau(H_\delta)$ | $\tau$ (B) | $\lg N_{01}H$ | $\tau$ (L) | $\lg N_{+}H$ | $\frac{\mathfrak{M}sh}{\mathfrak{M}_\odot}\cdot 10^{10}$ |
|---|---|---|---|---|---|---|---|---|---|---|
| φ Per | 14.5 | 250 | 20 | 8 | 5 | $10^{-3}$ | 17.2 | 1 | 22.1 | 1 |
| o And | 14.3 | 160 | 12 | 5 | 3 | $10^{-3}$ | 18.0 | 6 | 22.0 | 1 |
| γ Cas | 14.3 | 160 | 12 | 5 | 3 | $10^{-3}$ | 16.8 | 0.4 | 22.1 | 1 |
| ν Cem | 14.2 | 120 | 10 | 4 | 2.5 | $8\cdot 10^{-4}$ | 17.6 | 1.6 | 21.6 | 0.2 |
| ψ Per | 14.1 | 100 | 8 | 3 | 2 | $5\cdot 10^{-4}$ | 17.3 | 1 | 21.8 | 0.4 |
| c Per | 13.6 | 32 | 2.5 | 1 | 0.6 | $10^{-4}$ | 16.8 | 0.4 | 21.3 | 0.2 |
| ϰ Dra | 13.5 | 25 | 2 | 0.8 | 0.5 | $10^{-4}$ | 16.8 | 0.4 | 21.1 | 0.1 |
| 59 Cyg | 13.5 | 25 | 2 | 0.8 | 0.5 | $10^{-4}$ | 16.0 | 0.06 | 21.5 | 0.1 |
| 23 Tau | 12.9 | 6 | 0.5 | 0.02 | 0.001 | $4\cdot 10^{-5}$ | 16.5 | 0.1 | 20.8 | 0.02 |

The results of the determinations are given for each star in column 2 of Table 1.

In Figure 1 the dependence of $\log N_{02}H$ on the number of the line is represented for each star. In many cases, we obtain from the observations only a lower limit for the value of $\log N_{02}H$, but, as is evident from the form of the curves in Figure 1, the departure of the value found from the true one is probably not great.

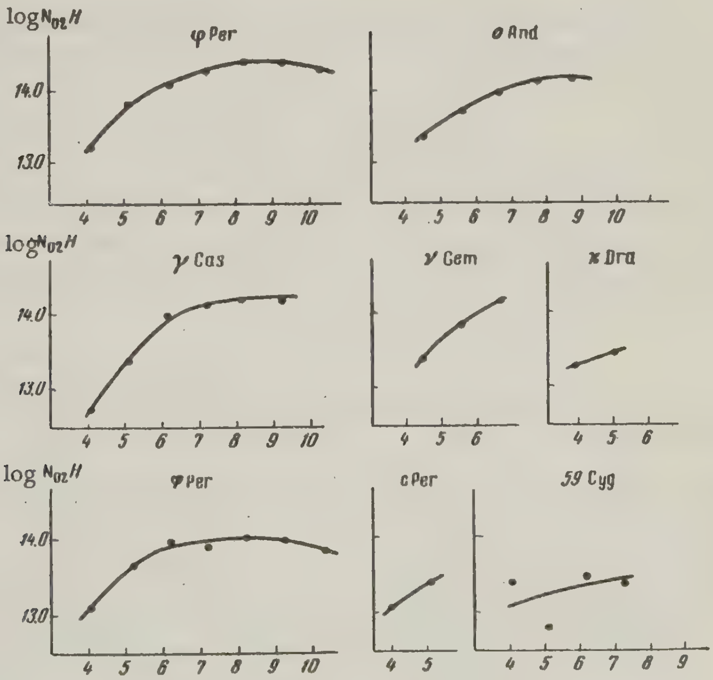

Fig. 1. Dependence of $\log N_{02}H$ on the number of the line.

The optical thickness of the shell of the Be star in the central portions of lines of the Balmer series and beyond its limit was determined by the formula:

$$\tau = kN_{02}\mathrm{H}, \qquad (2)$$

where k is the appropriate absorption coefficient, calculated per atom.

For the central portion of the line, k is determined by the following formula:

$$k_{\lambda_0} = \frac{\sqrt{\pi}\, e^2 \lambda}{m_e c v} f, \tag{3}$$

where v is the velocity of the atoms, f is the oscillator strength, and the rest of the symbols have their usual meaning.

The absorption coefficient beyond the series limit is

$$k = \frac{32\,\pi^2 e^6 R}{3\sqrt{3}\,\mathrm{ch}^3\,\nu^3\, n^5}\, g', \tag{4}$$

where n is the principal quantum number of the series, and g' is a certain correction factor which differs little from unity.

In columns 3-7 of Table 1 are given the values obtained for the optical thickness in $H_\alpha$–$H_\delta$ and beyond the Balmer series limit, $\tau(B)$ (at $\lambda = 3647$ A).

It is of great interest to determine the optical thickness of the shell beyond the Lyman limit. For this purpose it is necessary to know the value of $N_{01}H$, i.e., the number of atoms in the first energy level present in the shell above 1 cm² of its inner surface. In order to go over from $N_{02}H$ to $N_{01}H$, we make use of results of the theory of V.V. Sobolev [2].

This theory gives the distribution of atoms in the energy levels in relation to the stellar temperature and the parameter $x = \beta_{12}/W$. Here $\beta_{12}$ denotes the probability of escape of a quantum from the shell. This probability depends basically on the gradient of the projected velocity in the line of sight. In the shells of Be stars, such a gradient exists owing to the fact that different parts of the shell rotate at different rates. However, it is rather difficult to calculate the magnitude of this gradient, and we determined the parameter x by comparing the observed decrement of the Balmer emission lines with the theoretical one given in the work of Sobolev [2]. For the stars considered it was found that the quantity $x \approx 0.01$-$0.1$, i.e., $n_2/n_1$ is only 1/5 to 1/2 as large as the value expected from the Boltzmann formula for the same temperature. Since our calculations are approximate, we adopt a value of $n_2/n_1$,1/3 as large as that given by the Boltzmann distribution. At the same time, the error in $\log N_{01}H$ apparently will not exceed ± 0.5. The results of the calculations for $\log N_{01}H$ and $\tau(L)$ (at $\lambda = 912$ A) are given in Table 1 in columns 8 and 9.

From inspection of Table 1 it is possible to draw the following important conclusions:

1. The shells of Be stars are completely opaque in the central portions of the Balmer series lines – in its first members, $H_\alpha - H_\gamma$, at any rate.

2. The shells of Be stars are completely transparent beyond the limits of the Balmer and higher series. This means that self-absorption of the radiation of the shell is absent beyond the limits of these series.

3. The optical thickness of the shells of almost all the stars considered is less than or equal to unity beyond the Lyman limit. Since the absorption coefficient beyond the series limit is proportional to $\nu^{-3}$, it is impossible to consider that the shells of Be stars absorb all stellar radiation beyond the Lyman limit. From this, in particular, it follows that Zanstra's method of determining stellar temperatures is inapplicable to the majority of Be stars.

Let us determine the masses of Be-star shells. For this purpose it is necessary to allow for atoms which occur in an ionized state. The degree of ionization in the shell is determined by the following formula:

$$\frac{N_+H}{N_{01}H}\, n_e = \frac{n^+}{n_1}\, n_e = \frac{g^+ (2\pi mkT)^{3/2}}{g_1 h^3}\, e^{-\chi/kT}\, W, \tag{5}$$

where $N_+H$ is the number of hydrogen ions in the shell above 1 cm² of its inner surface, and W is the dilution coefficient in the shell.

According to this formula, taking $n_e = 10^{12}$ and $W = 0.05$, we have calculated column 10, Table 1, from which it is evident that hydrogen is completely ionized in the shells.

To determine the mass of a shell we must multiply the value of $N_+H$ by the surface area of the shell. Since our estimates of mass are approximate, we shall assume, for simplicity, that the shell is spherical. Hence,

$$\mathfrak{M}_{sh} = N_+H\, 4\pi R_{sh}^2 m_H. \qquad (6)$$

The results of the calculation are presented in column 11 of Table 1, from which it follows that the masses of Be-star shells are $10^{-10}$-$10^{-11}\, \mathfrak{M}_\odot$.

## The Dilution Coefficient and the Sizes of Shells in Be Stars

The determination of the dilution coefficient in the shells of Be stars is usually based on the assumption that the rotational velocity of the shell obeys the law of conservation of angular momentum:

$$vr = \text{const}, \qquad (7)$$

where $v$ is the linear rotational velocity at distance $r$ from the axis of rotation.

The question of the applicability of the law of conservation of angular momentum in the shells of Be stars has been discussed by Chandrasekhar [3], who concluded that it is valid in this case. Baldwin [4] came to the same conclusion on the basis of a comparison of the dimensions of the shell of $\gamma$ Cas, determined from the light-curve and the temperature, with the dimensions obtained from Equation (7). Furthermore, the law indicated is favored by the agreement in the dimensions of the shells of Be stars as determined from Equation (7) and from the intensity of the HeI line at λ3965 A [3].

If we denote by $v_0$ the rotational velocity of the reversing layer of the star, by R the radius of the star, and by $v$ the rotational velocity of the shell at distance $r$ from the axis of rotation, then on the basis of (7) we shall have

$$\frac{R}{r} = \frac{v}{v_0}. \qquad (8)$$

Thus, from the observed rotational velocities of the star and of the shell, we may find the size of the shell, expressed in units of the stellar radius, and consequently, the dilution coefficient:

$$W = \frac{1}{4}\left(\frac{R}{r}\right)^2 = \frac{1}{4}\left(\frac{v}{v_0}\right)^2. \qquad (9)$$

In this way, the whole procedure of determining the dilution coefficient boils down to the determination of the rotational velocity of the stellar reversing layer and the rotational velocity of the region of interest in the shell.

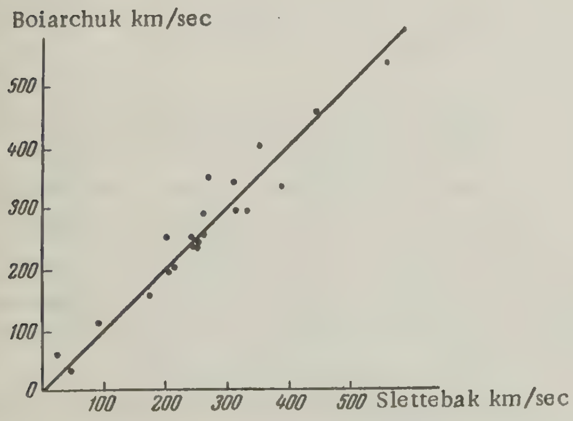

Fig. 2. Comparison of our determinations of stellar rotational velocity with those of Slettebak.

For the determination of the rotational velocity of the stars those lines are useful at which the influence of other kinds of line broadening is small compared with that of the Doppler effect. Because of the influence of the Stark effect on rotational velocity determination it is impossible to make use of the hydrogen lines. The most convenient lines to use are those of the ionized metals, in particular Mg II λ4481 A. The latter was in fact employed by us for determining stellar rotational velocities and only where it was absent from the spectrum did we use the lines of HeI λ4471 A and λ4388 A.

If line broadening arises only from rotation of the star, then half the interval between the violet and the red wing of the line, expressed in km/sec, will be equal to the rotational velocity of the star. By this

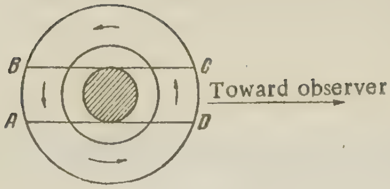

Fig. 3.

method we determined the stellar rotational velocities. The lines, especially narrow ones, are distorted by instrumental effects. The elimination of these effects was carried out following the method of Su-Shu Huang [5], according to the formula:

$$\Delta\lambda_D = \gamma\,[\Delta\lambda^2_{\text{meas}} - \Delta\lambda^2_{\text{instr}}\,]^{1/2}, \tag{10}$$

where $\Delta\lambda_{\text{meas}}$ is the measured line width, $\Delta\lambda_{\text{instr}}$ is the width of the instrumental contour, equal to 2.13 A at $H_\gamma$. $\gamma$ is a coefficient which is determined by comparing the rotational velocities determined by this method with the velocities obtained from the shape of the contour.

We compared our own measurements with the rotational velocities obtained by A. Slettebak [6]. The results of the comparison are presented in Figure 2.

As is apparent from this figure, good agreement was obtained, and the coefficient $\gamma$ entering into Formula (10) proved equal to unity.

In determining the rotational velocity of the shell we shall proceed from the following model of a Be star. A star, in the reversing layer of which broad absorption lines originate, is surrounded by a more or less spherical shell in which emission lines and narrower absorption lines arise. The observed absorption lines of the shell may be roughly divided into two groups: lines in which the central optical thickness is greater than unity, and lines in which the central optical thickness is less than unity. Lines of the second group originate in those regions of the shell CD which are projected onto the disc of the star (Figure 3). In this case, we obtain from the observations not the rotational velocity v of the shell, but its projection onto the line of sight v', which is connected with the velocity by the following relation:

$$v' = v\,\frac{R}{r}\,. \tag{11}$$

Because of the low value of v ≈ 50 km/sec, the observed profile of lines of this group, under our dispersion, appears to be purely instrumental. Moreover, all of these lines are very weak. Therefore, it was found impossible to utilize them for determining the rotational velocity of the shell.

Lines of the first group originate in the outer regions of the shell, regardless of whether a given part of the shell is projected onto the stellar disc.

The determination of the rotational velocity of the shell was made in the same way as was that of the rotational velocity of the stellar reversing layer.

In determining the rotational velocity and the dilution coefficient it is necessary to observe the following precautions.

1. One cannot make use of the ratio of widths of the emission and the diffuse absorption components in the case of the hydrogen lines, as is sometimes done, since the width of these absorption components, originating in the stellar reversing layer, depends on the Stark effect and not on the rotation of the star.

2. Strong hydrogen emission lines may have wings which are not the result of stellar rotation, but may be the result of the Stark effect and of radiation damping. Since the electron density in the shells of Be stars is low, of the order of $10^{12}$, the influence of the Stark effect will be perceptible only in high members of the Balmer series where emission is not present or is very weak. Therefore, it may be assumed that in Balmer lines having noticeable emission the influence of radiation damping will be greater than the influence of the Stark effect.

The width of the line, which is determined by damping due to radiation, decreases rather rapidly with the number of the line, since the number of radiating atoms producing a given line decreases in the first approximation according to the Boltzmann law. Therefore, it is necessary to determine the shell velocity from weak emission lines.

Taking all of these precautions into account, the dilution coefficients and the sizes of the shells of the Be stars were determined. The results of the calculations are collected in Table 2.

TABLE 2

| Star | $v \sin i$ | $v_{em}$ | $v_{abs}$ | $\frac{r_{em}}{R_{st}}$ | $\frac{r_{abs}}{R_{st}}$ | $\frac{r_{abs}-r_{em}}{R_{st}}$ | $W_{em}$ | $W_{abs}$ |
|---|---|---|---|---|---|---|---|---|
| φ Per | 530 | 325 | 135 | 1.6 | 3.9 | 2.3 | 0.09 | 0.016 |
| 59 Cyg | 450 | 300 | 128 | 1.5 | 3.5 | 2.0 | 0.11 | 0.020 |
| ψ Per | 330 | 200 | 85 | 1.6 | 3.9 | 2.3 | 0.09 | 0.016 |
| ν Cem | 330 | 210 | 86 | 1.6 | 3.8 | 2.2 | 0.10 | 0.016 |
| γ Cas | 310 | — | 125 | — | 2.5 | — | — | 0.040 |
| o And | 290 | — | 80 | — | 3.7 | — | — | 0.019 |
| 23 Tau | 285 | 200 | 112 | 1.4 | 2.5 | 1.1 | 0.12 | 0.040 |
| c Per | 250 | 137 | <68 | 1.8 | >3.7 | >1.9 | 0.07 | <0.018 |
| β CMi | 290 | 205 | — | 1.5 | — | — | 0.12 | — |
| η Tau | 210 | 130 | — | 1.6 | — | — | 0.09 | — |
| κ Dra | 250 | — | 80 | — | 3.2 | — | — | 0.023 |

In the first column, the star designation is given; in the second, the rotational velocity of the reversing layer; in the third and fourth, the rotational velocities of the emitting and absorbing parts of the shell; in the fifth and sixth, the sizes of the emitting and absorbing parts of the shell; and in the eighth and ninth, the dilution coefficients for the emitting and absorbing parts of the shell.

From inspection of Table 2, the following conclusions may be drawn:

1) There is stratification in the shells of Be stars; emission lines originate in those regions of the shell which are closer to the surface of the star, say at a distance of 0.6 $R_{st}$, whereas absorption lines originate in the outermost regions of the shell, at an average of 2.5 $R_{st}$ from the surface of the star.

2) The sizes of the shells of Be stars have a rather small dispersion, especially the sizes of the emitting regions, and do not show appreciable dependence on the rotational velocity of the star.

3) The dilution coefficients for different parts of the shell differ among themselves in order of magnitude: $\overline{W}_{em} = 0.1$ and $\overline{W}_{abs} = 0.02$. Consequently, it is necessary, in the study of Be-star shells, to consider the fact that the dilution coefficient is not the same for different parts of the shell.

## The Efflux of Matter from Be Stars

There is a rather widespread opinion that, because of the rapid axial rotation of Be stars, a continuous flow of matter emanates from their surfaces in the equatorial zone. The matter, abandoning the star, forms a shell around it.

Let us consider first what role stellar rotation plays in the formation of the shell. According to A. Slettebak [6], Be stars have an average rotational velocity that is 150 km/sec greater than that of B stars. This provides a basis for supposing that stellar rotation substantially assists shell formation. If the role of rotation in forming a shell is comparable with the role of other factors, then obviously there must be a statistical relation between the value of the rotational velocity of the star and the capacity of the shell surrounding the star. By the capacity of the shell we mean the total number of atoms forming it.

We cannot determine the capacity of the shell directly from the observations, but it is natural to suppose that at a given stellar temperature the capacity of the shell is greater the more intense the emission in the stellar spectrum. Because of the absence of quantitative data concerning the intensity of emission for a large number of stars, we made use of visual estimates of the intensity of the $H_\alpha$ emission line given by Merrill [7], as a measure of emission intensity, and consequently also of the capacity of the shell.

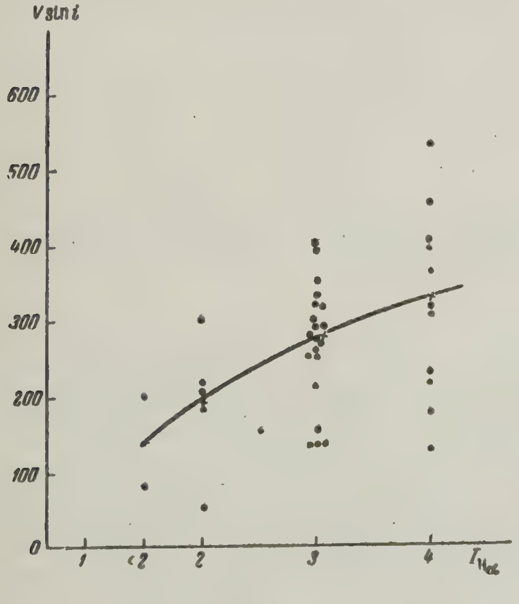

Fig. 4. Relation of intensity of emission in $H_\alpha$ to the velocity of stellar rotation.

The relation between the rotational velocity of the star and the emission intensity in $H_\alpha$ is illustrated in Figure 4. In order to eliminate possible temperature effects, we used stars in the spectral interval B0 – B3.

In spite of the rather large scatter of the points, it is evident from Figure 4 that there is a relation between the rotational velocity of the star and the intensity of $H_\alpha$ emission, i.e., the capacity of the shell. The scatter of the points is explained in part by the fact that we obtain from the observations the quantity $v \sin i$, i.e., the projection of the rotational velocity onto the line of sight. Thus, low observed values of $v \sin i$ at intensity 4 do not imply that the corresponding stars have low rotational velocities. We have averaged the rotational velocities in order to eliminate, to some extent, the effect of orientation of the axis of rotation. In Figure 4 the mark × denotes the mean. As was to be expected, the mean rotational velocities increase with increasing emission intensity.

Thus, the rotation of stars plays a rather large role in the formation of their shells.

If there exists a stable, continuous outward flow of matter from the surface of the star, we should observe either an expansion of the material of the shell or a continuous increase in its capacity. All observations of Be stars available up to now indicate that there is no monotonic increase in capacity of the shell over at least a few years. The emission intensity varies in an irregular manner, now increasing, now decreasing. Thus, in the case of a stable, continuous emanation of matter we must certainly observe expansion of the shell material.

We determined the rate of expansion of the shell material in the following way. As is well known, broad, diffuse absorption lines originating in the reversing layer of the star, and narrow shell absorption lines, are observed simultaneously in the spectra of Be stars. Obviously, the difference of velocity determined from the broad and the narrow lines gives us the velocity of shell material relative to the star. For some stars it was found possible to determine the radial velocities of the reversing layer and the shell. The measurements of the spectrograms were made with the aid of an Abbe comparator (one scale division = 0.001 mm). For the determination of the radial velocity of the stellar reversing layer the absorption lines of HeI λλ4471, 4388, 4026, 4009 A and MgII λ 4418 A were employed, while for the determination of the shell radial velocity all shell absorption lines were used which were visible in the spectrum of a given star. The procedure of measuring the spectrograms and their treatment were the usual ones [8]. For each star 3-4 spectrograms were used. The results are presented in Table 3.

TABLE 3

| Star | $v^{st}$, km/sec | $v^{sh}$, km/sec | $v^{sh} - v^{st}$, km/sec | V/R |
|---|---|---|---|---|
| ψ Pep | +9 | —13 | —22 | $V = 0.9R$ $(V < R)$ |
| o And | —38 | —36 | +2 | |
| c Per | —13 | —12 | +1 | $V = 1.1R$ $(V > R)$ |
| ϰ Dra | +13 | +15 | +2 | $V = 1.02R$ $(V = R)$ |

Furthermore, for some stars it was possible to find similar data in the literature. All the data, our own and that from the literature, were plotted in Figure 5, where the abscissa is the rotational velocity of the stellar reversing layer and the ordinate is the velocity of expansion of the shell:

$$v_{exp} = v^{sh} - v^{st}. \tag{12}$$

At abscissa 0 are plotted those stars for which the rotational velocities are unknown. Here class Ia supergiants and P Cygni stars were not considered, since they differ rather strongly in their characteristics from ordinary Be stars.

From Figure 5 it follows that there is no marked correlation between the rotational velocity of the star and the velocity of expansion of the shell. The mean shell expansion velocity, which is + 2 km/sec, suggests that on the average the shells of Be stars are contracting. Unfortunately, the small amount of material does not permit the present result to be considered conclusive.

However, one may extend this material if one takes into account the following circumstance. As is known,

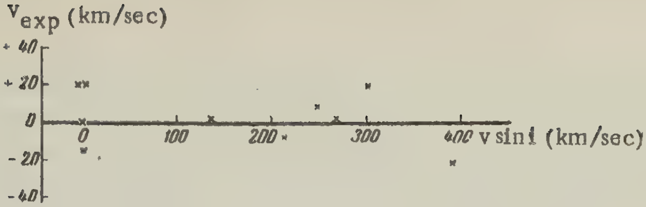

Fig. 5. Relation of the expansion velocity of the shell to the rotational velocity of the star.

the sharp absorption line of the shell divides the emission into two components, of which the red one may be designated R and the violet one V. Numerous investigations of the variations of emission line profiles have shown that the sharp absorption is always displaced in the direction of the component of lower intensity, and that this displacement is greater, the greater the difference in intensity between the two components; in other words, the ratio V/R may serve as a measure of the velocity of expansion of the shells of Be stars; if V > R the shell is contracting, if V < R it is expanding. In confirmation of what has been said, one may point out in particular the work of D. McLaughlin [9]. From this work it follows that such a variation of the ratio V/R cannot be explained by the presence of a velocity gradient in the shell. Comparison of the last two columns of Table 3 confirms the relation indicated between the ratio V/R and the expansion velocity of the shell.

The values of V/R found from our observations and from the literature have been plotted in Figure 6 as a function of the rotational velocity of the star. Inspection of this figure confirms the conclusion that Be star shells do not show a tendency to expand. Of the 37 stars considered in Figures 6 and 5, 13 shells are contracting, 15 are stationary, and only 9 are expanding.

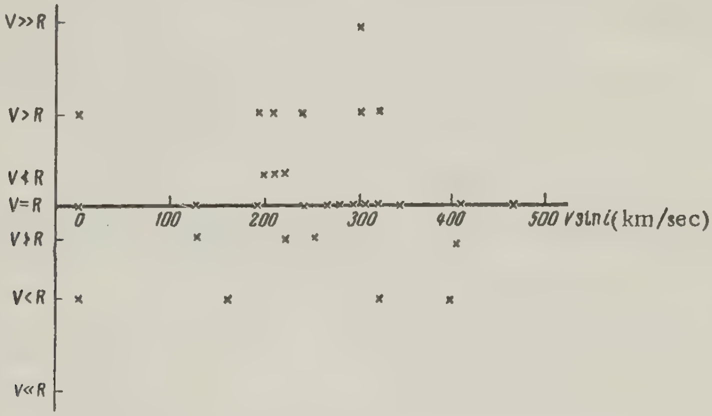

Fig. 6. Relation of V/R to the velocity of stellar rotation.

Moreover, from the point of view of a continuous escape of matter caused by rotation of the star, it is quite impossible to explain the variation of emission intensity and even its disappearance, as the rotational velocity of the star remains constant over a long period of time.

Thus, apparently, there does not exist a stable, continuous escape of matter from the surfaces of Be stars. Probably there is an outward flow in the form of discrete ejections, in which other forces play a fundamental role and stellar rotation only materially aids them.

The matter ejected in this way forms a shell, which is at a distance of about 1.5 $R_{st}$ from the surface of the star. This shell usually does not show a tendency to expand. Furthermore, all the observational data indicate that the material of the shell may not be dispersed into interstellar space. The parabolic velocity in the case of the shell $\mathfrak{M}_{st} = 20\ \mathfrak{M}_{\odot}$ and $R_{sh} = 15\ R_{\odot}$) must be of the order of 500 km/sec. We do not observe such velocities.

The rotational velocities of the shells and even of Be stars having shells seldom exceed 300 km/sec. The observed velocities of the shell with respect to the star do not exceed 40 km/sec. Besides that, they often appear to be variable.

Thus, on the basis of all that has been said, one may conclude that the matter thrown out of the star is retained, on the average at a distance of 1.5 $R_{st}$ from the stellar surface and forms a shell. At present it is difficult to say what forces maintain the material at this distance and promote the building of the shell. Possibly the general magnetic field of the star may play a decisive role here. But, unfortunately, because of the fast axial rotation of Be stars, it is impossible to detect a magnetic field directly.

The question of the ultimate fate of the shell, i.e., whether it dissipates into interstellar space or whether it returns to the surface of the star, requires further investigation. But from all that has been said above, there is good reason to think that the matter of the shell, to all appearances, returns to the star.

In conclusion, we shall briefly sum up the work done in studying the physical characteristics of Be star shells:

1. In the present work the optical thickness of the shells was first determined for different frequencies. It was found that the shells of Be stars are not transparent in the lines of the Balmer series. The optical thickness beyond the Balmer limit is much less than unity ($\tau(B) \ll 1$). And finally, the optical thickness beyond the Lyman limit for most shells is of the order of unity or smaller ($\tau(L) \ngtr 1$).

2. The masses of the shells were determined and were found to be of the order of $10^{-10}$-$10^{-11}\mathfrak{M}_{\odot}$

3. For 11 stars the sizes of the absorbing and emitting regions of the shells were determined and were found to average 3.5 $R_{st}$ and 1.7 $R_{st}$, respectively. The dispersion of the values is small, which is a rather interesting fact.

4. The question of a continuous escape of matter from Be stars was considered. It was shown that a stable, continuous efflux of matter does not exist in Be stars, and that stellar rotation plays a subsidiary role in the formation of the shell, while other active processes, possibly of type similar to solar prominences and chromospheric outbursts, play a fundamental role.

In conclusion, I wish to express my sincere thanks to Prof. E.R. Mustel' for very valuable advice.

## LITERATURE CITED

[1] A. Unsöld, Z. Astrophys. 21, 37 (1941).

[2] V.V. Sobolev, Moving Stellar Envelopes (Leningrad State University Press, 1946), p. 15.*

[3] O. Struve and K. Wurm, Astrophys. J. 88, 106 (1938).

[4] B. Baldwin, Astrophys. J. 92, 82 (1940).

[5] S.-S. Huang, Astrophys. J. 118, 285 (1953).

[6] A. Slettebak, Astrophys. J. 110, 498 (1949).

[7] P. Merrill et al., Astrophys. J. 76, 156 (1932).

[8] V.A. Al'bitskii et al., Course in Astrophysics and Stellar Astronomy, Vol. 1 (GITTL, Moscow-Leningrad, 1951), p. 301.*

[9] D. McLaughlin, Popular Astron. 46, 361 (1938).

Received November 19, 1956

Crimean Astrophysical Observatory
Academy of Sciences, USSR

---

*In Russian.

# OPEN STELLAR CLUSTER NGC 6811

## K. A. Barkhatova

The open stellar cluster NGC 6811 was photographed with the 15-inch Schmidt telescope at the Engelhardt Observatory. The diagrams for color index-apparent magnitude and the luminosity function were constructed for the stars in this cluster. The distance, corrected for light absorption (CE = $0.^{m}10$), equals 1000 parsecs. Angular diameter, derived from stellar counts, is 0°20'; linear diameter is 5.8 parsecs. The distance of the cluster from the galactic plane is +190 parsecs.

Stars in the region of cluster NGC 6811 ($\alpha_{1900} = 19^{n}35.^{m}2$, $\sigma_{1900} = 46°20'$) were photographed with a Schmidt camera at the Engelhardt Astronomical Observatory between March, 1954 and January, 1956. Altogether, sixteen pictures of the cluster and twelve pictures of standard regions were taken. Stars of Kapteyn area 39, registered on the same plate as the cluster, were used as a photographic standard. Plates Agfa Astro and Ilford Zenith were used in determining photographic stellar magnitudes; photovisual magnitudes were obtained on the plates Agfa ISS used in conjunction with a yellow filter, and also on a photovisual film prepared by Factory No. 8. Photovisual stellar magnitudes were determined with a microphotometer MF2 by means of comparing the stars with those of NPS and also with the stars of the Kapteyn area 40 (in this work the photovisual magnitudes of an unpublished work by Sears were used).

Photometric star measurements obtained on various emulsions agreed well with each other, and mean photographic magnitudes were determined from three plates of Ilford Zenith and from three of Agfa Astro.

Photovisual magnitudes obtained on Agfa ISS plates were introduced to the previously determined system of stellar magnitudes. Measurements obtained on seven plates and three films were used in obtaining photovisual magnitudes. All the photographic and photovisual magnitudes were corrected for light absorption in the earth's atmosphere.

In working with the observational data, stellar magnitudes were determined in the international system of photographic and photovisual stellar magnitudes. Average errors of area in the photographic magnitudes were $\pm 0.^{m}05$; for the photovisual magnitudes – $\pm 0.^{m}05$; and for the color index – $\pm 0.^{m}07$.

Cluster NGC 6811 was investigated in 1947 by Becker [1] and in 1953 by Becker and Stock [2]. Photographic magnitudes obtained by us agreed well with the photographic magnitudes of Becker, reduced to the international system.

Diagrams for color index-apparent magnitude for separate zones of concentration (Figures 1-6) were constructed on the basis of photographic and photovisual stellar magnitudes of 357 stars distributed through the cluster and in its neighborhood. Figure 7 shows the diagram for the color index – stellar magnitude of the probable members of the cluster, distributed in the first three zones. Figure 8 shows the photograph of the cluster. Figures 1-6 show that the magnitude can be determined exactly only for the main stars in the first three zones, while in the following zones the background stars predominate.

According to Trümpler [3], cluster NGC 6811 contains 37 stars of spectrum classes A3–G0 (among them 8 giants), and can be classified as type 2a–f.

According to Becker [2], stars of type A0 are the oldest.

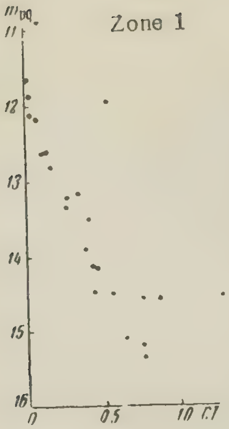

Fig. 1

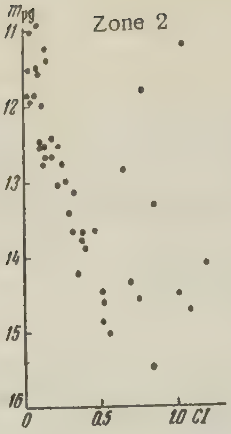

Fig. 2

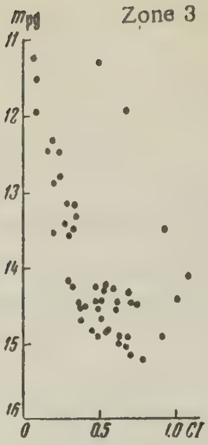

Fig. 3

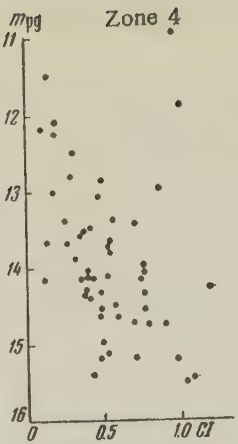

Fig. 4

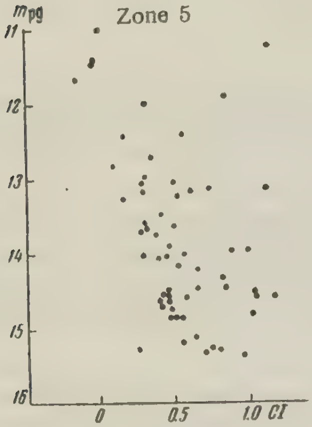

Fig. 5

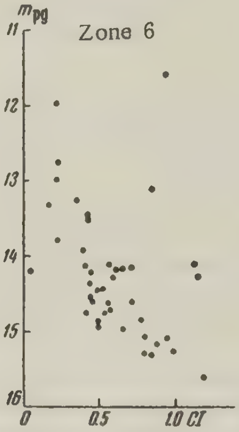

Fig. 6

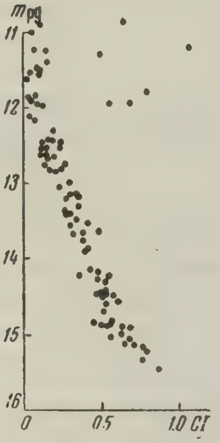

Fig. 7

Color excesses were determined by investigating the stars with known spectra. On the average, for 19 stars of spectrum classes A0-A9, color excess was found equal to $CE = 0.^{m}10$.

Apparent distance modulus, determined from the diagram for color index-stellar magnitude, amounts to $m - M = 10.^{m}50$. At $CE = 0.^{m}10$, light absorption in the direction toward the cluster is equal to $A_{pg} = 0.50$; consequently, the actual distance modulus is $m_0 - M = 10.^{m}0$ or $r = 1000$ parsecs, and agrees well with the data obtained by other investigators of this cluster [1-4]. Contrary to the vast majority of open clusters, this cluster is located at a considerable distance from the galactic plane ($Z = 190$ parsecs).

Angular distances were estimated by the method of Tseraskii who counted the stars of various magnitudes in annular zones.

Calculations of the number of stars showed that the angular diameter for this cluster was 0°20'-0°24', which agrees well with the data of Raab [5], who used the same method and found this diameter to be 0°19'-0°23'.

It can be seen from Figure 9 that for the stars of $m_{pg} < 14^{m}$ the apparent stellar density decreases gradually toward the edges of the cluster.

It should be noted that the distribution of densities for the stars of $14.^{m}0$-$15.^{m}25$ is somewhat irregular, and at a distance of 0°07' from the center the density of the cluster is considerably higher than, for instance, at a distance of 0°04' (Figure 10).

If we accept the angular diameter for this cluster as equal to 0°20', then the corresponding linear diameter will be 5.8 parsecs.

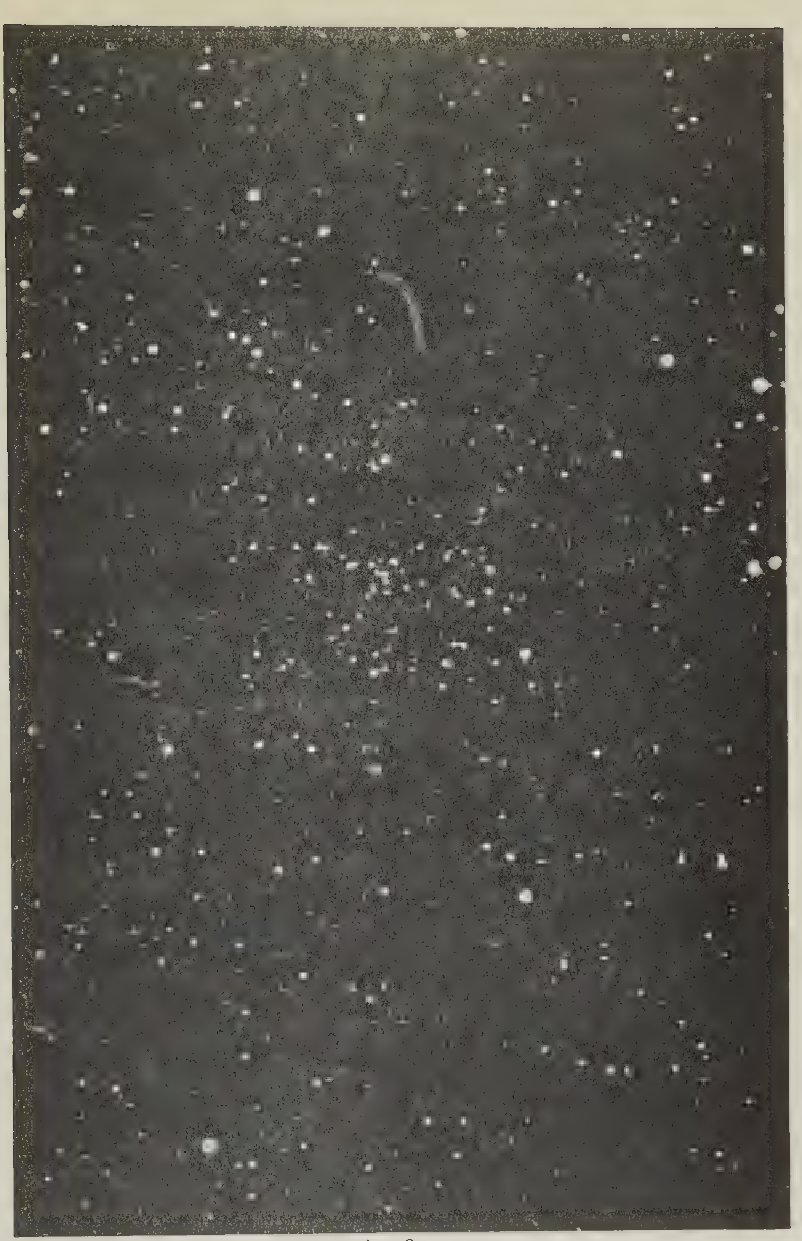

Fig. 8

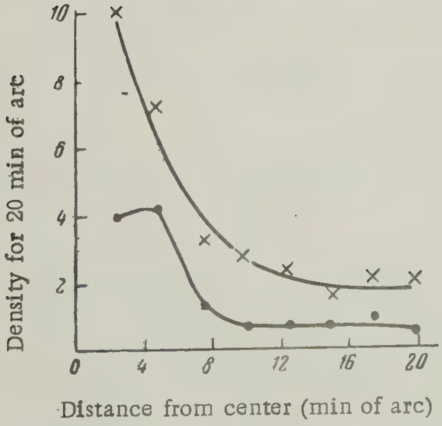

Fig. 9. ●) Stars of $m_{pg} < 12^m$; ×) stars of $12^m < m_{pg} < 14^m$.

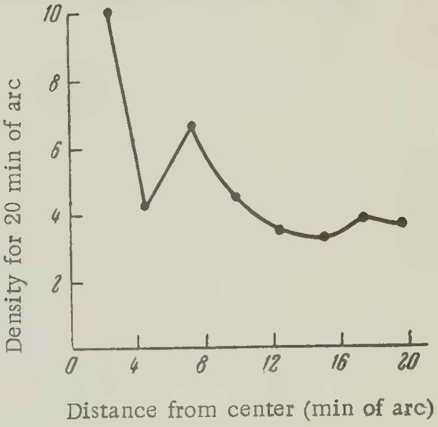

Fig. 10.

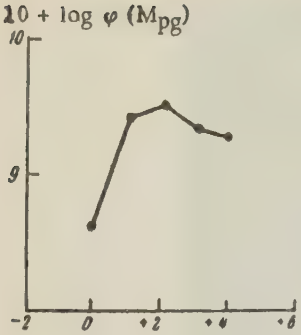

Fig. 11

The luminosity function of this cluster was determined from the diagram of color index-apparent magnitude and also from the stellar calculations which allowed us either to use or exclude some of the stars of the field. The luminosity function of the open cluster NGC 6811 rises steeply in comparison with the luminosity functions of the stars in the galactic field, and reaches its maximum at $M_{pg} = +2^m$ (Figure 11). Apparently, this cluster contains only an insignificant number of weak stars from $14.^m0$ to $15.^m0$. It has been shown by stellar calculations that the total number of stars up to $15.^m0$ in this cluster is 80.

In conclusion, the author takes this occasion to express his gratitude to his co-workers at the Engelhardt Astronomical Observatory, Sh.T. Khabibullin and Iu.A. Pupyshev, for their help in the collection of observational data.

## LITERATURE CITED

[1] W. Becker, Astron. Nachr. 275, 229 (1947).

[2] W. Becker and J. Stock, Zs. Astrophys. 34, 1 (1954).

[3] R. Trümpler, Lick. Obs. Bull. 14, 154 (1930).

[4] P. Collinder, Lund. Ann. 2 (1931).

[5] S. Raab, Lund. Medd. 2, No. 28 (1922).

Received August 25, 1956

P.K. Shternberg State Astronomical
Institute

# COLOR EXCESSES IN 102 RR LYRAE STARS

## I. F. Alaniia

The method used for determining color indexes of RR Lyrae stars at their maximum brightness is described briefly. The concept of normal colors is discussed. At present there are no reliable criteria for classifying the stars as belonging to any specific group. Therefore, the mean color index of stars with a galactic latitude greater than 60° (corrected for the differential light absorption caused by optical thickness) is accepted as the normal color. Observations indicate that 80% of these stars fall into one uniform group, according to their color characteristics. The absence of interdependence between the period and the color index is discussed. The mean absolute magnitude of 47 stars was determined as equal to $+0.^{m}2 \pm 0.^{m}2$. $M_{pg} = +0.^{m}3 \pm$ $\pm\ 0.^{m}1$ was accepted for the final value. The catalog of color excesses and other data are included. General results obtained by investigating spatial reddening of light are given. The parameters of Parenago's formula for absorption were determined in three galactic zones: 0°-30°, 30°-60°, and 60°-90°.

1. The state of our knowledge of interstellar light absorption and the importance to modern astronomy of investigating this problem in various directions and for different galactic depths is described in detail in the monograph of E.K. Kharadze [1]. The study of light absorption from the data of color excesses is based on the mass determinations of color indexes and the spectrum characteristic of the stars. It is difficult, however, to obtain the spectra for a great number of weak stars. At the present level of development of observational apparatus we are able to classify the stars to the 14th stellar magnitude. Moreover, our classification,even to this limit, is basically accomplished only in the selected Kapteyn areas. This condition, as well as the necessity for investigating the space reddening of light in the greatest possible number of directions, forces us to observe not only the common stars, but also those bodies which do not call for special spectrum classification. To the latter belong the variable RR Lyrae stars. The advantage of making use of these stars is also based on their great number and their high galactic latitudes, for which we have a small amount of data pertaining to the distribution of light-absorbing matter. Determination of color indexes for RR Lyrae stars is also independently valuable because it may lead to the determination of the physical nature of these stars.

2. In 1951 we initiated photographic observations of these stars with the help of the 360-444 mm Schmidt camera at the Abastuman Observatory. Our apparatus was described in the works [2, 3].

Investigation of RR Lyrae stars in order to learn about the selective light absorption in the galaxy presents a number of difficulties; the main one stems from the fact that the color of these stars changes with the alteration of their brightness. For this reason, the determination of light should always be made at a definite phase of brightness. In dealing with the long-period Cepheids, investigators, assuming that the light curves of these stars do not alter greatly for fairly long periods of time, often reduce their observations to one phase determined from the curves of Kukarkin and Parenago [3], or photograph them directly at the appropriate phases [4]. But this method of fixing definite phases cannot be used on the RR Lyrae stars. It is generally known that a great majority of such variable stars exhibit the results of the "Blazhko effect." In many cases the change of the brightness curve is accompanied by the alteration of the period and the amplitude, so that resorting to the standard curves becomes worthless.

Study of the existing data indicates that the spectrum characteristics of RR Lyrae stars are generally A0 to

A3, especially under the condition of maximum brightness; for this reason we decided to determine their color indexes at these phases.

Since our problem called for the study of selective light absorption in various directions, we should have investigated the greatest possible number of stars of a given type. But the process of observing every variable star in our catalog throughout the entire period of change of brightness would produce an extremely large accumulation of observational data. For this reason we were first faced with the question of what accuracy of the known elements would allow us to establish the moments of maxima in a preliminary manner.

To this end, we selected from our catalog 80 stars which had been more or less thoroughly studied, and for these we constructed the "O–C" diagrams; the analysis of these diagrams convinced us that the elements given in our OKPZ* catalog can be satisfied by a very small number of stars. Under these conditions we could not be satisfied with photographs of variable stars at the moments near the completed maxima, and we were forced to photograph each star in several phases and at such periods which would include the maximum moments throughout the night.

In determining the stellar color indexes, we made use of the method developed at the Abastuman Observatory by M.A. Vashakidze and E.K. Kharadze [5], which consists of the following: two images of a star in blue and in yellow light are obtained on a single panchromatic plate by means of appropriate movement of the plate holder. The advantages of this method consist of obtaining the negatives with two images produced under identical conditions, the short time needed for the developing of the negatives, the economical utilization of photographic material, etc.

The basic disadvantage of the method lies in the fact that the two images of the investigated star are not obtained simultaneously, but consecutively.

The photographs were taken slightly out of focus through the filters BG 3 and GG 11. All of the negatives were made on the highly sensitive films with emulsion "Izokhrom," produced by NIFKI, these films having been made to order to suit the conditions of our problems. The variable stars were photographed during completely cloudless nights and under favorable atmospheric conditions. Moments of maxima were previously computed and each star was photographed at 5 to 7 phases in such a way that the computed maximum moment would be included in a given group of exposures.

The intervals between the phases were set at 10 minutes to one hour, depending on the length of the period. Length of exposure for each star was selected in such a way that the straight segment of its characteristic curve could be utilized in determining stellar magnitudes at the maximum of brightness. Polar stars, which were to be used as standard stars, were photographed without being hidirated in the intervals between the phases, under identical conditions, and with an identical exposure. Because of the exact alignment of the telescope with respect to the azimuth and the latitude, and because of the excellent functioning of the time-measuring mechanism, star images of the polar and other regions of the sky are quite similar in appearance. Films were developed for ten minutes at a temperature of +18°C in the Chibisov developer.

Over 1200 negatives were obtained. Exact photometric determinations of the material were preceded by visual inspection of the brightness in order to select negatives with images at maximum phases. The subsequent photometric work was performed with a microphotometer MF-2. Because RR Lyrae stars are classified at their maxima as type A stars, in constructing the reduction curves we limited ourselves to the use of polar stars with color indexes not in excess of $0.^{m}5$.

Color indexes of the investigated stars were reduced to the zenithal distance of the pole according to the formula $\Delta m = 0.30 - 0.20F(Z)$, in which the transparency coefficient of the earth's atmosphere was taken as 0.74 and 0.89 for the photographic and photovisual rays, respectively.

Values of $F(Z)$ were obtained from the Bemporad Table for Z. Mean quadratic error for a single determination of color index was equal to $\pm 0.^{m}05$. In order to establish a reduction formula for converting our system to the international system of color coefficients, we made use of our numerous photographs of the northern polar region. Twelve of the spectrum type A stars are contained on the negatives of the pole within the area free of distortion; these stars have their photographic and photovisual magnitudes listed very exactly in the catalog of Seares and his co-workers [6]. The reducing formula has the form:

---

*Transliteration of Russian – Publisher's note.

$$C_{\text{int}} = 0.029 - 0.006\,m + 0.909\,C_{\text{knb}}.$$

Finally, we determined also the wavelengths of our system with the help of the spectra of the nearby AO-class stars. These spectra were obtained with the same camera and under the same conditions. An objective lens with a refraction angle of 5.5° placed in front of the correcting plate of the telescope was used as a dispersing system. The combined coefficient for the transparency of the earth's atmosphere, the optical elements of the instrument, the light filter and the light sensitivity of the emulsion were computed by the formula:

$$\lambda_{\text{eff}} = \frac{\int_{\lambda_1}^{\lambda_2} B(\lambda)\, F(\lambda)\, d(\lambda)}{\int_{\lambda_1}^{\lambda_2} \frac{1}{\lambda} B(\lambda)\, F(\lambda)\, d\lambda},$$

where B(λ) represents the energy distribution through the stellar spectrum; F(λ) is the combined coefficient of transparency of the earth's atmosphere, the optical part of the instrument, the light filter and the spectrum sensitivity of the emulsion, and is taken as $\lambda_{\text{eff}}^{\text{pg}} = 406$ mμ; $\lambda_{\text{eff}}^{\text{pv}} = 560$ mμ.

In our case $\lambda_{\text{eff}}^{\text{pv}}$ could not be determined exactly because of the smallness of dispersal in the photovisual part of the spectrum.

3. Table 1 contains a list of color indexes for 102 RR Lyrae stars, all of which were determined by the above method.

The second and third columns show the galactic coordinates computed from Olson's table.

The fourth column contains mean photographic magnitudes obtained from OKPZ. Whenever photographic magnitudes were missing in the above catalog, visual magnitudes were utilized by having the values of our color indexes added to them. The following two columns contain the periods (P) and the spectrum types obtained from the OKPZ. Asterisks indicate that the spectra were obtained from the work of P.P. Parenago [7]. The seventh column shows color indexes. The remaining columns are explained below.

4. Investigation of the cosmic light absorption by the method of color excesses calls for knowledge of the actual colors of the investigated stars. In determining normal colors of RR Lyrae stars it is important to clarify whether these stars form a uniform group or whether they represent a mixture of bodies of various origins. Several works published in the last ten years contain indications that these bodies are nonuniform. Thus, for instance, in 1946, Münch and Terrazas [8] studied qualitatively the spectra of eleven RR Lyrae stars. The study determined that their temperature variations corresponded to the spectrum types as determined by their metal lines and K lines of the ionized calcium. The intensity of Balmer series produced more advanced spectra. Spectra of SW And and AR Per do not show this anomaly. In 1953 there appeared the work of Iwanowska [9], dealing with the study of the spectra of 18 RR Lyrae stars. By comparing mean spectra classes with the periods, the author obtained one group of stars composed of BC Eri, AR Per, TZ Aur, RY Com, BB Pup, which she called a flat subsystem. We should note that RY Com has the galactic latitude of +80°, and that its color index does not differ from the indexes of other Cepheids of this constellation. B.V. Kukarkin [10] investigated space distribution and other features of the RR Lyrae stars. According to him, stars with periods between 0.425 and 0.435 days, contrary to the majority of stars of this type, form a somewhat flat system and are of a different origin. According to the length of their period, to this group belong SW And and AR Per. Aside from these stars, our catalog contains four more variables with periods within the same limits, but of latitudes not exceeding 40°; the latter fact is responsible for the reddening of their color indexes, which does not allow us to compare their color peculiarities with those of the stars at high galactic latitudes. The same can be said in respect to those stars in our catalog which, according to E.D. Pavlovskaia [11] belong to different groups. In his recent work, P.P. Parenago [7] refers RR Lyrae stars with Z-coordinates smaller than 300 parsecs and characterized by small velocity to the flat part of the galaxy. According to Parenago, stars RY Com belong to a spherical subsystem, which fact agrees with our findings. Thus, the above works indicate that the subsystems of RR Lyrae stars are nonuniform. This complicates the matter of normal colors because even those of the stars which are near to one another are subject to the reddening effect. It is possible, however, to state, on the basis of these works, that the stars in the flat part are rela-

TABLE 1

| Names of stars | $l$ | $b$ | $m$ | $P$ | Sp | Color Index | Color excess | $A_{pg}$ | $r$ | $Z$ |
|---|---|---|---|---|---|---|---|---|---|---|
| 1 | 2 | 3 | 4 | 5 | 6 | 7 | 8 | 9 | 10 | 11 |
| SW And | 84. | −32.9 | 9.8 | 0.44 | A3—F8 | −0.06 | 0.29 | 1.45 | 400 | 220 |
| AT And | 78.0 | −18.1 | 11.2 | 0.62 |  | +0.03 | 0.38 | 1.90 | 690 | 220 |
| SW Aqr | 19. | −32.7 | 11.5 | 0.46 | A3 | +0.12 | 0.47 | 2.35 | 600 | 320 |
| SX Aqr | 26. | −35.2 | 11.5 | 0.54 | A2 | −0.32 | 0.03 | 0.15 | 1660 | 960 |
| TZ Aqr | 21.8 | −45.6 | 12.0 | 0.57 |  | −0.16 | 0.09 | 0.95 | 1440 | 1030 |
| YZ Aqr | 17.4 | −51.0 | 11.7 | 0.55 |  | −0.25 | 0.10 | 0.50 | 1510 | 1170 |
| BR Aqr | 45.8 | −66.0 | 11.6 | 0.48 |  | +0.29 | 0.64 | 3.20 | 420 | 380 |
| CP Aqr | 17.2 | −32.6 | 12.7 | 0.46 |  | +0.34 | 0.69 | 3.45 | 600 | 320 |
| CY Aqr | 38.2 | −47.9 | 11.0 | 0.06 | A1—A9* | −0.10 | 0.25 | 1.25 | 760 | 560 |
| AA Aql | 11.0 | −26.4 | 11.4 | 0.36 |  | −0.18 | 0.17 | 0.85 | 1100 | 490 |
| V341 Aql | 13.7 | −23.5 | 10.9 | 0.58 |  | +0.11 | 0.46 | 2.30 | 460 | 180 |
| RV Ari | 118.4 | −39.5 | 12.2 | 0.09 |  | +0.41 | 0.76 | 3.80 | 420 | 270 |
| TZ Aur | 144.2 | +22.2 | 11.2 | 0.39 | A2—F3* | −0.21 | 0.14 | 0.70 | 1100 | 410 |
| RS Boo | 16.8 | +66.0 | 10.6 | 0.38 | A3—F4* | −0.21 | 0.14 | 0.70 | 830 | 760 |
| ST Boo | 23.9 | +54.0 | 11.0 | 0.62 |  | −0.04 | 0.31 | 1.55 | 690 | 560 |
| TV Boo | 44.4 | +66.1 | 10.7 | 0.31 | B9 | −0.52 | −0.17 | 0.00 | 1190 | 1050 |
| TW Boo | 36.7 | +61.9 | 10.8 | 0.53 |  | −0.36 | −0.01 | 0.00 | 1200 | 1060 |
| UU Boo | 22.8 | +56.8 | 12.0 | 0.46 |  | −0.33 | 0.02 | 0.10 | 2090 | 1750 |
| RZ Cam | 115.3 | +24.1 | 12.6 | 0.48 |  | −0.09 | 0.26 | 1.30 | 1590 | 650 |
| TY Cam | 117.2 | +16.4 | 13.2 | 0.67 |  | +0.01 | 0.36 | 1.80 | 1660 | 470 |
| SS Cnc | 166.6 | +27.7 | 12.0 | 0.37 |  | −0.32 | 0.03 | 0.15 | 2090 | 970 |
| TT Cnc | 180.0 | +29.9 | 11.2 | 0.56 | A2—F0* | −0.15 | 0.20 | 1.00 | 1100 | 550 |
| W CVn | 36.3 | +70.0 | 10.4 | 0.55 |  | −0.22 | 0.13 | 0.65 | 790 | 740 |
| RR CVn | 114.2 | +82.0 | 12.0 | 0.56 |  | −0.60 | −0.25 | 0.00 | 2080 | 2060 |
| RU CVn | 18.8 | +73.2 | 11.8 | 0.57 |  | −0.32 | 0.03 | 0.15 | 1820 | 1740 |
| RZ CVn | 25.4 | +76.0 | 11.4 | 0.57 |  | −0.26 | 0.09 | 0.45 | 1820 | 1740 |
| SS CVn | 47.2 | +71.9 | 11.8 | 0.48 |  | −0.22 | 0.13 | 0.65 | 1440 | 1370 |
| HU Cas | 93.4 | −5.3 | 12.6 | 0.41 |  | +0.33 | 0.68 | 3.40 | 600 | 60 |
| RZ Cep | 77.0 | +5.5 | 9.9 | 0.31 | A0—A3* | +0.30 | 0.65 | 3.25 | 190 | 18 |
| AQ Cep | 94.0 | +29.0 | 12.3 | 0.65 |  | +0.03 | 0.38 | 1.90 | 1050 | 510 |
| RR Cet | 113.3 | −59.0 | 9.7 | 0.55 | A5—F0* | −0.24 | 0.11 | 0.55 | 600 | 510 |
| RX Cet | 76.4 | −77.7 | 11.4 | 0.57 | A5—F0* | −0.24 | 0.11 | 0.55 | 1320 | 1290 |
| RZ Cet | 146.9 | −58.8 | 11.7 | 0.51 | A3—A7* | −0.05 | 0.30 | 1.50 | 960 | 820 |
| S Com | 187.5 | +87.2 | 11.3 | 0.59 |  | −0.31 | 0.04 | 0.20 | 1440 | 1440 |
| RY Com | 318.3 | +83.8 | 11.9 | 0.47 | A3—F2* | −0.31 | 0.04 | 0.20 | 1900 | 1890 |
| ST Com | 320.1 | +80.0 | 11.4 | 0.60 |  | −0.29 | 0.06 | 0.30 | 1440 | 1420 |
| RV CrB | 16.0 | +43.3 | 11.5 | 0.33 |  | −0.13 | 0.22 | 1.10 | 1050 | 720 |
| UY Cyg | 42.5 | −10.5 | 10.9 | 0.56 |  | −0.09 | 0.26 | 1.30 | 720 | 130 |
| XX Cyg | 59.8 | +14.0 | 12.1 | 0.13 |  | −0.10 | 0.25 | 1.25 | 1260 | 300 |
| XZ Cyg | 55.5 | +16.4 | 9.7 | 0.47 |  | +0.08 | 0.43 | 2.15 | 290 | 80 |
| DM Cyg | 47.4 | −13.2 | 11.7 | 0.42 |  | +0.29 | 0.64 | 3.20 | 440 | 100 |
| CK Del | 22.1 | −16.0 | 12.4 | 0.42 |  | −0.12 | 0.23 | 1.15 | 1580 | 440 |
| DX Del | 26.5 | −20.1 | 9.8 | 0.47 |  | −0.01 | 0.34 | 1.70 | 365 | 125 |
| RW Dra | 53.9 | +40.0 | 11.5 | 0.44 | A5 | −0.29 | 0.06 | 0.30 | 1510 | 970 |
| SU Dra | 99.6 | +48.8 | 9.9 | 0.66 | A2—A5* | −0.20 | 0.15 | 0.75 | 600 | 450 |
| SW Dra | 93.4 | +47.8 | 10.6 | 0.57 | F4 | −0.17 | 0.18 | 0.90 | 760 | 560 |
| WY Dra | 80.2 | +25.3 | 12.5 | 0.59 |  | 0.00 | 0.35 | 1.75 | 1260 | 540 |
| XZ Dra | 62.8 | +22.1 | 10.2 | 0.48 |  | −0.30 | 0.05 | 0.25 | 830 | 310 |
| AE Dra | 51.5 | +24.8 | 11.7 | 0.60 |  | −0.09 | 0.26 | 1.30 | 1050 | 440 |
| RX Eri | 181.7 | −32.4 | 9.0 | 0.59 |  | −0.20 | 0.15 | 0.75 | 400 | 210 |
| BK Eri | 324.2 | −50.3 | 12.5 | 0.35 |  | −0.26 | 0.09 | 0.45 | 2190 | 1690 |
| RR Gem | 155.0 | +21.0 | 11.6 | 0.40 | A8 | +0.18 | 0.53 | 2.65 | 520 | 190 |
| SZ Gem | 169.6 | +23.6 | 11.2 | 0.50 |  | −0.24 | 0.11 | 0.55 | 1200 | 480 |
| TW Her | 23.2 | +23.6 | 11.4 | 0.40 |  | −0.11 | 0.24 | 1.20 | 1000 | 400 |
| VX Her | 2.6 | +37.7 | 10.2 | 0.46 | A3—F0* | +0.04 | 0.39 | 1.95 | 380 | 230 |
| VZ Her | 26.5 | +33.4 | 11.1 | 0.44 |  | −0.24 | 0.11 | 0.55 | 1150 | 630 |
| AR Her | 41.4 | +47.2 | 11.2 | 0.47 |  | +0.05 | 0.40 | 2.00 | 600 | 440 |
| BD Her | 15.2 | +6.2 | 12.3 | 0.47 |  | +0.03 | 0.38 | 1.90 | 1050 | 110 |
| DY Her | 355.5 | +34.9 | 10.6 | 0.15 |  | +0.14 | 0.49 | 2.45 | 360 | 200 |
| EE Her | 359.0 | +41.6 | 12.3 | 0.50 |  | −0.23 | 0.12 | 0.60 | 1900 | 1260 |
| CQ Lac | 62.0 | −15.0 | 12.3 | 0.62 |  | −0.22 | 0.13 | 0.65 | 1820 | 470 |
| DE Lac | 60.9 | −12.8 | 10.9 | 0.25 |  | +0.36 | 0.71 | 3.55 | 260 | 60 |
| RR Leo | 176.4 | +54.5 | 11.0 | 0.45 | A0—F4* | −0.21 | 0.14 | 0.70 | 1000 | 810 |

TABLE 1 (continued)

| Names of stars | $l$ | $b$ | $m$ | $P$ | Sp | Color index | Color excess | $A_{pg}$ | $r$ | $z$ |
|---|---|---|---|---|---|---|---|---|---|---|
| 1 | 2 | 3 | 4 | 5 | 6 | 7 | 8 | 9 | 10 | 11 |
| SS Leo | 235.2 | +57.6 | 10.3 | 0.63 | | −0.28 | 0.07 | 0.35 | 870 | 740 |
| ST Leo | 223.9 | +67.0 | 11.0 | 0.48 | | −0.33 | 0.02 | 0.10 | 1320 | 1220 |
| SU Leo | 197·3 | +45.1 | 13.2 | 0.47 | | −0.08 | 0.27 | 1.35 | 2090 | 1480 |
| SZ Leo | 213.0 | +57.9 | 11.9 | 0.53 | | −0.09 | 0.26 | 1.30 | 1150 | 970 |
| TV Leo | 232.1 | +49.7 | 12.6 | 0.40 | A0—A6* | +0.04 | 0.39 | 1.95 | 1150 | 880 |
| AA Leo | 225.1 | +66.9 | 11.9 | 0.60 | | −0.25 | 0.10 | 0.50 | 1660 | 1530 |
| V LMi | 169.0 | +59.3 | 11.4 | 0.54 | A8 | −0.43 | −0.08 | 0.00 | 1585 | 1360 |
| TV Lib | 321.4 | +38.3 | 11·6 | 0.27 | | −0.18 | 0.17 | 0.85 | 1200 | 740 |
| EH Lib | 324.1 | +47.0 | 9.8 | 0.09 | A5—F0* | −0.13 | 0.22 | 1.10 | 480 | 350 |
| Y Lyr | 39.9 | +19.3 | 12.9 | 0.50 | | +0.01 | 0.36 | 1.80 | 1440 | 480 |
| RZ Lyr | 29.5 | +14.7 | 11.9 | 0.51 | A2 | +0.32 | 0.67 | 3.35 | 460 | 120 |
| EZ Lyr | 33.0 | +15.1 | 11.4 | 0.53 | | +0.46 | 0.81 | 4.05 | 250 | 70 |
| ST Oph | 350.1 | +15.1 | 11.4 | 0.45 | | +0.08 | 0.43 | 2.15 | 630 | 160 |
| VV Peg | 46.8 | −31.2 | 11.5 | 0.49 | | −0.03 | 0.32 | 1.60 | 830 | 430 |
| AO Peg | 38.0 | −23.5 | 13.0 | 0.52 | | −0.15 | 0.20 | 1.00 | 2190 | 870 |
| AV Peg | 45.6 | −24.8 | 10.7 | 0.39 | | −0.27 | 0.08 | 0.40 | 1000 | 420 |
| BF Peg | 58.0 | −31.0 | 12.4 | 0.50 | | −0.03 | 0.32 | 1.60 | 1260 | 650 |
| BH Peg | 54.0 | −39.0 | 10.6 | 0.64 | | +0.04 | 0.39 | 1.95 | 460 | 290 |
| DH Peg | 37.7 | −40.1 | 9.6 | 0.26 | | −0.04 | 0.31 | 1.55 | 360 | 230 |
| DY Peg | 59.6 | −40.1 | 11.0 | 0.07 | A3—A9* | +0.06 | 0.41 | 2.05 | 520 | 340 |
| DZ Peg | 69.9 | −41.9 | 11.8 | 0.61 | | −0.36 | −0.01 | 0.00 | 1900 | 1260 |
| AR Per | 122.7 | −1.2 | 10.7 | 0.43 | A3—F6* | +0.16 | 0.51 | 2.55 | 380 | 10 |
| SS Psc | 101.0 | −40.0 | 11.5 | 0.29 | F0 | −0.18 | 0.17 | 0.85 | 1150 | 740 |
| VY Ser | 334.2 | +42.6 | 10.1 | 0.71 | A7 | +0.06 | 0.41 | 2.05 | 350 | 240 |
| AN Ser | 351.4 | +43.7 | 11.1 | 0.52 | | −0.17 | 0.18 | 0.90 | 960 | 660 |
| AP Ser | 340.7 | +50.9 | 11.1 | 0.25 | | −0.35 | 0.00 | 0.00 | 1380 | 1070 |
| AT Ser | 343.8 | +40.9 | 11.1 | 0.75 | | −0.13 | 0.22 | 1.10 | 870 | 570 |
| T Sex | 204.1 | +41.7 | 10.1 | 0.32 | A2 | −0.16 | 0.19 | 0.95 | 580 | 390 |
| SS Tau | 148.1 | −37.2 | 11.9 | 0.37 | | −0.05 | 0.30 | 1.50 | 1050 | 630 |
| U Tri | 106.4 | −26.5 | 12.1 | 0.45 | | −0.35 | 0.00 | 0.00 | 2190 | 980 |
| RV UMa | 74.7 | +62.0 | 10.7 | 0.47 | F0 | −0.21 | 0.14 | 0.70 | 870 | 770 |
| SX UMa | 78.3 | +60.2 | 11.2 | 0.31 | | −0.19 | 0.16 | 0.80 | 1050 | 910 |
| TU UMa | 166.4 | +73.2 | 10.0 | 0.56 | A8 | −0.28 | 0.07 | 0.35 | 725 | 695 |
| ST Vir | 315.1 | +52.4 | 11.4 | 0.41 | | −0.48 | −0.13 | 0.00 | 1580 | 1250 |
| UU Vir | 251.6 | +60.8 | 10.2 | 0.48 | | −0.58 | 0.23 | 0.00 | 910 | 790 |
| UV Vir | 256.9 | +62.3 | 11.4 | 0.59 | | −0.32 | 0.03 | 0.15 | 1580 | 1400 |
| AT Vir | 274.6 | +57.0 | 11.0 | 0.53 | A2—A7* | −0.22 | 0.13 | 0.65 | 1050 | 880 |
| BB Vir | 310.1 | +63.3 | 11.0 | 0.47 | | −0.27 | 0.08 | 0.40 | 1150 | 1030 |
| BN Vul | 26.3 | +2.2 | 11.6 | 0.59 | B9 | +0.25 | 0.60 | 3.00 | 460 | 20 |

tively scarce (approximately 20%). Moreover, no valid criteria have been established so far for determining whether a star belongs to any specific group. Under these conditions, in determining normal light, we are forced to make use of stars lying at high galactic latitudes, without making any corrections. This is what we did. Cepheids lying at the latitude above 60° were selected from our catalog. They proved to be twenty-one in number. The mean value of the color index for seventeen of these stars was equal to $-0.^{m}27$ and showed the dispersal of ± 0.05. This dispersal is caused basically by two factors: by some actual dispersal of the color index and by observational errors. We have previously stated that spectrum types of these stars at their maximum lie between the limits A0 to A3, and that, consequently, similar variations should appear in their colors. By the observational errors we mean the discrepancies between the moments at which photographs were taken and the moments of maximum brightness. We have noted, while describing the method of observations, that a variable star was observed through the night at those periods which included the moments of maximum brightness. The negatives which served to determine color indexes for some stars may not correspond to the maxima of light curves, which fact would cause color indexes to be increased in various degrees. It can be seen from the color indexes, however, that the influence of this effect may be insignificant, because time intervals between consecutive photographs varied in relation to the lengths of the periods. The dispersal value of 0.05 cannot be considered as large. Greater dispersal of normal colors can be seen among the permanent stars of the same spectrum subclass. Table 2 includes, as an example, the values of dispersal for the stars B and A, taken from the works of E.K. Kharadze [1] and B.V. Nikonov [12].

If we take into consideration the causes for the variation in normal colors, we will realize that dispersal

TABLE 2

| Sp | Kharadze [1] | Nikonov [12] |
|---|---|---|
| B5 | – | 0.04 |
| B8 | 0.07 | 0.07 |
| B9 | – | 0.12 |
| A0 | 0.06 | 0.08 |
| A3 | 0.07 | – |
| A8 | 0.09 | – |

of 0.05 indicates that the 17 stars of our group are fairly uniform. As to the remaining four stars, TV Boo, UU Vir, RR CVn, and BR Aqr, we noted that they were different due to their anomalous colors, and for this reason they were not taken into consideration in arriving at our mean color index. The first three are characterized by extremely intense radiation of photographic light. On the other hand, BR Aqr appears to be too red for the latitude of 66°. It agrees very well with the data given in OKPZ, and for this reason the determination of its color was carried out for the exact maximum. We believe that in this case the reason for the reddening lies in the star itself. Most likely this star does not belong to the RR Lyrae group.

In this way, according to our data, the group of RR Lyrae comprising the spherical component of the galaxy represents a mixture of bodies in different physical conditions, but within this group at least 80% of the stars form a uniform group according to their color characteristics.

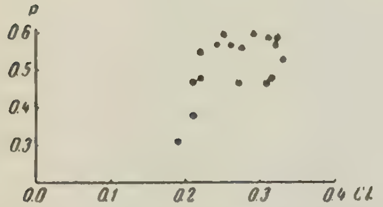

Fig. 1. Period-color index relationship.

Color indexes for the 17 stars are plotted on Figure 1 against the length of the periods. The relationships between these quantities are not apparent here. We should note that the spectrum class of RR Lyrae in our galaxy is not dependent on the period. On the other hand, it can be seen from the observations that the short-period Cepheids in the spherical clusters occupy definite places on the period-color index diagram [13], and are grouped according to their types as a, b, and c. In our case, however, the c-type are completely absent. Furthermore, the periods of the variables chosen by us lie mainly within the limits 0.46 to 0.60 days. According to the cited work, such stars of the spherical clusters show a weak correlation between their periods and their color indexes. In order to solve the problem completely it will be necessary to include the color determinations for the stars with periods lying beyond these limits.

Stars used by us in determining the normal color lie at great distances from the galactic plane, so that in dealing with them we must take into consideration the thickness of the selectively absorbing matter. A correction of $0.^{m}08$ was added to the determined color index; this correction corresponds to the full absorption of $0.^{m}4$ taken in the direction towards the galactic pole. Consequently, we obtain $0.^{m}35$ for the final value of the normal color of RR Lyrae. With the normal color known, it is easy to calculate color excesses for the investigated stars. These are shown in the eighth column of Table 1.

5. Our problem consisted not only of determining the selective color absorption in a given direction, but also of determining the corresponding depths of space for which we must know the mean absolute magnitudes of RR Lyrae stars. Up to this time there exist only two or three determinations of the magnitude obtained by Soviet astronomers. First of all, we must note the work of E.D. Pavlovskaia [11], based on the specific movements of 69 stars. For the mean absolute photographic magnitude Pavlovskaia obtained the value of $\overline{M}_{pg} = +0.^{m}5 \pm 0.^{m}2$

P.P. Parenago [14] obtained the value of $\overline{M}_{pg} = +0.^{m}53 \pm 0.^{m}4$, on the basis of dynamic considerations. According to his calculations, trigonometric parallaxes produce a smaller absolute magnitude of $+1^{m}.7 \pm 1.^{m}5$.

The mean absolute stellar magnitude obtained on the basis of specific movements is greatly influenced by the method used in estimating the effects of color absorption. E.D. Pavlovskaia [11] made use of Parenago's formula which gives very satisfactory results in statistical investigations. However, due to the tufted structure of the absorbing matter, total absorption in a given direction, as computed by Parenago's method, may be substantially different from the actual values. Taking this under consideration and making use of color excesses for 47 RR Lyrae stars investigated by Pavlovskaia, we undertook to calculate a new absolute magnitude.

In view of the fact that our determination of $\lambda_{eff}^{py}$ was not reliable, we decided not to use the transitional factor ($\gamma$) obtained from the computed effective wavelengths, and we took instead the value 5, which is usually employed for the international color system. The full absorptions obtained in this way are presented in Column 9 of Table 1.

All the necessary data for determining mean parallaxes were taken from the works of E.D. Pavlovskaia [11]. Our calculations yielded: $\pi_v = 0.00064 \pm 8$ : $\pi_T = 0.00083 \pm 13$. Consequently, $\pi = 0.00070 \pm 7$.

The corresponding mean absolute magnitude is usually calculated from Stromberg's formula [15]:

$$M = m + 5 + 5 \log \bar{\pi} - 5 \log C,$$

where $C^2 = \frac{\overline{\pi^2}}{\bar{\pi}^2}$.

When a group of stars is located at the same distance from us, then C = 1. In our case, $C^2 < 1$, and is equal to 0.93.

At the first glance this value may appear strange. However, a more thorough investigation of the problem convinced us that such a value could have been expected. Indeed, if $\overline{\pi^2}$ and $\bar{\pi}^2$ are computed directly from the known values of $\pi$ for various stars or from the very exact formulas interrelating $\pi$ with some known characteristics, then $C^2 \geq 1$, and the equality is obtained when the stars are located at the same distances. But when the known values of $\pi$ for individual stars are not available and when $\overline{\pi^2}$ and $\bar{\pi}^2$ are computed from some statistical formulas involving the components of specific motions, the radial velocities of stars and the mean parallax, the possible values of C are somewhat spread out in such a way that the expression $C^2 < 1$ cannot be equal to zero. For this reason, we can expect that in some cases, under the known conditions, our calculations will produce the value of C smaller than one. This will happen most frequently when the differences in the distances through the investigated stellar group are small and the actual value of C is very near to one. This condition is closely approached for the stars of our list. In view of all this we can accept the expression $C^2 = 1$ and the mean absolute magnitude for this stellar cluster will be found equal to $M = +0.^m2 \pm 0.^m2$. At the present time we can accept the value $\overline{M} = +0.^m3 \pm 0.^m1$ as the most reliable for the mean absolute magnitude of RR Lyrae stars; this value represents a weighted mean for our determinations and for those of P.P. Parenago. Calculated distances r for this value of the absolute magnitude are presented in the tenth column of Table 1. The eleventh column contains the coordinates of $z = r \sin b$.

6. It was previously stated that the basic aim of this investigation consisted of determining the differential light absorption in various directions of the galaxy. After some fairly laborious work we succeeded in compiling a list of color indexes for 102 RR Lyrae stars at the maximum of their brightness. Obviously, we cannot describe all the individual stars in our catalogs from the point of view of the space reddening of their light. Such a report will be published by the Abastuman Observatory.

We will present here only the results of more general character, which can be stated as follows:

a) According to our data, conspicuous reddening of the light at the middle and high galactic latitudes is not a rare phenomenon, which fact points to the presence of separate dispersing clouds even at great distances from the galactic plane. As examples of these we can take the stars: EH Lib, RV CrB, ST Boo, AR Her, TV Leo, DH, BH and DY Peg, RZ Cet and others.

b) Color excesses are large even in those directions which exhibit no obvious traces of darkening. As examples we can use the variables: BD Her, HU Cas, RZ Lyr, EZ Lyr, DX Del, DE Lac, AT And and others.

c) Our data does not allow us to investigate the distribution of differentially absorbing matter within small segments of the sky, because the stars investigated by us are scattered over the galactic longitudes and latitudes. Nevertheless, the Cepheids EZ and RZ Lyr, DE and CQ Lac, SW and CP Aqr, AA and V341 Aql lie fairly near to one another. To judge by their color excesses, the differential absorption in these segments is nonuniform.

d) In the zone between the longitudes 10° and 60° and the latitudes of −10° to −50° lie 20 stars of our catalog. Actually, this zone represents a southern extension of the equator of the region which, according to the investigations of V.B. Nikonov [12], exhibits a complex distribution of interstellar matter. An investigation of color excesses of stars in this zone indicates a varied picture of the distribution of dispersing matter. Here, apparently, lies hidden some interesting structural property of our galaxy, but the small number of stars in this zone makes it impossible for us to investigate it in detail.

e) Only six stars in our list differ greatly from others; these are ST Oph, BD Her, BN Vul, RZ Cep, HU Cas and AR Per, all of which are widely distributed along the longitudes 350° to 130°. As was expected, all of them are characterized by a strong reddening of their color. Moreover, this reddening is not uniform. Color indexes are within the limits of $0.^{m}38$ to $0.^{m}68$.

Stars Y Lyr, XX Cyg, CQ Lac, CK Del, AA Aql and others lie near to the galactic equator, but these stars are characterized by an insignificant reddening. This fact is in full agreement with our concept of the tufted structure of absorbing matter. It can also be said that among the RR Lyrae stars there exist some which radiate more strongly in the photographic part of the spectrum. Some of these stars may also be encountered at the lower galactic latitudes. A small visible reddening of these stars does not actually indicate a diminution of the dispersing matter. It may be that these stars belong to the "anomalous" cepheids. In view of what has been said they deserve a special investigation.

f) Mean color index for all the stars of our catalog at 100 parsecs is $0.^{m}05$. Our data is not sufficient for investigating the asymmetry in the distribution of absorbing matter, because in the southern galactic hemisphere we observed only the stars centered around the direction $l = 35°$, $b = -30°$.

7. P.P. Parenago [16] proposed the following formula for the investigation of general absorption:

$$A = (r, b) = \frac{a\beta}{\sin b}\left(1 - e^{-r \sin b/\beta}\right); \qquad (1)$$

this formula is widely used in the statistical investigations in the Soviet Union. Foreign astronomers have lately started using Parenago's theory. As an example we may cite the works of Zonn [17], Stibbs [18], and others.

Parameters for many directions, obtained from our data, are of interest. E.K. Kharadze [1] learned from his own catalog that the mean value of a is equal to $3.^{m}26$, and the mean value of β is 100 parsecs. In our case, with the absorption curves not available, the determination of a and β by Parenago's method (which was used by Kharadze) was impossible. We may attempt, however, to determine mean values for the absorption parameters of various galactic zones. The well-known method of factoring, with the members limited to those of the first order, produces

$$\frac{\beta_0}{\sin b}\left(1 - e^{-z/\beta_0}\right)(a - a_0) + \frac{a_0}{\sin b}\left(1 - e^{-z/\beta_0} + \frac{z}{\beta_0}e^{-z/\beta_0}\right)(\beta - \beta_0) + $$
$$+ \frac{a_0\beta_0}{\sin b}\left(1 - e^{-z/\beta_0}\right) - A(r, b) = 0. \qquad (2)$$

We will introduce the following designations:

$$a - a_0 = X; \quad \beta - \beta_0 = Y; \quad \frac{3_0}{\sin b}\left(1 - e^{-z/\beta_0}\right) = m;$$
$$\frac{a_0}{\sin b}\left(1 - e^{-z/\beta_0} + \frac{z}{\beta_0}e^{-z/\beta_0}\right) = n; \quad \frac{a_0\beta_0}{\sin b}\left(1 - e^{-z/\beta_0}\right) - A(r, b) = l.$$

Substituting these designations into Equation (2) transforms it into the form

$$mX + nY + l = 0. \qquad (3)$$

Systems of such equations were established for the galactic zones of 0° to 30°; 30° to 60° and 60° to 90°.

Solution of 34 equations by means of least square and with appropriate approximation, gave for the first zone

$a = 3\overset{m}{.}4 \pm 0\overset{m}{.}7$ per 1000 parsecs; $\beta = 141 \pm 28$ parsecs.

The value of a agrees well with those determined by Parenago, Kharadze, Zonn and others.

Coefficients m and n, established for the stars of the two other zones, were found to be approximately proportional, due to the insignificant influence of the exponential members. We know that in this case the separation of the unknowns is impossible. For this reason, we were unable to obtain values of the parameters for the zones 30° to 60° and 60° to 90° by this method. One of these parameters, however, can be determined, if we assume the other one to be known. We undertook to determine $\beta$, because some of the recent works allow us to conclude that the value $\underline{a}$ was determined quite reliably. Assuming that in Expression (2) $a = a_0 = 3^{m}.5$, we obtained: for the zone 30° to 60°, $\beta = 112$ parsecs, and for the zone 60° to 90°, $\beta = 92$ parsecs.

In this way, the value of $\beta$ remains constant (100 parsecs) for the entire galaxy (within limits of error about 20%).

In conclusion, I consider it my duty to express my gratitude to the Academicians of the Academy of Sciences GruzSSR, E.K. Kharadze, for suggesting this subject to me. I am also deeply indebted to Corresponding Member of the Academy of Sciences USSR, P.P. Parenago and to Professor B.V. Kukarkin for their valuable suggestions.

## LITERATURE CITED

[1] E.K. Kharadze, Biull. Abast. Obs. 12, 6 (1952).

[2] Sh.G. Gordeladze and E.K. Kharadze, Biull. Abast. Obs. 3, 133 (1938).

[3] M.A. Vashakidze, Biull. Abast. Obs. 13, 3 (1953).

[4] G.S. Badalian, Soobshch. Biur. Obs. 1948, No. 3 and others.

[5] M.A. Vashakidze and E.K. Kharadze, Soobshch. Gruz. Fil. AN SSSR 1, 673 (1940).

[6] F.H. Seares, F.E. Ross and M.C. Joyner, Publ. Carnegie Inst. N 532 (1941).

[7] P.P. Parenago, Peremennye Zvezdy 10, 193 (1955).

[8] G. Münch and L.R. Terrazas, Astrophys. J. 103, 371 (1946).

[9] W. Iwanowska, Torun. Bull. 11, 1 (1953).

[10] B.V. Kukarkin, Investigation of Structure and Development of Star Systems by Means of Studying Variable Stars* (GITTL, Moscow-Leningrad, 1949).

[11] E.D. Pavlovskaia, Peremennye Zvezdy 9, 349 (1953).

[12] B.V. Nikonov, Biull. Abast. Obs. 14, 3 (1953).

[13] M. Robert and A. Sandage, Astron. J. 60, 6, 185 (1955).

[14] P.P. Parenago, Astron. J. USSR 31, 425 (1954).

[15] G. Stromberg, Astrophys. J. 84, 555 (1936).

[16] P.P. Parenago, Astron. J. USSR 17, 21 (1940).

[17] W. Zonn, Acta Astronomica 6, I, 34 (1956).

[18] D.W. Stibbs, Monthly Notices, Roy. Astron. Soc. 115, 3, 323 (1955).

Received November 9, 1956

Abastuman Astronomical Observatory

---

*In Russian.

# INVESTIGATION OF THE SOLAR SUPERCORONA BY THE RECEPTION OF THE RADIO EMISSION FROM JUPITER

## V. V. Vitkevich

The investigation of the solar supercorona by studying the radio waves of Jupiter passing through it are discussed.

It is shown that such investigations are possible every year.

A new method of observation is proposed, the results of which are not affected by the radioemission from sunspots. The author stresses the importance of studying the supercorona during the years of maximum, as well as of minimum solar activity, for ascertaining its dependence on the phase of the solar cycle and its physical nature.

A radio method has been recently used with success for the study of the solar corona.

These investigations have been carried out by the method of studying the radio emission from the corona itself, as well as by transmission methods [1, 2].

Observations of this type, carried out at the FIAN [3, 4] and at Cambridge (England) [5, 6], have led to the discovery of the solar supercorona extending up to a distance of 15 $R_{\odot}$ from the photosphere.* The nature of the solar supercorona was established [4, 6]. It was found that it has a nonuniform structure. When radio waves propagate through it, they are scattered. In the nonuniform regions, the electron density reaches the value $10^3$-$10^4$ electrons/cm$^3$.

In the most recent work [7] the first attempt was made to construct a model for the solar supercorona and also to evaluate how the supercorona influences the radio emission from the sun itself when it is observed at the Earth.

In addition [7], the radio-frequency radiation associated with sunspots was observed and it was pointed out that the radio waves we receive from them are scattered by the supercorona. This scattering can reach the value of 1-2' at wavelengths of 3-6 m, but because the scattering effect increases proportionally to the square of the wavelength, at the longest wavelengths of the order of 12-15 m the degree of scattering must already be comparatively high and reach the value 15-20'. Thus, the problem of studying the supercorona is associated with the problem of studying the direct radio emission from the sun.

In all of this work the discrete source Taurus-A was used as the source of radio-frequency radiation for the transmission method.

At the present time, in connection with the information that has appeared on the radio emission from Jupiter, the question arises whether it is possible to use its radiation for the same purpose.** From the data available in the literature, the following conclusions can be drawn regarding the properties of the radiation (nonthermal) from this planet.

---

*The latest observations have enabled the supercorona to be found at distances of up to 20 $R_{\odot}$ from the photosphere.

**As this paper was being prepared for publication we received a paper by Shain (Australian J. Phys. 9, 1, 61, 1956) in which attention is drawn to the possibility of using the radio-frequency radiation from Jupiter for studying the corona by the transmission method.

1. The intensity of the radiation is fairly high at long wavelengths of the order of 12-15 m and the intensity is of the same order of magnitude as the radio-frequency radiation from the source Taurus-A. At shorter wavelengths the intensity sharply decreases.

2. The radiation is not constant, but is in the form of pulses.

3. The radiation is of nonthermal nature and is apparently associated with phenomena of the thunderstorm discharge type. There are times when it manifests itself very clearly; its duration is several months. At other times it disappears.

4. The dimensions of the emitting region are very small, in any case smaller than 1'.

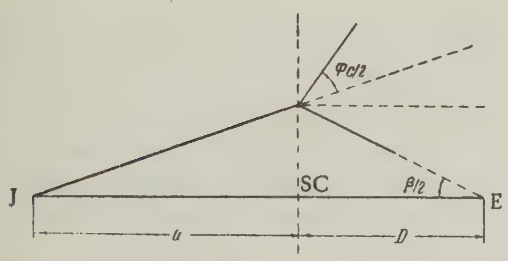

Fig. 1. The scattering of radio waves: J) Jupiter; SC) solar supercorona; E) Earth; $\Phi_c$) the scattering angle in the supercorona for an incident plane wave; $\beta$) the scattering angle when the source and receiver are placed at finite distances from the scatterer.

These properties of the radiation are very suitable for carrying out observations by the transmission method. The considerable intensity and the small angular dimensions of the source are an advantage for such measurements. It is also an advantage that the intensity is high at long wavelengths – this region of wavelength is of the greatest interest in studying the solar supercorona. The longer the wavelength, the farther away from the photosphere the solar supercorona can be seen. The fact that the radio emission consists of separate pulses does not impair the conditions for observation.

The fact is that the only effect which it is possible to observe at the moment is that of the "diffuseness" of the source. With the help of an interferometer, having base lines of various lengths, the angular dimensions of the source can be found whether it emits radiation which is constant in time or whether it emits separate pulses.

Unlike using the Crab Nebula, the distance to which is far greater than the distance between the Earth and the sun, in using Jupiter for the transmission method it is necessary to take into account the finiteness of the distance between the sun and this planet. The angle of scattering, which will be the angle subtended by the source, will not only depend on the scattering properties of the medium (in this case, the supercorona), but also on the distances d and D between the supercorona and the source and receiver (in our case, Jupiter and Earth), respectively.

If $\Phi_c$ is the scattering angle for a plane wave in the medium ($\Phi_c$ is not changed as the distance between the scatterer and the receiver varies), then in the general case the scattering angle, $\beta$, can be found from the following expression which follows from geometrical considerations:*

$$\operatorname{tg}\frac{\beta}{2}=\frac{D+d}{2D\operatorname{tg}\frac{\Phi_c}{2}}+\sqrt{\frac{(D+d)^2}{4D^2+\operatorname{tg}^2\frac{\Phi_c}{2}}+\frac{d}{D}}. \qquad (1)$$

For the case where $\Phi_c$ and $\beta$ are small, this expression can be simplified to

$$\operatorname{tg}\frac{\beta}{2}\approx\frac{d}{D+d}\operatorname{tg}\frac{\Phi_c}{2}, \qquad (2)$$

and, finally, which is even more approximate, but adequate for our purpose

$$\beta=\Phi_c\frac{d}{D+d}. \qquad (3)$$

Similar expressions are used in the problem of diffraction at individual inhomogeneities in the corona [8].

In order to plan the observations correctly it is useful to estimate beforehand the possible values of $\beta$. We give these estimates for wavelengths of 12 and 16 m, on the basis of our data for $\lambda = 6$ m ($\beta$ is expressed in minutes, $d = 5.2$ astronomical units). The results are given in Table 1.

---

*In this paper 'tg' ≡ 'tan' – Publisher.

TABLE 1

| $r$ | $\lambda = 6$ м | $\lambda = 12$ м | $\lambda = 16$ м | $\lambda = 12$ м | $\lambda = 16$ м |
|---|---|---|---|---|---|
| | $d = \infty$ | $d = \infty$ | $d = \infty$ | $d = 5.2$ | $d = 5.2$ |
| $10\ R_\odot$ | 17′ | 67′ | 120′ | 56′ | 100′ |
| $15\ R_\odot$ | 5′ | 20′ | 35′ | 17′ | 30′ |
| $20\ R_\odot$ | <3′ | <12′ | <21′ | <10′ | <18′ |

As can be seen, the scattering effect that will be observed will be somewhat smaller in the case of Jupiter than in the case of the source Taurus-A.

However, the extremely small angular dimensions of the source enable more accurate results to be obtained for the largest angular separation of the source from the sun since long interferometer base lines can be used. For example, at the wavelength of 12 m for this purpose we can use an interferometer base line having an angular resolution of 3-4', which will correspond to a distance between the antennas of the order of 12 km.

With these base lines, the danger of confusion arising from the sunspot radio emission is decreased since the latter will not produce interference effects with such narrow interference patterns. The importance of studying the supercorona in the presence of radio spots is undisputed. It is necessary to carry out observations on the supercorona during the periods of both maximum and minimum solar activity and to determine whether it is subject to an 11-year cycle.

The fact is that, at the present time, there is no reliable evidence that the supercorona is produced by the sun and is not the result of the ionization of the dust and gas clouds falling into the sun. Although there are some data which indicate that the supercorona is somewhat asymmetric: in the direction of the equator it is more prominent than in the direction of the poles, which is in favor of a solar origin of the supercorona, it is undoubtedly important to establish how it varies in the course of an 11-year cycle.

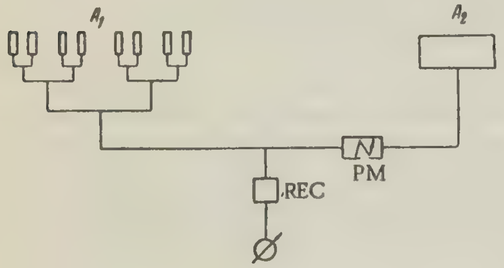

Fig. 2. An interferometer which uses as one of the antennas ($A_1$) a multi-wave interferometer.

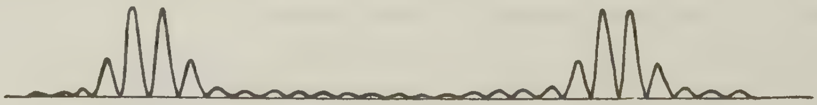

Fig. 3. Interference diagram for the system of Figure 2.

Let us note that there is another possibility for eliminating the confusing action of sunspots in observations of this type, irrespective of the source used in the transmission method. For this, we must use an interferometer with one antenna of the usual type (phase antenna or mirror having one main lobe), while the second antenna is in the form of a multi-wave interferometer, with the width of one lobe being of the order of 1° and the distance between the lobes being 5-6° (Figure 2).

This system (using, desirably, phase modulation) will enable the radiation from the sunspots and the source (Taurus-A, Jupiter) to be received separately.

We will now consider the final problem – when can such observations be carried out.

Figure 4 gives the dependence of the angular separation between the sun and Jupiter (as observed at the

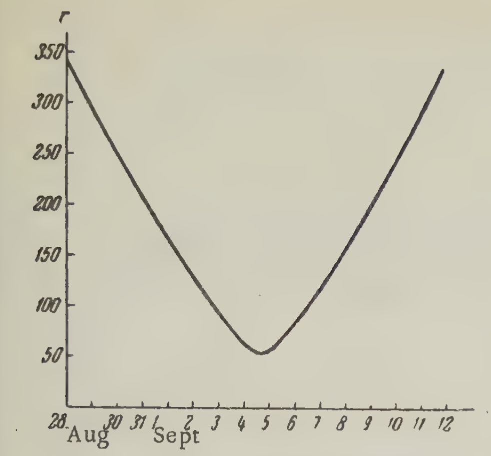

Fig. 4. The angular separation between Jupiter and the sun in minutes of arc as a function of the date (1956).

Earth) on the date of observation during 1956. As can be seen, on September 5th, 1956 the separation between them will be very small. The smallest distance, equal to 58', is smaller than that in the analogous case when the source Taurus-A is used in the transmission study of the corona.

This opportunity will occur annually, with this difference, however, that each year the date of occultation will change by approximately a month.

In Table 2, given below, these characteristic dates are given for several years. The minimum distance between Jupiter and the sun, as well as the declination of Jupiter, is given.

There is no doubt that this newly-discovered opportunity for expanding the investigations of the corona by the transmission method will be used and will lead to new results.

It is obvious that when radio emission from the other planets will be discovered, it can also be used for studying the solar corona, as well as the atmosphere of the moon, by the transmission method.

TABLE 2

| Date | Separation | Declination of Jupiter |
|---|---|---|
| September 5, 1956 | 58' | 7° |
| October 5, 1957 | 72' | −4° |
| November 5, 1958 | 56' | −15° |
| December 5, 1959 | 47' | −22° |

It must be pointed out, further, that using large mirrors at very short wavelengths, even thermal radio emission from the planets can apparently be used for this purpose. Its intensity is found to be adequate for carrying out such observations at centimeter and millimeter wavelengths.

Thus, the method indicated will probably be used in the future, for extending the investigations in this direction.

## LITERATURE CITED

[1] V.V. Vitkevich, Doklady Akad. Nauk SSSR 77, 4 (1951).

[2] V.V. Vitkevich, Astron. J. (USSR) 29, 4 (1952).

[3] V.V. Vitkevich, Astron. J. (USSR) 32, 2 (1955).

[4] V.V. Vitkevich, Doklady Akad. Nauk SSSR 101, 429 (1955).

[5] K.E. Machin and F.G. Smith, Nature 168, 599 (1951).

[6] Hewish, Proc. Roy. Soc. 228, 239 (1955).

[7] V.V. Vitkevich, Astron. J. (USSR) 33, 1 (1956).

[8] V.L. Ginsburg and V.V. Pisarev, Proceedings of the 5th Conference on Cosmogony (Izd. AN SSSR), p. 299.*

Received July 16, 1956

P.N. Lebedev Physics Institute
Academy of Sciences, USSR

---

*In Russian.

# ON THE ACCELERATION OF CHARGED PARTICLES IN THE ELECTROMAGNETIC FIELD OF SUNSPOTS

**P. E. Kolpakov**

Numerous observational data give evidence that electrons and protons with high energies ($10^6$-$10^9$ ev) are present in the solar atmosphere. Therefore, it is essential to investigate the possible processes for the acceleration of individual charged particles in the solar atmosphere. Acceleration caused by the electromagnetic field of a sunspot group is considered; other mechanisms of acceleration are not discussed. In the present paper, the mechanism of electron and proton acceleration by $E_\perp$, the component of an induced electric field (E) perpendicular to the magnetic field (H) of the spot is considered. This mechanism is not sufficiently effective and can increase the energy of the particles only by a factor of $10^2$-$10^3$, i.e., up to an energy of $10^5$-$10^6$ ev. The acceleration of charged particles by $E_\parallel$, the component of the induced field parallel to the magnetic field H is more effective and calculations show that the particles can be accelerated to an energy of $10^8$-$10^9$ ev.

## 1. On the Presence of Fast Particles in the Solar Atmosphere

Observational data obtained in the last few years show that, undoubtedly, in the solar atmosphere there are charged particles (ions and electrons) with high energies: $10^5$-$10^6$ and even $10^9$ ev. The number of such particles apparently changes with the time. Let us enumerate the data supporting this conclusion.

1. It is known that the passage of an active sunspot group across the central meridian of the solar disc is accompanied by sporadic radio emission in the form of a) radio emission connected with the sunspots and b) "radio bursts" which have a duration from 1 sec to several minutes. Meter radio waves are emitted by small regions of the corona in the vicinity of the sunspots and directly above the sunspots, at a height of 25,000-70,000 km or more above the photosphere. The radio temperature of the emitting regions reaches $10^8$-$10^{9\circ}$. (The radio temperature of the emitter is the temperature of a black body with the same angular dimensions which has an equal energy flux at the same radio frequency.) The radio temperature of the sun during large radio bursts reaches $10^{13\circ}$. However, if it is taken into account that the emission is from individual regions and not the whole sun, their temperature must be higher by one or two orders of magnitude. It is obvious that in this case there can be no "thermal" mechanism for the radio emission.

In the last few years, many authors [1-5] have considered that the sources of at least part of the sporadic radio emission by the sun are relativistic electrons moving in the magnetic field of the solar atmosphere. The presence of relativistic electrons in the chromospheric flares is, apparently, also probable [3].

2. From an analysis of the cosmic-ray-intensity variations connected with solar activity (these variations have a 27-day recurrence and some connection with magnetic storms), some authors [6-7] have concluded that:

a) solar activity changes the energy of the primary cosmic rays, perhaps through their acceleration when interacting with beams of atoms ejected from the solar active regions;

b) that the sun itself is a source of a small part of the cosmic rays. In particular, during powerful chromospheric flares on the sun cosmic-ray particles with an energy of $10^8$-$10^9$ ev are generated. A smaller number of cosmic-ray particles are apparently generated on the sun in connection with other phenomena: sunspots, prominances, etc. In any case, the mechanism producing a partial change of the primary-cosmic-ray spectrum (with a 27-day recurrence, a correlation with magnetic storms) is associated with processes taking place on the sun and accompanied by the production of high-energy particles.

3. It is known that the occurrence of chromospheric flares in an active region lying close to the central meridian of the solar disc is, in most cases, accompanied by magnetic storms, which commence on the earth several tens of hours after the flare, and ionospheric disturbances. Therefore, chromospheric flares are accompanied not only by bursts of radio emission and a variation in the intensity of the primary component of the cosmic radiation, but also by corpuscular streams. Consequently, the spatial region occupied by the chromospheric flare and the region of the corona in its immediate vicinity apparently contain particles with high (but not cosmic) energies.

4. A number of investigations by Soviet and foreign authors [8, 9, 3, 10] indicate that the sun emits x-rays with $\lambda \sim 7$-100 A which produce ionization in the earth's atmosphere (E layer) and a breakdown of radio communications. An approximate estimate of the intensity of the x-radiation with $\lambda \sim 10$ A, in a band 2 A wide, gives $10^{-4}$ ergs$\cdot$cm$^{-2}\cdot$sec$^{-1}$ at the top of the earth's atmosphere; in this estimate, intensity data obtained from rocket measurements were used. The x-radiation is in the nature of flares. An estimate made in Reference [3] shows that it is sufficient to have 250 electrons with an energy of $5 \cdot 10^9$ ev per 1 cm$^3$, in a region of the corona with a magnetic field intensity $H \sim 10$ oerst and of dimensions $\sim 10^{10}$ cm, for the x-radiation of the relativistic electrons in the magnetic field to be of the required intensity in the frequency range indicated. Thus, the sun is a powerful source of x-rays and their production indicates the presence in individual regions of the solar atmosphere of high-energy particles.

Taken together, this shows the necessity for investigating the possible mechanisms for accelerating individual particles in the solar atmosphere, particularly in the sunspot region. The acceleration of particles by electrostatic fields of a potential nature, producing large potential differences, cannot be considered since astrophysical observations and some theoretical ideas exclude the possibility of such fields being in existence. We can consider acceleration only by induced vortical electric fields. The present work is devoted to the investigation of the action of the induction mechanism for the acceleration in the sunspot regions. A number of the conclusions reached in the paper will probably be of a preliminary nature since, at the present time, the available data on the conditions of the solar atmosphere are not sufficient for more definite assertions to be made; nevertheless, they can be useful in further investigations of this problem.

## 2. Acceleration by the $E_\perp$, the Component of the Induced Electric Field Perpendicular to the Magnetic Field

The magnetic field H of a unipolar spot above the photosphere is axially symmetric and, in the first approximation, it can be taken as the field of a magnetic dipole with a magnetic moment

$$\mu = \frac{H_m \bar{a}^3}{\sqrt{1+3\cos^2\theta}},$$

directed along the radius of the sun. ($H_m$ is the intensity on the axis, $2\bar{a}$ is the length of the dipole, a value constant for a given sunspot.)

The determination of the length of the dipole $2\bar{a}$ presents some difficulty in the case of a unipolar spot. However, the dipole length can, apparently, be connected with the radius of the unipolar spot. Investigations show that the magnetic field of the dipole (unipolar spot) whose length is $2\bar{a} \cong 1.6$ b (b is the radius of the spot penumbra), in the plane, perpendicular to the dipole axis, extended at a distance $z = a =$ constant, has a distribution H with sunspot area, close to the distribution found by Broxon [11] and to the distribution found by Grotrian and Mattig [12], even if it does not accurately agree with either of them. The change of the magnetic flux $\Phi$ of the spot gives rise to a vortical electric field, E, directed along concentric circles and determined by the relation:

$$\oint E_l dl = -\frac{1}{c}\int_S \frac{\partial H_n}{\partial t} ds = -\frac{2\pi}{c}\int_0^r \frac{\partial H_n(r)}{\partial t} r dr, \qquad (1)$$

where $E_l$ is the projection of the electric-field intensity on the contour of integration, r is the distance from the center of the spot and the permeability is taken equal to unity. If Broxon's equation for the variation of the magnetic-field strength along the radius of a normal solar unipolar spot (circular in shape), $H(r) = H_m[1 - (r^2/b^2)]$, is used we have

$$E_l = -\frac{r}{2c}\left(1 - \frac{r^2}{2b^2}\right)\frac{\partial H_m}{\partial t}, \tag{2}$$

where b is the radius of the spot to the inner boundary of the penumbra, r the distance from the center, $H_m$ the maximum intensity of the magnetic field at the center. The degree of nonuniformity of the fields (at the level of the photosphere) is very small. The gradient of the magnetic-field intensity H(r) along the radius, at a given time, $\partial H(r)/\partial r = -H_m 2r/b^2$ oerst · cm$^{-1}$ has a small value from $\sim 3 \cdot 10^{-10}\, H_m$ to $\sim 19 \cdot 10^{-10}\, H_m$ oerst · cm$^{-1}$ for a spot of radius $b = 10^9$ cm.

The gradient of the induced electric field along the radius, $\frac{\partial E_l}{\partial r} = -\left(1 - \frac{2r^2}{2b^2}\right)\frac{1}{2c}\frac{\partial H_m}{\partial t}$, is also small. For a spot with $b = 10^9$ cm, at a distance from the center between $r = 0$ and $r = 0.816b$ the gradient is positive (i.e., the magnitude of $E_l$ grows at a given time) and the value of the gradient lies between $+0.915\,\frac{1}{2c}\frac{\partial H_m}{\partial t}$ and $+0.155 \cdot \frac{1}{2c}\frac{\partial H_m}{\partial t}$. From $r = 0.816b$ to $r = \sqrt{2}b$, the gradient $\frac{\partial E_l}{\partial r}$ is negative and has a value between $-0.085\,\frac{1}{2c}\frac{\partial H_m}{\partial t}$ and $-2.80\,\frac{1}{2c}\frac{\partial H_m}{\partial t}$.

Therefore, there will be a comparatively high degree of nonuniformity in the magnetic and induced electric fields near the boundary of the spot (approximately, in the penumbra).

Taking into account the small nonuniformity of the magnetic field in the remaining region (at the same height), instead of Equation (2) we can use a simpler equation:

$$E_l = -\frac{r}{2c}\frac{\partial H_m}{\partial t}. \tag{3}$$

In a more general form (for any height above the photosphere) Equation (3) can be obtained from the expression for the intensity of the electric field of an alternating dipole with a magnetic moment $\mu$ [13, 14]:

$$\mathbf{E} = \frac{1}{cr^3}[\mathbf{r}\bar{\mu}]\frac{1}{\mu}\frac{d\mu}{dt}, \tag{4}$$

$$E_l = \frac{r}{c}\frac{\sin\theta}{\sqrt{1 + 3\cos^2\theta}}\frac{\partial H_m}{\partial t}\left(\frac{\bar{a}}{r}\right)^3 = \frac{r_0}{c\sqrt{1 + 3\cos^2\theta}}\frac{\partial H_m}{\partial t}\left(\frac{\bar{a}}{r}\right)^3, \tag{4'}$$

where $\theta$ is the angle between the radius vector **r** and the magnetic moment $\bar{\mu}$, and $r_0$ is the radius of the circular integration contour.

The lines of force of the induced electric field **E** will be circular and, according to (4), will be perpendicular to the magnetic field **H**.

In a uniform, stationary or quasistationary magnetic field the trajectories of a moving charged particle will be a circle whose plane is perpendicular to the magnetic field (if $v_H = 0$). The radius of this circle will be

$$R = \frac{cmv_\perp}{eH}, \tag{5}$$

where $mv_\perp$ is the momentum of a nonrelativistic particle in the plane of the circle. In the case of a relativistic particle $R = \frac{cmv_\perp}{en\sqrt{1 - (v^2/c^2)}}$.

It is known that in the case of superimposed magnetic and electric fields, having an angle between them different from zero or $\pi$, the charged particle and the aggregate of charged particles (plasma) will experience a drift with velocity $\mathbf{u} = -\frac{c\,[\mathbf{HE}]}{H^2}$.

In the lower layers of the chromosphere and in the photosphere with fields $H < 10^2$ oerst, when $\omega_e \tau_e \sim 1$ for electrons and $\omega_i \tau_i \ll 1$ for ions (where $\tau$ is the mean free time, $\omega = eH/cm$ is the angular frequency), an electric current with density $\mathbf{j}$ arises in the direction of the field $\mathbf{E}$ and the plasma begins to move under the action of the force $\mathbf{F} = (1/c)[\mathbf{jH}]$. It can be easily shown that with the growth of the field ($dH/dt > 0$), the drift and the ponderomotive force are directed toward the axis of the spot, while with decreasing field ($dH/dt < 0$), away from the axis.

During the drift and motion of the plasma under the action of this force, a field will be induced in the plasma $E_{\perp}^{\mathrm{ind}}$, which will almost completely destroy the action of the transverse component of the field applied on the plasma, if this plasma can be considered completely mobile (without the property of inertia) and if there is no obstruction to the movement of the plasma as a whole.

The assumption that the plasma is inertialess, however, is not strictly accurate. In addition, if there are factors which impede the movement (drift) of the plasma, then in the plasma there can and will exist an electric field, $E \neq 0$, induced by the sunspot. Such factors can be: 1) nonuniformity of density (pressure) arising from a compression of matter towards the axis of the sunspot field, and 2) the nonuniformity of the magnetic field in a direction perpendicular to H (particularly in the penumbral regions of the spot). The nonuniformity of the density and the magnetic field in the neighborhood of a unipolar spot will produce a drift of the charged particles [15, 16]:

$$\mathbf{u}_1 = -\frac{c}{eH^2}\left[\mathbf{H} \times \left(\frac{1}{n}\,\mathrm{grad}\,\mathrm{p} - \mu_1\,\mathrm{grad}\,\mathbf{H}\right)\right],$$

where $\mu_1 = W_{\perp}/H$ is the magnetic moment of the dipole equivalent to the circular current $\pi e R^2/cT_1$, produced by the particle motion; $p = nkT$ is the pressure. The direction of the drift velocity depends on the charge of the particle and it will be different for electrons and positive ions. Therefore, because of the presence of the drift $\mathbf{u}_1$, a ring current arises with a density $j_{\varphi} = neu_1$. An increase of the ring currents $j_{\varphi}$ produces a further compression of the matter in the chromosphere and corona along the axis of the sunspot field. According to the evaluation of S.B. Pikel'ner [17], the pressure gradient can increase by several tens of times and the transverse component of the field, $E_{\perp}$, will not be appreciably destroyed by the motion.

Let us suppose that this case occurs in the region of a unipolar sunspot. We consider the case of charged-particle acceleration by $E_{\perp}$, the transverse component of the induced field.

The charged particle, during its motion in a varying magnetic field of the sunspot, will gain energy at the expense of the varying magnetic flux cutting the contour described by the particle which moves in a plane perpendicular to the magnetic field. The increase of the energy of the particle (in the nonrelativistic case) is

$$\frac{dw_{\perp}}{dt} = eE_t v = \frac{mv_{\perp}^2}{2}\,\frac{1}{H}\,\frac{dH}{dt} = w_{\perp}\,\frac{1}{H}\cdot\frac{dH}{dt},$$

from which we obtain after integrating

$$w_{\perp} = (w_{\perp})_0\,\frac{H}{H_0}, \qquad (6)$$

i.e., the energy of a nonrelativistic particle will increase proportionately to the increase of the magnetic field, $H/H_0$. $H_0$ is the original magnitude of the magnetic field, $(w_{\perp})_0$ is the initial kinetic energy of the particle, determined by $(v_{\perp})_0$.

The latter Equation (6) also follows from the existence of the adiabatic invariant $I = \oint \mathbf{P}_1 dr$ for a particle moving in a slowly-changing magnetic field [18]. ($\mathbf{P}_{\perp} = \mathbf{p}_{\perp} + \frac{e}{c}\mathbf{A}$ is the projection of the generalized momentum onto the plane perpendicular to H, and A is the vector potential of the magnetic field):

$$I = \oint \mathbf{P}_\perp d\mathbf{r} = \oint \mathbf{p}_\perp d\mathbf{r} + \frac{e}{c}\oint \mathbf{A} d\mathbf{r} = \frac{3\pi c p_\perp^2}{eH} = \frac{6\pi c m w_\perp}{eH}, \qquad (7)$$

At the time t = 0, we have

$$I = \frac{6\pi c m (w_\perp)_0}{eH_0}.$$

From a comparison of the last two equations we will obtain Equation (6).

To determine the energy increase for a relativistic particle during a systematic growth of the magnetic field intensity H, in the adiabatic invariant we substitute the energy, $\mathcal{E}$, for the momentum, using the well known relation between the two quantities:

$$I = 3\pi c\left(\frac{\mathcal{E}^2}{c^2} - m_0^2 c^2\right) / \, eH. \qquad (7')$$

From which

$$\frac{d}{dt}\ln\mathcal{E} = \frac{v_0^2(\mathcal{E})}{2c^2}\frac{d}{dt}\ln H \qquad (8)$$

or in integrated form

$$\mathcal{E} = \mathcal{E}_0\sqrt{\left(\frac{H}{H_0} - 1\right)\frac{v_0^2}{c^2} + 1}, \qquad (9)$$

where $\mathcal{E}_0$ is the initial energy of a relativistic particle. The initial velocity of a relativistic particle $v_0 \sim c$, therefore

$$\mathcal{E} \sim \mathcal{E}_0\sqrt{\frac{H}{H_0}}. \qquad (9')$$

Let us consider Equation (6); it gives the upper limit for the energy gained by a particle in a varying magnetic field without taking into account energy losses in elastic and inelastic collisions.

Let a unipolar spot have a magnetic moment $\mu \sim 4 \cdot 10^{30}$ oerst · cm$^3$, a maximum magnetic field intensity at its center of $H_m = 10^3$ or $2 \cdot 10^3$ oerst, and let the field before the appearance of the spot be $H_0 = 1$-3 oerst. Thus, for such a spot we take $H/H_0 \sim 10^3$. According to Equation (6) the energy of a nonrelativistic particle will increase by approximately $10^3$ times.

The gases of the solar atmosphere are in a heated and ionized condition; the degree of ionization is particularly large in the corona and the upper chromosphere. The gases of the solar atmosphere form what is known as plasma, which, with sufficient accuracy, has a Maxwellian distribution of velocities [19, 20]:

$$dn_v = 4\pi n\left(\frac{m}{2\pi kT}\right)^{3/2} e^{-mv^2/2kT}\, v^2 dv \qquad (10)$$

(in unperturbed regions and in the absence of an external electric field).

The results of the calculation of the velocities and energies of the particles in various layers of the solar atmosphere and the data used are given in Table 1 for electrons and Table 2 for protons. In the last column of the tables, the maximum velocities and energies of the particles (the number of particles is taken to be several tens per 1 cm$^3$) which are possible on account of the Maxwellian distribution at the given temperature are shown. (In the calculations, for electrons $\Delta v$ was taken as $\sim 10^7$-$10^8$ cm/sec and for protons as $10^5$-$10^6$ cm/sec.) Thus, in the upper chromosphere a small fraction of the particles (several tens of electrons and protons per cm$^3$) have an energy of 15-30 ev. With an increase of the magnetic field by $H/H_0 \sim 10^3$ times the energy of these particles

TABLE 1

For Electrons

| Region of the atmosphere | Height in 1000 km | Number of electrons in 1 cm³, $n_e$ | Kinetic temperature, $T_e$ | Most probable value at given temperature | | Maximum possible values | | |
|---|---|---|---|---|---|---|---|---|
| | | | | velocity (cm/sec) | energy in ev | velocity in cm/sec | energy in ev | number of particles with these energies |
| Photosphere | 0 | | | | | | | |
| Chromo" | 0.5 | $4 \cdot 10^{11}$ | $5 \cdot 10^3$ | $3.88 \cdot 10^7$ | $\sim 0.2$ | $1.95 \cdot 10^8$ | $\sim 10.8$ | $\sim 81$ |
| » | 5 | $2 \cdot 10^{10}$ | $6 \cdot 10^3$ | $4.25 \cdot 10^7$ | $\sim 0.5$ | $2.05 \cdot 10^8$ | $\sim 11.9$ | $\sim 25$ |
| » | 10 | $2 \cdot 10^9$ | $10^4$ | $5.48 \cdot 10^7$ | $\sim 1$ | $2.45 \cdot 10^8$ | $\sim 17$ | $\sim 33$ |
| » | 15 | $10^9$ | $2 \cdot 10^4$ | $7.76 \cdot 10^7$ | $\sim 1.6$ | $3.45 \cdot 10^8$ | $\sim 33$ | $\sim 15$ |
| Corona | 40 | $2 \cdot 10^8$ | $10^6$ | $5.48 \cdot 10^8$ | $\sim 84$ | $2.25 \cdot 10^9$ | $\sim 1.4 \cdot 10^3$ | $\sim 57$ |
| » | 100 | $10^8$ | $10^6$ | $5.48 \cdot 10^8$ | $\sim 84$ | $2.25 \cdot 10^9$ | $\sim 1.4 \cdot 10^3$ | $\sim 30$ |
| » | 100 | $10^8$ | $1.5 \cdot 10^6$ | $6.72 \cdot 10^8$ | $\sim 128$ | $2.75 \cdot 10^9$ | $\sim 2.1 \cdot 10^3$ | $\sim 31$ |

could increase to $1.3 \cdot 10^4$-$3 \cdot 10^4$ ev. In the inner regions of the corona a small fraction of the particles (several tens of electrons and protons per cm³) have an energy of $1.4 \cdot 10^3$-$2.2 \cdot 10^3$ ev. With an increase of the magnetic field by $10^3$ times their energy could increase to 1-2 Mev.

TABLE 2

For **H** and **H$_+$**

| Region of the atmosphere | Height in 1000 km | Number of particles in 1 cm³ | | Kinetic temperature, T | Most probable value at given temperature | | Maximum possible value | | |
|---|---|---|---|---|---|---|---|---|---|
| | | $H$ | $H_+$ | | velocity in cm/sec | energy in ev | velocity in cm/sec | energy in ev | number of particles with these energies |
| Photosphere | 0 | | | | | | | | |
| Chromosphere | 0.5 | $3 \cdot 10^{13}$ | $4 \cdot 10^{11}$ | $5 \cdot 10^3$ | $9.06 \cdot 10^5$ | $\sim 0.43$ | $4.55 \cdot 10^6$ | $\sim 10.8$ | $\sim 33$ |
| » | 5 | $4 \cdot 10^{10}$ | $2 \cdot 10^{10}$ | $6 \cdot 10^3$ | $9.92 \cdot 10^5$ | $\sim 0.50$ | $4.65 \cdot 10^6$ | $\sim 11.5$ | $\sim 28$ |
| » | 10 | $3 \cdot 10^9$ | $2 \cdot 10^9$ | $8 \cdot 10^3$ | $1.01 \cdot 10^6$ | $\sim 0.51$ | $5.15 \cdot 10^6$ | $\sim 13.8$ | $\sim 33$ |
| » | 15 | | $10^9$ | $10^4$ | $1.28 \cdot 10^6$ | $\sim 0.63$ | $5.55 \cdot 10^6$ | $\sim 16.2$ | $\sim 49$ |
| Corona | 40 | $10^3$ | $2 \cdot 10^8$ | $6 \cdot 10^5$ | $9.92 \cdot 10^6$ | $\sim 52$ | $4.05 \cdot 10^7$ | $\sim 857$ | $\sim 24$ |
| » | 100 | | $10^8$ | $10^6$ | $1.28 \cdot 10^7$ | $\sim 85$ | $5.05 \cdot 10^7$ | $1.33 \cdot 10^3$ | $\sim 23$ |
| » | 100 | | $10^8$ | $1.5 \cdot 10^6$ | $1.57 \cdot 10^7$ | $\sim 128$ | $6.55 \cdot 10^7$ | $2.2 \cdot 10^3$ | $\sim 9$ |

Inasmuch as the particle energy $w_{\perp} = w_{\perp 0}\frac{H}{H_0}$ is determined by the final value of the magnetic field, when the latter increases it is obvious that the time in which the particles are accelerated is equal to the time in which the field of the spot increases.

## 3. Retardation of the Particles

In considering the motion of particles in the solar atmosphere, we cannot take the latter to be a vacuum even if its upper layers are sufficiently rarefied. Therefore, in considering the problem of the acceleration of particles, in addition to taking the accelerating factors into account, it is also necessary to take into account the interaction between the moving particles and the medium, i.e., to take into account those factors which produce retardation. In moving through the medium, the particle suffers retardation – energy losses because of the following processes:

a) It is known that a charged particle (electron, positive ion) moving through a gaseous plasma containing electrons with a velocity higher than the thermal velocity ($v > v_m$) will suffer an energy loss due to the plasma. The interaction between a moving electron and the plasma electrons has been treated by a number of authors [20-22]. The retardation of an electron moving with a velocity higher than the thermal velocity of plasma electrons will be caused predominantly by the plasma electrons and the retardation by ions can be neglected. The magnitude of the retardation will be

$$-\left(\frac{d\mathcal{E}}{dz}\right)_{\text{ret}} = \frac{4\pi e^4 n_e}{m_e v^2}\ln\frac{m_e v_e^2}{e^2 n^{1/3}}\ \text{erg}\cdot\text{cm}^{-1}. \tag{11}$$

The retardation of ions by electrons will have the magnitude

$$-\left(\frac{d\mathcal{E}}{dz}\right)_{\text{ret}} = \frac{4\pi z^2 e^4 n_e}{\mu v^2}\ln\left(\frac{\mu v^2}{z e^2 n^{1/3}}\right), \tag{12}$$

where $\mu$ is the reduced mass.

b) The energy losses in the ionization of atoms by electron impact are

$$-\left(\frac{d\mathcal{E}}{dz}\right)_{\text{ion}} = \frac{2\pi e^4 n}{m_e v^2}\left\{\ln\frac{m v^2 w}{2\bar{\chi}^2(1-v^2/c^2)} - \right.$$
$$\left. -\ln 2\left(2\sqrt{1-\frac{v^2}{c^2}} - 1 + \frac{v^2}{c^2}\right) + 1 - \frac{v^2}{c^2}\right\}\ \text{erg}\cdot\text{cm}^{-1}, \tag{13}$$

where $\bar{\chi}$ is the average ionization potential of the remaining non-ionized atoms, $w$ is the relativistic kinetic energy of the electron and $n$ the number of non-ionized atoms.

The ionization losses of the ions are determined by the expression:

$$-\left(\frac{d\mathcal{E}}{dz}\right)_{\text{ion}} = \frac{4\pi z^2 e^4 n}{m v^2}\left(\ln\frac{2mv^2}{\bar{\chi}(1-v^2/c^2)} - \frac{v^2}{c^2}\right)\ \text{erg}\cdot\text{cm}^{-1}. \tag{14}$$

c) In an inelastic collision with atoms and complex ions the energy of the electron can go into the excitation of discrete optical levels. The probability for the excitation of atoms by ions (protons) at energies below $10^3$ ev is usually small and we will not take it into account in our calculations.

Knowing the total cross section for excitation by fast electrons (whose energy, $w$, is large by comparison with the excitation potential)

$$\sigma_{in} = \frac{16\pi^3 m_e e}{h^2} M_{in}\frac{1}{w}\ln\frac{4w}{U_a} \tag{15}$$

(where $M_{in}$ is the matrix element for the dipole transition), the energy losses of an electron which lead to optical excitation of atoms and ions could be evaluated.

d) The energy losses of a fast electron due to radiation in a magnetic field are

$$-\left(\frac{d\mathcal{E}}{dz}\right)_{\text{mag}} = \frac{2}{3}\frac{v}{c}\left(\frac{l^2}{m_e c^2}\right)^2 H_\perp^2\left(\frac{\mathcal{E}}{m_e c^2}\right)^2\ \text{erg}\cdot\text{cm}^{-1}. \tag{16}$$

e) The energy losses of an electron in the inverse-Compton effect are

$$-\left(\frac{d\mathcal{E}}{dz}\right)_{\text{compt.}} = \frac{8\pi}{3}\left(\frac{e^2}{m_e c^2}\right)^2 \bar{n}_\Phi\,\mathcal{E}_\Phi\left(\frac{\mathcal{E}}{m_e c^2}\right)^2\ \text{erg}\cdot\text{cm}^{-1}, \tag{17}$$

where $\mathcal{E}_\Phi$ is the mean energy, and $\bar{n}_\Phi$ the mean number, of scattering photons.

f) The disappearance and the creation of pairs of fast particles will not be taken into account. Also, the radiation losses during the acceleration of an electron will not be taken into account.

In view of the fact that the upper layers of the chromosphere and the inner layers of the photosphere are almost completely ionized and the predominant element is hydrogen, the excitation and ionization losses can be neglected. The presence of a small proportion of ionized atoms of other elements [23] does not make these losses appreciable. The radiation by the electrons in the magnetic field (especially at the beginning of the acceleration, when the energy is still low) are also not important. Thus, for example, in the case of electrons with a velocity of $3 \cdot 10^9$ cm/sec, these losses are almost six orders of magnitude less than the retardation losses. The radiation by high-energy electrons in the magnetic field of the solar atmosphere must be considered separately. Therefore, we will only consider as important (particularly at energies $\sim 10^3$-$10^4$ ev) the energy losses necessary to overcome the retardation by the plasma.

Hence, because of the induced field, the charged particle is under the action of an accelerating force

$$eE_{\text{ind}} = e\frac{r}{2c}\frac{\partial H}{\partial t} = \frac{mv_\perp}{2H}\frac{\partial H}{\partial t};$$

and because of the plasma it is under the action of a retarding force

$$F_{\text{ret}} = \frac{4\pi e^4 n_e}{m_e v^2}\ln\frac{m_e v_e^2}{e^2 n^{1/3}}.$$

The particle will be accelerated and will gain energy if the accelerating force is greater than the retarding force

$$eE_{\text{ind}} \geqslant F_{\text{ret}}. \tag{18}$$

Since the retarding force is inversely proportional to the particle energy, not all of the particles will be accelerated to high energies in a given varying magnetic field. From Inequality (18) the value of the velocity can be found for which the particle will be accelerated, given the values of H and dH/dt:

$$v^3 \geqslant \frac{2 \cdot 4\pi e^4 n_e HL}{m_e^2 (dH/dt)}, \tag{19}$$

where $L = \ln\frac{m_e v^2}{e^2 n^{1/3}}$. On the other hand, we can consider what is the necessary value of the rate of change of the magnetic field, dH/dt, for which particles with a given velocity will be accelerated to high energies:

$$\frac{dH}{dt} \geqslant \frac{2 \cdot 4\pi e^4 n_e HL}{m_e^2 v^3}. \tag{20}$$

It must be pointed out that Inequality (19) must be satisfied at the initial time of formation of the sunspot magnetic field. As the magnetic field intensity H rises, the particle velocity $\underline{v}$ will also increase, in the nonrelativistic case proportionately to H according to (6). Simultaneously, the velocity of the plasma electrons will also increase (i.e., the electron temperature will increase) which will lead to a decrease of the retarding force. Therefore, if at the initial time $t = 0$, in some regions of the chromosphere or the corona, Inequality (19) is satisfied for the given type of particle with $H_0$, then also subsequently, for $t > 0$, this inequality will also be satisfied for the increasing values of H (with one and the same value of dH/dt).

In addition, from Inequality (19) or the equation $eE_{\text{ind}} = mv_\perp/2H \cdot dH/dt$, it follows that the regions most favorable for the acceleration of particles will be those areas of the sunspot field where the value of H is not large, i.e., the outer regions of the magnetic field of the sunspot.

For the inner corona, this value of $H_0$ can be taken to be several oersteds or even several tens of oersteds. Taking $dH/dt \approx 2 \cdot 10^{-2}$ oerst/sec, i.e., 72 oerst/hour, or $dH/dt \approx 3 \cdot 10^{-2}$, i.e., 108 oerst/hour, let us determine from Inequality (19) the initial limiting velocity, starting from which the electrons can be accelerated to high energies in the increasing magnetic field, given:

$$v_e^3 \geqslant \frac{4\pi e^4 n_e HL}{m_e^2 (dH/dt)} \approx \frac{4\pi (4.8)^4 \cdot 10^{-40} \cdot 5 \cdot 10^7 \cdot 0.5 \cdot 17}{(9.1)^2 \cdot 10^{-56} \cdot 2 \cdot 10^{-2}};$$

$$v_e \geqslant 2.58 \cdot 10^9 \text{ cm/sec} \qquad (\text{with } dH/dt \; 2 \cdot 10^{-2} \text{ oersted/sec})$$

and

$$v_e \geqslant 2.25 \cdot 10^9 \text{ cm/sec} \qquad (\text{with } dH/dt \; 3 \cdot 10^{-2} \text{ oersted/sec}). \tag{21}$$

The values of the various quantities used can be seen from the calculation. In addition, it is assumed that $(v_e)_{rel} = \sqrt{2} \cdot v_e$.

The results of the calculations of the electron-velocity distribution, given in Table 1, show that in the inner corona there are several tens of electrons in 1 cm$^3$ whose velocities exceed the limiting velocity given by (21).

Consequently, these electrons can be accelerated in the increasing magnetic field of the sunspot to an energy

$$w = w_0 (H / H_0) \sim 10^5 - 10^6 \text{ ev.}$$

The protons (ions) in moving through the chromosphere-corona plasma will suffer retardation essentially due to the protons.

The value of the retardation will be

$$-\frac{d\mathcal{E}}{dz} = \frac{4\pi e^4 n_e}{3kT_e} \ln\left(\frac{3kT_e}{e^2 n^{1/3}}\right). \tag{22}$$

Inequality (19) for protons will be

$$v_{pr} \geqslant \frac{4\pi e^4 n_e \cdot 2HL}{m_{pr} 3kT\,(dH/dt)}. \tag{23}$$

Taking dH/dt ~ $2 \cdot 10^{-2}$ oerst/sec, $H_0 = 0.5$ oerst, T ~ $10^{6°}$, we have

$$v_{pr} \geqslant 3.74 \cdot 10^7 \text{ cm/sec,}$$

and

$$v_{pr} \geqslant 6.73 \cdot 10^7 \text{ cm/sec,} \tag{24}$$

for dH/dt ~ $1.4 \cdot 10^{-2}$ oerst/sec, $H_0 = 0.5$ oerst, T ~ $10^{6°}$.

According to Table 2, in the inner corona there are several tens of protons in 1 cm$^3$ whose velocities exceed the limiting velocity given by (25). These protons can be accelerated by the increasing magnetic field of the sunspot to an energy

$$w = w_0 \frac{H}{H_0} \sim 10^5 - 10^6 \text{ ev.}$$

## SUMMARY

The results obtained can be summarized as follows:

1. In the increasing magnetic field of a sunspot group, charged particles (electrons, protons and other ions) can be accelerated to an energy

$$w = w_0 \frac{H}{H_0}.$$

2. The presence of retarding forces eliminates an overwhelming majority of the particles from the process of acceleration to the energies indicated in item 1. Only those particles for which Inequality (18) is satisfied, i.e., the particles which have a sufficiently high initial energy $w_0$ (as it were, an injection energy), can be accelerated to the energy indicated.

3. Particles which do not satisfy the Inequality (18) will not be accelerated to high energies, but they can gain a small amount of energy (several electron volts) from the induced sunspot field ($E_{ind}$) and can be the source of additional thermal, radiation and other effects.

4. The more favorable regions for the acceleration of charged particles in the increasing magnetic field of a sunspot group will be the regions of the chromosphere-corona plasma situated in the boundary areas of the magnetic field of this group.

It seems to us that this conclusion is in agreement with the well-known fact that some of the phenomena associated with solar activity (chromospheric flares, prominences, emission of filaments, etc.) during observations can be projected back, not on the spot itself, but onto its periphery or even onto regions in the immediate vicinity of the sunspot.

5. The acceleration of particles, and phenomena associated with these processes, will then be most clearly defined when the rate of change of the magnetic field, $dH/dt$, is high, i.e., when the sunspot group is in the active stage of its existence. This is also in agreement with observations.

## LITERATURE CITED

[1] M. Ryle, Uspekhi Fiz. Nauk 46, 508 (1952).*

[2] V.L. Ginsburg, Doklady Akad. Nauk SSSR 76, 377 (1951); Uspekhi Fiz. Nauk 51, 342 (1952).

[3] I.M. Gordon, Doklady Akad. Nauk SSSR 94, 813 (1954).

[4] G.G. Getmantsev, Uspekhi Fiz. Nauk 44, 527 (1951).

[5] G.G. Getmantsev and V.L. Ginsburg, Doklady Akad. Nauk SSSR 87, 187 (1952).

[6] J. Simpson and W. Foner, Phys. Rev. 85, 366 (1952); J. Simpson, Phys. Rev. 94, 426 (1954).

[7] V. Sarabhai and R. Kane, Phys. Rev. 90, 204 (1953).

[8] S.L. Mandel'shtam, Uspekhi Fiz. Nauk 46, 145 (1952).

[9] E. Byram and T. Chubb, Phys. Rev. 92, 1066 (1953).

[10] I.S. Shklovskii, Doklady Akad. Nauk SSSR 64, 38 (1949).

[11] J. Broxon, Phys. Rev. 62, 521 (1942).

[12] W. Mattig, Z. Ap. 31, No. 4, 273 (1953); W. Grotrian, Atti Convegni. Acaad. No. 11, 257 (1953).

[13] Ia.P. Terletskii, Vestnik Moskov. Univ. No. 11, 53 (1949).

[14] P.E. Kolpakov, Astronomical J. (USSR) 29, 638 (1952).

[15] H. Alfven, Cosmical Electrodynamics (IL, 1952).*

[16] A. Schlüter, Zs. f. Naturforsch. 5-a, 72 (1950).

[17] S.B. Pikel'ner, Izv. Krymskoi Astrofiz. Obs. 7, 99 (1951).

[18] L.D. Landau and E.M. Lifshits, Field Theory (GTTL, 1948).**

[19] V.A. Ambartsumian et al., Theoretical Astrophysics (GTTL, 1952).**

[20] A.A. Vlasov, Multi-Particle Theory (GTTL, 1950).**

[21] B.I. Davydov, J. Exptl.-Theoret. Phys. (USSR) 7, 1069 (1937).

[22] S.G. Gvozdover, J. Exptl.-Theoret. Phys. (USSR) 7, 867 (1937).

[23] I.S. Shklovskii, Solar Corona (GTTL, 1951).**

[24] V.L. Granovskii, Electric Current in a Gas, I (GTTL, 1952).**

Received March 17, 1956

---

*Russian translation.

**In Russian.

# CORONAL STREAMERS

## E. Ia. Bugoslavskaia

The dependence of the directions of coronal streamers on the phase of solar activity and heliographic latitude of coronal formations is discussed. New dependencies are shown to be present and are given in figures in the text.

A number of problems connected with the form of the solar corona and the directions of coronal streamers are considered in the present paper, leading to an extension of earlier results. Already, in 1897, A.P. Ganskii showed that the form of the solar corona is determined by the eruptive activity on the sun. He successfully predicted the form of the solar corona of 1900.

We shall not describe here all the coronal formations and their dependence on the formations on the solar surface which were established earlier, but shall refer the reader to previous papers [1, 2]. We merely shall state that coronal forms are determined by formations on the solar surface. The most pronounced formations in the corona are the dome-like streamers above prominences and strong fans which include them; for this reason the form of the solar corona depends, in the main, on the disposition of these strong formations.

On a quiet sun, on which there are no prominences or spots, the corona stretches down the solar equator, the corona of May 28th, 1900, and particularly that of June 30th, 1954, being good examples; the rays of the solar corona bend towards the equator and stretch out down its plane in the form of thin streamers.

During a maximum of solar activity, when the prominences reach up to the poles, the corona has an irregular form and the rays spread out on all sides. The coronas of 1905 and 1927 are particularly characteristic. In a corona of the intermediate type the main coronal streamers concentrate in the mean latitudes of the sun, which correspond to the maximum eruptive activity.

From the minimum form the solar corona gradually goes over to a maximum form, and then fairly quickly takes up an intermediate form as the high-latitude prominences disappear.

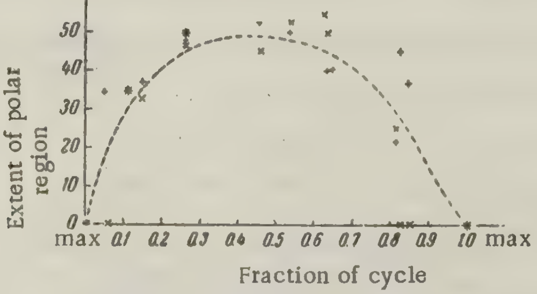

Fig. 1. The extent of the region of polar rays of the solar corona as a function of the phase of solar activity.

The extent of the region of polar rays changes, depending on the disposition of prominences, and in the maximum corona these rays are not observed at all (Figure 1).

The form of the corona depends not only on the disposition of the prominences but also on the inclination of the corresponding dome-like streamers to the normal to the solar surface, which also changes with the phase of the solar activity.

The inclination of the axes of the domes in a given system of prominences are near to each other, to within 2-5°, but may differ in a given corona between different groups. The domes of the second type which have thin luminous apexes usually have a smaller inclination to the normal than the domes of the first type (Table 1). However, the dependence of the inclination of coronal streamers above the prominences on the phase of solar activity shows up quite definitely. The nearer one is to a minimum of solar activity the more these domes bend towards the equator; during a minimum (1901, 1914) their inclination reaches 50° in the latitude of about 50°, the domes become almost parallel to the plane of the equator, and the angles of the axes of the domes with the normals at their bases decrease with latitude.

TABLE 1

| Date of the eclipse | $\varphi$ | $i$* | Type |
|---|---|---|---|
| January 24, 1925 | +54° W | 0° | 2 |
| | +30 W | +20 | 1 |
| June 19, 1936 | —60 W | +5 | 2 |
| | +58 W | +20 | 1 |
| September 21, 1941 | —40—75 E | +25 | 1 |
| | +48 E | +12 | 2 |
| | —48 W | 0 | 2 |
| | —55 W | 0 | 2 |
| | +60 W | +28 | 1 |
| | +44 W | +12 | 1 |
| June 9, 1945 | —13 W | +3 | 2 |
| | —50 E | +35 | 1 |
| | —40 W | +40 | 1 |
| | —45 W | +25 | 1 |

---

*Plus indicates inclination toward equator.

On an ascending arm of solar activity the inclination of the axes of domes (and fans) gradually decreases, during a maximum the domes in low and mean latitudes are normal to the surface of the sun, while those near the poles bend towards them as if mutually attracted and approach parallelism with the solar axis. Their angles to the normal are up to 30° in latitudes of 50-70° (1905, 1908, 1927). After a maximum, and with the disappearance of prominences which are close to the poles, the domes become inclined to the equator. Figure 2 shows the

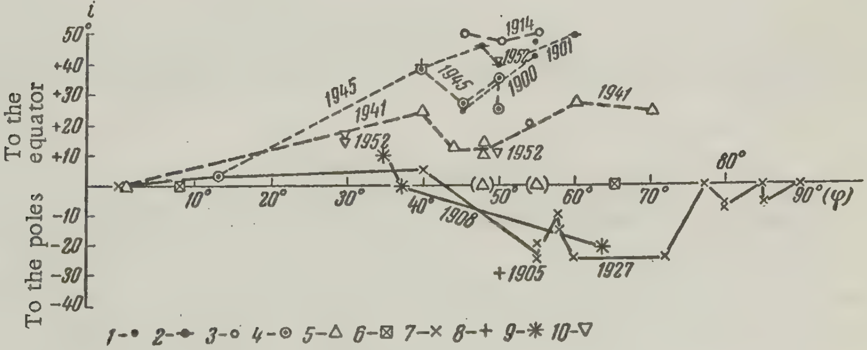

Fig. 2. Inclination of the axes of dome-like streamers as function of heliographic latitude for different eclipses. Notation: 1) May 28, 1900; 2) May 18, 1901; 3) August 9, 1914; 4) July 9, 1945; 5) September 21, 1941; 6) January 14, 1926; 7) June 29, 1927; 8) August 30, 1905; 9) January 3, 1908; 10) February 25, 1952.

inclination of domes as a function of latitude after different eclipses. Figure 3 shows the inclination of the axes of the domes and fans as functions of the phase of solar activity after prominences. The increase in the inclination of the axes of domes after a maximum is faster than its decrease on an ascending arm of solar activity.

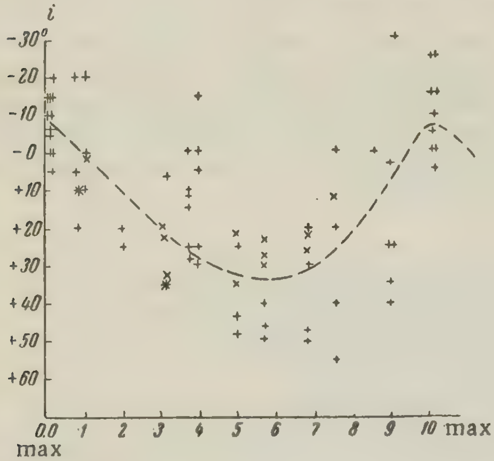

Fig. 3. Inclination of the axes of domes and fans as functions of phase of solar activity. + – domes; x – fans.

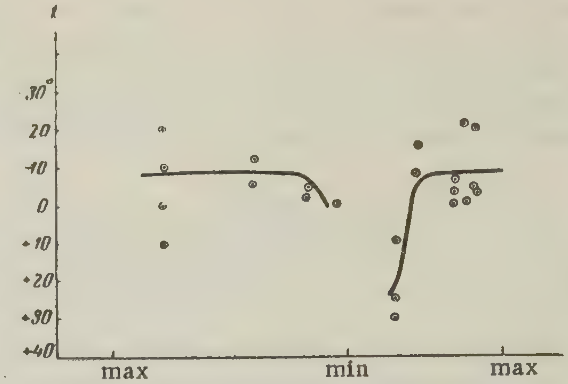

Fig. 4. Inclinations of the axes of beams of rays above faculas as functions of phase of solar activity. Minus – inclination to the pole; plus – inclination to the equator.

The form of the variation in the inclination of the axes of domes corresponds to changes in the latitudes of prominences and influences the general form of the corona, increasing the rapidity of its transition from a maximum type to an intermediate type.

Straight coronal rays which correspond to facular fields are subject to different regularities.

These rays are not very divergent and behave as if they were mutually attracted. The inclination of the axes of beams of such rays to the normal is usually small, although rays corresponding to smaller fields may appreciably bend away from the normal and towards the stronger streamers of facular rays, tending to become parallel to them; some cases of intersection of such streamers with the plane of the solar equator have been observed (the coronas of 1927 [2] and 1952 [3]).

In a corona of intermediate or maximum form, the rays above faculae have a small inclination towards the poles which is on the average constant within the limits 0-20°, and only near the minimum of activity do the rays above faculae incline towards the equator (Figure 4). No obvious dependence of the inclination of rays on latitude has been found.

The regularities in the directions of coronal streamers described above indicate once more the existence on the sun of a general magnetic field and local force fields, showing that the intensity of the latter depends on the phase of solar activity.

## LITERATURE CITED

[1] S.K. Vsekhsviatskii, E.Ia. Bugoslavskaia and A. Deutsch, "Report of the expedition to observe the full solar eclipse on June 19th, 1936" 1, 27 (1938).

[2] E.Ia. Bugoslavskaia, Trudy GAISh 19 (1951).

[3] E.Ia. Bugoslavskaia, Soobshcheniia GAISh 1954, No. 96, 36.

Received October 15, 1956

P.K. Shternberg State Astronomical
Institute

# RADIAL SYSTEMS IN THE HEAD OF THE COMET 1908 III (MOOREHOUSE)

## S. V. Orlov

A. Eddington [1] studied the evolution of envelopes in the head of the comet 1908 III and concluded that the envelopes were formed exclusively by massive repulsive accelerations due to the sun (from 700 to 16,000 in the units of solar gravitational acceleration) with initial emission velocities of molecules from the nucleus of from 10 to 100 km/sec. Since accelerations in the tails of comets (found from the motion of cloud formations) are only 200, with initial velocities of about 1 km/sec, accelerations in the heads of the comets should be about unity, and the velocity less than 1 km/sec.

The author [2] has shown that the solution of the problem can be reduced to two equations with three unknowns and is therefore indeterminate.*

Eddington used only one of the possible solutions ($M_2 - M_1 = \tau_2 - \tau_1$). If one assumes that the nuclei of comets rotate and that the emission of molecules from the nucleus is due to thermal energy then the values $1 + \mu < 5$ are physically admissible, the initial velocities being $q < 1$ km/sec. The spectra of the ends of envelopes, as well as, in general, of the heads of comets, should consist of CN (or $C_2$) bands.

A. Eddington [1] succeeded in tracing the appearance and evolution of envelopes in the head of the comet 1908 III. His investigations were helped by the large scale photographs (reflector D = 30" and 1 mm = 1') and the very short exposures (about $10^m$). The top of the envelope appeared first, then the envelope itself, extending left and right, entered the nucleus and enveloped it with its rapidly lengthening ends. These ends, like leaves of a fan, quickly crossed and finally merged with the tail, and the envelope disappeared. At the same time, at the point where the top of the first envelope was formed, the top of the second new envelope appeared and this went through an identical evolutionary cycle.

In order to explain these shifts, Eddington [1] assumed that the emission of molecules from the nucleus took place in bursts. At any moment in such a burst the initial velocities of all the molecules emitted in all the possible directions will be close to each other because otherwise the sharp outlines of envelopes would not appear. The velocities of emission of molecules towards the end of an outburst systematically decrease. Two or more envelopes could be observed at the same time.

Near the head of the comet, the force field due to the sun is practically uniform and this means that the molecules emitted from the nucleus with velocities $\underline{g}$ move under the action of a repulsive acceleration $1 + \mu$ due to the sun and along parabolas relative to the comet. For this reason the outline of the head of the comet is also a parabola, with the nucleus as the focus, and the head itself is a paraboloid of revolution [2].

The equation of the envelope in terms of cometocentric coordinates $\xi, \eta$ (the origin of the coordinate system being at the nucleus while the $\xi$-axis is along the radius vector and the $\eta$-axis is perpendicular to both the $\xi$-axis and the line of sight) has the form

$$\eta^2 = 2\xi\eta_0 + \eta_0^2,$$

---

*This indeterminacy is quite understandable on purely mechanical grounds: it is impossible to determine acceleration from two measurements of position (in Eddington's case, two positions of the envelope and the interval of time between them).

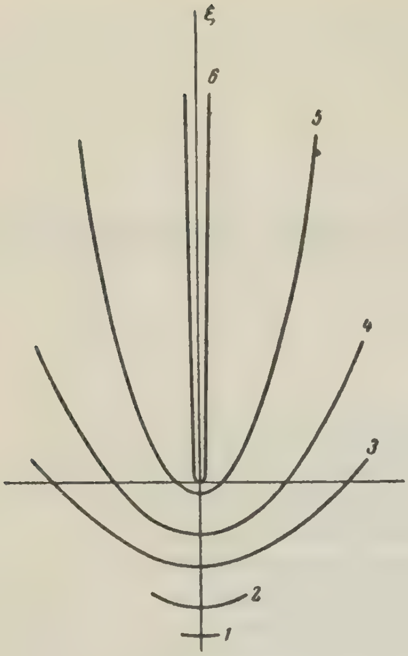

Fig. 1.

where $\eta_0 = \frac{g^2}{R}$, and $R = \frac{k^2(1+\mu)}{r^2}$.

The time $\tau$ necessary for a particle to reach the envelope after emission from the nucleus is given by

$$\tau = \sqrt{\frac{2}{R}}\sqrt[4]{\xi^2 + \eta^2}.$$

The envelopes are undoubtedly gaseous and the repulsive forces due to the sun are none other than the radiation pressure and therefore the quantities $1 + \mu$ should be discrete, and we are justified in assuming that any separate envelope is formed only by one definite repulsive force due to the sun.

If one takes two photographs of the head, one after another, at the moments $M_1$ and $M_2$, and on each of them one determines the coordinates $\xi$ and $\eta$ for a number of points and hence $\eta_0 = -\xi + \sqrt{\xi^2 + \eta^2}$, then it is always possible to find points having the same $\eta_0$ on both the first and the second photographs.

Since $\eta_0 = g^2/R$ and R is the same for all points in an envelope, it follows that g (the initial velocity) increases with increasing $\xi$ (cf. Table 2), for example, points 5 and 11 for which $\eta_0 = 0.20 \cdot 10^{-3}$. Molecules at these points are emitted from the nucleus with the same velocity ($g^2 = R\eta_0$) and therefore, according to Eddington, simultaneously (Table 2).

It is therefore possible to write

$$\tau_1 = \sqrt{\frac{2}{R}}\sqrt[4]{\xi_1^2 + \eta_1^2} \quad \text{and} \quad \tau_2 = \sqrt{\frac{2}{R}}\sqrt[4]{\xi_2^2 + \eta_2^2}.$$

The quantities $\tau_1$, $\tau_2$ and R are unknown to us but since, according to Eddington, the molecules are emitted from the nucleus simultaneously $\tau_2 - \tau_1 = M_2 - M_1$ and from the formula

$$M_2 - M_1 = \sqrt{\frac{2}{R}}\left(\sqrt[4]{\xi_2^2 + \eta_2^2} - \sqrt[4]{\xi_1^2 + \eta_1^2}\right)$$

TABLE 1

| Data | $1+\mu$ |
|---|---|
| September 17 | 4 000 |
| October 2 | 730 |
| 2 | 930 |
| 14 | 8 000 |
| 15 | 10 500 |
| 27 | 12 000 |
| 27 | 11 000 |
| 27 | 16 000 |
| 27 | 12 000 |
| November 3 | 700 |
| 10 | 3 500 |

it is possible to calculate R and consequently $1 + \mu$ and g. Eddington [1] obtained the values given in Table 1 for $1 + \mu$.

These enormous values of accelerations $1 + \mu$ (from 700 to 16,000) and initial velocities g (from 10 to 100 km/sec) differ considerably from the well known values of $1 + \mu$ and g in the tails of comets (obtained from motion of cloud formations; $1 + \mu$ from 25 to 200 and g = 1 km/sec approx.) and in the head ($1 + \mu$ from 0.5 to 4.5 and g about 1 km/sec).

Eddington himself thought that the values he obtained were improbable, but he could not find any other suitable mechanism which could explain the observed shifts of envelopes.

The mechanism of the bursts remained incomprehensible (enormous velocities of up to 100 km/sec, their systematic decrease, and the strange property of giving the same velocity to the emitted molecules to begin with [the tops of the envelopes usually appear at the same distances from the nucleus]).

Apparently, there is only one admissible mechanism which leads to the emission of molecules from the surface layers of nuclei, i.e., their thermal energy. It should be noted that at a given temperature an appreciable number of molecules have thermal velocities which do not differ very much from the most probable velocities,

TABLE 2

| | $\zeta \cdot 10^{-8}$ | $\eta \cdot 10^{-8}$ | $\sqrt{\zeta^2+\eta^2} \cdot 10^{-8}$ | $\eta_0 \cdot 10^{-8}$ |
|---|---|---|---|---|
| | | 17.3417 September | | |
| 1 | −0.062 | 0.20 | 0.209 | 0.26 |
| 2 | +0.42 | 0.55 | 0.687 | 0.28 |
| 3 | 1.59 | 1.06 | 1.910 | 0.32 |
| | | 17.3792 September | | |
| 4 | 0.240 | 0.162 | 0.163 | 0.14 |
| 5 | 0.648 | 0.539 | 0.843 | 0.20 |
| 6 | 1.47 | 0.848 | 1.697 | 0.23 |
| 7 | 3.73 | 1.617 | 4.069 | 0.34 |
| 8 | 5.21 | 2.004 | 5.578 | 0.37 |
| | | 17.4196 September | | |
| 9 | 0.258 | 0.248 | 0.359 | 0.10 |
| 10 | 1.250 | 0.649 | 1.408 | 0.16 |
| 11 | 2.595 | 1.039 | 2.795 | 0.20 |
| 12 | 5.857 | 2.013 | 6.193 | 0.34 |

which at a distance r from the sun are given by

$$g = \frac{2.02}{\sqrt{M}\sqrt[4]{r}}\ \text{km/sec} \qquad \text{or} \qquad g = \frac{2.51}{\sqrt{M}\sqrt[4]{r}}\ \text{km/sec},$$

the first of these expressions being applicable to surface layers which transmit thermal energy into the nucleus, and the second to completely nonthermally conducting surfaces. For $C_2N_2$ ($M = 52$) at a distance $r = 1.3$ AU from the sun (September 17th) we have $g = 0.3$-$0.5$ km/sec while Eddington obtained 10-100 km/sec.

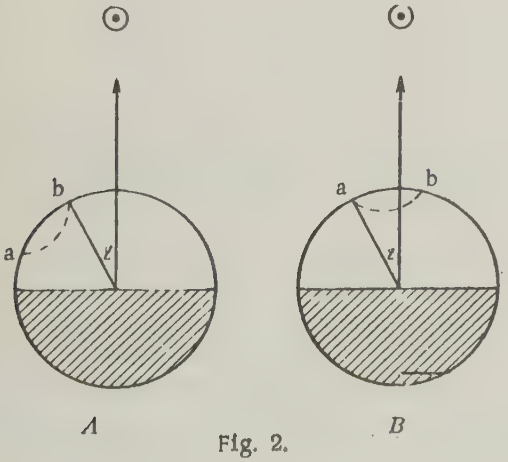

Fig. 2.

TABLE 3

| $1+\mu$ | $\eta_0 \cdot 10^{-8}$ | $\Delta\tau$ | g, km/sec |
|---|---|---|---|
| 3 000 | 0.20 | $0\overset{\mathrm{h}}{.}04$ | 20 |
| 1 000 | 0.20 | 0.07 | 12 |
| 500 | 0.20 | 0.10 | 7.4 |
| 5 | 0.20 | 1.0 | 0.83 |
| 1 | 0.20 | 2.22 | 0.37 |

In the case of the rotation of the nucleus and the thermal velocities a repetition of the same values of g after finite time intervals is inevitable. Then $M_2 - M_1 < \tau_2 - \tau_1$ and from all these possible values one must choose the admissible one. Here it is better to replace $\tau_2 - \tau_1$ by $\Delta\tau$.

Suppose that on the surface of the nucleus there is a region ab where a preferred emission of molecules occurs. The highest temperature in this region will occur when its center is as close as possible to the radius vector, and this will, of course, also correspond to maximum speed of molecules (Figure 2). We may assume that the degree of heating at various points of the region will be proportional to cos z (Figure 2). In the position A, the point b, heated by solar rays, will have a definite temperature and therefore also definite emission velocities, and the point a will for a time have the same temperature. In this case $\Delta\tau$ will not be equal to $M_2 - M_1$. Herein lies the solution to the problem of the enormous accelerations obtained by Eddington. In fact, we have two equations with three unknowns R, g and $\Delta\tau$:

$$\eta^2 = 2\xi\frac{g^2}{R} + \frac{g^4}{R^2} \quad \text{and} \quad \Delta\tau = \sqrt{\frac{2}{R}}\left(\sqrt[4]{\xi_2^2 + \eta_2^2} - \sqrt[4]{\xi_1^2 + \eta_1^2}\right).$$

From all of the possible solutions (cf. Table 3) we should choose only those which are physically admissible assuming that the reason for the emission of molecules is thermal energy of the surface layers of the nucleus. Hence g cannot be greater than 1 km/sec and 1 + $\mu$ cannot be greater than 5 (cf. Footnote on page 231).

A few solutions of the equation

$$\Delta\tau = \sqrt{\frac{2}{R}}\left(\sqrt[4]{\xi_2^2+\eta_2^2} - \sqrt[4]{\xi_1^2 + \eta_1^2}\right)$$

are given in Table 3 with $\eta_0 = 0.20 \cdot 10^{-3}$ and arbitrary values of 1 + $\mu$ (3000, 1000, etc.).

I would maintain that enormous accelerations and large initial velocities are not in fact present. Radial systems are nothing but the ends of envelopes with the associated small repulsive accelerations ~1 and initial velocities ~1 km/sec. In the spectra of these ends of envelopes one should see CN or $C_2$ bands just as, in general, in all heads of comets.

## LITERATURE CITED

[1] A. Eddington, Monthly Notices, Roy. Astron. Soc. 70, 442 (1910).

[2] S.V. Orlov, The Head of a Comet and the Classification of Cometary Forms (State Technical Press, 1945), p. 31.

Received August 17, 1956

Shternberg State Astronomical Institute

# DISTRIBUTION OF METEORIC RADIO ECHOES ACCORDING TO THEIR DURATION

## E. I. Fialko

The distribution of signals reflected from stable meteor trails according to their duration is considered.

A simplified analytical expression is given for the distribution of meteoric reflections of the stable type as a function of duration. Results are given of an experiment on a wavelength of $\lambda = 10$ m carried out during observations of sporadic meteors.

The agreement between experimental and theoretical data is satisfactory.

### 1. Preliminary Remarks

The duration of reflected radio signals from a meteoric trail depends on the level at which the duration is measured, the latter being determined by a number of parameters associated with the meteoric trail and the radio-locator.

For stable (long) meteoric trails [1] ($\alpha > 2.4 \cdot 10^{12}$)

$$\tau = 1.124 \cdot 10^{-12} \frac{\lambda^2}{16\pi^2 D} \cdot \alpha, \tag{1}$$

and for unstable (short) trails ($\alpha < 2.4 \cdot 10^{12}$)

$$\tau = \frac{\lambda^2}{16\pi^2 D}, \tag{2}$$

where $\tau$ is the duration of the reflected signal reckoned at the level $U_{max}/e$; $U_{max}$ is the maximum value of amplitude of the reflected signal; D is the coefficient of diffusion; $\lambda$ is the wavelength on which the radio-locator is operating, and $\alpha$ is the linear density of electrons in the meteoric trail.

The duration of a meteoric reflection of the unstable type (with visual or photographic recording) depends on the relation between $U_{max}$ and the noise level, since the time of observation of signals is the time during which the signal exceeds the noise level (Figure 1). The duration of a stable reflection [1] is not very dependent upon the relation between $U_{max}$ and the noise level since both the rise and the decay of echo amplitudes take place very rapidly in this case (Figure 1).

With usual radio locational observations of meteors, using photorecording of echo signals on a film which moves with the speed of a few cm/min, the duration of reflections can be sufficiently accurately measured in a few tenths of a second (or more).

Let us consider what kind of reflections corresponds to durations of $\tau \geq \tau_{min}$. From Equation (1)

$$\alpha_{min} = \tau_{min} \frac{16\pi^2 D \cdot 10^{12}}{1.124\lambda^2}. \tag{3}$$

If $\alpha > 2.4 \cdot 10^{12}$ then $\tau \geq \tau_{min}$ corresponds, in the main, to trails of the stable type.

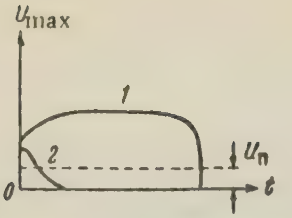

Fig. 1. The variation of the amplitude of the reflected signal: 1) $\alpha = 2 \cdot 10^{13}$ el/cm; 2) $\alpha = 2 \cdot 10^{12}$ el/cm; $U_n$ is the noise level.

If $\alpha < 2.4 \cdot 10^{12}$ then $\tau \geq \tau_{min}$ corresponds to trails of both types.

In the region of the meteoric zone [3] D ≈ 2-20 m²/sec. In the case $\lambda = 10$ m and $\tau_{min} \approx 1$ sec

$$\alpha_{min} \approx (2.8 - 28)\, 10^{12},$$

i.e., reflections longer than 1 sec are mainly due to stable trails.

If $\lambda = 10$ m the duration of a stable reflection is determined by the linear electron density $\alpha$ and by the coefficient of diffusion D:

$$\tau = 0.72 \cdot 10^{-12} \frac{\alpha}{D}. \tag{4}$$

The distribution of meteors with respect to $\tau$ depends on the distribution of meteors with respect to $\alpha$ and D.

The linear electron density is equal to [2]

$$\alpha = \frac{\beta}{\mu H} \cos\chi \cdot \frac{p}{p_{max}} \left[1 - \frac{1}{3} \frac{p}{p_{max}}\right] m, \tag{5}$$

where $\beta$ is the probability that as a result of evaporation of one meteoric atom, one free electron will be liberated; $\mu$ is the mass of the meteoric atom; H is the height of a uniform atmosphere (at the point of reflection); $\chi$ is the zenith distance of the radiant of the meteor; p is the atmospheric pressure (at the point of reflection of the radio waves); $p_{max}$ is the pressure at the point of the most intense evaporation of the meteoric body; m is the mass of the meteoric body (before the beginning of the evaporation process). From (4) and (5)

$$\tau = A_1 m, \tag{6}$$

where

$$A_1 = 0.72 \cdot 10^{-12} \frac{\beta}{\mu H} \cos\chi \cdot \frac{p}{p_{max}} \left[1 - \frac{1}{3} \frac{p}{p_{max}}\right]^2 \frac{1}{D}. \tag{7}$$

The coefficient $A_1$ depends on the zenith distance of the radiant of the meteor, the speed of the meteor, the height where the reflecting part of the meteor body is located, etc.

Thus, in order to discover the law of distribution of meteors as a function of the duration of reflections it is necessary to know the law of distribution of meteoric bodies as functions of mass, radiants, velocity, etc.

A rigorous solution of this problem presents considerable difficulties and is beyond the scope of the present work.

## 2. A Simplified Representation of the Distribution of Meteors According to the Duration of Reflections

Let us consider, as a first very rough approximation, that the functional dependence $\tau(m)$ is of the form

$$\tau = cm, \tag{7}$$

where c is a constant.

The differential law of distribution of meteoric bodies with mass is usually presented in the form [2]:

$$p_m(m) = \frac{b}{m^S}, \tag{8}$$

where b and S are constants.

The differential law of distribution of meteors with duration will, as is easily shown using (7) and (8), have the form

$$p_\tau(\tau) = \frac{A_2}{\tau^S}, \tag{9}$$

where $A_2 = bc^{S-1}$.

The integral law of distribution of meteors with duration is

$$P_\tau(\tau) = \int_\tau^\infty p_\tau(\tau)\, d\tau = \frac{A_2}{S-1} \frac{1}{\tau^{S-1}}. \tag{10}$$

In considering the duration of reflections $\tau \geq \tau_{min}$ we shall normalize $P_\tau(\tau_{min})$:

$$P_\tau(\tau_{min}) = 1. \tag{11}$$

From (10) and (11)

$$\frac{A_2}{S-1} = \tau_{min}^{S-1} \tag{12}$$

and thus

$$P_\tau(\tau) = \frac{\tau_{min}^{S-1}}{\tau^{S-1}}. \tag{13}$$

The number of meteors N giving reflections with the duration $\tau \geq \tau_{min}$ will be

$$N = N_\Sigma P_\tau(\tau) = N_\Sigma \frac{\tau_{min}^{S-1}}{\tau^{S-1}}, \tag{14}$$

where $N_\Sigma$ is the total number of recorded meteoric echoes.

In the case of sporadic meteors $S \approx 2$ [2] and

$$N = N_\Sigma \frac{\tau_{min}}{\tau}. \tag{15}$$

## 3. Experimental Results

Table 1 gives the meteoric reflections having durations not less than 0.5 sec.

During 6 hours 4 minutes of continuous observations 223 of such reflections were observed (out of a total number of 976).

These observations were carried out on September 13, 1956 in the Tomsk district using a radio-locator constructed at the Tomsk Polytechnical Institute for radio-locational observations of meteors.

The main characteristics of the apparatus were: wavelength $\lambda = 10$ m; pulse length $\tau_p = 5\ \mu$sec; power per pulse, $p \approx 100$ kilowatt; the antenna was a horizontal half-wave vibrator placed above the earth's surface at a height of $\lambda/3$; the frequency $F_p = 300$-$600$ pulses per sec; a provision was made for sending out of "divided" pulses, and the meteoric echo was fixed on a photographic film moving continuously with the speed of 60 mm/min.

From the observational data (Table 1) the number N of meteors with durations exceeding 0.5, 1, 1.5, 2, 3, 4, 5, 10 and 60 secs (Table 2) was counted.

In Figure 2 the experimental data are represented by points and the dotted line is obtained from Equation (15) for $N_\Sigma = 223$ and $\tau_{min} = 0.5$ sec.

TABLE 1

Meteoric Reflections with Duration ≥0.5 sec (from photographic recording of meteoric radio echoes)

| No. of film | No. of meteors | Local time | Distance, km | Duration, sec | No. of film | No. of meteors | Local time | Distance, km | Duration, sec |
|---|---|---|---|---|---|---|---|---|---|
| 11 | 1 | $1^h02^m$ | 210 | 2.1 | | 64 | — | 240 | 1 |
| | 2 | — | 260 | 0.5 | | 65 | $2^h26^m$ | 150 | 2 |
| | 3 | — | 350 | 1.5 | | 66 | 2 28 | 170 | 0.5 |
| | 4 | 1 03 | 110 | 0.8 | | 67 | — | 130 | 2 |
| | 5 | 1 07 | 140 | 2.2 | | 68 | — | 120 | 0.8 |
| | 6 | 1 08 | 130 | 0.8 | | 69 | 2 30 | 140 | 1 |
| | 7 | 1 09 | 140 | 0.9 | | 70 | 2 31 | 140 | 1 |
| | 8 | 1 12 | 220 | 1 | | 71 | — | 180 | 0.8 |
| | 9 | 1 13 | 130 | 1 | | 72 | 2 33 | 240 | 0.8 |
| | 10 | 1 18 | 130 | 1 | | 73 | — | 140 | 0.6 |
| | 11 | — | 170 | 0.5 | | 74 | 2 34 | 170 | 4 |
| | 12 | 1 20 | 200 | 1 | | 75 | — | 180 | 33 |
| | 13 | 1 21 | 380 | 1 | | 76 | 2 35 | 140 | 0.6 |
| | 14 | — | 150 | 5.0 | | 77 | 2 36 | 160 | 0.5 |
| | 15 | 1 22 | 370 | 0.7 | | 78 | 2 38 | 190 | 1.5 |
| | 16 | — | 110 | 0.9 | | 79 | — | 170 | 2 |
| | 17 | 1 24 | 160 | 0.8 | | 80 | 2 43 | 160 | 0.5 |
| | 18 | 1 25 | 140 | 0.9 | | 81 | 2 44 | 200 | 10 |
| | 19 | 1 26 | 270 | 5.0 | | 82 | — | 180 | 1 |
| 10 | 20 | 1 31 | 140 | 0.5 | | 83 | — | 180 | 1 |
| | 21 | 1 34 | 180 | 1.5 | | 84 | 2 46 | 130 | 0.5 |
| | 22 | 1 36 | 110 | 1 | | 85 | — | 130 | 0.5 |
| | 23 | 1 44 | 155 | 1 | | 86 | 2 47 | 280 | 2 |
| | 24 | 1 45 | 200 | 1.5 | | 87 | 2 49 | 200 | 0.6 |
| | 25 | — | 180 | 10 | | 88 | — | 270 | 3 |
| | 26 | 1 48 | 140 | 2 | | 89 | 2 50 | 130 | 1 |
| | 27 | 1 49 | 260 | 0.5 | | 90 | 2 53 | 110 | 1 |
| | 28 | 1 50 | 110 | 0.5 | | 91 | — | 150 | 1 |
| | 29 | 1 51 | 130 | 1 | | 92 | — | 160 | 1.5 |
| | 30 | 1 53 | 220 | 0.8 | | 93 | 2 55 | 120 | 0.5 |
| | 31 | 1 53 | 180 | 1 | 8 | 94 | 3 05 | 140 | 3 |
| | 32 | 1 54 | 160 | 3 | | 95 | 3 06 | 120 | 2.5 |
| | 33 | 1 56 | 230 | 0.5 | | 96 | 3 07 | 170 | 5 |
| | 34 | 1 58 | 180 | 3 | | 97 | — | 150 | 1 |
| | 35 | — | 170 | 0.5 | | 98 | — | 140 | 0.5 |
| | 36 | 1 59 | 130 | 1.5 | | 99 | 3 08 | 160 | 0.5 |
| | 37 | 2 01 | 150 | 0.5 | | 100 | — | 200 | 0.5 |
| | 38 | 2 03 | 130 | 1 | | 101 | 3 08 | 165 | 0.5 |
| | 39 | 2 04 | 180 | 1 | | 102 | 3 08 | 130 | 1 |
| | 40 | — | 110 | 0.5 | | 103 | 3 09 | 140 | 0.6 |
| | 41 | 2 05 | 140 | 0.5 | | 104 | — | 220 | 0.5 |
| | 42 | — | 130 | 0.5 | | 105 | 3 10 | 150 | 0.5 |
| | 43 | — | 160 | 1.5 | | 106 | 3 11 | 120 | 1.2 |
| | 44 | 2 06 | 130 | 1 | | 107 | — | 140 | 0.5 |
| | 45 | 2 07 | 180 | 1 | | 108 | 3 12 | 165 | 0.8 |
| | 46 | 2 08 | 220 | 0.5 | | 109 | 3 14 | 230 | 0.5 |
| | 47 | 2 09 | 220 | 2 | | 110 | 3 18 | 240 | 0.5 |
| | 48 | 2 10 | 175 | 2 | | 111 | 3 20 | 180 | 1 |
| | 49 | — | 150 | 3 | | 112 | 3 23 | 160 | 0.5 |
| | 50 | — | 180 | 12 | | 113 | 3 24 | 200 | 0.5 |
| | 51 | 2 16 | 150 | 0.5 | | 114 | 3 25 | 200 | 2.5 |
| | 52 | — | 240 | 0.5 | | 115 | 3 35 | 130 | 2 |
| | 53 | 2 17—18 | 190 | 3 | | 116 | — | 110 | 1 |
| | 54 | — | 180 | 1.5 | | 117 | 3 37 | 310 | 0.8 |
| | 55 | — | 190 | 0.5 | 7 | 118 | 3 38 | 220 | 1.5 |
| | 56 | 2 19 | 180 | 1.5 | | 119 | 3 39 | 150 | 0.5 |
| | 57 | — | 170 | 0.5 | | 120 | 3 41 | 180 | 16 |
| | 58 | 2 20 | 140 | 0.5 | | 121 | 3 42 | 170 | 1.5 |
| | 59 | 2 21 | 140 | 1.2 | | 122 | 3 43 | 200 | 1.5 |
| | 60 | — | 160 | 0.5 | | 123 | — | 220 | 0.8 |
| | 61 | 2 22 | 260 | 1 | | 124 | — | 210 | 0.5 |
| | 62 | 2 23 | 170 | 1 | | 125 | 3 44 | 170 | 0.5 |
| | 63 | 2 24 | 200 | 0.5 | | 126 | 3 45 | 160 | 0.5 |

TABLE 1 (continued)

| No. of film | No. of meteors | Local time | Distance, km | Duration, sec |
|---|---|---|---|---|
| | 127 | $3^h46^m$ | 250 | 1.5 |
| | 128 | — | 170 | 0.8 |
| | 129 | — | 220 | 1 |
| | 130 | 3 47 | 145 | 1 |
| | 131 | 3 48 | 250 | 3 |
| | 132 | 3 49 | 170 | 1.5 |
| | 133 | … | 140 | 0.8 |
| | 134 | 3 54 | 120 | 2.5 |
| | 135 | — | 200 | 7 |
| | 136 | 4 00 | 115 | 0.8 |
| | 137 | 4 03 | 290 | 1 |
| | 138 | — | 320 | 4 |
| | 139 | 4 04 | 120 | 1 |
| | 140 | 4 07 | 220 | 102 |
| | 141 | — | 160 | 7 |
| | 142 | 4 08 | 160 | 1 |
| | 143 | 4 12 | 205 | 7 |
| 6 | 144 | 4 15 | 190 | 0.5 |
| | 145 | 4 15 | 190 | 1 |
| | 146 | 4 16 | 100 | 1 |
| | 147 | 4 17 | 160 | 0.8 |
| | 148 | 4 23 | 150 | 0.5 |
| | 149 | 4 36 | 140 | 3 |
| | 150 | — | 120 | 2 |
| | 151 | 4 37 | 130 | 0.8 |
| | 152 | 4 41 | 130 | 2 |
| | 153 | 4 43 | 180 | 0.8 |
| | 154 | — | 160 | 2 |
| | 155 | — | 110 | 0.8 |
| | 156 | 4 44 | 200 | 0.5 |
| | 157 | 4 46 | 270 | 0.8 |
| | 158 | — | 140 | 0.5 |
| | 159 | — | 190 | 1.2 |
| | 160 | 4 49 | 230 | 0.5 |
| | 161 | 4 51 | 170 | 0.8 |
| | 162 | 4 52 | 120 | 0.5 |
| 5 | 163 | 5 00 | 160 | 4 |
| | 164 | 5 07 | 240 | 0.8 |
| | 165 | 5 08 | 110 | 3 |
| | 166 | — | 150 | 0.6 |
| | 167 | 5 09 | 140 | 0.8 |
| | 168 | — | 120 | 0.5 |
| | 169 | — | 150 | 0.5 |
| | 170 | 5 11 | 120 | 1 |
| | 171 | 5 12 | 150 | 0.8 |
| | 172 | 5 13 | 180 | 2 |
| | 173 | 5 16 | 160 | 4.5 |
| | 174 | 5 18 | 170 | 0.5 |
| | 175 | 5 23 | 200 | 3 |
| | 176 | 5 31 | 150 | 1 |
| 4 | 177 | $5^h32^m$ | 190 | 1 |
| | 178 | 5 34 | 120 | 0.8 |
| | 179 | 5 36 | 110 | 0.6 |
| | 180 | 5 38 | 330 | 0.8 |
| | 181 | 5 39 | 165 | 1.3 |
| | 182 | 4 40 | 260 | 0.7 |
| | 183 | 5 41 | 170 | 4.5 |
| | 184 | 5 43 | 315 | 0.5 |
| | 185 | 5 48 | 190 | 1.5 |
| | 186 | — | 250 | 1.2 |
| | 187 | 5 54 | 200 | 0.6 |
| | 188 | 6 02 | 170 | 0.8 |
| | 189 | — | 215 | 3.5 |
| | 190 | 6 04 | 170 | 0.5 |
| | 191 | 6 05 | 150 | 0.5 |
| | 192 | 6 12 | 190 | 1.2 |
| | 193 | — | 160 | 1.8 |
| | 194 | 6 16 | 230 | 2.5 |
| | 195 | 6 17 | 150 | 2.0 |
| | 196 | 6 20 | 170 | 1 |
| | 197 | — | 270 | 6 |
| | 198 | 6 23 | 210 | 0.8 |
| | 199 | 6 24 | 150 | 5 |
| | 200 | 6 27 | 150 | 3.5 |
| | 201 | 6 32 | 150 | 4.2 |
| | 202 | 6 33 | 170 | 6 |
| | 203 | — | 160 | 0.5 |
| | 204 | 6 35 | 150 | 0.5 |
| | 205 | 6 35 | 180 | 20.8 |
| | 206 | — | 170 | 1 |
| | 207 | 6 36 | 130 | 2 |
| | 208 | 6 37 | 150 | 2 |
| | 209 | 6 38 | 260 | 0.5 |
| 2 | 210 | 6 39—40 | 140 | 0.5 |
| | 211 | — | 130 | 0.5 |
| | 212 | — | 110 | 0.8 |
| | 213 | 7 01 | 210 | 0.5 |
| | 214 | 7 03 | 110 | 0.5 |
| | 215 | — | 110 | 10.5 |
| | 216 | 7 07 | 100 | 1 |
| | 217 | 7 12 | 130 | 0.5 |
| | 218 | 7 13 | 300 | 4 |
| | 219 | — | 120 | 0.8 |
| | 220 | 7 14 | 140 | 5.5 |
| 1 | 221 | 7 22 | 160 | 3.5 |
| | 222 | 7 26 | 145 | 1.5 |
| | 223 | 7 29 | 125 | 1.5 |

TABLE 2

| $\tau \geqslant \tau_{\min}$ sec | $\tau \geqslant 0.5$ | $\tau \geqslant 1$ | $\tau \geqslant 1.5$ | $\tau \geqslant 2$ | $\tau \geqslant 3$ | $\tau \geqslant 4$ | $\tau \geqslant 5$ | $\tau \geqslant 10$ | $\tau \geqslant 60$ |
|---|---|---|---|---|---|---|---|---|---|
| $N$ | 223 | 121 | 76 | 60 | 39 | 25 | 18 | 8 | 1 |

$$N = \frac{111.5}{\tau}. \tag{16}$$

The curve which approximates to the experimental results may be presented in the form

$$N = \frac{c_1}{\tau^n}, \qquad (17)$$

where $c_1$ and n are constants. The exponent n is found from

$$n = \frac{\log \frac{N_1}{N_2}}{\log \frac{\tau_2}{\tau_1}}, \qquad (18)$$

where $N_1$ and $N_2$ are the numbers of reflections with durations exceeding $\tau_1$ and $\tau_2$, respectively.

When $\tau_1 = 0.5$ sec, $N_1 = 223$; $\tau_2 = 10$ sec, $N_2 = 8$, and $n \approx 1.11$, i.e.,

$$N \sim \frac{1}{\tau^{1.11}}. \qquad (19)$$

In spite of the fact that the analytical expression for the distribution of meteors with duration of reflections (15) was obtained on the basis of very rough assumptions, (7), and in spite of the fact that in the experimental data which included reflections with $0.5 < \tau < 1$ sec, to which echoes of the intermediate type correspond ($\alpha \approx 10^{12}$), the divergence between experimental and analytical data is not very great.

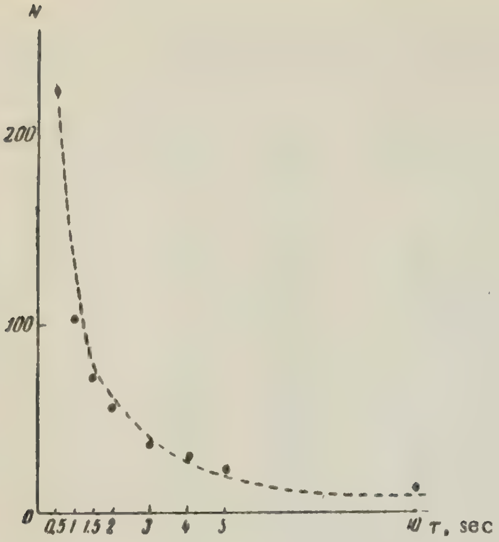

Fig. 2. The distribution of meteors with the duration of reflections from ionized trails. N = number of meteors with durations not less than $\tau_{(\mathrm{sec})}$. The curve is constructed using analytical data; points – from experiment.

I wish to thank F.I. Peregudov and E.K. Nemirova for carrying out the observations.

## SUMMARY

The number of sporadic meteors which give rise to reflections of the stable type ($\alpha > 2.4 \cdot 10^{12}$) with durations exceeding some value $\tau$ is inversely proportional to the duration, i.e., $N \sim 1/\tau$.

## LITERATURE CITED

[1] T.R. Kaiser and R.L. Closs, Phil. Mag. 43, No. 336 (1952).

[2] T.R. Kaiser, S. Adv. Phys. 2, No.8 (1953).

[3] J.S. Greenhow and E.L. Neufeld, J. Atmospheric Terrest. Phys. 6, No. 2-3 (1955).

Received November 20, 1956

Kirov Polytechnical Institute, Tomsk

# THE INFRARED SPECTRUM OF THE NORTHERN NIGHT SKY IN THE REGION 9500-11,500 A

## N. I. Fedorova

Determinations were made of the relative intensity of hydroxyl bands in the 9,500-11,500 A region of the Northern night-sky spectrum, obtained in February, 1955, in the Murmansk area, using a spectrograph with an electron optical transducer, dispersion ~230 A/mm. Results of the measurement were compared with the absolute intensities of hydroxyl bands in the near infrared region, computed by Roach. Appreciable discrepancies occurred.

A considerable portion of the radiation in auroral spectra obtained in 1955 in the Murmansk area was attributable to the night sky. In his recent paper, Roach [1] adduced the absolute intensities of hydroxyl bands in the near infrared, obtained by appropriate conversion of the data of Roach, Pettit and Williams [2] for the visible region, according to transition probabilities computed by I.S. Shklovskii [3]. The absolute intensity of hydroxyl radiation in the region extending from $4.4\mu$ to the border of the visible spectrum, based on Roach's data, is equal to $10^6$ R* (the night-sky green-line intensity, expressed in the same units, is equal to 250 R), for which reason it is not surprising that hydroxyl bands stood out sharply on some of our exposures, where the auroral display was weak. One of these spectra** is shown in Figure 1, while Figure 2 gives the corresponding intensity distribution, but without corrections for atmospheric absorption.

This spectrum was obtained on February 19-21, 1955, with a 24-hour exposure using the apparatus and procedure described in an earlier paper [5]. While the exposures were being made, the spectrograph was trained to the north at an angle roughly 45° to the horizon. 3-0 bands were present in the spectrum, as Johnson reported. The Q branch of the spectrum was clearly visible and lines of the P branch were resolved, although the 3-0 band, as V.I. Krasovskii has shown [6], is very weak. The $P_1$ and $P_2$ lines of the 4-1 band showed poor resolution, although they were clearly resolved in other bands, while, in addition, the intensity in this region was unusually high. Probably, as has been already suggested in a previous paper [5], there is in this region an enhancement of radiation originating from a nonhydroxyl source.

Roach's paper provides absolute intensities for the hydroxyl bands in terms of R units. The intensities for the spectral region concerned in our discussion are given in Table 2. In the 4th column, for convenience, intensity is reported relative to the 4-1 band. In the 5th and subsequent columns, rough evaluations of the relative intensities of hydroxyl bands in our spectrum are given, expressed in arbitrary units. These evaluations were made without correction for atmospheric absorption.

The intensity of the 6-3 band is not given, since it was determined with very poor accuracy owing to a falloff in the sensitivity of the apparatus in this region and, in addition, it was set for the region of strong water-vapor absorption.

---

*The new unit of measurement for night-sky brightness, the "Rayleigh" (R), adopted at the Conference of the Special International Committee on the IGY, at Barcelona, defined by the formula $4\pi B = 1$ rayleigh = 1 R.

**Wavelength measurements for this spectrum were in rather good agreement with the measurements and calculations, reported by several authors [4], for the hydroxyl spectrum in this region, although there are several discrepancies, as is clear from Table 1, where, together with our measurements, the latest measurements performed by Johnson [4] are presented.

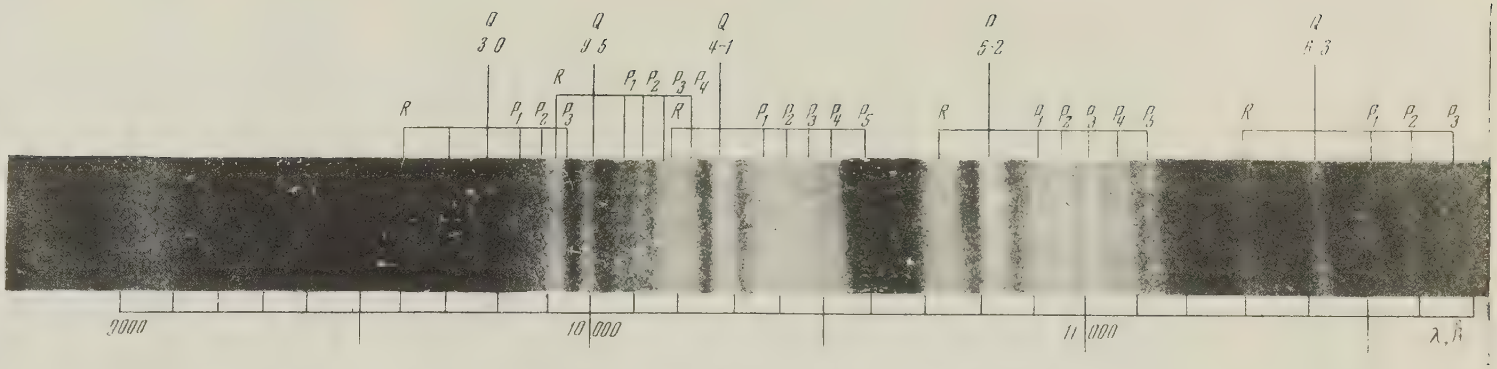

Fig. 1.

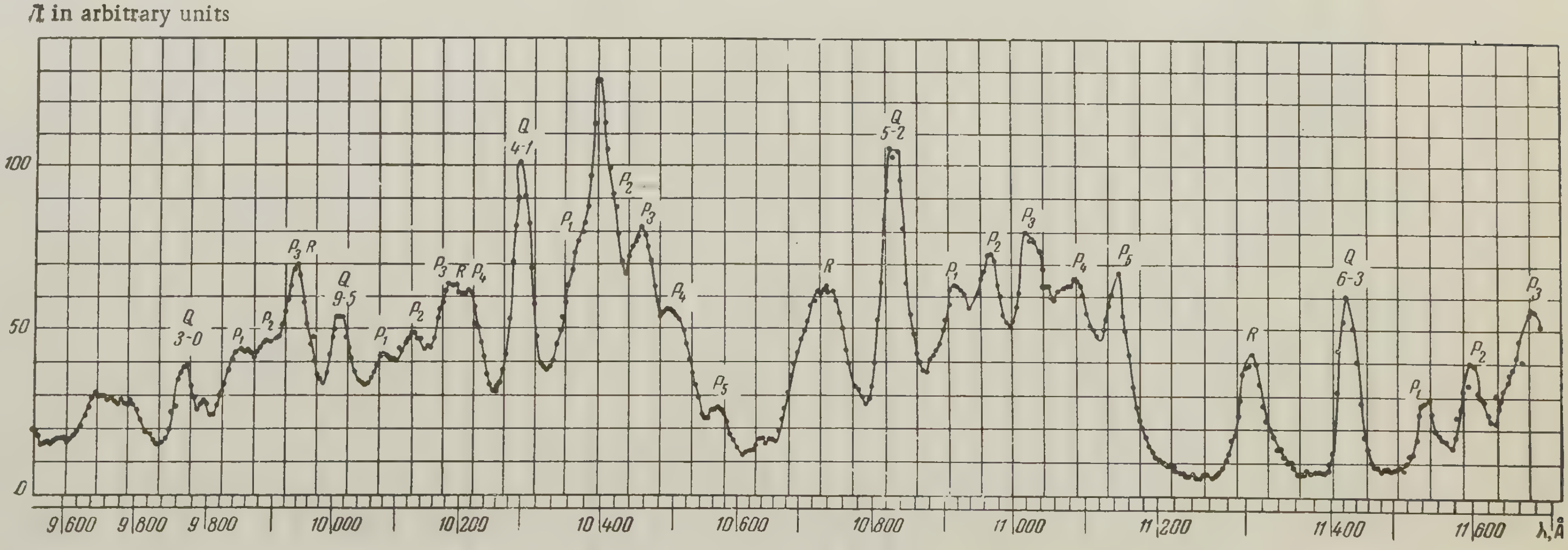

Fig. 2. Relative intensities of hydroxyl bands in northern night-sky spectrum.

TABLE 1

| Wavelength measurements, A | Identification | Johnson's data | Measurements | Identification | Johnson's data |
|---|---|---|---|---|---|
| 9793 | (3—0) OH | 9796 | 10446 | P (4) (4—1) OH | 10469 |
| 9868 | *P* (2) (3—0) OH | 9875 | 10520 | *P* (5) (4—1) OH | |
| 9894 | *P* (3) (3—0) OH | 9917 | 10578 | *P* (6) (4—1) OH | 10831 |
| 10014 | *Q* (9—5) OH | 10015 | 10924 | *P* (2) (5—2) OH | 10923 |
| 10076 | *P* (2) (9—5) OH | 10086 | 10968 | *P* (3) (5—2) OH | 10972 |
| 10122 | *P* (3) (9—5) OH | 10124 | 11026 | *P* (4) (5—2) OH | |
| 10163 | *P* (4) (9—5) OH | 10171 | 11084 | *P* (5) (5—2) OH | |
| 10218 | *P* (5) (9—5) OH | 10224 | 11140 | *P* (6) (5—2) OH | |
| 10290 | *Q* (1) (4—1) OH | 10287 | 11430 | *Q* (6—3) OH | |
| 10360 | *P* (2) (4—1) OH | 10373 | 11536 | *P* (2) (6—3) OH | |
| 10410 | *P* (3) (4—1) OH | 10418 | 11594 | *P* (3) (6—3) OH | |
| | | | 11656 | *P* (4) (6—3) OH | |

Measurements for the P branch refer to the strong component.

TABLE 2

| λ, A | $V'-V''$ | Intensity, R (Roach) | $I/I_{4-1}$ | $I_Q$ | $I_Q/I_{Q\,(4-1)}$ | I-bands | $I_b/I_{b(4-1)}$ |
|---|---|---|---|---|---|---|---|
| 9788 | 3—0 | 440 | 0.26 | 14 | 0.4 | 82 | 0.4 |
| 10010 | 9—5 | 5770 | 3.41 | 20 | 0.5 | 95 | 0.5 |
| 10380 | 4—1 | 1690 | 1.0 | 39 | 1.0 | 192 | 1.0 |
| 10380 | 5—2 | 4000 | 2.37 | 45 | 1.1 | 246 | 1.3 |
| 14440 | 6—3 | 7000 | 4.14 | — | — | — | — |

$I_Q$ is the intensity of Q branch; $I_b$ is the integral intensity of band.

As is clear from Figure 2 and Table 1, Roach's data agree closely with our measurements. According to our measurements, the 5-2 band is only slightly more intense than the 4-1 band. A correction for atmospheric absorption can have a material effect only on the last lines of the P branch, which hardly affects the over-all intensity of the band. The intensities of the Q branches of the bands are approximately identical. Discrepancies in evaluation of the 9-5 band intensity are even more substantial. Its intensity, as reported by Roach, is rather high. According to our findings, it is slightly greater in intensity than the 3-0 band, but appreciably weaker than the 4-1 and 5-2 bands. Our evaluations of the hydroxyl-band intensities coincide with evaluations reported by V.T. Lukashenia and V.I. Krasovskii [7].

## LITERATURE CITED

[1] Roach, Manual for photometric observations of the airglow during the International Geophysical Year., meeting of CSAGJ at Barcelona (September, 1956).

[2] Roach, Pettit and Williams, J. Geophys. Research 55, 183 (1950).

[3] I.S. Shklovskii,"The intensity of vibrational-rotational hydroxyl bands, Report to the Conference on Molecular Spectroscopy (June, 1956).*

[4] I.S. Shklovskii, Izvestiya Krymskoi Astrofizicheskoi Observatorii 7, 34 (1955); A. Vallance Jones, Nature 175, 950 (1955); R.C. Herman and G.A. Hornbeck, Astrophys. J. 118, 214 (1953); A.B. Meinel, Astrophys. J. 111, 55 (1950).

[5] B.A. Bagariatskii and N.I. Fedorova, Proc. Acad. Sci. USSR 103, 6, 1009 (1955).

[6] V.I. Krasovskii, Proc. Acad. Sci. USSR 77, 3, 395 (1951); V.I. Krasovskii, V.T. Lukashenia, Proc. Acad. Sci. USSR 80, 5, 241 (1951).

---

*In Russian.

[7] V.T. Lukashenia and V.I. Krasovskii, Proc. Acad. Sci. USSR 79, 2, 241 (1951).

Received November 13, 1956

Institute of Atmospheric Physics
Academy of Sciences, USSR

# A NEW METHOD FOR DETERMINING THE PHOTOGRAPHIC POSITIONS OF CELESTIAL OBJECTS

Kh. I. Potter

A new method is proposed for solving the classical problem of photographic astrometry – the determination of the position of a celestial object near the optical center, using reference stars. This method differs from that of Turner (6 constants) and Merton ("position lines") in that the angles between the directions from the optical center to separate stars are used. If these angles are measured, the influence of radial aberrations is wholly excluded, i.e., coma, astigmatism, lateral chromatic aberration, distortion and also an inaccurate scale value, the possible difference of the scale in different azimuths or the curvature of the focal plane if reflectors of the Maksutov or Schmidt type are used. As the stellar images are symmetrical to radial directions, the accidental errors of measurement are decreased considerably. The proposed method is expedient if there are few reference stars on the plate, unsymmetrically distributed around the object and far from the optical center. Such cases may arise if long-focus astrographs with a small field are used, and also for photographic observations of the moon, when the central part of the plate is fogged.

§1. The most widely used method for determining the exact position of a celestial object on a photographic plate is considered to be the method of six constants, advanced by Turner in 1893 [1]. In some special cases (plates with a large field, low zenith distances), a modification of the Turner method is resorted to, with quadratic terms included in the equation. Both the Turner method and the Schlesinger "method of dependences" derived from it require measurements of the rectangular coordinates of reference stars and of the object to be determined [2, 3].

In 1953, G. Merton worked out the so-called "position line method," which requires measurement of the distances from the object to be determined to reference stars [4]. This technique may be utilized with the simplest type of measuring device on hand, since it demands measurements on only one coordinate. However, the derivation of corrections to be applied to the measured quantities and the graphic method for finding unknown quantities are not sufficiently rigorous. The Merton method should therefore be assigned to the category of approximate methods – those which resolve a problem with the aid of a limited number of reference stars (cf. the Deutsch, König, Kaiser, Blazhko, etc., methods [5]). We mention this method in the present discussion, since it has a certain interest from the methodological standpoint.

There exist a number of astrometric problems which require the highest order of accuracy in solutions using astrophotographic methods. Among such problems may be included, for example: the determination of the positions of asteroids (Eros, et al.) for the derivation of the value of the solar parallax; observations of selected asteroids for the orientation of star catalogs; lunar observations for the determination of ephemeris time and for the solution of some geodetic problems. The rigor of the requirements for the distribution of the reference stars (proximity to the optical center and to the object to be determined, uniformity of stellar magnitudes and spectral classes) demands the use of small-scale astrographs with medium focal length, for the solution of such problems. The limited number of stars in the zone catalogs acts as an obstacle to the use of long-focus astrographs with a small field. Particular difficulty is encountered in the choice of reference stars for photographs of the moon, because of considerable fogging over a wide area adjoining the center of the plate.

The method proposed in the present paper for measurement and treatment of photographs makes it possible to eliminate some of the causes having a negative effect on the accuracy of results where an unfortunate distribution of reference stars is involved. It makes it possible to utilize the stars at a considerable distance from the center, without running the risk of causing random and systematic errors.

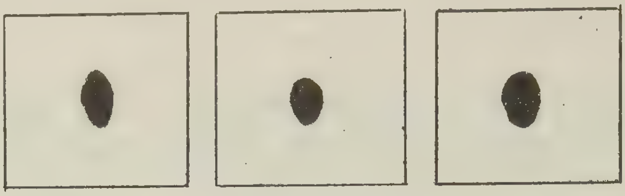

Fig. 1.

§ 2. In the measurement of stars very close to the edge of the plate, asymmetry of the stellar images due to the effect of various off-axis aberrations of the objective is encountered. Coma and astigmatism, in the first instance, may be assigned to that category of aberrations, as well as lateral chromatic aberration, exerting a different effect for stars of different spectral classes. The position of the geometric center of the image is displaced relative to the center of blackening, the position of which becomes blurred. Figure 1 shows a view of stellar images of the 8-9th magnitude at a distance of $\approx 1°$ from the center of the plates of the Pulkov normal astrograph. Distortion, though it does not disturb the symmetry of the image, leads to a displacement of the star by an amount proportional to the cube of the distance from the center of the plate. It is important to note that all of the aberrations enumerated which distort the stellar image on the edge act in a radial direction.

The setting of the micrometer thread in measuring such asymmetric star images in rectangular coordinates is very difficult (Figure 2a). For this reason, stars located far from the center of the plate are neglected in measurements when photographs are mapped in rectangular coordinates. But this is not always feasible, as, for instance, in the case of observations of the moon using astrographs of medium focal length ($\sim$3-5 m). The uncertainty of the position of the center of the stellar image enters fully in direct measurement of the distance between a star and an object located in the vicinity of the optical center of the plate (Figure 2b). The method of treatment suggested by Merton is, in this sense, a sort of extreme example compared to methods requiring measurements of rectangular coordinates.

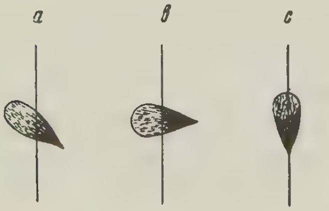

Fig. 2.

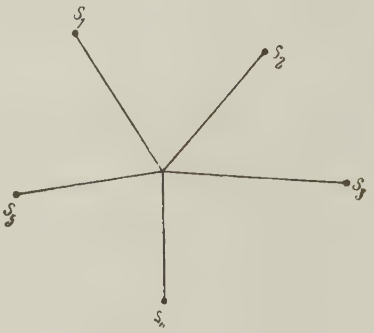

Fig. 3.

If it were possible, in taking measurements, to limit the sightings on a stellar image to a sighting along its axis of symmetry (Figure 2c), then, obviously, the influence of those factors acting in a radial direction would be excluded. In addition to the complete elimination of systematic errors, significant advantage would be gained in an accidental sense, since a sighting so carried out could be performed with greater reliability. The method proposed for treating the photograph is based primarily on the principle of measuring the stellar images in a radial direction, i.e., along their axis of symmetry.

§3. If the angles between the direction lines leading from the object of interest P to various reference stars, $S_i$, are measured with known coordinates, it will obviously be possible to find the coordinates of the object to be measured as well (Figure 3). If the point P is located close to the optical center, directions $PS_i$ will not be affected at all by coma, astigmatism, lateral chromatic aberration, distortion, the scale of the plate, or by the possibility of nonuniformity of the scale with respect to different azimuths. These directions are also independent of the curvature of the focal plane, if the photograph is obtained with the aid of Maksutov or Schmidt reflectors. There is a rather great probability that the distortion of the photographic layer will take place in a radial direction; the effect of this source of systematic errors will then also be canceled out, or, at least, attenuated.

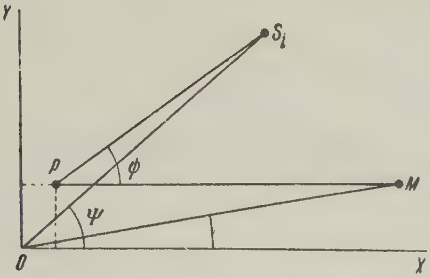

Fig. 4.

The problem of determining the coordinates of a point along the measured angles between the direction lines leading out from that point to a series of other points having given coordinates is known in geodesy as the Potenot problem. Let us now consider an analytical solution of this problem applicable to our case of central projection of a portion of the celestial sphere on the surface of the plate.

Consider an object P to be measured, located close to the optical center, O (Figure 4). In this case, the coordinates of the optical center A,D may be taken as the approximate values of the coordinates of the object. In actual practice, this is almost always what happens. Consider next a case where the conditions of proximity of the object to be determined, with reference to the optical center, are not fulfilled. For the reference stars $S_i$, at given coordinates of the optical center A,D, it is possible to find the standard coordinates X,Y according to known formulas. In that case, it is entirely immaterial that the scale used to compute those values be close to the actual scale of the plate. Let us set

$$X_i = R_i \cos \Psi_i, \quad Y_i = R_i \sin \Psi_i.$$

Here $\Psi_i = < S_iOX$ can be termed the standard position angle for star $S_i$ by analogy with rectangular coordinates. These angles can be easily found for all reference stars from the ratios:*

$$\operatorname{tg} \Psi_i = \frac{Y_i}{X_i}. \tag{1}$$

Let us assume that, by some given method, angles $\psi$ between the directions leading from the object of interest respectively to all reference stars and to some constant point M, connected with the plate, are measured on the plate. These angles are assumed corrected for the action of differential refraction by the corrections $\Delta\psi$, the derivation of which will be given further on. Coordinates p,q of point M in frame of reference XOY are not known to us. It is possible to put

$$p = \rho \cos \beta, \quad q = \rho \sin \beta,$$

where $\rho, \beta$ are unknowns and, in essence, polar coordinates of the point M which are not of interest to us. The desired values are coordinates $X_0, Y_0$ of point P with respect to the optical center. Points $S_i(X_i, Y_i)$ and M(p,q) are seen, looking out from the optical center O, at an angle $\Psi_i - \beta$, and from point P, at an angle $\psi_i$. These angles are close to each other, if $X_0$ and $Y_0$ are small when compared to R and $\rho$.

Let us introduce equations which connect the desired coordinates $X_0, Y_0$ with the small difference $(\Psi_i - \beta) - \psi_i$. For this we use the well-known ratio from analytic geometry:

$$\operatorname{tg}(\Psi_i - \beta) = \frac{X_i q - Y_i p}{X_i p + Y_i q},$$

$$\operatorname{tg} \psi_i = \frac{(X_i - X_0)(q - Y_0) - (Y_i - Y_0)(p - X_0)}{(X_i - X_0)(p - X_0) + (Y_i - Y_0)(q - Y_0)}.$$

---

*In this paper 'tg' ≡ 'tan' — Publisher.

Compute the difference of these equations and transform it, taking $X_0, Y_0$ small and retaining only the first degrees of the values $X_0/R$, $Y_0/R$, $X_0/\rho$, $Y_0/\rho$. After not very complicated, but long calculations, we get

$$\sin(\Psi_i - \beta - \psi_i) = \frac{1}{R_i}(X_0 \sin \Psi_i - Y_0 \cos \Psi_i) + \frac{1}{\rho}(-X_0 \sin \beta + Y_0 \cos \beta).$$

Replacing the sine of the small angle on the left-hand side by the value of the argument, we find

$$\Psi_i - \psi_i = \frac{\sin \Psi_i}{R_i \sin 1''} X_0 - \frac{\cos \Psi_i}{R_i \sin 1''} Y_0 + \beta + \frac{1}{\rho \sin 1''}(-X_0 \sin \beta + Y_0 \cos \beta).$$

The last two terms in the expressions arrived at are not dependent on the coordinates of the reference stars; let us designate their sum by $\Psi_0$. The desired ratio then takes on the following form:

$$\Psi_i - \psi_i = A_i X_0 + B_i Y_0 + \Psi_0, \tag{2}$$

where

$$A_i = \frac{\sin \Psi_i}{R_i \sin 1''} = \frac{Y_i}{(X_i^2 + Y_i^2) \sin 1''},$$
$$B_i = -\frac{\cos \Psi_i}{R_i \sin 1''} = -\frac{Y_i}{(X_i^2 + Y_i^2) \sin 1''}. \tag{3}$$

Set up Equations (2) for all reference stars, $S_i$. The value $\Psi_0$ depends on the coordinates of an arbitrarily chosen point M, serving as a reference point for the measured angles $\psi_i$; its value has no interest for us. The coordinates of the object of interest P, after solution of Equations (2), are found from the relations

$$\alpha_P = A + X_0 \sec D, \quad \delta_P = D + Y_0. \tag{4}$$

It is obvious that, for the complete solution of the problem, at least three reference stars are needed.

If the object to be determined is located at some distance from the optical center (OP > 1-2 mm), it will be necessary to know its approximate rectangular coordinates $a_0$ and $b_0$. The problem is resolved with the aid of analogous formulas, but instead of $X_i$ and $Y_i$, it will be necessary to take, in each case, $X_i - a_0$ and $Y_i - b_0$. The definitive coordinates of the object to be determined will, in that case, be found from the relations:

$$\alpha_P = A + (a_0 + X_0) \sec D, \quad \delta_P = D + (b_0 + Y_0). \tag{5}$$

The solution of the problem is also possible in a case where the object to be determined is situated at a very considerable distance from the center, as for example, at the edge of the plate. Its coordinates $\alpha_P, \delta_P$ may then be calculated by taking into account the noncoincidence of the plane of the plate and the portion of the celestial sphere according to formulas known from astrophotography.

§4. It is also fitting to examine the question of what effects may act to distort a directly measured angle between directions leading out from the object to be determined to a reference star and an arbitrary point, M. The following effects must, of necessity, be included: differential refraction, differential aberration, and the inclination of the plate to the optical axis. It is suggested that, in computing standard coordinates $X_i$, $Y_i$, $\Psi_i$, referred to the equinox of the reference-star catalog, the proper motions of the stars over the difference of the epochs of the catalog and of the plate be taken into account. The plate scale, as we saw previously, has no effect on the standard position angles, $\Psi_i$.

Let us inquire into the changes occurring in the measured angles, $\psi_i$, under the action of the effects indicated. For this purpose, we shall use the familiar expressions for corrections of measured rectangular coordinates [5]:

$$\Delta x = \beta k_3 x + \beta k_1 (k_2 - \operatorname{tg} D) y - \beta k_1 k_3 x^2 - 2\beta k_1^2 k_2 xy -$$
$$- \beta k_1 k_4 y^2 + 2\beta' (1 + k_1^2 + k_2^2) k_1 (k_1 x + k_2 y);$$

$$\Delta y = \beta k_1 (k_2 + \operatorname{tg} D)\, x + \beta k_4 y - \beta k_2 k_3 x^2 - 2\beta k_1 k_2^2 xy - \beta k_2 k_4 y^2 + 2\beta' (1 + k_1^2 + k_2^2)\, k_2 (k_1 x + k_2 y), \tag{6}$$

where

$$k_1 = \operatorname{tg}\zeta \sin\chi, \quad k_2 = \operatorname{tg}\zeta\cos\chi, \quad k_3 = 1 + k_1^2,$$
$$k_4 = 1 + k_2^2, \quad \beta = \beta_0 \frac{273}{273 + t}\frac{H}{760}, \quad \beta' = -0''.087, \quad \beta_0 = 61''.24.$$

$\zeta$ and $\chi$ are the zenith distance and parallactic angle of the optical center of the plate at the time of exposure:

$$\Delta x = Qx - R\operatorname{tg} Dy + Sxy + \frac{1}{2} R (x^2 - y^2);$$
$$\Delta y = R\operatorname{tg} Dx + Qy + Rxy - \frac{1}{2} S (x^2 - y^2),$$

where values Q, R, S depend on the aberration constant k = 20".47 and on the coordinates of the apex of the earth's motion:

$$\Delta x = \alpha y - x(\gamma_1 x + \gamma_2 y), \qquad \Delta y = -\alpha x - y(\gamma_1 x + \gamma_2 y),$$

where values $\alpha$, $\gamma_1$, $\gamma_2$ characterize the angle of inclination of the plate to the optical axis.

The expressions cited include orthogonal terms of the following form:

$$\Delta x = ax - by, \qquad \Delta y = bx + ay.$$

It is not difficult to demonstrate that the effect of these terms on measured angles $\psi_i$ is reduced to a constant number:

$$\begin{aligned} x &= r\cos\psi, \\ y &= r\sin\psi, \end{aligned} \qquad \Delta\psi = \frac{x\Delta y - y\Delta x}{x^2 + y^2} = b,$$

independent of the position of the star. Accordingly, it is not necessary to take into account the effect of the orthogonal terms, since the constant correction term of the measured angle enters into the unknown $\psi_0$ in the solution of Equations (2). The remaining quadratic terms in the corrections for differential aberration and for the inclination of the plate to the optical axis are vanishingly small for astrographs with a small field at an allowable plate inclination. It is thus shown that the measured angles $\psi_i$ need be corrected only for the effect of nonorthogonal terms of differential refraction.

To derive the corresponding correction, we substitute into equation

$$\Delta\psi_i = \frac{x\Delta y - y\Delta x}{x^2 + y^2}$$

the values Δx and Δy from (6), first excluding orthogonal terms. After a series of transformations, we get

$$\Delta\psi_i = U_i\beta + V_i R_i + W_i, \tag{7}$$

where

$$\begin{gathered} U_i = \operatorname{tg}^2\zeta \sin 2(\chi + \Psi_i), \\ V_i = -\beta_0 \sin 1' \operatorname{tg}\zeta\,[1 + \operatorname{tg}^2\zeta \sin^2(\chi + \Psi_i)]\cos(\chi + \Psi_i), \\ W_i = \beta' \operatorname{tg}^2\zeta \sec^2\zeta \sin 2(\chi + \Psi_i), \\ R_i = \sqrt{X_i^2 + Y_i^2} \ \text{(in minutes of arc)} \end{gathered} \tag{8}$$

For values V and W, which need be taken into account only for large zenith distances, a double-entry table may be set up ($\zeta$, $\chi + \psi$). These tables, as well as a small table for $\beta$ with arguments t and H, are given at the end of the present discussion. The zenith distance and parallactic angle of the center of the plate for the average time of exposure ($\zeta$, $\chi$) are computed on the basis of known formulas. However, the values $\tan^2\zeta$ and $\chi$ entering into the expression U. may be tabulated according to the arguments of the declination and hour angle of the center of the plate (D and s−A) for the given latitude. These tables have been set up for Pulkov; they facilitate to some considerable degree the computation of differential refraction. For not very large zenith distances, the calculation of differential refraction assumes a very simple form:

$$\Delta\psi_i = \beta\,\mathrm{tg}^2\zeta \sin 2(\chi + \Psi_i). \tag{9}$$

Corrections $V_i \cdot R_i$ and $W_i$ come into play starting only with zenith distances of 50 and 60°, respectively.

§5. Let us now take up the question of how an accurate measurement of the angles $\psi_i$ may be made on the plate. Measuring devices provided with accurately divided circles for this purpose are not met with in practice in astrographic work. We shall not go into details on the possible design of a device which might serve for angular measurements on a plate, but we shall draw attention to another technique leading to the same goal. The latter requires a measuring machine which can enable the users to carry out simultaneous measurements of two rectangular coordinates of points on the plate. The difference from a 90° angle given by the device must be carefully studied. Among devices of that type may be included the Zeiss system coordinate-measuring machine [6]. The recently studied Pulkov specimen of this type of system had high quality with respect to scales, guiding bars and micrometers [7]. Preliminary investigations on the nonperpendicularity of the coordinate axes of the machine showed that the corrections of the measured coordinates for obliquity of the system were extremely small.

In performing measurements, we placed a plate in the device with the aid of a turntable so that the line, $PS_i$, was parallel to one of the coordinate axes, say, X (Figure 5). In this case, in setting the micrometer thread on the reference star, $S_i$, the principle of measuring the radial asymmetry of star images, which underlies the method, was fully observed. A second direction, determining an angle $\psi_i$, led through the arbitrary point, M, on the plate edge. Any defect in the film, or an artificial marker introduced with the aid of a special gauge, will serve to represent such a point. The criterion for a marker is that it should be as symmetrical as possible. A setting at its center may then be reliably carried out using any given position angles, while, in measuring different reference stars, the platform of the measuring machine must be rotated.

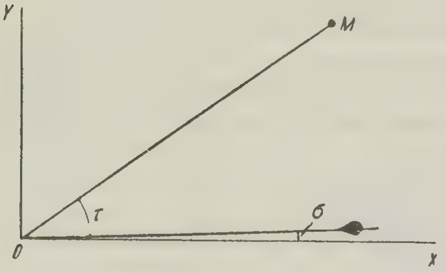

Fig. 5.

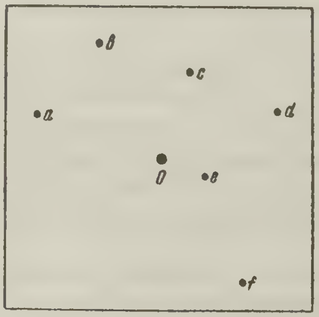

Fig. 6.

If the rectangular coordinates of three points, P, $S_i$, M, are measured with the plate, oriented in the manner indicated, in a stationary position, determination of the angle $\psi_i$ will be given by the relations:

$$\psi = \tau - \sigma, \qquad \mathrm{tg}\,\tau = \frac{y_M - y_P}{x_M - x_P}, \qquad \sigma'' = \frac{1}{\sin 1''}\,\frac{y_{S_i} - y_P}{x_{S_i} - x_P}. \tag{10}$$

In view of the small value of $y_{S_i} - y_P$, the distance of the comparison star from the object to be determined may be known only to an approximation.

§6. As an illustration of the method outlined, let us cite the results of the treatment on a photograph recording the asteroid Pallas, obtained by A.N. Deutsch on a Pulkov normal astrograph on August 30, 1951, and which he was kind enough to place at the disposal of the author. Six reference stars were selected on the plate, their positions known from the Yale Observatory catalog [8]. The distribution of these stars (a,b,c,d,e,f, Figure 6) was felt to be very unfortunate. In the first place, symmetry with respect to the optical center was impaired; in the second place, several stars are placed so close to the edge of the field that their images suffer considerable distortion due to aberrations (in Figure 2, stars a,b,c, from the plate examined). The distance of the selected stars from the optical center (field of normal astrograph 2° x 2°) are such as indicated in Table 1.

The position of the asteroid, found at a distance of 6′.10 from the optical center, was determined by three independent methods.

A – by measuring the rectangular coordinates using the method of six constants;

B – by measuring the distances from the planet to reference stars (Merton);

C – by measuring position angles, $\psi$, using the method outlined above.

TABLE 1

| | | | |
|---|---|---|---|
| *a* | 68′.1 | *d* | 65′.7 |
| *b* | 69′.5 | *e* | 24′.0 |
| *c* | 48′.9 | *f* | 77′.1 |

TABLE 2

| | $\alpha_P$ | $\delta_P$ |
|---|---|---|
| *A* | 292°27′ 51″.72 | +12°21′ 34″.36 |
| *B* | 292°27′ 51″.54 | +12°21′ 34″.25 |
| *C* | 292°27′ 51″.84 | +12°21′ 34″.69 |

Determination of the coordinates of the planet by the Merton method were carried out not by the graphic, but by the analytic method, which permitted the use of any number of reference stars. In measuring $\psi_i$ angles by the method cited in §5, a KIM-3 coordinate-measuring machine from the Pulkov Observatory was used. No corrections were introduced in the measuring process for the obliquity of the system of coordinates; to exclude any possible nonperpendicularity of the axes, each reference star was measured in four plate positions at 90° angles to each other.

Regardless of what technique is employed in measuring angles $\psi_i$ on the plate, the error of the angle measured will always be inversely proportional to the lengths of the sides of angle $PS_i$ and PM. If the marker, M, is assumed to be located at the very edge of the plate, the error of the measured angle is

$$\varepsilon_{\psi_i} \sim \frac{1}{R_i}.$$

In solving Equations (2) by the method of least squares, it is thus necessary to take into account the weight of the various separate equations equal to $R_i^2$. To bring Equations (2) to uniform, weighted values, we multiply each of them by $R_i$; the system, in its final form, is then:

$$R_i(\Psi_i - \psi_i)\sin 1'' = X_0 \sin \Psi_i - Y_0 \cos \Psi_i + \Psi_0 R_i \sin 1''. \tag{11}$$

TABLE 3

| No. | No. of stars | Stars | No. | No. of stars | Stars |
|---|---|---|---|---|---|
| 1 | 5 | *a, b, c, d, e* | 9 | 4 | *c, d, e, f* |
| 2 | 5 | *b, c, d, e, f* | 10 | 4 | *d, e, f, a* |
| 3 | 5 | *c, d, e, f, a* | 11 | 4 | *e, f, a, b* |
| 4 | 5 | *d, e, f, a, b* | 12 | 4 | *f, a, b, c* |
| 5 | 5 | *e, f, a, b, c* | 13 | 4 | *a, c, d, f* |
| 6 | 5 | *f, a, b, c, d* | 14 | 4 | *a, c, e, f* |
| 7 | 4 | *a, b, c, d* | 15 | 4 | *b, c, e, f* |
| 8 | 4 | *b, c, d, e* | 16 | 4 | *b, c, d, f* |

The desired coordinates of the asteroid, when treated by the various methods, are obtained as given in Table 2. Preference should be given to the solution by method C, since that method is the one most free from the influence of random errors, which exert an effect when stars are measured at the edge of a plate. In confirmation of the above, we employed the following approach. From the six reference stars, different combinations of four and five stars were selected, the coordinates of the asteroid being determined from them. Those combinations are tabulated below in Table 3.

It is readily seen that in all variants used, the inadequacies in the distribution of reference stars about the object to be determined are significantly increased. The results of the solution of all the variants by the three methods cited are shown in Figure 7 separately, for cases of five and four reference stars (variants 1-6 and 7-16). The scale measured along axis $\alpha$ is reduced by $\cos\delta$ times.

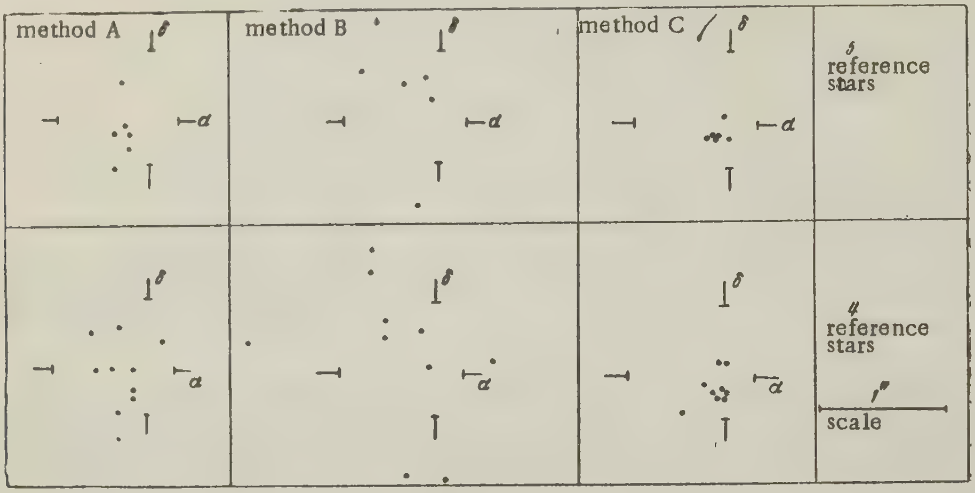

Fig. 7.

The data presented in Figure 7 are very significant. Large systematic errors in measurement of stars remote from the center, using methods A and B, led to quite a degree of inconstancy in the solution. On the other hand, the result based on the measurement of angles $\psi_i$ (method C) was much less dependent on the choice of comparison stars and,in the last analysis, was determined by the errors inherent in the catalog positions of those stars. The reciprocals of the sums of the squares of the deviations of individual points on the graphs cited from their arithmetic mean, for the various methods, are found by the following relation:

$A:B:C = 1.0:0.2:4.9$ for variants with five reference stars,

$A:B:C = 1.0:0.2:2.1$ for variants with four reference stars.

Roughly the same relationship holds between the reciprocals of the sums of the squares of the remaining deviations in solving the equations for the different stars by the three methods, respectively: $A:B:C = 1.0:0.4:4.0$.

In carrying out the present investigation, we did not in any way take as our goal the deprecation of the method of six constants or of the position-line method. The point was simply that the reference-star distribution decided upon was highly unfavorable for the application of those techniques. Our problem was to show that the position-line method, examined in the present discussion, may be employed with success even where such a distribution of stars prevails. In the presence of a sufficient number of reference stars, close to the object to be measured, it must be expected that the result will have uniform accuracy when treated by any one of the three methods.

§7. The cases of reference-star distribution reviewed in the present paper are by no means a mere academic exercise. Practical work in photographic observations of the moon at Pulkovo [9] demonstrated that such cases may very well occur for normal-type astrographs. As is clear from the charts in Figure 7, the employment of the traditional six-constants method may lead to an uncertainty in the solution reaching $0''.3-0''.4$. The application of the position-angle method for the determination of lunar coordinates would result in a considerable in-

## TABLE 4*

$$V = -\beta_0 \sin 1' \tan \zeta \, [1 + \tan^2 \zeta \sin^2 (\chi + \psi)] \cos (\chi + \psi)$$

| $\chi + \psi$ | 180° | 170° | 160° | 150° | 140° | 130° | 120° | 110° | 100° | 90° |
|---|---|---|---|---|---|---|---|---|---|---|
| $\zeta$ | 180 | 190 | 200 | 210 | 220 | 230 | 240 | 250 | 260 | 270 |
| 50° | 0.02 | 0.02 | 0.02 | 0.02 | 0.02 | 0.02 | 0.02 | 0.01 | 0.01 | 0.00 |
| 51 | 0.02 | 0.02 | 0.02 | 0.02 | 0.03 | 0.03 | 0.02 | 0.02 | 0.01 | 0 |
| 52 | 0.02 | 0.02 | 0.02 | 0,03 | 0.03 | 0.03 | 0.02 | 0.02 | 0.01 | 0 |
| 53 | 0.02 | 0.02 | 0.02 | 0.03 | 0.03 | 0.03 | 0.03 | 0.02 | 0.01 | 0 |
| 54 | 0.02 | 0.02 | 0.03 | 0.03 | 0.03 | 0.03 | 0.03 | 0.02 | 0.01 | 0 |
| 55 | 0.02 | 0.02 | 0.03 | 0.03 | 0.03 | 0.03 | 0.03 | 0.02 | 0.01 | 0 |
| 56 | 0.02 | 0.03 | 0.03 | 0.03 | 0.04 | 0.04 | 0.03 | 0.03 | 0.01 | 0 |
| 57 | 0.03 | 0.03 | 0.03 | 0.04 | 0.04 | 0.04 | 0.04 | 0.03 | 0.02 | 0 |
| 58 | 0.03 | 0.03 | 0.03 | 0.04 | 0.04 | 0.04 | 0.04 | 0.03 | 0.02 | 0 |
| 59 | 0.03 | 0.03 | 0.03 | 0.04 | 0.04 | 0.05 | 0.04 | 0.03 | 0.02 | 0 |
| 60 | 0.03 | 0.03 | 0.04 | 0.04 | 0.05 | 0.05 | 0.05 | 0.04 | 0.02 | 0 |
| 61 | 0.03 | 0.03 | 0.04 | 0.05 | 0.06 | 0.06 | 0.06 | 0.04 | 0.02 | 0 |
| 62 | 0.03 | 0.04 | 0.04 | 0.05 | 0.06 | 0.06 | 0.06 | 0.04 | 0.03 | 0 |
| 63 | 0.03 | 0.04 | 0.04 | 0.06 | 0.06 | 0.07 | 0.06 | 0.05 | 0.03 | 0 |
| 64 | 0.04 | 0.04 | 0.05 | 0.06 | 0.07 | 0.08 | 0.08 | 0.06 | 0.03 | 0 |
| 65 | 0.04 | 0.04 | 0.05 | 0.07 | 0.08 | 0.08 | 0.08 | 0.06 | 0.03 | 0 |
| 66 | 0.04 | 0.04 | 0.06 | 0.08 | 0.09 | 0.10 | 0.09 | 0.07 | 0.04 | 0 |
| 67 | 0.04 | 0.05 | 0.06 | 0.08 | 0.10 | 0.11 | 0.10 | 0.08 | 0.04 | 0 |
| 68 | 0.04 | 0.05 | 0.07 | 0.09 | 0.11 | 0.12 | 0.12 | 0.09 | 0.05 | 0 |
| 69 | 0.04 | 0.05 | 0.07 | 0.10 | 0.13 | 0.14 | 0.13 | 0.10 | 0.06 | 0 |
| 70 | 0.05 | 0.06 | 0.08 | 0.12 | 0.15 | 0.16 | 0.16 | 0.12 | 0.07 | 0 |
| 71 | 0.05 | 0.06 | 0.09 | 0.13 | 0.17 | 0.19 | 0.18 | 0.14 | 0.08 | 0 |
| 72 | 0.05 | 0.06 | 0.10 | 0.15 | 0.20 | 0.22 | 0.21 | 0.16 | 0.19 | 0 |
| 73 | 0,06 | 0.07 | 0.12 | 0.18 | 0.23 | 0.26 | 0.25 | 0.20 | 0.11 | 0 |
| 74 | 0.06 | 0.08 | 0.13 | 0.21 | 0.27 | 0.31 | 0.30 | 0.22 | 0.13 | 0 |
| $\zeta$ | 0° | 10° | 20° | 30° | 40° | 50° | 60° | 70° | 80° | 90° |
| $\chi + \psi$ | 0 | 350 | 340 | 330 | 320 | 310 | 300 | 290 | 280 | 270 |

## TABLE 5

$$W = \beta' \tan^2 \zeta \sec^2 \zeta \sin 2 (\chi + \psi)$$

| $\chi + \psi$ | 90° | 95° | 100° | 105° | 110° | 115° | 120° | 125° | 130° | 135° |
|---|---|---|---|---|---|---|---|---|---|---|
|  | 180 | 175 | 170 | 165 | 160 | 155 | 150 | 145 | 140 | 135 |
|  | 270 | 275 | 280 | 285 | 290 | 295 | 300 | 305 | 310 | 315 |
| $\zeta$ | 0° | 355 | 350 | 345 | 340 | 335 | 330 | 325 | 320 | 315 |
| 60° | 0″ | 0″ | 0″ | 0″ | 1″ | 1″ | 1″ | 1″ | 1″ | 1″ |
| 62 | 0 | 0 | 0 | 1 | 1 | 1 | 1 | 1 | 1 | 1 |
| 64 | 0 | 0 | 1 | 1 | 1 | 2 | 2 | 2 | 2 | 2 |
| 66 | 0 | 0 | 1 | 1 | 2 | 2 | 2 | 2 | 3 | 3 |
| 68 | 0 | 1 | 1 | 2 | 2 | 3 | 3 | 4 | 4 | 4 |
| 70 | 0 | 1 | 2 | 3 | 4 | 4 | 5 | 5 | 6 | 6 |
| 72 | 0 | 2 | 3 | 4 | 6 | 7 | 8 | 8 | 9 | 9 |
| 74 | 0 | 2 | 5 | 7 | 9 | 11 | 12 | 13 | 14 | 14 |
| $\zeta$ | 0° | 5° | 10° | 15° | 20° | 25° | 30° | 35° | 40° | 45° |
|  | 90° | 85 | 80 | 75 | 70 | 65 | 60 | 55 | 50 | 45 |
|  | 180° | 185 | 190 | 195 | 200 | 205 | 210 | 215 | 220 | 225 |
| $\chi + \psi$ | 270 | 265 | 260 | 255 | 250 | 245 | 240 | 235 | 230 | 225 |

---

*In Tables 4 and 5, the value of the function which corresponds to the argument reading from the bottom of the table upward has a minus sign.

TABLE 6

$$\beta = \beta_0 \frac{273}{273 + t^\circ} \cdot \frac{H}{1013.2} \text{ (}H\text{ in millibars)}$$

| $t^\circ$ | H | | | | | |
|---|---|---|---|---|---|---|
| | 980 | 990 | 1000 | 1010 | 1020 | 1030 |
| — 20° | 63″9 | 64″6 | 65″2 | 65″9 | 66″5 | 67″2 |
| — 18° | 63·4 | 64·1 | 64·7 | 65·3 | 66·0 | 66·6 |
| — 16° | 62·9 | 63·6 | 64·2 | 64·8 | 65·5 | 66·1 |
| — 14° | 62·4 | 63·1 | 63·7 | 64·3 | 65·0 | 65·6 |
| — 12° | 61·9 | 62·6 | 63·2 | 63·8 | 64·5 | 65·1 |
| — 10° | 61·5 | 62·1 | 62·7 | 63·4 | 64·0 | 64·6 |
| — 8° | 61·0 | 61·6 | 62·3 | 62·9 | 63·5 | 64·1 |
| — 6° | 60·6 | 61·2 | 61·8 | 62·4 | 63·0 | 63·6 |
| — 4° | 60·1 | 60·7 | 61·3 | 61·9 | 62·6 | 63·2 |
| — 2° | 59·7 | 60·3 | 60·9 | 61·5 | 62·1 | 62·7 |
| 0° | 59·2 | 59·8 | 60·4 | 61·0 | 61·6 | 62·2 |
| + 2° | 58·8 | 59·4 | 60·0 | 60·6 | 61·2 | 61·8 |
| + 4° | 58·4 | 59·0 | 59·6 | 60·2 | 60·8 | 61·3 |
| + 6° | 59·9 | 58·5 | 59·1 | 59·7 | 60·3 | 60·9 |
| + 8° | 57·5 | 58·1 | 58·7 | 59·3 | 59·9 | 60·5 |
| + 10° | 57·1 | 57·7 | 58·3 | 58·9 | 59·5 | 60·0 |
| + 12° | 56·7 | 57·3 | 57·9 | 58·5 | 59·0 | 59·6 |
| + 14° | 56·3 | 56·9 | 57·5 | 58·1 | 58·6 | 59·2 |
| + 16° | 55·9 | 56·5 | 57·1 | 57.7 | 58·2 | 58·8 |
| + 18° | 55·6 | 56·1 | 56·7 | 57·3 | 57·8 | 58·4 |
| + 20° | 55·2 | 55·7 | 56·3 | 56·9 | 57·4 | 58·0 |

crease in accuracy. That method may also prove to be useful for the utilization of astrographs of poor optical design, giving an excessively small field with good images, and also for long-focus astrographs.

It should be noted that at the present time the accuracy of photographic determinations of the positions of celestial objects is comparable with the accuracy of catalog positions of reference stars. Attempts to achieve a more absolute accuracy will have a real foundation only in the future, when catalog errors will be considerably less than the accuracy with which the interrelation between objects and reference stars is determined. The value of the position-line method, which assures a more reliable tie-up of the objects and the catalog, will then be obviously substantial.

The determination of position angles, $\psi$, on the plate by means of linear measurements (§5) is a more tedious undertaking than the measurement of rectangular coordinates or, even more so, measurement of the distances between two objects on the plate. It is therefore desirable to construct an apparatus with a divided circle for the measurement of those angles. The design of such an apparatus will not be very complicated; as a constructional basis, individual parts (divided circle, microscope-micrometer) of portable astronomical-geodetic instruments could be utilized.

## LITERATURE CITED

[1] H. Turner, Monthly Notices Roy. Astron. Soc. 54, 11 (1894).

[2] F. Schlesinger, Astron. J. Vol. 37 (1926).

[3] A.N. Deutsch, A.N. 249, 102, 1933.

[4] G. Merton, Monthly Notices Roy. Astron. Soc. 113, 4 (1953).

[5] Course in Astrophysics and Stellar Astronomy (1951).*

[6] A. König, A.N. 246, 5893, 1932.

[7] Kh.I. Potter and O.N. Chudovicheva, Transaction of 12th Astronomical Conference of USSR (in press).*

[8] Transact. Yale Observ. 19, 1948.

[9] A.A. Mikhailov and Kh.I. Potter, Transaction of 12th Astronomical Conference of USSR (in press).*

Received November 9, 1956

Main Astronomical Observatory
Academy of Sciences, USSR

---

*In Russian.

# ASTRONOMICAL EPHEMERIDES

D.H. Sadler

The calculation and publication of astronomical ephemerides, both in the past and at the present time, are considered, particularly from the point of view of the international exchange of data ; the further development of this work is also discussed. The increasing accuracy and complexity of the calculations will demand the fullest international cooperation and exchange of data in the future, in spite of the availability of high-speed automatic computing machines.

## 1. Introduction and Historical Review

The basic purpose of this paper, which was written at the invitation of the Editor of the Journal, is to outline the measures being taken at the present time for the calculation and publication of astronomical ephemerides and to consider future needs in accordance with modern computing methods.

Starting in 1911, when collaboration in astronomical computing work was first established by agreements on an international scale, the computation of ephemerides was divided among the principal national almanac offices; it proved to be one of the most effective and enduring examples of international scientific cooperation. Conditions have changed since 1911, but the demand for joint work here is as great as it was formerly.

The original reason which prompted the Bureau des Longitudes to summon the "International Congress of Astronomical Ephemerides" was formulated as follows in the letter of invitation by the Director of the Bureau, B. Baillaud:

"In particular, it appears that by a suitable distribution of the work it would be possible, without increasing the annual expenditure, to enlarge considerably the number of stars for which ephemerides are published annually."

But the Conference set broader goals for itself and was not satisfied with the standards for the calculation and publication of the apparent places of more than 3000 stars. Recommendations were made (and carried out) in regard to standardization of the principles on which the calculations were based and publication of the results of the calculations in a unified form, and also in regard to the mutual exchange of calculations of fundamental ephemerides, eclipses and occultations, physical ephemerides, and ephemerides of satellites; it was specified that calculations of fundamental ephemerides (high-precision positions of the Sun, Moon, and planets) and of eclipses be performed independently at two locations. The agreement also touched on the calculation and publication of ephemerides of minor planets and variable stars. Although there were, naturally, some further changes, the most important recommendations of the Conference are being carried out even now.

The International Astronomical Union, created in 1920-1922, made its appearance as a permanent organization, ideally suited to the direction of international cooperation; its Commission 4 continued to put into practice the proposals of the conference of 1911.

In 1911 primary emphasis was placed upon the distribution of the computational work. It was also agreed to support special publications, by the Office of the Berliner Jahrbuch, serving all astronomers in regard to minor planets and variable stars. But each of the principal national almanacs continued to publish, in addition to the fundamental ephemerides and other data, the apparent places of stars on its own list. Meanwhile, the following proposal had already been recorded in the proceedings of the Conference:

"As for the others (stars not on the list of bright navigational stars), is it not suitable to gather them all together (along with the preceding ones) in a separate brochure, of an international character, to the preparation of which the principal observatories particularly intestested in this publication might contribute ?"

This proposal was not adopted, but an agreement was reached, on the strength of which O. Blacklund at Pulkovo undertook to publish the apparent places of stars on the Blacklund-Hough list, which were computed in Great Britain by the Nautical Almanac Office.

Thus, although observers were now guaranteed the apparent places of more than 3000 stars, they still had to look for them in the five principal almanacs (Almanaque Nautico, American Ephemeris, Berliner Jahrbuch, Connaissance des Temps, Nautical Almanac), in the Turin Annuario Astronomico, and in the special Pulkovo publication.

Changes in the accepted fundamental catalog gave rise to changes in the lists of stars, until at last, with the adoption of the FK3 as the fundamental catalog, it was decided in 1935 to publish the apparent places in a separate international publication under the supervision of the I.A.U. The first volume was published in 1941; the calculations for it were performed in France, Germany, Spain, and the United States; the summarizing of the results, proofreading, and publication were done in Great Britain.

As a result of the redistribution of the computations in 1948, the apparent places for this volume were also calculated by the Institute of Theoretical Astronomy of the U.S.S.R. and by the Nautical Almanac Office.

The publication of minor planet ephemerides was done in Germany until 1945, and since then at the Institute of Theoretical Astronomy of the U.S.S.R., which shares the minor planet work with Cincinnati, Heidelberg, and many individual orbit computers.

The variable star ephemerides, although included in the program of the 1911 Conference, have long since lost connection with the other epehemerides, and are not now considered as pertaining to the scope of Commission 4.

## 2. Current Measures

At the 1955 (Dublin) meeting of the I.A.U. an agreement was reached concerning the redistribution of the computations for the national ephemerides, which is to come into effect beginning with the ephemerides for 1960. The redistribution became desirable for many reasons: first, the use of analytical computing machines made it more expedient to commission one institution to do the whole of any one kind of computation; second, the need arose for increasing the accuracy and uniformity of the basic materials used for the computations; third, for the sake of possible economy in publication. These changes are in conformity with the introduction into the ephemerides of ephemeris time, new methods of calculating reduction quantities and apparent places of stars, and new elements for the fundamental ephemerides of the Moon and planets (see the reports and recommendations of Commission 4).

A basic change lies in the fact that, as of 1960, Apparent Places of Fundamental Stars will be published by the Astronomisches Rechen-Institut at Heidelberg. They will be printed from an original obtained directly from punched cards with the aid of a printing tabulator, similar to those available at Washington and Herstmonceux; the task will be facilitated by the fact that all the calculations of the apparent places of 10-day stars will be centralized in one institute, so that the results will have exactly the form needed for the printing mechanism. On punched-card machines the calculations for a large number of stars will not require markedly greater labor than those for a few stars.

The calculation of apparent places of circumpolar stars was shared between the Connaissance des Temps and the Almanaque Nautico.

At one time the possibility of publishing a single international collection of fundamental ephemerides of the Sun, Moon, and planets (under the title International Fundamental Astronomical Ephemeris) was considered by the Directors of the national ephemerides, but it was acknowledged to be impracticable for various reasons. The principal advantages of such a single collection of fundamental ephemerides would be its unitary and binding character, and also its economy of labor and facilities.

To a certain extent, both of these advantages might be realized by photographic printing from a fundamental original; such reproduction guarantees (except for negligible imperfections) uniformity and accuracy, while the necessary labor and its cost are not great. By the agreement of 1911, the calculation of the fundamental ephemerides of the Sun, Moon, and planets (which duplicate the calculations based on the tables of Le Verrier and Gaillot which the Office of the Connaissance des Temps was obliged to continue) was assigned to the Nautical Almanac Office, where it is being done up to the present time; but from 1960 onward, the fundamental data for the Moon and the five outer planets will be obtained from calculations performed on electronic computing machines in the United States; for the Moon, by direct calculation of the trigonometric expressions of Brown's theory; for the planets, by direct numerical integration of the equations of motion. In addition to copies of these data sent around to the other almanac offices, the Nautical Almanac Office can supply, in a form specially adapted for direct photographing, galley proofs of the whole of the first part.

The advantage of this method of exchanging astronomical data, which eliminates not only repetitious computation but also typographical expenses and the labor of proof-reading, is basic to the unification of the Nautical Almanac and the American Ephemeris. As of 1960, this will be a single publication, printed in both countries from the same material. The second part of the almanac will be printed in the United States and then reproduced photographically, as in the case of the first part. This fusion is very much simplified by a common language; otherwise, complete unification would be impossible. But language is not an obstacle to the use of the ephemerides themselves; any part of them may be reproduced by photolithography after first gluing on headings in another language, if this is necessary. This kind of reproduction from the unified British and American nautical and air almanacs is already being applied in a number of countries. The Air Almanac was unified beginning in 1953, and the Nautical Almanac will be unified in the same way as of 1958. The Astronomisch-Geodätisches Jahrbuch, published by the Astronomisches Rechen-Institut in Heidelberg, will cease to appear after 1957 and in place of it the American Ephemeris and the Nautical Almanac will be used, while the facilities and manpower will be employed on the Apparent Places of Fundamental Stars. A few small changes in the distribution of computations were made, chiefly with the aim of centralizing all the computations of any one kind in one Office. Thus the Nautical Almanac Office has taken upon itself the calculation of the elements of occultations; it even guarantees all subsequent phases – their prediction and processing.

## 3. Future Tasks

The astronomical ephemerides serve four different purposes, which may be stated as follows:

a) Preliminary computation, i.e. lists of observed phenomena, positions of observed celestial objects which serve for setting the telescope, and other material of assistance to the observer; and for minor planets, data to aid in their identification.

b) Practical reduction of observations needed for the determination of time, for geodetic work, in navigation, etc.

c) Comparison of the observations with theory, for which apparent positions are required (or data from which they may be obtained) which are in strict conformity with the underlying theory.

d) The furnishing of fundamental data for the calculation of further predictions (for example, for comets and minor planets) and for theoretical investigations.

Originally, a single ephemeris satisfied all these needs. But now there is already a division; thus ephemerides for navigational purposes are now separated everywhere from those intended for astronomical purposes – to the great benefit of aerial and marine pilots, who now have precisely what they need, and moreover in a form that is more convenient for them. Similarly, the international publication Apparent Places of Fundamental Stars provides for time service and geodetic work; and in certain countries there are special publications (such as, for example, the British Star Almanac) useful in topographic work.

There is also a tendency to unite in one volume data for prediction and data for representation of observations; but fundamental data, such as the rectangular coordinates of the planets referred to a standard equinox, it is now found preferable to publish separately. These collections of Planetary Coordinates are designed for a special purpose – the calculation of perturbations of comets and minor planets. For the majority of minor planets, the accuracy of the published ephemerides is sufficient only to insure their identification and observation.

The inclusion, in one volume, of accurate ephemerides serving for comparison with observation, and of approximate ones, which only facilitate observations, means that the majority of purchasers will not make use of the full accuracy provided; but the advantages of separate publication are not so great in current practice.

The trend toward use of automatic recording of observations and the application of electronic equipment in computing, however, will rapidly create conditions to change the situation. The comparison of theory with observations will probably be made, to an ever increasing extent, not by independent observers, but in a centralized manner, at a small number of computing centers equipped with appropriate facilities. And whereas it would be best to provide in printed form the preliminary computations necessary to each observer, highly accurate ephemerides will be necessary only for the programming of computing machines. And for this purpose the printed form is not suitable, since taking copies from it (on punched cards) is a waste and an abundant source of errors. In this case all data must be reported in the form of punched cards which, fortunately, are standard all over the world. They are more easily exchanged than printed data. The exchange of data among the American Ephemeris, the (British) Nautical Almanac, and the Rechen-Institut now usually takes place by means of punched cards, and the Institute of Theoretical Astronomy of the U.S.S.R. and the Minor Planet Center in Cincinnati also make wide use of punched cards in their computations. Many star catalogs and mathematical tables exist only in the form of punched cards, and in such form are available to all who have need of them. Thus, in the near future, the exchange of data in the form of punched cards apparently will prove to be the most convenient means of comparison of observation with theory.

Printed epehemerides of high precision will naturally be indispensable for reference; but for this purpose there is no need to give them together with the approximate ephemerides intended for observers.

Computing has entered a new era in which the routine calculations connected with the construction of ephemerides are no longer substantial. Electronic machines are now in operation which, for example, can compute all the Apparent Places of Fundamental Stars in less than one minute! With the availability of such powerful facilities (and we may be sure that astronomers will have such machines at their disposal in the not too distant future) one might think that it would be simpler to reduce each observation from fundamental data, or to calculate independently everything that is necessary in each computing office. But this is incorrect. Not all astronomers will have access to electronic machines, so that values computed beforehand will still be required for a long time; indeed, this was the case even with logarithms, which up to now have been used by astronomers who do not have calculating machines. Furthermore, the actual computing time is only a small part of the time required for the elaboration of the problem and for programming it for the machine. With the increasing complexity of fundamental computations it is necessary that there be one accepted fundamental standard with which it would be possible to compare observations. This pertains not only to fundamental constants and orbital elements, but also to current ephemerides. No one, indeed, will want to recompute, without very sound motives, the lunar ephemeris according to Brown's theory, though the time required for the purely arithmetical operations is reckoned in hours; and the existence of two independent and discordant calculations would be perplexing.

The fastest computing machines have been used primarily for computing special perturbations or motion over a short period of time, and their capacity has been as yet poorly utilized for calculations in general theory. But when this is done (in particular, for minor planets), there is very little likelihood that the resulting theories should have the form of tables like Newcomb's for the Sun and Brown's for the Moon; it is preferable to calculate the ephemerides directly from the theoretical formulae, as was recently done for the Moon. And in this event the exchange of results among astronomical institutions would be extremely productive.

It seems, therefore, that the principal ephemeris offices must organize the exchange of data in a form more convenient for computing machines than manuscript, typescript, or printed text. It is true that, since it is possible, in theory at least, to translate from one language to another with the help of machines, it is also possible to read written or printed matter by photoelectric means and then to translate it into a form more convenient for computing. But this requires large resources, and the universally adopted punched cards are much more suitable for this purpose; it is true that they are more cumbersome for transport and storage. Probably best of all in this respect would be magnetic tape, from the point of view of space occupied and of transport, and also the speed of the work; but it will be some years still, before it enters the daily life of astronomers.

Even in the area of preliminary calculations the universal mode of supplying observers with material in printed form may not always be efficient; thus, in regard to preliminary calculations of lunar occultations in

1960 and afterwards, the Nautical Almanac Office will furnish all observers not provided with printed material, with sheets (prepared by automatic machines from punched cards) giving the preliminary calculations for the nearest station.

The general character of contemporary astronomical ephemerides is not likely, therefore, to change rapidly, except for short-cuts brought about by the striving of each country to minimize unproductive expenses connected with printing (proofreading is especially burdensome). Fundamental computations will be distributed as before and will be performed much more rapidly than before, but the need for skilled work on the part of collaborators in the ephemeris offices will become still greater; the new computing machines, which reveal the possibility of solving many problems of celestial mechanics and ephemeris astronomy, are insatiable and are ever demanding fresh problems, the programs of which appear to be their nourishment. And hence there is an urgent need for astronomers working in this field to reduce to a minimum the routine work and proofreading, which are inseparable from the production of printed ephemerides; possibly full cooperation and exchange of data will be powerful means for the attainment of this goal.

Nautical Almanac Office
Great Britain

Received July 25, 1956.

# ON THE ERRORS OF INTERPOLATION AND REPRESENTATION IN DETAILED GRAVIMETRIC SURVEYS, THE ACCURACY OF CHARTS, AND THE BEST DISTRIBUTION OF STATIONS

N. P. Grushinskii

The results of an investigation of interpolation and representation errors in detailed gravimetric surveys based on a considerable amount of data are reported. It is emphasized that the accuracy of gravimetric charts is governed by interpolation errors, and a method for the calculation of a rational density distribution and accuracy of determination of gravimetric stations is developed. In conclusion, new recommendations are made with regard to the accuracy prescribed in the instruction for gravimetric prospecting surveys.

The concept of representation error was introduced by Graf-Khenter who defined it as the mean square error at an arbitrarily chosen point which represents the gravitational anomaly over a certain area. In order to obtain the representation error for a square with sides $x$ and $y$, uniformly covered by gravimetric stations, one uses the formula

$$E = \pm\sqrt{\frac{\Sigma\,(\Delta g_m - \Delta g_i)^2}{n-1}}\,,$$

where $\Delta g_m$ is the mean anomaly for all the points of the square, $\Delta g_i$ is the value of the anomaly at the i-th point, and $n$ is the number of stations.

Graf-Khenter established an empirical relation between the representation error and $x$, $y$:

$$\overline{E} = k(\sqrt{x} + \sqrt{y}). \tag{1}$$

Using the data obtained during a pendulum gravimetric survey carried out in India, he found the value of $k$ to be 0.55. The same value of the coefficient $k$ was obtained by A.M. Lozinskaia in 1937 and A.I. Baiborodin [1] with L.A. Govorova, also from pendulum survey data. In the above work representation errors were determined for areas 0.5° x 1° or more in size, with a mean distance of 30 km between stations. In his "Basic Problems of Geodesic Gravimetry" [2], M.S. Molodenskii discusses representation errors using data from variometric surveys for small areas (8 x 8 and 16 x 16 km) and shows that in this case also, the value of $k$ is close to 0.55.

By analogy with the representation error, M.S. Molodenskii introduced the idea of interpolation error. This is defined as the mean square error associated with the force of gravity obtained by interpolation at an arbitrary point on the chart. The interpolation error is given by

$$\overline{E} = \pm\sqrt{\frac{\Sigma\,(\Delta g_{obs} - \Delta g_{int})^2}{n-1}}\,,$$

where $\Delta g_{obs}$ is the anomaly observed at the given point, $\Delta g_{int}$ is the interpolated value of the anomaly at this point, and $n$ is the number of points involved.

Comparing the interpolation and the representation errors obtained by A.M. Lozinskaia, M.S. Molodenskii found an unexpected approximate equality between them.

By analogy with representation errors one can write the Relation (1) for interpolation errors

$$\bar{E} = k'(\sqrt{x} + \sqrt{y}),$$

where x and y are the mean distances between points along two orthogonal directions, or

$$\bar{E} = 2k\sqrt{x} \tag{2}$$

if the area is covered uniformly by the points and k = 2k'.

Interpolation errors obtained directly from a gravimetric chart, and including errors of determination of anomalies, are usually known as total interpolation errors. On the other hand, interpolation errors which are free from the errors of determination of anomalies are usually called pure interpolation errors. The connection between the total and pure interpolation errors is given by

$$\bar{E}^2 = E^2 + m^2, \tag{3}$$

which applies to random errors, and where $\bar{E}$ is the total error, E is the pure error, and m is the error involved in the determination of the anomaly.

The magnitude of the interpolation errors depends, first of all, on the distance between the stations in the survey. We shall assume that this dependence is given by Equation (2). In addition, the magnitude of these errors is a function of the field anomaly. For a "quiet" field with slowly varying anomalies, the interpolation error will be less than for a field which has large and irregularly varying anomalies. This dependence can be expressed in Equation (2) by having k different for different fields. In view of the above, the magnitude of the interpolation error at a constant interstation distance, or the magnitude of the coefficient k (independently of the chosen distance) may be used as criteria for the degree of anomality. This criterion, being independent of the intuition of the observer, appears to be objective and therefore also reliable. All the above applies also to representation errors.

Interpolation and representation errors determine the accuracy of a gravimetric chart. In fact, by the accuracy of a chart we understand the accuracy with which it is possible to obtain from a given chart the anomaly at any arbitrarily taken point. This accuracy is characterized either by the interpolation error, if we determine the anomaly by interpolation using points in the neighborhood of the given point, or by the representation error, if the anomaly ascribed to the given point is obtained by averaging over the points on the area.

The application of the concepts of interpolation and representation errors introduces clarity into the concept of accuracy of gravimetric charts, and allows one to approach the solution of the problem of the rational distribution of stations, the choice of the accuracy of determination of anomalies, and the choice of the profile of "isoanomals."

In fact, if the accuracy of a chart is given, then one has an indication of the magnitude of the admissible (for this chart) interpolation and representation error, and if there exists a simple relation connecting these errors with the mean distance between points, such as, for example, some relation analogous to that given by Graf-Khenter, then it is easy to obtain the distance by which the stations should be separated on a given area:

$$x = E^2/k^2. \tag{4}$$

The difficulty is that in order to determine x it is necessary to know k and the latter is only known if the survey has already been carried out and x has been established. For new areas which have not been investigated we cannot, strictly speaking, know k since k is a function of the anomaly of the gravitational field. It is necessary to discover whether Equation (2) can be applied to detailed gravimetric surveys, and the variation in k from a survey to a survey, i.e., how stable is k and to what extent can one use the value of k obtained from a number of surveys in new areas. Finally, it is of interest to compare interpolation and representation errors, as this will throw light on the problem of chart construction.

To solve these problems we use the values of representation and interpolation errors calculated for different gravimetric surveys. Results of such calculations are collected together in Tables 1 and 2.

TABLE 1

Interpolation Errors for Different Areas

| Area | Scale | Mean distance, km | $\bar{E}$, mgl* | $E = (\bar{E}^2 - 0.4^2)^{1/2}$ |
|---|---|---|---|---|
| I | 1 : 2 | 3.0 | 1.08 | 1.00 |
| | 1 : 4 | 4.2 | 1.28 | 1.22 |
| | 1 : 8 | 6.0 | 1.63 | 1.58 |
| | 1 : 16 | 8.5 | 2.01 | 1.97 |
| II | 1 : 2 | 4.5 | 1.35 | 1.29 |
| | 1 : 4 | 6.2 | 1.72 | 1.67 |
| | 1 : 8 | 9.0 | 2.00 | 1.97 |
| III | 1 : 2 | 2.7 | 0.5 | 0.30 |
| | 1 : 4 | 3.8 | — | — |
| | 1 : 8 | 5.4 | 0.7 | 0.58 |
| | 1 : 30 | 10.4 | 1.85 | 1.81 |
| IV | 1 : 2 | 2.8 | 0.74 | 0.62 |
| | 1 : 4 | 4.0 | 0.71 | 0.59 |
| | 1 : 8 | 5.6 | 0.83 | 0.73 |
| V | 1 : 2 | 2.7 | 0.52 | 0.33 |
| | 1 : 4 | 3.8 | 0.63 | 0.49 |
| | 1 : 8 | 5.4 | 0.74 | 0.62 |
| VI | 1 : 2 | 3.2 | 0.89 | 0.79 |
| | 1 : 4 | 4.5 | 1.07 | 0.99 |
| | 1 : 8 | 6.4 | 1.27 | 1.20 |
| VII | 1 : 2 | 1.4 | 0.38 | 0.22 |
| | 1 : 4 | 2.1 | 0.38 | 0.22 |
| | 1 : 8 | 2.95 | 0.47 | 0.36 |
| | 1 : 32 | 6.2 | 0.71 | 0.64 |
| | 1 : 64 | 8.6 | 1.02 | 0.97 |
| | 1 : 128 | 12.1 | 1.78 | 1.75 |

Table 1 gives the interpolation errors obtained in seven different gravimetric surveys carried out in the course of geological prospecting. In this table Column 1 gives the number assigned to a given region, Column 2 gives the scale of the survey in relation to the density of stations on the initial chart, Column 3 gives the mean distance between stations for the given survey and scale, and Column 4 gives the interpolation error. The last column gives pure interpolation errors which were obtained on the assumption that the accuracy of determination of the anomaly was given by the mean square error of ± 0.4 mgl.* In these calculations charts involving 2000-3000 or more stations and covering areas of 3 to 20 thousand km$^2$ were used. Each of the errors is obtained from not less than 1000 differences. The calculations of interpolation errors for areas I, VII, III were carried out by graduate students Papendik, T.S. Chesnokova and N.P. Kezhutin. The values for the areas IV, V, VI were obtained at TsNIIGAiK [3].

Table 2 gives the values for representation errors obtained for areas of 25, 100, 400 and 900 km$^2$.

Column 1 of this table gives the number of the region. The numbering in Tables 1 and 2 is the same. Column 2 gives the size of the areas for which representation errors were calculated, and Column 3 gives the representation errors. Calculations for the areas I, II, VII, XI, XII, XIII, XIV were carried out in the Department of Gravimetry and the remaining quantities were obtained at the TsNIIGAiK.

In order to verify Graf-Khenter's formula for detailed surveys we shall calculate for each value of the error of interpolation and representation the coefficient $\underline{k}$ from the formula

$$\bar{E} = k\sqrt{x}, \tag{4'}$$

---

* milligalileo

TABLE 2

Representation Errors for Different Areas

| Region | Area, km$^2$ | $\bar{E}$, mgl | $k = \frac{E}{x}$ | Region | Area, km$^2$ | $\bar{E}$,mgl | $k = \frac{E}{x}$ |
|---|---|---|---|---|---|---|---|
| I | 5×5 | 1.98 | 0.40 | VIII | 5×5 | 1.8 | — |
| | 10×10 | 3.66 | 0.37 | | 10×10 | 3.2 | — |
| | 20×20 | 6.07 | 0.30 | | 20×20 | 5.1 | — |
| | 40×40 | 9.74 | 0.24 | | 30×30 | 8.1 | — |
| II | 10×10 | 2.34 | 0.23 | IX | 5×5 | 1.7 | — |
| | 20×20 | 3.45 | 0.17 | | 10×10 | 2.7 | — |
| | 30×30 | 4.5 | 0.15 | | 20×20 | 4.7 | — |
| | 40×40 | 5.3 | 0.13 | | 30×30 | 8.2 | — |
| III | 5×5 | 1.7 | 0.34 | X | 5×5 | 1.4 | — |
| | 10×10 | 3.4 | 0.34 | | 10×10 | 2.1 | — |
| | 20×20 | 4.4 | 0.22 | | 20×20 | 3.0 | — |
| | 30×30 | 8.2 | 0.27 | | 30×30 | 5.0 | — |
| IV | 5×5 | 1.7 | 0.34 | XI | 5×5 | 1.12 | — |
| | 10×10 | 3.6 | 0.36 | | 10×10 | 2.2 | — |
| | 20×20 | 6.0 | 0.30 | | 20×20 | 3.3 | — |
| | 30×30 | 8.7 | 0.29 | | | | |
| V | 5×5 | 1.3 | 0.26 | XII | 10×10 | 1.8 | — |
| | 10×10 | 2.3 | 0.23 | | 20×20 | 2.9 | — |
| | 20×20 | 4.7 | 0.24 | | 40×40 | 4.3 | — |
| | 30×30 | 6.1 | 0.20 | | | | |
| VI | 5×5 | 1.8 | 0.36 | | 10×10 | 1.4 | — |
| | 10×10 | 2.9 | 0.29 | | 20×20 | 2.2 | — |
| | 20×20 | 3.6 | 0.18 | | 40×40 | 3.3 | — |
| | 30×30 | 7.1 | 0.24 | | | | |
| VII | 2.5××2.5 | 0.6 | — | XIV | 10×10 | 3.9 | — |
| | 5×5 | 1.1 | — | | 20×20 | 6.1 | — |
| | 10×10 | 2.0 | — | | 40×40 | 8.8 | — |
| | 20×20 | 3.5 | — | | | | |

where x is the length of one side of the square which the given point represents, or the mean distance between stations in km, and k equals the 2k of Equation (2).

The degree of constancy of the coefficient will serve as an indication of the applicability of (4'). The variation of this coefficient from region to region should show its dependence on the nature of the anomality of the gravitational field. Table 3 gives the values of the coefficient k obtained using (4') for both the representation and interpolation errors for the areas listed in Tables 1 and 2.

As can be seen from this table, Expression (4') represents interpolation errors quite well for distances between stations of up to 10 km. It can also be seen that in the case of representation errors k clearly depends on the size of the chosen areas and this means that here Expression (4') does not hold so well. Let us consider the dependence of representation and interpolation errors on distance given by

$$\bar{E} = kx^n, \tag{5}$$

in which k and n can be found by the method of least squares. Results of such a treatment of the data are given in Table 4.

The values of k and n for interpolation errors are given in part (a) of Table 4. These values were obtained using the values of interpolation errors given in Table 1 by solving a set of equations of the form

$$\log \bar{E} = \log x + n \log x,$$

TABLE 3

| For interpolation errors | | | For representation errors | | | | | |
|---|---|---|---|---|---|---|---|---|
| area | mean distance $\bar{x}$ in km | $k$ | area | mean distance $\bar{x}$ in km | $k$ | area | mean distance $\bar{x}$ in km | $k$ |
| I | 3.0 | 0.62 | I | 5 | 0.88 | VIII | 5 | 0.80 |
| | 4.2 | 0.62 | | 10 | 1.16 | | 10 | 0.90 |
| | 6.0 | 0.66 | | 20 | 1.20 | | 20 | 1.14 |
| | 8.5 | 0.70 | | 40 | 1.52 | | 30 | 1.46 |
| II | 4.5 | 0.64 | II | 10 | 0.72 | IX | 5 | 0.76 |
| | 6.3 | 0.66 | | 20 | 0.76 | | 10 | 0.86 |
| | 9.0 | 0.68 | | 30 | 0.82 | | 20 | 1.04 |
| | | | | 40 | 0.84 | | 30 | 1.50 |
| III | 2.7 | 0.30 | III | 5 | 0.76 | X | 5 | 0.62 |
| | 5.4 | 0.30 | | 10 | 1.08 | | 10 | 0.66 |
| | 10.4 | 0.58 | | 20 | 0.98 | | 20 | 0.66 |
| | | | | 30 | 1.32 | | 30 | 0.90 |
| IV | 2.3 | 0.44 | IV | 5 | 0.76 | XI | 5 | 0.50 |
| | 4.0 | 0.36 | | 10 | 1.14 | | 10 | 0.70 |
| | 5.6 | 0.36 | | 20 | 1.34 | | 20 | 0.74 |
| | | | | 30 | 1.58 | | | |
| V | 2.7 | 0.32 | V | 5 | 0.58 | XII | 10 | 0.57 |
| | 3.8 | 0.32 | | 10 | 0.74 | | 20 | 0.65 |
| | 5.4 | 0.32 | | 20 | 1.04 | | 40 | 0.68 |
| | | | | 30 | 1.12 | | | |
| VI | 3.2 | 0.52 | VI | 5 | 0.80 | XIII | 10 | 0.44 |
| | 4.5 | 0.50 | | 10 | 0.92 | | 20 | 0.50 |
| | 6.4 | 0.46 | | 20 | 0.80 | | 40 | 0.52 |
| | | | | 30 | 1.28 | | | |
| VII | 1.4 | 0.32 | VII | 2.5 | 0.38 | XIV | 10 | 1.24 |
| | 2.1 | 0.26 | | 5 | 0.49 | | 20 | 1.37 |
| | 3.0 | 0.28 | | 10 | 0.63 | | 40 | 1.39 |
| | 6.2 | 0.28 | | 20 | 0.70 | | | |
| | 8.6 | 0.36 | | | | | | |
| | 12.1 | 0.52 | | | | | | |

TABLE 4

The Quantities $\underline{k}$ and $\underline{n}$ in the Formula $\overline{E} = kx^n$ for the Areas Listed in Tables 1 and 2

| For interpolation | | | For the determined values (representation) | | |
|---|---|---|---|---|---|
| area | $k$ | $n$ | area | $k$ | $n$ |
| I | 0.48 | 0.66 | I | 0.62 | 0.76 |
| II | 0.52 | 0.61 | II | 0.57 | 0.60 |
| III | 0.12 | 0.95 | III | 0.47 | 0.81 |
| IV | 0.47 | 0.23 | IV | 0.42 | 0.89 |
| V | 0.14 | 0.90 | V | 0.27 | 0.93 |
| VI | 0.36 | 0.67 | VI | 0.57 | 0.69 |
| VII | 0.13 | 0.98 | VII | 0.17 | 1.04 |
| | | | VIII | 0.49 | 0.81 |
| | | | IX | 0.40 | 0.86 |
| Mean | 0.31±0.07 | 0.7±0.10 | X | 0.40 | 0.71 |
| | | | XI | 0.27 | 0.86 |
| | | | XII | 0.43 | 0.63 |
| | | | XIII | 0.28 | 0.67 |
| | | | XIV | 1.02 | 0.59 |
| | | | Mean | 0.47±0.06 | 0.78±0.04 |

by the method of least squares. Part (b) of this table gives these values for representation errors.

Table 4 shows that when Equation (5) is applied to interpolation errors the coefficient k will be less, by a factor of 1.5, than in the case of representation errors for the same values of n. We have the same result on comparing the values of k obtained for the same mean values of both interpolation and representation errors calculated from (4). Such a comparison is given in Table 5.

Tables 4 and 5 show that in detailed gravimetric surveys it is necessary to use, as has been the practice, interpretation charts, while in calculations of the distribution of stations one should start with interpolation errors.

The surveys which we have considered are different according to the intensity and division of the field. Thus area I has a strongly variable field with considerable gradients of the order of 1.5-2 mgl per km. For this area both errors are large. Area III has a weakly variable field having large horizontal gradients of the order of 1.5-2 mgl per km. Here, because the isoanomalies are almost parallel, the interpolation is very accurate and hence the interpolation error is small while the representation error is large. Area VII has a weakly variable field with small gradients of the order of 0.5 mgl per km. For this area both the interpolation and representation errors are small.

TABLE 5

A Comparison of Interpolation and Representation Errors According to the Values of k Obtained from the Formula $\bar{E} = k\sqrt{x}$

| No. of arc a | Mean distance in km | Interpolation error | Representation error |
|---|---|---|---|
| I | 5 | 0.64 | 0.88 |
| III | 5 | 0.30 | 0.76 |
| IV | 5 | 0.36 | 0.76 |
| V | 5 | 0.32 | 0.58 |
| VI | 5 | 0.50 | 0.80 |
| VII | 5 | 0.28 | 0.49 |
| Mean | | 0.40±0.14 | 0.71±0.14 |
| I | 10 | 0.70 | 1.16 |
| II | 10 | 0.68 | 0.72 |
| III | 10 | 0.58 | 1.08 |
| VII | 10 | 0.40 | 0.63 |
| Mean | | 0.59±0.12 | 0.90±0.26 |

We tried to treat charts with both very steady and rapidly varying gravitational fields. In such cases interpolation and representation errors change appreciably depending on the nature of the field.

Thus, in considering k and n in the case of interpolation errors [Table 4 (a)], we can divide all the areas into two groups. One of these consists of areas I, II, IV and VI and the other III, V and VII, and for the first of these areas $k_{mean} = 0.46$ and $n = 0.57 \approx 0.5$. The interpolation errors for these surveys are well represented by

$$\bar{E} = 0.46\sqrt{x}.$$

For areas III, V and VII, $k_{mean} = 0.13$ and $n_{mean} \approx 1$. For those surveys, interpolation errors can be represented by

$$\bar{E} = 0.13x.$$

It would be possible to divide a country according to the intensity of anomalies, taking k as the criterion (cf. Tables 1, 2 and 3). Such an approximate division would allow a more accurate planning of gravimetric surveys,

TABLE 6

| Profile | Accuracy of chart, mgl | Scale | Accuracy of determination and mean distance between | | | | | |
|---|---|---|---|---|---|---|---|---|
| | | | calculated using $E = 0.3^{0.7}$ | | calculated in [5] | | according to the "Instruction" | |
| | | | $m$, mgl | $x$, km | $m$, mgl | $x$, km | $m$, mgl | $x$, km |
| 10 | 4 | 1 : 1 000 000 | 2.8 | 38.6 | 2.8 | 39 | 4 | 10—7 |
| 5 | 2 | 1 : 500 000 | 1.4 | 14.3 | 1.4 | 9.8 | 2 | 3 |
| 2 | 0.8 | 1 : 100 000 | 0.6 | 3.9 | 0.6 | 1.6 | 0.8 | 1.5 |
| 1 | 0.4 | 1 : 50 000 | 0.3 | 1.4 | 0.3 | 0.4 | 0.4 | 0.2 |
| 0.5 | 0.5 | 1 : 25 000 | 0.1 | 0.5 | 0.1 | 0.1 | 0.2 | 0.1 |

but it requires a very laborious study of extensive data. A large error will not be introduced if one uses for all plane areas the general formula $\overline{E} = kx^n$ with constant k and n, remembering that the errors thus introduced will be smaller than those obtained with arbitrary planning, the more so since strongly variable, intensely anomalous fields are relatively rare. In our calculations we used the following expression:

$$\overline{E} = 0.3\,x^{0.7}. \tag{5*}$$

The application of numerical characteristics such as interpolation errors to the planning of surveys allows one, though admittedly less rigorously, to approach the solution of the problem of establishing the accuracy of the survey. The accuracy of a chart, of which the interpretation error is a measure, depends on the accuracy of interpolation and the accuracy of determination of the anomalies. This dependence is given by Equation (3). Clearly the components of Equation (3) cannot be arbitrary. Thus, in the case of "rare" survey and low accuracy of interpolation it is futile to seek high accuracy of determination, and, conversely, in the case of a "dense" survey, when interpolation is carried out accurately, it is necessary to increase the accuracy of the determination of anomalies. If the latter is of the order of the accuracy of interpolation, further increase in the density, i.e., an increase in the accuracy of interpolation, is irrational, and beyond a certain limit quite futile.

In order to establish the necessary accuracy of determination of anomalies we shall consider that the error in the determination of anomalies should be equal to the pure interpolation error (cf. Table 1) so that $m = E$, but since $\overline{E}^2 = E^2 + m^2$, we find for the admissible error in the determination of anomalies the following simple relation

$$m = 0.7\,\overline{E}. \tag{6}$$

Formulas (5*) and (6) may be used to calculate the density of stations and the accuracy of determination of anomalies. A calculation of the density of gravimetric stations has already been carried out in [4] using the concept of interpolation error. However, the latter calculations were based on the data of only two surveys. We are now in a position to correct the results obtained in [5] using much more extensive data.

TABLE 7

| No. | Accuracy of chart mgl | Profile, mgl | Error in determination of anomalies, mgl | Mean distance km | Scale |
|---|---|---|---|---|---|
| 1 | 4 | 10 | ±2.8 | 35 | 1 : 1 000 000—1 : 500 000 |
| 2 | 2 | 5 | 1.4 | 10 | 1 : 500 000—1 : 200 000 |
| 3 | 1 | 2.5 | 0.7 | 5 | 1 : 500 000—1 : 200 000 |
| 4 | 0.8 | 2.0 | 0.6 | 3 | 1 : 200 000—1 : 100 000 |
| 5 | 0.4 | 1.0 | 0.3 | 1 | 1 : 100 000—1 : 50 000 |
| 6 | 0.2 | 0.5 | 0.1 | 0.5 | 1 : 50 000—1 : 25 000 |
| 7 | 0.1 | 0.25 | 0.05 | 0.2 | 1 : 50 000—1 : 10 000 |

Table 6 gives a comparison of the accuracy of determination of anomalies m and the density of stations x calculated from (5*) and (6) (Columns 4 and 5) with the corresponding values obtained in [4] (Columns 6 and 7) and the values given in "Instruction for Gravitational Surveys with Gravimeters" [5] (Columns 8 and 9). Columns 1 and 3 give the profile of the charts and the scale, Column 2 gives the accuracy of the chart taken as equal to the interpolation error for the given chart. This quantity was shown as equal to the value of the error of determination given in Table 7. The profile given in Column 1 was determined in accordance with the above Instructions as the mean quadratic error in the determination of anomalies multiplied by 2.5. It is natural to take the interpolation error multiplied by 2.5 as equal to the profile of the "isoanomals." In the table the profiles obtained from the Instruction and from our calculations agree since we are comparing these quantities for the same accuracy of charts and errors of determination of anomalies according to the Instruction.

It is clear from Table 6 that the density of stations required by the Instructions is excessively large. On the other hand, its requirements in relation to the accuracy of determination of anomalies are not sufficiently stringent. This conclusion has already been reached in [4]. The increased volume of data now available not only confirms this conclusion but shows that in the majority of cases one can increase the mean distance between stations, compared with the distance suggested by us earlier, without loss of accuracy of the chart. In gravimetric survey practice we often come across excessive densities of stations when these densities could be cut down by a factor of 2 or even 3 without a loss of accuracy of the chart. The introduction of numerical criteria in the planning of gravimetric surveys will allow a reduction in the number of such cases and will introduce a considerable economy and thus increase the rate at which gravimetric work is being carried out. As a rough guide to the admissible accuracies and distributions of stations in gravimetric surveys one may recommend Table 7 in which approximate mean values of the quantities involved which were obtained by us are given.

Naturally, the mean values given in the above table may turn out to be unsatisfactory in special cases. Clearly, when regions of strong anomaly are present it is necessary to allow for a greater density of stations. Furthermore, in the case of a well-defined run of anomalies it is necessary to increase the density of points on profiles directed along the run.

The following appear to be the main conclusions of the above discussion of the numerical values of interpolation and representation errors:

1. The interpolation error in detailed gravimetric surveys is, as a rule, approximately 1.5 times smaller than the representation error.

2. The requirements for detailed gravimetric surveys, as formulated in the "Instruction" mentioned above, are not quite stringent enough as far as the accuracy of determination of anomalies is concerned, and are definitely excessive in respect to the density of stations. New tolerances must be introduced into the "Instruction" based on the concept of interpolation error.

3. The errors of interpolation in detailed gravimetric surveys on a plain, in the case of an average field anomality, may be calculated from the approximate empirical formula

$$\bar{E} = 0.3\,x^{0.7},$$

where x is the mean distance between stations in km, and $\bar{E}$ is the interpolation error in mgl.

## LITERATURE CITED

[1] A.I. Baiborodin, Trudy TsNIIGAiK* 1951, No. 86.

[2] M.S. Molodenskii, Trudy TsNIIGAiK* 1945, No. 42.

[3] L.A. Govorova, Sbornik Referatov TsNIIGAiK* 1955, No. 4.

[4] N.P. Grushinskii, Razvedochnaia Promyslovaia Geofizika 1956, No. 15.

[5] Instruction for Gravimetric Surveys with Gravimeters [in Russian] (Geological Publishing House, 1952).

Received June 19, 1956

P.K. Shternberg State Astronomical Institute

---

*Central Scientific Research Institute of Geodesy, Aerial Surveying and Cartography.

# SOME METHODS OF PLOTTING AN INTERMEDIATE ORBIT FOR ASTEROIDS OF THE TROJAN GROUP. I.

Iu. A. Riabov

A method for computing an intermediate orbit for the "Trojans" is considered, based on the application of what is termed the single averaged variant of the Delaunay-Hill problem. Some of the essential characteristics of this orbit are studied, using integrals of the intermediate orbit, and the results are compared with observational data accumulated for the "Trojans." The intermediate orbit for asteroid No. 884, Priamus, is constructed, using mechanical quadratures.

In the present article we consider a technique for constructing an intermediate orbit for the "Trojans" based on the application of the single-averaged variant of the Delaunay-Hill problem, which was first introduced by N.D. Moiseev [1, 2]. The formulas for the osculating elements are obtained in explicit form, while it is necessary to resort, in part, to mechanical quadratures, since an intermediate orbit must be plotted separately for each "Trojan."

The method under consideration is applied to "Trojans" whose orbits exhibit a relatively large inclination to the ecliptic.

## 1. Setting Up of Initial Equations of Motion for the "Trojans"

We shall view the "Trojans" as ordinary asteroids lacking any relationship to "triangular" points of libration, but moving about the sun in a manner such that their mean motion is close to the mean motion of Jupiter (a close commensurability of mean motions of the type 1 : 1).

As an initial problem, let us take the scheme of the restricted elliptic problem of three bodies and use for our investigation the ordinary motions with respect to the osculating elements of the orbits of the "Trojans" about the sun.

We shall select our units of length and time such that the semimajor axis of the orbit of Jupiter a' and the gravitational constant $k^2$ will be equal to unity. As unit of mass, let us take the sum of the masses of the sun $M_S$ and of Jupiter m' and assume:

$$M_S = 1 - m, \quad m' = m.$$

We shall consider the osculating elements of the orbits of the "Trojans" referred to the plane of the ecliptic. The equations with respect to the osculating elements – semimajor axis $\underline{a}$, eccentricity $\underline{e}$, longitude of the perihelion $\bar{\omega}$, longitude of the node $\Omega$, inclination $\underline{i}$, mean anomaly M – are written in the following manner:

$$\frac{da}{dt} = 2\sqrt{a}\,\frac{\partial W}{\partial M},$$

$$\frac{de}{dt} = \frac{1-e^2}{e\sqrt{a}}\,\frac{\partial W}{\partial M} - \frac{\sqrt{1-e^2}}{e\sqrt{a}}\,\frac{\partial W}{\partial \bar{\omega}},$$

$$\frac{d\bar{\omega}}{dt} = \frac{\sqrt{1-e^2}}{e\sqrt{a}}\,\frac{\partial W}{\partial e} + \frac{\tan\frac{i}{2}}{\sqrt{a(1-e^2)}}\,\frac{\partial W}{\partial i}, \qquad (1) \text{ (continued)}$$

$$\frac{dM}{dt} = \frac{1}{a\sqrt{a}} - \frac{1-e^2}{e\sqrt{a}}\frac{\partial W}{\partial e} - 2\sqrt{a}\frac{\partial W}{\partial a},$$

$$\frac{d\Omega}{dt} = \frac{1}{\sqrt{a(1-e^2)}}\frac{1}{\sin i}\frac{\partial W}{\partial i},$$

$$\frac{di}{dt} = -\frac{\tan\frac{i}{2}}{\sqrt{a(1-e^2)}}\frac{\partial W}{\partial \bar{\omega}} - \frac{1}{\sqrt{a(1-e^2)}}\frac{1}{\sin i}\frac{\partial W}{\partial \Omega},$$

(1)
(continued)

where W denotes the disturbing function.

If we use $\underline{r}$, r', Δ to designate the corresponding mutual distances between the sun S, Jupiter J and any given "Trojan" P, and θ to designate the angle between directions SP and SJ (Figure 1), then the disturbing function W may be written in the form:

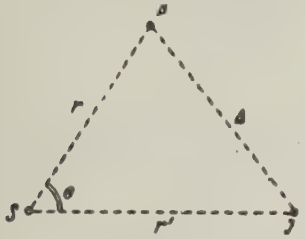

Fig. 1

$$W = m\left(-\frac{1}{r} + \frac{1}{\Delta} - \frac{r\cos\theta}{r'^2}\right). \tag{2}$$

For convenience in further investigation, we may designate

$$\Delta^2 = r'^2 + \rho,$$

where

$$\rho = r^2 - 2rr'\cos\theta,$$

and rewrite W in the form:

$$W = m\left[-\frac{1}{r} - \frac{1}{2}\frac{r^2}{r'^2} + \frac{1}{r'}R(\bar{\rho}) + rr'\cos\theta\left(\frac{1}{r'^2} - \frac{1}{r'^3}\right)\right], \tag{3}$$

where

$$R(\bar{\rho}) = \frac{1}{\sqrt{1+\bar{\rho}}} - 1 + \frac{1}{2}\bar{\rho}, \quad \bar{\rho} = \frac{\rho}{r'}.$$

Using known formulas for nondisturbed elliptic motion, we may represent W in the form of a series which expands in integral positive powers of the eccentricity of the orbit of Jupiter e', and also of the inclination of the orbit of the "Trojan" in question. Neglecting the inclination of the orbit of Jupiter, for W we obtain the expression:

$$W = \sum_{k=0}^{\infty}(W_{k0} + i^2W_{k2} + i^4W_{k4} + \ldots)e'^k, \tag{4}$$

with $W_{00}$ and $W_{02}$ defined by the formulas:

$$W_{00} = m\left\{-\frac{1}{r} - \frac{1}{2}r^2 + \frac{1}{\sqrt{1+\rho_{00}}} - 1 + \frac{1}{2}\rho_{00}\right\},$$

$$W_{02} = \frac{1}{2}\rho_{02}\left[1-(1+\rho_{00})^{-3/2}\right], \tag{5}$$

where

$$\rho_{00} = r^2 - 2r\cos(\bar{\omega} + v - \lambda'),$$

$$\rho_{02} = -r\sin\Omega\sin(\bar{\omega} - \Omega + \lambda'). \tag{6}$$

## 2. On the Method of Constructing an Intermediate Orbit

It can be shown that the solution of the initial Equations (1) may be found in the form of series expanded in integral positive powers of small parameters, which are e' and the initial value of i:

$$\text{э}_s = \text{э}_{s0} + \sum_{n=1}^{\infty} \sum_{j=0}^{\infty} \text{э}_s^{(jn)} \alpha^n e'^j,$$

where $\alpha$ denotes the initial value of i, and $\text{э}_1, \text{э}_2, \ldots, \text{э}_6$ designate the osculating elements under consideration.

We may consider the first terms of these series, $\text{э}_{s0}$, when they are used to express long-period changes, as the osculating elements of our intermediate orbit. Equations for the first terms of those series are written in the form:

$$\begin{aligned}
\frac{da_0}{dt} &= 2\sqrt{a_0}\left(\frac{\partial W_{00}}{\partial M}\right)_0, \\
\frac{de_0}{dt} &= \frac{1-e_0^2}{e_0\sqrt{a_0}}\left(\frac{\partial W_{00}}{\partial M}\right)_0 - \frac{\sqrt{1-e_0^2}}{e_0\sqrt{a_0}}\left(\frac{\partial W_0}{\partial \bar{\omega}}\right)_0, \\
\frac{d\bar{\omega}_0}{dt} &= \frac{\sqrt{1-e_0^2}}{e_0\sqrt{a_0}}\left(\frac{\partial W_{00}}{\partial e}\right)_0, \\
\frac{dM_0}{dt} &= \frac{1}{a_0\sqrt{a_0}} - \frac{1-e_0^2}{e_0\sqrt{a_0}}\left(\frac{\partial W_{00}}{\partial e}\right)_0 - 2\sqrt{a_0}\left(\frac{\partial W_{00}}{\partial a}\right)_0. \\
\frac{d\text{☊}_0}{dt} &= \frac{2}{\sqrt{a_0(1-e_0^2)}}(W_{02})_0, \\
\frac{di_0}{dt} &= 0,
\end{aligned} \tag{7}$$

where $\left(\frac{\partial W_{00}}{\partial M}\right)_0 = \left(\frac{\partial W_{00}}{\partial M}\right)_{a=a_0,\ldots}$.

At $t = t_0$, the values of $a_0', e_0' \ldots, i_0'$ coincide with the initial values of the desired osculating elements.

Since the mean motions of the "Trojans" are close to the Jovian mean motion, i.e., a (1 : 1) commensurability of the mean motions of the perturbed and perturbing body takes place, then, in order to work out the long-period part of the solution of the Equations (7), we shall find it expedient to apply the single-averaged variant of the Delaunay-Hill problem of the limited plane circular problem of three points, considered for the first time by N.D. Moiseev [1, 2]. That method consists of the following.

Let there be given the following equations with respect to the osculating elements a, e, $\omega$, M of the plane circular problem of three points:

$$\begin{aligned}
\frac{da}{dt} &= 2\sqrt{a}\,\frac{\partial W}{\partial M}, \\
\frac{de}{dt} &= \frac{1-e^2}{e\sqrt{a}}\,\frac{\partial W}{\partial M} - \frac{\sqrt{1-e^2}}{e\sqrt{a}}\,\frac{\partial W}{\partial \omega}, \\
\frac{d\omega}{dt} &= \frac{\sqrt{1-e^2}}{e\sqrt{a}}\,\frac{\partial W}{\partial a}, \\
\frac{dM}{dt} &= \frac{1}{a\sqrt{a}} - 2\sqrt{a}\,\frac{\partial W}{\partial a} - \frac{1-e^2}{e\sqrt{a}}\,\frac{\partial W}{\partial e},
\end{aligned} \tag{8}$$

where W is the disturbing function which may be represented, as is known, in the form:

$$W = \sum_{q=0}^{\infty} \sum_{s=-\infty}^{\infty} C_{qs}(a, e) \cos[qM + s(\omega - n't)],$$

where $C_{qs}$ are dependent only on $a$ and $e$.

In terms of the units of time which we selected, the mean motion of the perturbing body n' is equal to unity.

Consider a close commensurability of the mean motions $n$ and n' of the perturbed and perturbing bodies, i.e.,

$$\frac{n}{n'} \approx \frac{s^*}{q^*},$$

where s*, q* are two integral positive numbers.

Let us further introduce the quantity D, termed the Delaunay anomaly, and equal to

$$D = q^* M + s^* (\omega - n't), \tag{9}$$

after which the function W may be rewritten in the form:

$$W = \sum_{q=0}^{\infty} \sum_{s=-\infty}^{\infty} C_{qs} \cos\left[\frac{qs^* - sq^*}{s^*} M + \frac{s}{s^*} D\right]. \tag{10}$$

Putting $q = \chi q^*$, $s = \chi s^*$, where $\chi = 0, 1, 2, \ldots$, we obtain a set of terms in the disturbing function dependent only on $a$, $e$, D.

For the mean anomaly M we have, in general, the expression:

$$M = \overline{M}_0(t) + \int_{t_0}^{t} n(t)\,dt,$$

where $\overline{M}_0(t)$ denotes the mean anomaly of the initial epoch $t_0$.

Using the mean value theorem for definite integrals, we may rewrite this expression in the form:

$$\overline{M} = M_0(t) + \overline{n}(t - t_0),$$

where $\overline{n}$ is some mean value of $n$ in the time interval $t - t_0$, which, naturally, varies with increase in $t - t_0$. $\overline{n}$ and $\overline{M}_0$ thereby change comparatively slowly.

Having rewritten the Delaunay anomaly in the form

$$D = (q^*\overline{n} - s^*n')\,t + q^*\overline{M}_0 + s^*\omega,$$

we see that, by virtue of the close commensurability of $n$, n', and also of $\overline{n}$, n', it changes in each case in the course of significant intervals of time at a very slow rate, and that the set of terms in W, dependent solely on $a$, $e$, D, represents the secular and long-period part of the perturbatory function.

The working out of the secular and long-period part of the disturbing function, which we shall designate as [W], may be effected either directly on the basis of the Series (10), or with the aid of the following averaging of the disturbing function:

$$[W] = \frac{1}{2\pi s^*} \int\limits_{M=0}^{2\pi s^*} W dM,$$

where integration is performed under the conditions:

1. Instead of $\omega - n't$, an expression D for the Delaunay anomaly is introduced into the disturbing function.

2. In the process of integration, the Delaunay anomaly D and the osculating elements $\underline{a}$, $\underline{e}$ are assumed constant.

3. The mean anomaly M is not dependent on D.

The values of the function [W] correspond closely with the sense of such an averaging to the mean value of W, in the course of the osculating period of revolution of the perturbed body. This function will be explicitly dependent only on $\underline{a}$, $\underline{e}$, D, whereby D is expressed by means of the Formula (9).

Let us now replace W in Equations (8) by [W], thereby taking into account the fact that

$$\frac{\partial [W]}{\partial M} = \frac{\partial [W]}{\partial D} q^*, \qquad \frac{\partial [W]}{\partial \omega} = \frac{\partial [W]}{\partial D} s^*.$$

We then obtain the following equations:

$$\begin{aligned} \frac{da}{dt} &= 2\sqrt{a}\, q^* \frac{\partial [W]}{\partial D}, \\ \frac{de}{dt} &= \frac{q^*(1-e^2) - s^*\sqrt{1-e^2}}{e\sqrt{a}} \frac{\partial [W]}{\partial D}, \\ \frac{d\omega}{dt} &= \frac{\sqrt{1-e^2}}{e\sqrt{a}} \frac{\partial [W]}{\partial e}, \\ \frac{dM}{dt} &= \frac{1}{a\sqrt{a}} - 2\sqrt{a} \frac{\partial [W]}{\partial a} - \frac{1-e^2}{e\sqrt{a}} \frac{\partial [W]}{\partial e}. \end{aligned} \tag{11}$$

In solving these equations, we may then consider that the most essential secular and long-period perturbations of the desired osculating elements will be worked out in the process.

Equations (11) have, as is known, two integrals:

$$\begin{aligned} s^*\sqrt{a} &= q^*\sqrt{a(1-e^2)} + \text{const} \\ \frac{1}{2a} + n'\sqrt{a(1-e^2)} + [W] &= \text{const} \end{aligned} \tag{11*}$$

The last integral is a Jacobi integral.

In virtue of the presence of those two integrals, the solution of Equations (11) may be reduced to quadratures.

We shall plot our intermediate orbit, using the method of averaging the perturbatory function in the Delaunay-Hill problem, with some changes.

In the given case, a 1:1 commensurability of the mean motions occurs, and the Delaunay anomaly is equal to

$$D = \bar{\omega} + M - \lambda',$$

i.e., is the difference between the mean longitudes of the "Trojans" and of Jupiter.

In accordance with the above, we have to replace the function $W_{00}$ in (8) by its averaged value $[W_{00}]$:

$$[W_{00}] = \frac{m}{2\pi} \int\limits_{M=0}^{2\pi} \left[ -\frac{1}{r} - \frac{1}{2} r^2 + R(\rho_{00}) \right] dM,$$

where, on integrating, the quantities $\underline{r}$ and $\rho_{00}$ must be expressed in terms of the elements $\underline{a}$, $\underline{e}$, M and the Delaunay anomaly D, and the conditions indicated above must also be fulfilled.

This method of working out the secular and long-period parts of $W_{00}$ will prove convenient, if it is possible to expand $W_{00}$ in a series in ascending powers of the eccentricity $\underline{e}$. But, to obtain such a series, it is first of all necessary to expand the function $R(\rho_{00})$ into a series in powers of $\underline{e}$. However, this last approach is hardly expedient at all, since $\rho_{00}$, in its changes, attains comparatively high values for the observed "Trojans": 0.3, 0.5 and higher. For the "Trojan" No. 1173, $\rho_{00}$ reaches, for example, values so high as to exceed 0.91. Therefore, we must refrain from expanding the function $R(\rho_{00})$ into a power series in $\underline{e}$. But it will then be expedient for us to resort to some simplified variant of the method of averaging the disturbing function.

The function $W_{00}$ is dependent on the osculating elements through its dependence on the intermediate arguments $\underline{r}$ and $\rho_{00}$. To obtain from $W_{00}$ constant terms and terms not dependent on M, we average not the function W, taken in its entirety, but the intermediate arguments $\underline{r}$ and $\rho_{00}$. We set

$$[r] = \frac{1}{2\pi} \int\limits_{M=0}^{2\pi} r\,dM, \quad [\rho] = \frac{1}{2\pi} \int\limits_{M=0}^{2\pi} \rho_{00}\,dM,$$

where, on integration, all the conditions indicated above are fulfilled, and replacing in $W_{00}$ the values of $\underline{r}$ and $\rho_{00}$ with the values of [r], [ρ], we get the averaged function $[\overline{W}_{00}]$ in the form:

$$[\overline{W}_{00}] = W_{00}([r],\ [\rho]).$$

Such a simplified procedure for averaging makes it possible to work out, in $W_{00}$, not all of the constants and long-period terms, but, given the condition of the smallness of the values of the osculating eccentricity $\underline{e}$, the more significant ones. It may be shown that, in carrying out such an averaging operation, terms having an order of $e^2$ or higher are not considered.

Using simplified averaging, we obtain $[\overline{W}_{00}]$ in a rather simple form, and all the calculations are carried out in more or less simple fashion in constructing the intermediate orbit. Given its mechanical interpretation, our averaging operation differs from the exact operation in that it gives not the average value of $W_{00}$, over a time interval equal to the osculating period of revolution of the "Trojans," but the value of $W_{00}$ at mean distances $\underline{r}$ and $\rho_{00}$ for that time interval.

## 3. Setting Up Differential Equations Determining the Intermediate Orbit

Making use of the familiar series of a nonperturbed elliptic motion for values $\underline{r}$, $r\cos(\nu - M)$, $r\sin(\nu - M)$, we may write $\underline{r}$ and $\rho_{00}$ in the form:

$$\begin{aligned} \frac{r}{a} &= 1 - e\cos M + e^2\left(\frac{1}{2} - \frac{1}{2}\cos 2M\right) + e^3\left(\frac{3}{8}\cos N - \frac{3}{8}\cos 3M\right) + \\ &\quad + e^4\left(\frac{1}{3}\cos 2M - \frac{1}{3}\cos 4M\right) + \ldots, \qquad (12) \\ \rho_{00} &= a^2 - 2a\cos D + e[-2a^2\cos M - a\cos(D+M) + 3a\cos(D-M)] + \\ &\quad + e^2\left[\frac{3}{2}a^2 + a\cos D - \frac{1}{2}a^2\cos M - \frac{3}{4}a\cos(D+2M) - \right. \\ &\quad \left. - \frac{1}{4}a\cos(D-2M)\right] + e^3\left[\frac{1}{4}a^2\cos M - \frac{1}{4}a\cos 3M + \right. \\ &\quad \left. + \frac{3}{4}a\cos(D+M) - \frac{2}{3}a\cos(D+3M) - \frac{1}{12}a\cos(D-3M)\right] + \\ &\quad + e^4\left[\frac{1}{32}a\cos D + \frac{1}{6}a^2\cos 2M - \frac{1}{6}a^2\cos 4M + 2a\cos(D+2M) - \right. \\ &\quad \left. - \frac{4}{3}a\cos(D-2M) - \frac{299}{192}a\cos(D+4M) + \frac{165}{192}a\cos(D-4M)\right] + \ldots, \end{aligned}$$

where terms higher than the 4th order with respect to $e$ are discarded.

Expanding the constant and long-period part of $r$ and $\rho_{00}$, we obtain with accuracy up to 4th order terms:

$$[r] = a\left(1 + \frac{1}{2}e^2\right), \tag{13}$$

$$[\rho] = a^2 - 2a\cos D + \frac{3}{2}a^2e^2 + a\left(e^2 + \frac{1}{32}e^4\right)\cos D.$$

We may write the averaged perturbing function $\overline{[W_{00}]}$ in the form:

$$\overline{[W_{00}]} = m\left\{-\frac{1}{[r]} - \frac{1}{2}[r]^2 + R\left([\rho]\right)\right\} \tag{14}$$

or

$$\overline{[W_{00}]} = m\left\{-\frac{1}{a} - \frac{1}{2}a^2 + \frac{1}{2}e^2\left(\frac{1}{a} - a^2\right) + \frac{1}{4}\left(-\frac{1}{a} - \frac{1}{2}a^2\right) + \right.$$

$$\left. + \frac{1}{\sqrt{1+[\rho]}} - 1 + \frac{1}{2}[\rho]\right\}. \tag{15}$$

Replacing $W_{00}$ in Equations (7) by $\overline{[W_{00}]}$ and taking into account the fact that $W_{02}$ does not contain constant and long-period terms, we obtain the following equations (in order to stress the fact that we are dealing not with the exact Equations (7), but with modified equations, we replace the variables $a_0$, $e_0$, $\bar{\omega}_0$, $M_0$, $\Omega_0$, $i_0$, by the variables $a_*$, $e_*$, $\bar{\omega}_*$, $M_*$, $\Omega_*$, $i_*$):

$$\begin{aligned}
\frac{da_*}{dt} &= 2\sqrt{a_*}\left(\frac{\partial\overline{[W_{00}]}}{\partial D}\right)_*,\\
\frac{de_*}{dt} &= \frac{1-e_*^2-\sqrt{1-e_*^2}}{e_*\sqrt{a_*}}\left(\frac{\partial\overline{[W_{00}]}}{\partial D}\right)_*,\\
\frac{d\bar{\omega}_*}{dt} &= \frac{\sqrt{1-e_*^2}}{e_*\sqrt{a_*}}\left(\frac{\partial\overline{[W_{00}]}}{\partial e}\right)_*,\\
\frac{dM_*}{dt} &= \frac{1}{a_*\sqrt{a_*}} - \frac{1-e_*^2}{e_*\sqrt{a_*}}\left(\frac{\partial\overline{[W_{00}]}}{\partial e}\right)_* - 2\sqrt{a_*}\left(\frac{\partial\overline{[W_{00}]}}{\partial a}\right)_*\\
\frac{d\Omega_*}{dt} &= 0, \quad \frac{di_*}{dt} = 0,
\end{aligned} \tag{16}$$

where the subscript $*$ attached to the derivatives of function $\overline{[W_{00}]}$ denotes the fact that, after carrying out the differentiation, those terms contain, instead of $a$, $e$, $\bar{\omega}$, $M$, $D$, the substituted terms $a_*$, $e_*$, $\bar{\omega}_*$, $M_*$, $D_*$, whereby

$$D_* = \bar{\omega}_* + M_* - \lambda'. \tag{16*}$$

Equations (16) are initial equations defining our intermediate orbit. The variables $a_*$, $e_*$, $\bar{\omega}_*$, $M_*$, $\Omega_*$, $i_*$ are osculating elements of that intermediate orbit.

## 4. Method of Solving Equations for the Intermediate Orbit

Equations (16) have four integrals. Let us note, first of all, that in the simplified averaging over the intermediate arguments, integrals of the form (11*), obtained in the exact averaging operation, are retained. We therefore obtain the integral:

$$\sqrt{a_*}\left(1 - \sqrt{1-e_*^2}\right) = \gamma, \tag{17}$$

and the Jacobi integral:

$$\frac{1}{2a_*} + \sqrt{a_*(1-e_*^2)} + [\overline{W}_{00}] = C, \tag{18}$$

where $\gamma$ and C are arbitrary constants. Let us note that $\gamma$ is small and has the order of $e_*^2$.

In addition, we immediately get

$$\Omega_* = \text{const}, \; i_* = \text{const}.$$

With the aid of Integral (17), we may express $e_*$ in terms of $a_*$:

$$e_*^2 = \frac{\gamma}{\sqrt{a_*}}\left(2 - \frac{\gamma}{\sqrt{a_*}}\right). \tag{19}$$

The Jacobi Integral (18) may, with the aid of (19), be written in the form:

$$\frac{1}{2a_*} + \sqrt{a_*} + [\overline{W}_{00}] = \overline{\beta}, \tag{20}$$

where $\overline{\beta}$ is a constant.

Substituting into $[\overline{W}_{00}]$, instead of $e_*$, its expression in terms of $a_*$, we obtain a relation linking $a_*$ and $D_*$:

$$\Phi(a_*, \; D_*) = \overline{\beta}. \tag{21}$$

On the basis of (21), $D_*$ may be expressed as a function of $a_*$:

$$D_* = D_*(a_*) \tag{22}$$

or, conversely, it is possible to express $a_*$ as a function of $D_*$:

$$a_* = a_*(D_*).$$

Using, for example, (19) and (22), we may express the right-hand parts of the equations for $a_*$ and $\overline{\omega}_*$ in terms of $a_*$. We then get

$$\frac{da_*}{dt} = F_1(a_*), \tag{23}$$

$$\frac{d\overline{\omega}_*}{dt} = F_2(a_*). \tag{24}$$

Solving the equation for $a_*$, we obtain $a_*$ as a function of time _t_:

$$a_* = a_*(t).$$

Substituting the expression for $a_*$ into (24), and integrating, we get

$$\overline{\omega}_* = \overline{\omega}_*(t).$$

On the basis of (16*), we may further express, in terms of $a_*$ and $\overline{\omega}_*$, the mean anomaly $M_*$:

$$M_* = D_*(a_*) - \overline{\omega}_* + \lambda', \tag{25}$$

We thus see that the values $a_*$ and $\overline{\omega}_*$ may be determined as a time function with the aid of quadratures, and then expressed on the basis of the corresponding formulas of $e_*$, $M_*$, in terms of $a_*$ and $\overline{\omega}_*$. Since $\Omega_*$, $i_*$ remain constant, the intermediate orbit will then be fully determined after that point.

## 5. Investigation of the Jacobian Integral. Some General Properties of the Intermediate Orbit

Since, for the "Trojans," the semimajor axis of their osculating orbits is close to unity, and the difference in the average longitudes of the "Trojans" and Jupiter still does not differ appreciably from +60° or −60°, for convenience in further investigations it is expedient to introduce the variables $x$, $\psi$, setting

$$a_* = 1 + x, \quad \psi = 1 - 2\cos D_*. \tag{26}$$

Expanding $(1+x)^{-1/2}$, $(1+x)^{-1}$ into a power series in $x$, Integral (19) may be rewritten in the form:

$$e_*^2 = \gamma\left[2 - \gamma + (-1+\gamma)x + \frac{3}{4}x^2 + \dots\right], \tag{27}$$

where terms higher than the 3rd order with respect to $\gamma$ and $x$ are discarded.

For the "Trojans," it follows from observational data and findings which will be supplied below that $\gamma$ and $|x|$ are not in excess of 0.01-0.02. In practice, we discard in the perturbing function $[\overline{W}_{00}]$ terms higher than the 5th order relative to $e_*$, which guarantees accuracy to the 5th decimal place. Therefore, in all further calculations, we have the full right to restrict ourselves to terms of the 3rd degree relative to $\gamma$ and $x$ which, in any case, retains such accuracy.

Substituting into (20) the expression for $e_*^2$ and going on to the variables $x$, $\psi$, we may, after rearranging terms, write the integral in the form

$$\Phi(x, \psi) \equiv f(x) + mR([\rho]) - \beta = 0, \tag{28}$$

where

$$f(x) = 3m(-\gamma+\gamma^2)x + \left[\frac{3}{8} - \frac{3}{2}m(1-\gamma)\right]x^2 + \left(-\frac{7}{16} + m\right)x^3 + \dots,$$

$$R([\rho]) = \frac{1}{\sqrt{1+[\rho]}} - 1 + \frac{1}{2}[\rho],$$

$$[\rho] = 4\gamma - \frac{31}{16}\gamma^2 + \left(1 + 5\gamma - \frac{9}{2}\gamma^2\right)x + (1+\gamma)x^2 +$$
$$+ \left[1 - \gamma + \frac{7}{16}\gamma^2 + \left(1 - \frac{1}{2}\gamma\right)x - \frac{1}{8}\gamma x^2\right]\psi,$$

and $\beta$ is the constant of the given integral.

In $f(x)$ and $[\rho]$, all terms higher than the 3rd order with respect to $\gamma$ and $x$ are discarded. If we designate

$$\begin{aligned}
&A_1 = 3m(-\gamma+\gamma^2), && \alpha_0 = 4\gamma - \frac{31}{16}\gamma^2, && \delta_0 = 1 - \gamma + \frac{7}{16}\gamma^2,\\
&A_2 = \frac{3}{8} - \frac{3}{2}m(1-\gamma), && \alpha_1 = 1 + 5\gamma - \frac{9}{2}\gamma^2, && \delta_1 = 1 - \frac{1}{2}\gamma,\\
&A_3 = -\frac{7}{16} + m, && \alpha_2 = 1 + \gamma, && \delta_2 = -\frac{1}{8}\gamma,\\
& && \alpha = \alpha_0 + \alpha_1 x + \alpha_2 x^2, && \delta = \delta_0 + \delta_1 x + \delta_2 x^2,
\end{aligned} \tag{29}$$

then $f(x)$ and $[\rho]$ are written in the form:

$$\begin{gathered}
f(x) = A_1 x + A_2 x^2 + A_3 x^3 + \dots,\\
[\rho] = \alpha(x) + \delta(x)\psi.
\end{gathered} \tag{30}$$

If the constant $\beta$ of the Integral (28) is not large, which is actually the case for the "Trojans" considered in the present discussion, as we shall see later on, then it is not difficult to grasp that the equation:

$$f(x) - \beta = 0 \tag{31}$$

has three real roots: $c_1, c_2, c_3$. $c_1$ and $c_2$ are thereby roughly equal to $-\sqrt{\frac{8}{3}\beta}$ and $+\sqrt{\frac{8}{3}\beta}$, respectively, while $c_3 \approx \frac{6}{7}$.

Computing the values of the left-hand member of Equation (31) as a function of $\underline{x}$, and plotting it on a graph, we obtain the following result.

At the values $c_1 < x < c_2$ we have $f(x) - \beta < 0$, while, at the values $c_2 < x < c_3$ and $x < c_1$ we have $f(x) - \beta > 0$ (Figure 2).

The function $R([\rho])$, at $[\rho] \neq 0$, takes on only positive values. Therefore, when the value of $\underline{x}$ at the initial moment of time $t_0$ falls within the region $(c_1, c_2)$, values of $\underline{x}$ may not fall outside of that region for any $t \geq t_0$. Actually at $x < c_1$ or, as soon as $\underline{x}$, in changing, exceeds the value of $c_2$, we will have

$$f(x) - \beta > 0, \quad R([\rho]) > 0,$$

which contradicts Integral (28).

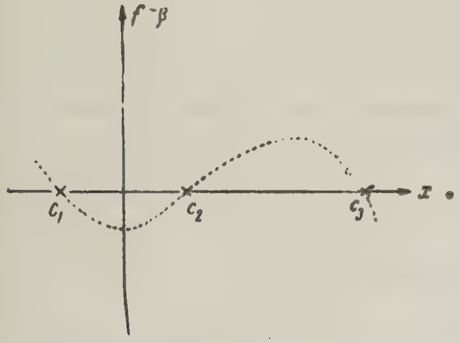

Fig. 2.

If $\underline{x}$ changes within the limits extending from $c_1$ to $c_2$, then, on the basis of Integral (28), and also on the basis of Formulas (26), (30), it is possible to conclude that $[\rho]$ and $\psi$ will also be restricted. We obtain the approximate values for the limits of the change of $[\rho]$ by solving the equation

$$mR([\rho]) - \beta = 0,$$

which has two real roots, one positive and the other negative. The formulas for a more precise determination of the limits of the change in $[\rho]$ will be derived later.

Accordingly, in this case $\underline{x}$, $[\rho]$, $\psi$, and together with them, $a_*$, $D_*$ of our intermediate orbit will be bounded by certain limits $a_1$, $a_2$, $D_1$, $D_2$ and there will take place a so-called "libration" of the arguments of $a_*$ and $D_*$ (let us note that this term has nothing in common with the libration solution of Lagrange or with the "triangular" points of libration).

If the equation

$$f(x) - \beta = 0$$

has only one real root, then the Integral (28) does not give us a "libration" for the arguments of $a_*$ and $D_*$. But, in that case, the constant $\beta$, as it is not difficult to prove, should reach a value of roughly 0.03-0.04. For all observed "Trojans," the value of the constant $\beta$ is considerably less, so that the case of the absence of "librations" for the arguments of $a_*$, $D_*$ of our intermediate orbit is excluded for them.

To derive the corresponding formulas for $a_1$, $a_2$, $D_1$, $D_2$, on the basis of (28), it should be noted that $\underline{x}$ reaches an extremum at the value $[\rho] = 0$, i.e., at $|D_*| \approx 60°$, while $\psi$, $D_*$ reach extrema at values of $\underline{x}$ close to zero.

The values of $a_1$ and $a_2$ are determined by the formulas

$$a_1 = 1 + c_1, \quad a_2 = 1 + c_2,$$

where $c_1$ and $c_2$ are the least roots, in absolute value, of Equation (28), with $c_1 < 0$ and $c_2 > 0$. This equation may be written in the form:

$$x^2 - Ax^3 - \bar{\alpha}^2 - \varepsilon x = 0,$$

where

$$\varepsilon = -\frac{A_1}{A_2} > 0, \quad A = -\frac{A_3}{A_2} > 0, \quad \bar{\alpha}^2 = \frac{\beta}{A_2}.$$

Constants $\bar{\alpha}$ and $\epsilon$ are sufficiently small when compared with unity and A, while, for the "Trojans" under discussion, $\epsilon/\bar{\alpha}$ is also small. Therefore, taking $\epsilon = 0$, we may find the greater part of the roots $c_1$ and $c_2$ in the form of series expanded in ascending powers of $\bar{\alpha}$. Subsequent terms, at $\epsilon \neq 0$, may then be found in the form of power series expanded in ascending powers of $\epsilon$. After the corresponding operations, we obtain the formulas:

$$c_1 = x_{\text{min}} = -\bar{\alpha} + \frac{1}{2} A\bar{\alpha}^2 - \left(\frac{3}{4} A - \frac{1}{8} A^2\right)\bar{\alpha}^3 +$$

$$+ \frac{\varepsilon}{2 + 3\bar{\alpha}A} - \frac{\varepsilon^2}{\bar{\alpha}}\left(\frac{1}{(2 + 3\bar{\alpha}A)^2} + \frac{1}{8}\right) + \ldots,$$

$$c_2 = x_{\text{max}} = \bar{\alpha} + \frac{1}{2} A\bar{\alpha}^2 + \left(\frac{3}{4} A - \frac{1}{8} A^2\right)\bar{\alpha}^3 +$$

$$+ \frac{\varepsilon}{2 - 3\bar{\alpha}A} + \frac{\varepsilon^2}{\bar{\alpha}}\left(\frac{1}{(2 - 3\bar{\alpha}A)^2} + \frac{1}{8}\right) + \ldots$$

At small values of x, we may seek $\psi$ by starting out from Integral (28) in the form of a series expanded in integral positive powers of x. After corresponding manipulations, we obtain

$$\psi = \psi_0 + \psi_1 \nu + \psi_2 \nu^2 + \psi_3 \nu^3 + \ldots, \tag{32}$$

where $\nu = x/\sqrt{m}$, and the coefficients $\psi_1$, $\psi_2$, $\psi_3$ are defined by the formulas:

$$\begin{aligned}
\psi_1 &= \frac{1}{\delta_0}(d_1 - \alpha_1 \sqrt{m} - \delta_1 \sqrt{m}\,\psi_0),\\
\psi_2 &= \frac{1}{\delta_0}(d_2 - \alpha_2 m - \delta_1 \sqrt{m}\,\psi_1 - \delta_2 m\psi_0),\\
\psi_3 &= \frac{1}{\delta_0}(d_3 - \delta_1 \sqrt{m}\,\psi_2 - \delta_2 m\,\psi_1),\\
d_1 &= -\frac{1}{R_0'}\frac{A_1}{\sqrt{m}},\\
d_2 &= -\frac{A_2}{K_0'} - \frac{1}{2} d_1^2 \frac{R_0''}{R_0'},\\
d_3 &= -\frac{A_3\sqrt{m}}{R_0'} - d_1 d_2 \frac{R_0''}{R_0'} - \frac{1}{6} d_1^3 \frac{R_0'''}{R_0'},\\
R_0' &= \frac{1}{2} - \frac{1}{2}(1 + \alpha_0 + \delta_0 \psi_0)^{-3/2},\\
R_0'' &= \frac{3}{4}(1 + \alpha_0 + \delta_0 \psi_0)^{-5/2},\\
R_0''' &= -\frac{15}{8}(1 + \alpha_0 + \delta_0 \psi_0)^{-7/2},
\end{aligned} \tag{33}$$

with $\psi_0$ being found from the equation

$$\frac{1}{\sqrt{1 + \alpha_0 + \delta_0\psi_0}} - 1 + \frac{1}{2}(\alpha_0 + \delta_0 \psi_0) - \frac{\beta}{m} = 0. \tag{34}$$

Let us note that Equation (34) has two solutions with respect to

$$\psi_0 : \psi_0^{(1)} < 0 \quad \text{and} \quad \psi_0^{(2)} > 0.$$

It should be stressed that Series (32) is suitable for use only at small values of $|\nu|$. As the calculations show, even at values of $|\nu|$ as low as 0.3, which is the case for many "Trojans" even when the values of $x$ are rather remote from the extremal values, terms of the Series (32) slowly fall off and the convergence of the series, generally speaking, comes into question.

Accordingly, Series (32) should in no case be used for all values of $x$ over the course of our intermediate orbit. However, as a consequence of the fact that $\psi$ reaches its extremum value at values of $x$ close to zero, this series is fully suitable for use in computing extremal values of $\psi$.

With the help of conventional rules of mathematical analysis, after performing the necessary operations we obtain the following formulas:

$$\begin{aligned} \psi_{\min} &= \psi_0^{(1)} + \nu_m \psi_1 + \nu_m^2 \psi_2 + \ldots, \\ \psi_{\max} &= \psi_0^{(2)} + \nu_m \psi_1 + \nu_m^2 \psi_2 + \ldots, \end{aligned} \tag{35}$$

where $\nu_m$ is expressed by a series expanded in ascending powers of the small value $\psi_1$:

$$\nu_m = -\frac{1}{\psi_2}\psi_1 - \frac{3}{8}\frac{\psi_3}{\psi_2^3}\psi_1^2 + \ldots$$

The extremal values of $D_1$ and $D_2$ are determined in accordance with the formulas:

$$\cos D_1 = \frac{1}{2}(1 - \psi_{\min}),$$

$$\cos D_2 = \frac{1}{2}(1 - \psi_{\max}).$$

Since $c_1 > 0$, $c_2 > 0$ and $\psi_{\min} < 0$, $\psi_{\max} > 0$, then $a_1 < 1$, $a_2 > 1$, $|D_1| < 60°$, $|D_2| > 60°$.

Let us consider the point $\bar{P}$, moving along our intermediate orbit. In order to investigate the general character of the motion of $\bar{P}$ relative to the sun S and to Jupiter J, we may neglect the inclination of the intermediate orbit $i$ and the inclination of the orbit of Jupiter $i'$ to the ecliptic, i.e., assume that $\bar{P}$ and J are moving in the plane of the ecliptic. Let us further select, in the plane of the Jovian orbit J (corresponding, in our simplified procedure, with the plane of the ecliptic) a mobile frame of reference X,Y with the origin at S such that the axis SX always passes through J. The position of the point $\bar{P}$ in this system of coordinates is defined by the values of the radius-vector $r$ and the difference $u$ between the true longitudes of $\bar{P}$ and J.

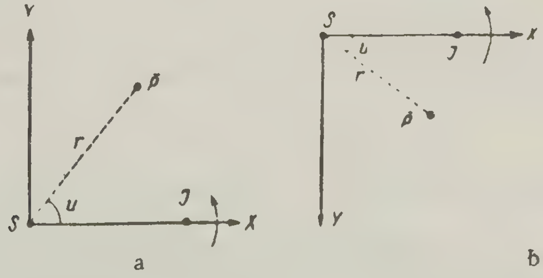

Fig. 3. a) For Trojans leading Jupiter; b) for Trojans lagging Jupiter.

In the XY-plane, $r$ and $u$ may be viewed as the polar coordinates of $\bar{P}$ (Figure 3).

The change in r and u over the course of small time intervals will be defined, basically, by the undisturbed orbital motion of $\bar{P}$ and J about the origin S. Therefore, for an approximate investigation of the motion of $\bar{P}$ in the selected system of coordinates, over the course of small time intervals, we may safely assume that the elements $a_*$, $e_*$, $\bar{\omega}_*$ of the orbit of $\bar{P}$, as well as the Delaunay anomaly $D_*$, representing the difference between the mean longitudes of $\bar{P}$ and J, remain unchanged.

For u, we have the expression:

$$u = \bar{\omega}_* + \nu_* - \bar{\omega}' - \nu',$$

where $\nu_*$, $\bar{\omega}_*$ denote the true anomaly and the longitude of the perihelion of $\bar{P}$, and $\nu'$, $\bar{\omega}'$ denote the true anomaly and the longitude of the perihelion of J.

Expressing r and u with the aid of series for elliptic unperturbed motion, we obtain

$$r = a_* - a_* e_* \cos M_* + \ldots,$$
$$u = D_* + 2(e_* \sin M_* - e' \sin M') + \ldots,$$

where terms higher than the first order relative to $e_*$ and e' are discarded.

Now let us consider further the point $\bar{\bar{P}}$, whose position is defined by coordinates:

$$X = a_* \cos D_*, \quad Y = a_* \sin D_*,$$

and choose a mobile frame of reference $\xi, \eta$, with the origin of the frame of reference at $\bar{\bar{P}}$, so that the axis $\bar{\bar{P}}\xi$ will be directed along the line of $S\bar{\bar{P}}$ (Figure 4).

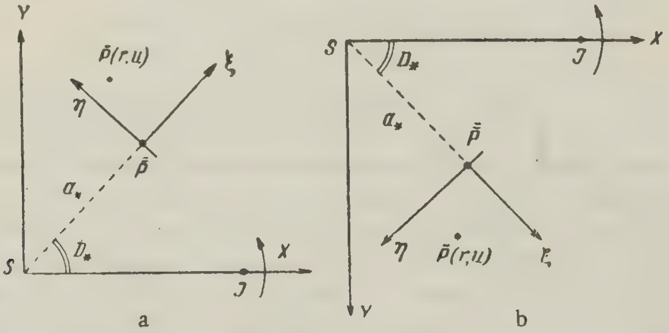

Fig. 4. a) For Trojans leading Jupiter; b) for Trojans lagging Jupiter.

The coordinates $\xi, \eta$ of point $\bar{P}$ are linked to the coordinates r,u in accordance with the relations:

$$\xi = r \cos(u - D_*) - a_*,$$
$$\eta = r \sin(u - D_*).$$

Using the expression for r,u, we may write ξ and η in the form of series expanded in ascending powers of $e_*$ and e'. Limiting ourselves to first-order terms with respect to $e_*$ and e', we get

$$\xi = -a_* e_* \cos M_* + \ldots, \quad \eta = 2a_* (e_* \sin M_* - e' \sin M') + \ldots \tag{36}$$

Neglecting the eccentricity of the orbit of Jupiter e', these formulas define, in the XY system of coordinates, motion along an ellipse (in a clockwise direction) with the center at $\bar{\bar{P}}$ and with semiaxes $a_* e_*$ and $2a_* e_*$.

The period of this motion is equal to the period of the unperturbed motion of $\overline{P}$ with respect to the sun.

Of course, if the series are written out in full, completely defining $\xi$ and $\eta$, then the exact formulas for $\xi, \eta$ will correspond, generally speaking, to nonperiodic motion along an open curve. However, it may be represented approximately as motion along the ellipse considered.

Accordingly, point $\overline{\overline{P}}$ with coordinates

$$X = a_* \cos D_*, \quad Y = a_* \sin D_*$$

determines, in the XY-plane, over the course of small time intervals, some mean position of the point $\overline{P}$, about which $\overline{P}$ traces out, in 11-12 years, a curve somewhat resembling an ellipse, as shown in Figure 5.

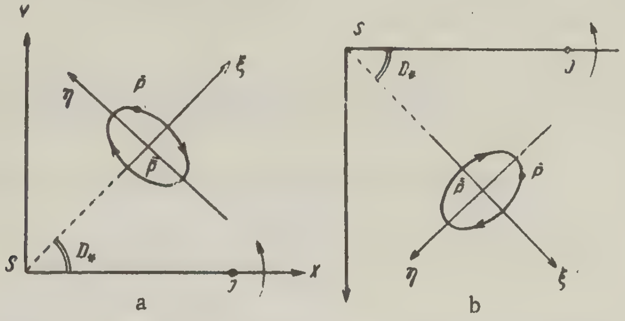

Fig. 5. a) for Trojans leading Jupiter; b) for Trojans lagging Jupiter.

In examining the motion of $\overline{P}$ over protracted time intervals, it is necessary to take into consideration changes in the osculating elements of the orbit of $\overline{P}$. In the course of time, $a_*$ and $D_*$ undergo changes, although slowly, and the point $\overline{P}$, which is the origin of our frame of reference with coordinates $\xi, \eta$, is displaced on the XY-plane.

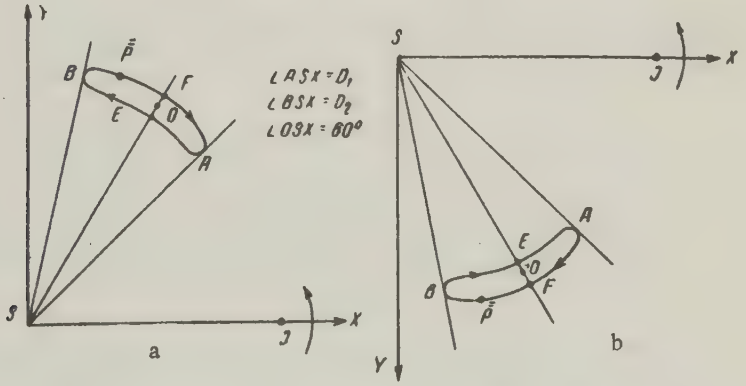

Fig. 6. a) Trojans leading Jupiter; b) Trojans lagging Jupiter.

The trajectory swept out by point $\overline{\overline{P}}$ in the XY system of coordinates may be examined. The investigation of the integral cited earlier shows that, for our intermediate orbit, $a_*$ and $D_*$ undergo changes, remaining confined between the limits $a_1$, $a_2$, $D_1$, $D_2$. The trajectory of $\overline{\overline{P}}$ in the XY system of coordinates assumes the form of a closed curve, encompassing the point O with coordinates:

$$X = \cos 60°, \quad Y = \sin 60°,$$

and having, as shown by calculations, approximately the form shown in Figure 6.

The dimensions of that trajectory are determined by the magnitudes of $a_1$, $a_2$, $D_1$, $D_2$. The distance EF is approximately equal to $a_2 - a_1$, while the distance $AB = a' \, |D_2 - D_1|$ where a' is the semimajor axis of the orbit of Jupiter, and $D_1$, $D_2$ are expressed in radians.

Let us note that in our system of coordinates, "triangular" points of libration of the circular, as well as of the elliptic, problem of three bodies fail to retain their position unaltered and do not coincide, in general, with the point O. However, point O is sufficiently close to the "triangular" point of libration of the elliptic problem $\tilde{L}_4$ (or $\tilde{L}_5$), which has coordinates in the XY-plane:

$$X = r' \cos 60^\circ, \quad Y = r' \sin 60^\circ.$$

Points $\tilde{L}_4$ (or $\tilde{L}_5$) are situated, in our frame of reference, always on the line SO and fluctuate near the point O, never leaving the neighborhood of that point by a distance in excess of a'e'.

As will be shown later, $a_*$ and $D_*$ are, for our intermediate orbit, periodic time functions. The period of their change, i.e., the period during which $\bar{\bar{P}}$ traces out the curve about O, referred to above, is approximately equal to 150-160 years.

We thus obtain the following schematic pattern in the XY frame of reference (Figure 7).

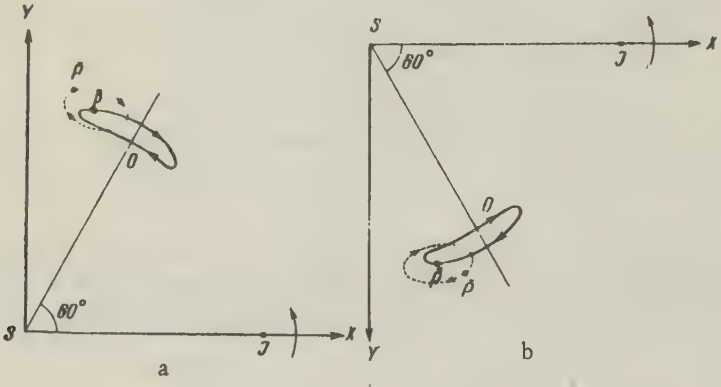

Fig. 7. a) for Trojans leading Jupiter; b) for Trojans lagging Jupiter.

In the course of 150-160 years, the point $\bar{\bar{P}}$, defining some mean position of $\bar{P}$ for a short time interval (11-12 years), describes a trajectory about some center O, close to the "triangular" point of libration of the restricted elliptic problem of three bodies $\tilde{L}_4$ (or $\tilde{L}_5$). The displacement of $\bar{\bar{P}}$ is then determined, for the most part, by the change suffered by the osculating elements of the orbit of the point $\bar{P}$. (Let us note that the Delaunay anomaly $D_*$ will also change when only the undisturbed orbital motion of $\bar{P}$ and J is considered, if the mean motion of $\bar{P}$ and J differ from each other in magnitude.)

In the course of 11-12 years, the point $\bar{P}$ traces out a trajectory about $\bar{\bar{P}}$ which may be represented approximately by an ellipse, such as that depicted in Figure 5. The displacement of $\bar{P}$ relative to $\bar{\bar{P}}$ is due chiefly to the unperturbed orbital motion of $\bar{P}$ and J about the sun.

We thus arrive at the result which was advanced in our previous article [3], namely, that the coördinates of the "Trojans" in the rotating system of coordinates under discussion experience both short-term and long-period changes, the short-period changes being due, for the most part, to the undisturbed motions of the "Trojans" and the long-period changes, to their perturbations. The amplitude of the short-period changes reaches, according to the formulas supplied above, 2ae, where $\underline{a,e}$ are the osculating semimajor axis and eccentricity, while the amplitude of the changes of long period is $a'D_2 - D_1$, where a' denotes the semimajor axis of the orbit of Jupiter, and $D_1$, $D_2$ are limits of changes in D, expressed in radians.

In accordance with the discussion outlined above for the determination of the osculating elements of our intermediate orbit, it is necessary to express, with the aid of the Integral (28), one of the variables $\underline{x}, \psi$ as an explicit function of the other variable. The investigation of (28) shows that it is not possible to obtain a simple expression of $\underline{x}$ in terms of $\psi$, although it is entirely feasible to express $\psi$ as an explicit function of $\underline{x}$. With that in mind, let us rewrite (28) in the form:

$$R([\rho]) = \frac{\beta - f(x)}{m}$$

or

$$\frac{1}{\sqrt{1+[\rho]}} - 1 + \frac{1}{2}[\rho] = q^2, \tag{37}$$

where

$$q = \frac{1}{\sqrt{m}}\sqrt{\beta - f(x)}.$$

Viewing (37) as an equation for $[\rho]$ and assuming $\underline{q}$ to take on small values, we shall look for the solution of the equation in the form of a series expanded in integral positive powers of $\underline{q}$:

$$[\rho] = \rho_1 q + \rho_2 q^2 + \rho_3 q^3 + \ldots \tag{38}$$

Let us then note that at the required $\underline{x}$, we obtain two solutions for $[\rho]$: $[\rho]_1 > 0$ and $[\rho]_2 < 0$.

Performing the necessary operations, we get

$$\begin{aligned} [\rho]_1 &= 1.6330\,q + 1.1111\,q^2 + 0.3023\,q^3 - 0.0332\,q^4 - 0.0240\,q^5 + \ldots, \\ [\rho]_2 &= -1.6330\,q + 1.1111\,q^2 - 0.3023\,q^3 - 0.0332\,q^4 + 0.0240\,q^5 + \ldots \end{aligned} \tag{39}$$

The larger the values taken on by $\underline{q}$, the slower the series converge and the more in doubt stands the possibility of utilizing the series. However, for all observed "Trojans" (with the exception, possibly, of asteroid No. 1208), the values of $\underline{q}$ are not in excess of 0.40-0.45. Substituting these values into (39), computing $[\rho]_1$, $[\rho]_2$ and then verifying directly whether or not Equation (37) yields the given value of $\underline{q}$ at the $[\rho]_1$, $[\rho]_2$ obtained, we find that Formulas (39) provide a reliable result with an accuracy to five decimal places. Accordingly, Expressions (39), when limited to the terms worked out, are suitable for computing the changes in $\underline{x}$ and $\psi$ over the whole interval, with the same accuracy.

For each value of $\underline{x}$, we obtain two values of $\psi$ ($\psi^{(1)} > 0$ and $\psi^{(2)} < 0$) and two values of $D_*$ ($D_*^{(1)}$ and $D_*^{(2)}$), defined by the formulas

$$\begin{aligned} \psi^{(j)} &= \frac{1}{8}[-\alpha + [\rho]_j], \\ \cos D_*^{(j)} &= \frac{1}{2}(1 - \psi^{(j)}) \quad (j = 1, 2). \end{aligned} \tag{40}$$

## 6. Observational Data on the Motion of "Trojans." Some Quantitative Characteristics of Intermediate Orbits for Asteroids Nos. 588, 659, 884, 1143, 1173.

In the capacity of the initial moment, which we encounter in solving the equations of the intermediate orbit, the epoch $t_0 = 1948$, VII, 28.0 was chosen.

First of all, it is necessary to the view the question of the initial elements of the Jovian orbit. Within the framework of our problem (the restricted elliptic three-body problem) we assume that Jupiter moves along an unperturbed elliptic orbit. However, as we know, the motion of Jupiter is not such as a consequence of the presence of perturbations due to other planets in our solar system. We are actually dealing with the osculating elliptic orbit of Jupiter, whose elements vary with the course of time, although very slowly. Neglecting changes in the osculating elements of Jupiter's orbit, we must center on the values of those elements for any given moment of time. It is most natural, in this context, to select as such an epoch either the initial epoch of our problem or an epoch close to the initial one.

Since the values of the osculating elements of the orbit of Jupiter are not given in the ephemerides, we decided to calculate them on the basis of the two heliocentric positions of Jupiter for epochs close to 1950.0. We took from the tables of the perturbed motion of Jupiter [4] the values of the heliocentric rectangular (equatorial) coordinates of Jupiter for the epochs $t_1$ = 1949, X, 11.0 and $t_2$ = 1950, VI, 80:

$$X_1 = 2.8794387, \qquad X_2 = 4.1367020,$$
$$Y_1 = -3.8447716, \qquad Y_2 = -2.5863121,$$
$$Z_1 = -1.7198351, \qquad Z_2 = -1.2106886.$$

Computing the elements of the orbit in accordance with the two heliocentric positions led to the following result*:

$$a' = 5.20279, \qquad i' = 1°18'24''{\cdot}9,$$
$$e' = 0.0489132, \qquad M'(t_2) = 315°49'37''{\cdot}2,$$
$$\omega' = -86°18'28''{\cdot}5, \qquad n' = 299''{\cdot}1295 = 0°.08309153,$$
$$\Omega' = 99°57'44''.2, \qquad \lambda'(t_0) = 272°58'44''.4.$$

At the present time, 14 "Trojans" are known. We present a table containing the values of their osculating elements, compiled on the basis of data in the compendium "Ephemerides for Asteroids for 1948" and Thüring's papers [5]:

TABLE 1

| Planet number | $a$ | $e$ | $\omega$ | $\Omega$ | $i$ | $M$ | $n''$ | $D$ | Epoch |
|---|---|---|---|---|---|---|---|---|---|
| | | | 1950.0 | | | | | | |
| 588 | 5.2112 | 0.14829 | 83″701 | 316°063 | 10°316 | 244°304 | 298.264 | 55.025 | 1948, VII 28.0 |
| 617 | 5.2068 | 0.14057 | 347.631 | 43.856 | 22.075 | 230.460 | 298.645 | —54.778 | |
| 624 | 5.1211 | 0.02485 | 164.200 | 342.091 | 18.281 | 164.662 | 306.170 | 55.998 | |
| 659 | 5.2368 | 0.11060 | 323.592 | 350.559 | 4.520 | 18.522 | 296.080 | 69.135 | |
| 884 | 5.2164 | 0.12052 | 272.053 | 301.049 | 8.890 | 288.145 | 297.841 | —72.781 | |
| 911 | 5.1328 | 0.06488 | 55.615 | 337.272 | 21.94 | 280.651 | 305.120 | 63.397 | |
| 1143 | 5.1860 | 0.09113 | 94.248 | 220.664 | 3.149 | 248.293 | 300.443 | 69.562 | |
| 1172 | 5.1881 | 0.10290 | 292.401 | 256.784 | 16.69 | 270.604 | 300.254 | 69.864 | |
| 1173 | 5.0958 | 0.13767 | 314.842 | 284.132 | 6.980 | 263.474 | 308.455 | —54.663 | |
| 1208 | 5.1595 | 0.09235 | 340.550 | 47.985 | 33.694 | 232.454 | 302.757 | —59.865 | |
| 1404 | 5.1631 | 0.11182 | 29.517 | 332.320 | 18.132 | 323.367 | 302.437 | 80.015 | |
| 1437 | 5.1431 | 0.04360 | 82.101 | 315.330 | 20.563 | 229.476 | 304.209 | 38.708 | |
| 1949 SA | 5.430 | | | 356.3 | 18.8 | | 280.43 | | 1949, X, 8, 390 |
| 1949 SB | 5.2344 | 0.09432 | 88.263 | 340.882 | 6.098 | | 296.257 | | 1952, III, 15, 928 |

The method outlined above for constructing an intermediate orbit for the "Trojans" is all the more expedient, the lesser the inclination of the osculating orbits of the planetoids. From the table supplied, it is clear that the inclination i for the asteroids Nos. 617, 624, 911, 1172, 1208, 1404, 1437, 1949SA is rather large. In addition, it is convenient to select such "Trojans" as have already been under observation for an appreciably protracted length of time, in order to assure the possibility of comparing theory with observations. By virtue of the above, we shall consider five "Trojans," viz.: Nos. 588, 659, 884, 1143, 1173.

Making use of the materials kindly presented to us at the Institute for Theoretical Astronomy of the Academy of Sciences of the USSR, we compiled tables giving the values of the osculating elements of orbits of the

---

*Of course, these are not the actual osculating elements of the orbits, but rather some mean elements for the period falling between $t_1$ and $t_2$. But they are closer to the osculating elements for the moment 1950, I, 1.0, than the elements cited in the "American Ephemeris and Nautical Almanac."

"Trojans" referred to above, for different epochs. These values for the osculating elements are partly based on observations and partly based on data obtained from numerical integration provided at the Institute for Theoretical Astronomy, taking into account the perturbations brought into play by Jupiter and Saturn. The elements $\omega$, $\Omega$, $i$ are given in the tables for the equinox and equator of 1950.0. The tables also provide the magnitudes

$$x = \frac{a}{a'} - 1, \quad D = \lambda - \lambda',$$

which we made use of in the preceding paragraphs, and which characterize the position of the "Trojans" relative to the sun and Jupiter.

TABLE 2

| № 588 | 1948,VII, 28. | 1941, II,2.0 | 1938, II,1.0 | 1933, X, 25.0 | 1924, XII, 11.0 | 1907,V, 28.0 |
|---|---|---|---|---|---|---|
| $a$ | 5.2112 | 5.2116 | 5.2233 | 5.2267 | 5.2372 | 5.2382 |
| $e$ | 0.14829 | 0.14981 | 0.15021 | 0.14857 | 0.14957 | 0.14960 |
| $\bar{\omega}$ | 83°.701 | 83°.928 | 82°.879 | 83°.141 | 81°.900 | 81°.767 |
| ☊ | 316°.063 | 316°.101 | 316°.101 | 316°.117 | 316°.139 | 316°.156 |
| $i$ | 10°.316 | 10°.316 | 10°.315 | 10°.311 | 10°.308 | 10°.308 |
| $M$ | 244°.304 | 17°.219 | 287°.307 | 158°.046 | 251°.614 | 84°.012 |
| $n$ | 298″.264 | 298″.233 | 297″.230 | 296″.940 | 296″.047 | 295″.963 |
| $D$ | 55°.025 | 55°.257 | 55°.447 | 55°.961 | 57°.615 | 62°.247 |
| $x$ | 0.001613 | 0.001690 | 0.003939 | 0.004593 | 0.006611 | 0.006803 |

TABLE 3

| № 884 | 1948, VII, 28.0 | 1940, VII, 31.0 | 1938, II, 1.0 | 1931, III, 10.0 | 1925, I, 1.0 | 1917, IX, 25.0 |
|---|---|---|---|---|---|---|
| $a$ | 5.2164 | 5.2313 | 5.2341 | 5.2472 | 5.2564 | 5.2618 |
| $e$ | 0.12052 | 0.12007 | 0.12072 | 0.11896 | 0.11808 | 0.11946 |
| $\bar{\omega}$ | 272°.053 | 271°.569 | 271°.090 | 270°.874 | 270°.695 | 270°.849 |
| ☊ | 301°.049 | 301°.102 | 301°.104 | 301°.062 | 301°.141 | 301°.157 |
| $i$ | 8°.890 | 8°.873 | 8°.872 | 8°.884 | 8°.860 | 8°.859 |
| $M$ | 288°.145 | 47°.591 | 332°.930 | 125°.889 | 300°.455 | 82°.999 |
| $n$ | 297″.814 | 296″.542 | 296″.312 | 295″.198 | 294″.427 | 293″.976 |
| D | —72°.781 | —71°.275 | —70°.719 | —68°.585 | —66°.494 | —63°.188 |
| $x$ | 0.002613 | 0.005477 | 0.006015 | 0.008533 | 0.010301 | 0.011340 |

TABLE 4

| № 659 | 1948, VII, 28.0 | 1941, III 3.0 | 1938, II. 1.0 | 1934, VIII, 1.0 | 1926. VI, I7,0 | 1908, IV, I2.0 |
|---|---|---|---|---|---|---|
| $a$ | 5.2368 | 5.2319 | 5.2221 | 5.2142 | 5.2028 | 5.1770 |
| $e$ | 0.11060 | 0.10892 | 0.11036 | 0.10921 | 0.10963 | 0.10661 |
| $\bar{\omega}$ | 323°.592 | 323°.916 | 323°.255 | 322°.731 | 322°.618 | 319°.711 |
| ☊ | 350°.559 | 350°.559 | 350°.538 | 350°.524 | 350°.494 | 350°.567 |
| $i$ | 4°.520 | 4°.523 | 4°.524 | 4°.527 | 4°.529 | 4°.535 |
| $M$ | 18°.522 | 155°.231 | 62°.928 | 317°.522 | 71°.466 | 239°.891 |
| $n$ | 296″.080 | 296″.496 | 297″.326 | 298″.005 | 298″.989 | 301″.219 |
| $D$ | 69°.135 | 70°.842 | 71°.444 | 71°.872 | 69°.743 | 69°.481 |
| $x$ | 0.006534 | 0.005592 | 0.003708 | 0.002190 | 0.000000 | —0.004960 |

The computed constants $\gamma, \beta$ associated with the integrals in (17), (28), as well as the magnitudes for $[\rho]$ at the initial epoch $t_0$ = 1948, VII, 28.0 on the basis of the values of the osculating elements, give the following result:

|  | № 588 | № 659 | № 1143 | № 1173 | № 884 |
|---|---|---|---|---|---|
| $\gamma$ | 0.011066 | 0.0061552 | 0.0041547 | 0.0094240 | 0.0072896 |
| $\beta \cdot 10^4$ | 0.047673 | 0.44504 | 0.31668 | 1.6980 | 0.52709 |
| $[\rho]$ | —0.099293 | 0.31880 | 0.31211 | —0.13567 | 0.43674 |

TABLE 5

| № 1143 | 1948, VII, 28.0 | 1941, I, 15.0 | 1938, II, 1. 0 | 1934, II, 22.0 | 1930, III, 15. 0 |
|---|---|---|---|---|---|
| $a$ | 5.1860 | 5.1748 | 5.1723 | 5.1660 | 5.1621 |
| $e$ | 0.091135 | 0.093346 | 0.092390 | 0.092404 | 0.091135 |
| $\bar{\omega}$ | 94°.248 | 93°.968 | 93°.374 | 94°.374 | 94°.188 |
| ☊ | 220°.664 | 220°.673 | 220°.677 | 220°.649 | 220°.647 |
| $i$ | 3°.149 | 3°.150 | 3°.150 | 3°·154 | 3°.155 |
| $M$ | 248°.293 | 18°.219 | 288°.282 | 166°.375 | 45°.399 |
| $n$ | 300″.443 | 301″.406 | 301″.637 | 302″.185 | 302″.530 |
| $D$ | 69°.562 | 66°.793 | 66°.917 | 65°.635 | 64°.152 |
| $x$ | —0.00323 | —0.00538 | —0.00586 | —0.00707 | —0.00782 |

TABLE 6

| № 1173 | 1948, VII, 28.0 | 1940, VIII, 25.0 | 1938, II, 1.0 | 1930, III, 15.0 |
|---|---|---|---|---|
| $a$ | 5.0958 | 5.0926 | 5.0948 | 5.1037 |
| $e$ | 0.13767 | 0.13768 | 0.13753 | 0.13663 |
| $\bar{\omega}$ | 314.°842 | 314.°471 | 313.°948 | 314.°238 |
| ☊ | 284.°132 | 284.°179 | 284.°183 | 284.°117 |
| $i$ | 6.°980 | 6.°976 | 6.°975 | 6.°972 |
| $M$ | 263.°474 | 14.°656 | 295.°663 | 48.°617 |
| $n$ | 308.″455 | 308.″737 | 308.″544 | 307.″733 |
| $D$ | —54.°663 | —63.°385 | —65.°128 | —72.°580 |
| $x$ | —0.02057 | —0.02118 | —0.02076 | —0.02005 |

For parameters $\bar{\alpha}$ and $\epsilon$, entering into the formulas for computing the extrema of $\underline{x}$, the following values were obtained:

|  | № 588 | № 659 | № 884 | № 1143 | № 1173 |
|---|---|---|---|---|---|
| $\bar{\alpha}$ | 0.0035723 | 0.010915 | 0.011879 | 0.0092070 | 0.021319 |
| $\varepsilon \cdot 10^4$ | 0.83899 | 0.46860 | 0.54580 | 0.31693 | 0.71508 |

The calculations of the extremal values of $a_*$ (in astronomical units), $\underline{x}$ (in the units selected by us), and $D_*$ gave the results listed in Table 7 (here, values are also cited for $[\rho]$, corresponding to the extremal values of D).

In looking over the tables for the osculating elements of the "Trojans," the following may be noted:

For asteroid No. 588, in the period falling between 1907, V, 28.0 and 1924, XII, 11.0, the semimajor axis of the orbit $\underline{a}$ had the largest value, while the Delaunay anomaly D was close to 60°.

For asteroid No. 659, in the period falling between 1926, VI, 17.0 and 1938, II, 1.0, D had the largest value, going to a maximum (i.e., a maximum distance removed from Jupiter on the basis of mean longitude was observed), while the value of the semimajor axis was close in magnitude to the semimajor axis of Jupiter.

TABLE 7

| | № 588 | № 659 | № 884 | № 1143 | № 1173 |
|---|---|---|---|---|---|
| $x_{\max}$ | 0.003623 | 0.011010 | 0.011990 | 0.009237 | 0.021629 |
| $x_{\min}$ | —0.003524 | —0.010823 | —0.011771 | —0.009143 | —0.021026 |
| $a_2$ | 5.2216 | 5.2601 | 5.2652 | 5.2510 | 5.3153 |
| $a_1$ | 5.1845 | 5.1465 | 5.1416 | 5.1552 | 5.0934 |
| $D_2$ | 62.537 | 71.998 | —73.379 | 70.157 | —83.698 |
| $D_1$ | 54.695 | 48.290 | —47.221 | 50.195 | —38.882 |
| $[\rho]_2$ | 0.12106 | 0.40728 | 0.44885 | 0.33604 | 0.90738 |
| $[\rho]_1$ | —0.10995 | —0.30390 | —0.32640 | —0.26240 | —0.51382 |

For asteroids Nos. 884 and 1143, over the course of the entire period encompassed by the observations performed, D increased in absolute magnitude, not reaching its extremum by 1948, VII, 28.0, but being apparently in the neighborhood of its extremum.

For asteroid No. 1173, in the period falling between 1940, VIII, 25.0 and 1948, VII, 28.0, the semimajor axis of the osculating orbit had its lowest value, passing through a minimum, and the Delaunay anomaly D was close to −60°.

Comparing the extremal computed values of $a_*$, $D_*$ given in Table 7 with the observed values of a, D in the vicinity of the extremal values, it may be inferred that our computations, on the whole, are not at variance with observation.

As was indicated above (in Section 5), the coordinates of the "Trojans" in the rotating system of coordinates XY, fixed and invariant with respect to the Sun and Jupiter, undergo both short-period and long-period changes, while the amplitudes of the long-period changes reach 2ae, where a,e are the osculating semimajor axis and osculating eccentricity of the orbit of the "Trojans," and the amplitude of the short-period changes is $a'|D_2 - D_1|$, where a' is used to denote the semimajor axis of Jupiter's orbit, and $D_1$, $D_2$ are the extremal values of the Delaunay anomaly expressed in radians. Performing an approximate calculation of these amplitudes in astronomical units for the "Trojans" involved, in accordance with the data available in Tables 2-4 and 7, we obtain

| | № 588 | № 659 | № 884 | № 1143 | № 1173 |
|---|---|---|---|---|---|
| $A_{\text{short}}$ | 1.55 | 1.16 | 1.26 | 0.95 | 1.40 |
| $A_{\text{long}}$ | 0.71 | 2.15 | 2.37 | 1.81 | 4.07 |

The figures obtained show that the amplitudes of those short-period and long-period changes are rather large and, generally speaking, comparable with one another as to magnitude.

## 7. Intermediate Orbit for the Asteroid No. 884

For one of the asteroids under consideration, namely, No. 884, the calculation of the intermediate orbit was effected in its entirety. Without dwelling on the computational operations, during which mechanical quadratures were applied to the solution of the equations for $a_*$ and $\omega_*$, and methods of practical harmonic (Fourier) analysis were also used, let us indicate the definitive formulas for the intermediate orbit, providing five significant figures:

$$\begin{aligned} a_* &= 1 + x; \\ x &= 0.000062 + 0.003071\cos\tau - 0.011359\sin\tau + \\ &\quad - 0.000590\cos 2\tau + 0.000920\sin 2\tau + \\ &\quad + 0.000083\cos 3\tau - 0.000075\sin 3\tau + \\ &\quad - 0.000008\cos 4\tau + \\ &\quad + 0.000001\cos 5\tau - 0.000003\sin 5\tau + \\ &\quad - 0.000005\cos 6\tau; \end{aligned}$$

$$
\begin{aligned}
\bar{\omega}_* = 272^\circ.053 - 0^\circ.0077541\,(t-t_0) &+ 0^\circ.772\sin\tau + 0.257\,(1-\cos\tau)\\
&- 0^\circ.106\sin 2\tau - 0.074\,(1-\cos 2\tau)\\
&+ 0^\circ.019\sin 3\tau + 0^\circ.013\,(1-\cos 3\tau)\\
&- 0^\circ.004\sin 4\tau + 0^\circ.002\,(1-\cos 4\tau)\\
&- 0^\circ.002\sin 5\tau + 0^\circ.003\,(1-\cos 5\tau)\\
&+ 0^\circ.002\sin 6\tau;
\end{aligned}
$$

$$M_* = D_* - \bar{\omega}_* + 272^\circ.979 + (t-t_0);$$

$$e_*^2 = \frac{1}{1+x}\left(0.014597\sqrt{1+x} - 0.000053\right);$$

$$2\cos D_* = 1 - \frac{1}{1.99272 + 9.99635\,x}\,[\pm 1.6330\,q + 1.1111\,q^2 \pm 0.3023\,q^3 -$$

$$- 0.0332\,q^4 \mp 0.0240\,q^5 - 0.029091 - 1.0363\,x - 1.0073\,x^2];$$

$$q = 32.3782\,(0.000052709 + 0.000020390\,x - 0.37358\,x^2 + 0.43655\,x^3)^{1/2};$$

$$\Omega = 301^\circ.049; \quad i_* = 8^\circ.890; \quad \tau = 4^\circ.4928\,(t-t_0).^* \tag{41}$$

Calculation in accordance with these formulas of the values of the osculating elements of the intermediate orbit, for the moments cited in Table 3, in which observed values of the osculating elements of asteroid No. 884 are given, as well as a comparison of observed and calculated osculating elements, yielded the following results:

TABLE 8

| | 1948, VII, 28.0 | 1940, VII, 31.0 | 1938, II. 1.0 | 1931, III, 10.0 | 1925, I, 1.0 | 1917, IX 25.0 |
|---|---|---|---|---|---|---|
| $a_*$ | 5.2164 | 5.2325 | 5.2373 | 5.2490 | 5.2574 | 5.2637 |
| $a_O$ | 5.2164 | 5.2313 | 5.2341 | 5.2472 | 5.2564 | 5.2618 |
| $a_O - a_*$ | | —12 | —32 | —18 | —10 | —19 |
| $e_*$ | 0.12052 | 0.12043 | 0.12040 | 0.12023 | 0.12029 | 0.12025 |
| $e_O$ | 0.12052 | 0.12007 | 0.12072 | 0.11896 | 0.11808 | 0.11946 |
| $e_O - e_*$ | | —36 | +32 | —137 | —221 | —79 |
| $\bar{\omega}_*$ | 272°.053 | 271°.923 | 271°.850 | 271°.728 | 271°.642 | 271°.584 |
| $\bar{\omega}_O$ | 272.053 | 271.569 | 271.090 | 270.874 | 270.695 | 270.849 |
| $\bar{\omega}_O - \bar{\omega}_*$ | | —0.354 | —0.760 | —0.854 | —0.947 | —0·735 |
| $M_*$ | 288.145 | 47.399 | 332.504 | 125.870 | 300.860 | 83.970 |
| $M_O$ | 288.145 | 47.591 | 332.930 | 125.889 | 300.455 | 82.999 |
| $M_O - M_*$ | | 0.192 | 0.426 | 0.019 | —0.405 | —0.971 |
| $i_*$ | 8.890 | 8.890 | 8.890 | 8.890 | 8.890 | 8.890 |
| $i_O$ | 8.890 | 8.873 | 8.872 | 8.884 | 8.860 | 8.859 |
| $i_O - i_*$ | | —0.017 | —0.018 | —0.006 | —0.030 | —0.031 |
| $\Omega_*$ | 301.049 | 301.049 | 301.049 | 301.049 | 301.049 | 301.049 |
| $\Omega_O$ | 301.049 | 301.102 | 301.104 | 301.062 | 301.141 | 301.157 |
| $\Omega_O - \Omega_*$ | | 0.053 | 0.055 | 0.013 | 0.092 | 0.108 |
| $D_*$ | —72.781 | —71.113 | —70.385 | —67.750 | —65.142 | —61.482 |
| $D_O$ | —72.781 | —71.275 | —70.719 | —68.585 | —66.494 | —63.188 |
| $D_O - D_*$ | | —0.162 | —0.334 | —0.835 | —1.352 | —1.706 |
| $D^{(0)}$ | —72.781 | —71.714 | —71.381 | —70.461 | —69.635 | -68.665 |
| $D_O - D^{(0)}$ | | 0.439 | 0.662 | 1.876 | 3.141 | 5.477 |

---

* The unit of time is equal to 689°.5503 mean solar days.

where $a_0$, $e_0$, $\bar{\omega}_0$, $M_0$, $i_0$, $\Omega_0$, $D_0$ represent observed values, and $a_*$, $e_*$, $\bar{\omega}_*$, $M_*$, $i_*$, $\Omega_*$, $D$, $D^{(0)}$ represent computed osculating elements, with $D_0$ being the value of the Delaunay anomaly, computed for unperturbed motion using the initial osculating elements.

As we readily see on inspection of the table, the elements of the intermediate orbit reflect rather well, on the whole, the real changes in the osculating elements of the orbit of asteroid No. 884. The given intermediate orbit may therefore be considered acceptable, viewing it,of course, not as the final result, but rather as the starting point for further calculations. In conjunction with the preceding, it should be kept in mind that the divergences are still large. If we were to compare our intermediate orbit with the observed right ascension and declination of the "Trojan" under discussion, we would encounter deviations of the same order as in the case of $D_0 - D_*$. The drawback of that particular intermediate orbit resides in the fact that we did not have recourse to varying the parameters associated with the orbit. In a subsequent article, we shall employ a somewhat different method for constructing an intermediate orbit, which will make it possible to avert the pitfall referred to, and to obtain better agreement with observation.

## LITERATURE CITED

[1] N.D. Moiseev, Trudy GAISh (Trans.of the Shternberg State Astronomical Institute) 15, 100 (1945).

[2] N.D. Moiseev, Trudy GAISh (Trans. of the Shternberg State Astronomical Institute) 20, 147 (1950).

[3] Iu.A. Raibov, Astron. J. (USSR) 33, 936 (1956).

[4] Astronomical Papers No. 12 (Washington, 1951).

[5] B. Thüring, Astron. Nachr. 279, 211 (1950).

Received April 19, 1956

P.K. Shternberg State Astronomical
Institute

# LETTERS TO THE EDITOR

## ON THE PAPER BY A. M. MIKISHA AND F. A. TSITSIN "SOME PROBLEMS OF THE THEORY OF GALACTIC POTENTIAL"

G. M. Idlis

It is shown that the paper by A.M. Mikisha and F.A. Tsitsin [1] is physically inconsistent since in considering galactic models it introduces negative (!) densities. It is noted that all their "critical remarks" on the work of P.P. Parenago and G.M. Idlis are based on a misunderstanding and a misinterpretation of the generally accepted view of Newtonian potential.

A.M. Mikisha and F.A. Tsitsin [1] determined the gravitational potential Φ, and considered it basic to the determination of the force of attraction through the expression

$$\mathbf{F} = \operatorname{grad} \Phi, \tag{1}$$

i.e., to within an undetermined additive constant of integration C, in distinction to other authors who by "potential" always understand the so-called "exit work" from the system, i.e., the potential tending to zero at infinity (this uniquely determines the corresponding value of the additive constant C). The latter method has long been generally accepted in all work on Newtonian potential following Green (1828), Gauss (1834-1840) and others, and beginning with standard textbooks (F.R. Mul'ton [2], M.F. Subbotin [3] and so on), and the special monographs (N.I. Idel'son [4], P. Appel' [5], N.M. Giunter [6] and so on) in which potential is defined by

$$\Phi(\mathbf{r}) = \iiint \frac{G\delta(\mathbf{r}')}{|\mathbf{r} - \mathbf{r}'|} \, dV, \tag{2}$$

which is equal to the work done by the force of attraction in moving a unit mass from infinity to the point whose position vector is $\mathbf{r}$ (G is the gravitational constant, $\mathbf{r}'$ is the running position vector, δ is the mass density, and dV is a volume element within the gravitating system over which the integration is carried out). Formula (2) is quoted at the very beginning of my work [7] since only gravitational potential is considered in that paper.

For this reason it is difficult to understand the surprise expressed by A.M. Mikisha and F.A. Tsitsin [1], when they note that P.P. Parenago [8-10], and G.M. Idlis [7, 11] define potential as the "exit work" [2], which is basic in deriving the force of attraction but which does not involve any indeterminacy with respect to an additive constant. The concept of "exit work" introduced by the authors of [1] was introduced into science more than one hundred years ago and has always been identified with the concept of gravitational potential., Thus, an attempt to find the numerical value of the additive constant in the expression for the potential which is obtained by integration of (1) should not surprise the authors of [1], unless they ascribe to others their own terminology.

A.M. Mikisha and F.A. Tsitsin [1] write the following expression for the "exit work" (potential) in the galactic plane of symmetry at an arbitrary distance R from the axis of symmetry

$$\Phi(R) = \frac{\Phi_c}{1 + \varkappa R^2}, \tag{3}$$

without noting that at infinity and for any values of $\kappa$ and $\Phi_c$ the function $\Phi$ does not satisfy the necessary boundary condition for a system with a finite mass M. In fact, the following condition should be satisfied [4]:

$$\lim_{R\to\infty} \frac{-\partial\Phi / \partial R}{GM / R^2} = 1, \tag{4}$$

and in the case of Expression (3) we have

$$\lim_{R\to\infty} \frac{-\partial\Phi / \partial R}{GM / R^2} = \lim_{R\to\infty} \frac{2\varkappa\Phi_c R^3}{GM (1 + \varkappa R^2)^2} = 0. \tag{5}$$

It is this, and not the imaginary "misunderstanding" of the formal difference between the generally accepted terminology and the terminology used by the authors of [1], which was the reason for my reconsideration [7], and further development of the work of P.P. Parenago on galactic potential [8, 9]. Expression (3) and even the more general expression

$$\Phi(R) = \frac{\Phi_c}{1 + \varkappa R^2} + C, \tag{6}$$

which is obtained in the case of identification of circular velocity with the usual expression for the velocity of centroids of plane sub-systems

$$v_c = \frac{\sqrt{2\varkappa\Phi_c}\, R}{1 + \varkappa R^2}, \tag{7}$$

cannot represent the potential ("exit work") for any large values of R if the system under consideration has only a finite mass (in the case of infinite mass the use of these concepts of Newtonian mechanics is improper). For this reason the system with these properties should, in spite of the statement made by A.M. Mikisha and F.A. Tsitsin [1], have limited dimensions; i.e., the Formulas (6) and (7) which can be deduced from each other can only apply in the case of a definite finite value $R_0$ beyond which its use has no physical meaning. But this was precisely what the authors of [1] did in deriving Expression (6a) for the "exit work" in the case of P.P. Parenago's model.

In considering the spherically symmetric model of the galaxy which leads to the potential (6), A.M. Mikisha and F.A. Tsitsin find (p. 887 of [1]), using Poisson's equation, an expression for the density:

$$\delta(R) = \frac{\varkappa\Phi_c}{2\pi G} \frac{3 - \varkappa R^2}{(1 + \varkappa R^2)^3}, \tag{8}$$

and write: "it is easy to see that for $R = R_0 = \sqrt{3/\kappa}$ the density is equal to zero and for $R > R_0$ it becomes negative, which, as G.M. Idlis points out, has no physical meaning.

For this reason G.M. Idlis assumes ([7] and [11])

$$\left.\begin{aligned} \delta(R) &= \frac{\varkappa\Phi_c}{2\pi G} \frac{3 - \varkappa R^2}{(1 + \varkappa R^2)^3} \quad \text{for} \quad R \leqslant R_0. \\ \delta(R) &\equiv 0 \quad \text{for} \quad R \geqslant R_0. \end{aligned}\right\}\text{»} \tag{9}$$

On the following page (p. 888) the same authors of [1] quite calmly compute "exit work" for their galactic model (8), (3) using negative densities which have no physical meaning and are at the same time shown by them in Figure 1 graphically! With such an arbitrary attitude to elementary logic (apart from physical sense) it is possible to "show" practically anything and not only the "inconsistency of the criticism by G.M. Idlis of the work of P.P. Parenago on galactic potential" as was declared in an annotation to [1].

Observations show that the density of real finite stellar systems does not have a discontinuity (break) at the boundaries of these systems (A.M. Mikisha and F.A. Tsitsin erroneously assume that the density falls off asymptotically to zero at infinity, although there is no observational evidence for this). For this reason the spherically symmetrical model of the galaxy with (6) as the potential within it, and which is finite (its radius cannot exceed $\sqrt{3/\kappa}$ for an arbitrary value of C) should extend up to the distance $R = R_0 = \sqrt{3/\kappa}$, i.e., our solution (9) is in this case the only physically sensible solution, and from it, as can be easily shown [7], one can uniquely obtain the corresponding value of the additive constant $C = \frac{1}{8}\Phi_C$. In the analogous case of the plane model, the radius is somewhat larger and C is smaller by a factor of 1.7. In the intermediate models one obtains mean characteristics of the system. Taking this into account, P.P. Parenago in the new edition of his "Course in Stellar Astronomy" [10], points out that the additive constant C in Equation (6) which determined the rate of evacuation in the galactic plane (within the galaxy)

$$v_\infty(R) = \sqrt{2\Phi(R)}, \tag{10}$$

is different from zero and is of the order of 0.1 $\Phi_C$. For $C = 0$ one obtains a low value for the above quantity which does not correspond to any physically sensible model (with a positive density and finite mass). Analogous erroneous values for the rate of evacuation obtained by rejecting the finite additive constant are found in the paper by K.F. Ogorodnikov [12] which was quoted by the authors of [1] (cf. [7]).

Thus, all the four points stated at the conclusion of the paper by A.M. Mikisha and F.A. Tsitsin [1] are erroneous and their groundless attempt to contradict or even generalize the work of G.M. Idlis and P.P. Parenago on galactic potential (instead of considering them as complementary, is a result of a trivial misunderstanding and an arbitrary attitude to the physical meaning of the quantities involved. We note finally that the irresponsible attitude of A.M. Mikisha and F.A. Tsitsin to their readers can be seen from the quite fantastic density graphs given in [1], which have no relation at all (apart from the signs) to the corresponding formulas in the text: on their scale the region of negative values for the Expression (8) should practically coincide with the axis of the abscissa and the mutually identical positive parts of the curves (8) and (9) have a point of inflection and are convex towards the origin [7] and not away from it (in [1] these parts almost coincide with a circular arc drawn with the origin as the center).

## LITERATURE CITED

[1] A.M. Mikisha and F.A. Tsitsin, Astron. J. (USSR) 33, 885 (1956).

[2] F.R. Mul'ton, Introduction to Stellar Mechanics [in Russian] (ONTI, Moscow-Leningrad, 1935).

[3] M.F. Subbotin, A Course in Stellar Mechanics [in Russian] Vol. III (GITTL, Leningrad-Moscow, 1949).

[4] N.I. Idel'son, Potential Theory [in Russian] (ONTI, Leningrad-Moscow, 1936).

[5] P. Appel', Equilibrium Shapes of a Rotating Uniform Liquid [in Russian] (ONTI, Leningrad-Moscow, 1936).

[6] N.M. Giunter, Theory of Potential and its Application to Basic Problems of Mathematical Physics [in Russian] (GITTL, Moscow, 1953).

[7] G.M. Idlis, Cosmic Fields of Force and Certain Problems of the Structure and Evolution of Galactic Matter (Dissertation, Alma-Ata, 1954). Izvest. Astrophys. Inst. AN Kazakh. SSR 4, 3 (1957).

[8] P.P. Parenago, Astron. J. (USSR) 27, 329 (1950).

[9] P.P. Parenago, Astron. J. (USSR) 29, 245 (1952).

[10] P.P. Parenago, A Course in Stellar Astronomy [in Russian] 3rd ed. (GITTL, Moscow, 1954).

[11] G.M. Idlis, Astron. J. (USSR) 33, 20 (1956).

[12] K.F. Ogorodnikov, Uspekhi Astron. Nauk 4, 3 (1948).

Received February 18, 1956

Astrophysical Institute of the
Academy of Sciences, Kazakh. SSR

# CHRONICLE

## A SYMPOSIUM ON "ELECTROMAGNETIC PHENOMENA IN COSMIC PHYSICS" IN STOCKHOLM ON AUGUST 27-31, 1956

At the end of the last century it was noted that some lines in the spectra of sunspots split into components. Somewhat later, in 1908, G. Hale showed that this splitting was due to the magnetic field associated with sunspots. For this reason 1908 can be considered as the year during which a new branch of astrophysics, namely, cosmic electrodynamics, was born. However, cosmic electrodynamics has only reached an equality with other branches of astrophysics during the last two decades, when new observational data on cosmic rays, cosmic radio emission, magnetic fields of stars and the sun, etc., have shown the very great importance of electromagnetic phenomena in cosmic processes.

In 1942, H. Alfven predicted theoretically the possibility of the appearance in a conducting medium of the so-called magneto-hydrodynamic waves and thus discovered a new direction for investigations in cosmic electrodynamics. At the same time, the necessity for a close cooperation between physicists and astrophysicists became clear. In order to widen and develop such a cooperation the International Astronomical Union decided to call a Symposium on cosmic electrodynamics, and this took place between the 27th and 31st of August, 1956 at Stockholm.

In accordance with the plan mentioned above, many physicists, geophysicists and astrophysicists participated in the Symposium, with a total of 70 scientists from various countries. The delegation from the Soviet Union, which was led by Academician L.A. Artsimovich, consisted of six members. Because of the small number of delegates at the Symposium, it was not necessary to work in separate sections, and this contributed considerably to the success of the Symposium. However, the daily program required some intensive work by the participants because of the relatively wide range of subjects.

The papers read at the Symposium may, according to their contents, be divided into four groups: theory and experiment in hydrodynamics, solar electrodynamics, stellar magnetism and the interstellar magnetic field. Papers with a geophysicalbasis, equally interesting to both astronomers and physicists, formed a separate group.

The Symposium was opened on the 27th of August with an opening address by Prof. Alfven, after which there were papers on theoretical magneto-hydrodynamics. A review of the state of the theory and its more important problems was given by H.C. van de Hulst. Papers on the separate problems of the theory were mainly concerned with the course of magneto-hydrodynamic processes, starting with the corresponding equations. Thus, for example, A. Banos,Jr. considered uniform plane magneto-hydrodynamic waves, starting with equations set up by him which take into account compressibility, viscosity, thermal and electrical capacity, as well as the finite thermal and electrical conductivity of the medium. He discovered six types of magneto-hydrodynamic waves, which include, however, already known types, for example, Alfven's waves. L. Davis,Jr. considered the possibility of an increase of the originally weak magnetic field in cosmic objects in accordance with the theory of self-excitation ("dynamo" theory). A. Kipper gave an exposition of his statistical theory of magnetic fields of stars which is based on a close analogy between magneto-hydrodynamics and the theory of turbulent motion of a viscous liquid.

Experiments which were demonstrated as illustrations to theoretical papers excited great interest. In opening remarks which preceded the experiments, B. Lehnert showed that contemporary technical means make it possible to simulate cosmic conditions on laboratory scale using the theory of similarity. Thus, the participants in the Symposium were given an opportunity to "see for themselves" things which are usually known only from theoretical considerations.

In a whole series of papers on the problems of magneto-hydrodynamics the behavior of an ionized gas in the presence of a magnetic field was considered. In considering an ionized gas consisting of a number of components (electron, proton, and other gases) each of which separately behaves according to some quasi-hydrodynamic equations with additional terms, A. Schluter reached similar conclusions to those presented by Ia.P. Terletskii. The aims of the paper by E. Astrom were similar to those by Schluter and Terletskii, and the paper was devoted to a study of waves in a heated ionized gas, although Astrom's method of solution of the problem was somewhat different from the method employed by the other two authors.

Of major astrophysical interest were the reported results of various experiments on the motion of ionized matter in a strong magnetic field and the effect of electrical currents on an ionized gas in presence of a strong magnetic field. The corresponding results reported by W.H. Bostick, R.S. Pease, L.A. Artsimovich and I.N. Golovin will contribute considerably to a better understanding of high energy processes on the sun and stars. P.A. Sweet spoke on the magneto-hydrodynamics of ionized gases and considered the behavior of a liquid having a high electrical conductivity and near a magnetic neutral point. He showed that here the motion is unstable if the pressure is below a certain limiting value. This, according to the author, should be of some importance in the theory of sunspots and other similar formations. J.W. Dungey reported on the theory of chromospheric flares and based it on the theory of electrical discharge at a magnetic neutral point. This paper was at the same time a reply to the criticisms from T.G. Cowling.

A separate cycle of subjects in the work of the Symposium consisted of papers on the electrodynamics of the sun. In a historical review which formed a part of his opening remarks, Cowling listed the major steps in the development of studies of the different electrodynamic phenomena on the sun. He touched on the problem relating to mechanical effects of the magnetic field, the theory of chromospheric flares and other formations in the solar atmosphere. In considering the problem of the presence and the appearance of the general magnetic field on the sun, Cowling brought to the attention of the Symposium a number of mistakes involved in the hypotheses suggested so far. Thus, the role of self-induction in cosmic electrodynamical processes is not always satisfactorily taken into account.

A.B. Severnyi reported on the motion in the regions of major activity on the sun and the role of magneto-hydrodynamics in this. A.B. Severnyi considered the data obtained from observations of prominences, chromospheric flares, and other nonstationary processes on the sun, and showed in his analysis the specific properties of the corresponding motions which appear in the form of bursts, emission of corpuscles, as well as other spectroscopic properties.

J.H. Piddington reported on phenomena associated with a strong heating of certain parts of the atmosphere of the sun and processes which take part in the formation of chromospheric flares in which the magnetic field takes a part. The role of the magnetic field on the sun in the formation and the development of prominences was considered in the paper by S. Rosseland, E. Jensen, and E. Tandberg-Hanssen, who showed that the general magnetic field on the sun may lower the heat exchange between a prominence and the corona,and weakens turbulent winds as a result of which the stability of prominences in a hot corona becomes more understandable.

Schluter and St. Temesvary, and also Jensen, spoke on the structure of sunspots and the processes that take place within them and their connection with magneto-hydrodynamics. In the first of these papers it was shown that, on the basis of known premises, the properties of spots do not depend very strongly on the physical processes within the sun. This conclusion contradicts, to some extent, the conclusions of Alfven in whose opinion sunspots are originally formed within the sun. Jensen considered the Evershed effect and established that during the flow of gas, predominantly along magnetic lines of force, there appear forces directed away from the spot and leading to flow known as the Evershed effect. The dependence of the structure of the solar corona on the solar magnetic field was considered by T. Gold. He thought it probable that in the hydrodynamics of the corona the general magnetic field predominates over the inertial forces and makes possible only those motions which are connected with changes in gas pressure. The dependence of the structure of the solar corona on the magnetic field was also pointed out by A.B. Severnyi in the paper mentioned above.

H.W. and H.D. Babcock reported results of measurements of the solar magnetic field. 635 magnetograms of the solar surface were obtained since 1952, and these indicate a complex structure of the magnetic field, the latter including fields of a few tenths of a gauss. During a discussion some shortcomings in these measurements were pointed out.

Both theoretical and observational studies of stellar magnetism were described during the Symposium. The most extensive papers on these problems were read by Spitzer and Babcock. A review of the theory of stellar magnetism was given in the first of these, and in the second some results of measurements of changes in stellar magnetic fields, which have for some time been measured at Mount Wilson and Palomar, were reported. Among the 39 stars which were studied there are some which change their magnetic fields regularly and some irregularly. Babcock suggests that the variation in the magnetic field with time is not due to the fact that the axis of rotation does not coincide with the magnetic axis of a star.

E.R. Mustel pointed out that electromagnetic phenomena play a considerable role in astrophysics. He showed that the motion of a gas thrown out during the explosion of a new star is regulated by the magnetic field of the star and that a part of the magnetic field is carried off by the emitted envelope into the interstellar space.

Spectral changes which take place simultaneously with changes in the field are observed in the spectra of stars with variable magnetic fields. Using the method of harmonic analysis,A.J. Deutsch showed that the simultaneous change in the magnetic field and the spectrum of stars is closely connected with peculiarities in the chemical composition of these objects. The same problem was considered from a somewhat different point of view by G. Burbidge,who discussed the connection between stellar magnetic fields and nuclear reactions assumed to take place in the surface layers of stars.

One of the most interesting results which emerged from studies of the structure of the galaxy was the discovery in it of a magnetic field. This was done by G.A. Shain on the basis of studies of a structure of nebulae. Because of the sudden death of Academician G.A. Shain, his paper was read from a text submitted to the Symposium. On the basis of considerable observational material obtained in $H_\alpha$ and other lines, using 450 and 640 mm cameras with large fields of view, G.A. Shain showed that, during their expansion in the presence of the galactic magnetic field which takes place predominantly in the direction of the lines of force, nebulae remain visible during longer periods of time than in the absence of the magnetic field. The elongation of nebulae which is often observed also suggests that the expansion takes place with different velocities in different directions. G.A. Shain points out the preferential orientation of the major axes of dark nebulae relative to the center of the galaxy and draws conclusions about the structure of the magnetic field of the galaxy. In studying the connection between the forms of nebulae and the polarization of stellar light,G.A. Shain reaches some very important results relating to the magnetic field of the galaxy.

Alfven and Serkowski considered, in their papers, the problems connected with the magnetic field in interplanetary and interstellar space. In the first of these papers an analysis was made of a model of interplanetary magnetic field which explains fairly well observations of magnetic storms, cosmic rays, and other phenomena. Serkowski studied the polarization of stellar light near the double cluster, in Perseus, and reported some results in connection with the interstellar magnetic field in this part of the galaxy.

Towards the end of the Symposium there was a whole series of papers devoted to geophysical problems such as magnetic storms, short-period variations in the intensity of cosmic rays and other phenomena. S.F. Forbush reported on a 27-day cycle in the intensity of cosmic rays which is connected with geomagnetic activity, W.H. Bennett and E.D. Hulburt reported on the "stermertron" and its application to the study of flow of charged particles in the field of a magnetic dipole, A. Ehmert spoke on the intensity of cosmic rays generated by the sun in connection with interplanetary magnetic field. V.C.A. Ferraro, L. Block, S.F. Singer and several others reported on the theory of magnetic storms. A cinefilm showing experiments with the "stermertron" was very interesting.

During the third day of the Symposium an excursion to the Stockholm Observatory was organized. Prof. B. Lindblad gave a review of the work of the Observatory. The Stockholm Observatory is situated on a rocky hill in a picturesque place, while the old Observatory, situated in Stockholm itself, has been made into a museum.

The research work carried out at the Stockholm Observatory is very varied. The work of Lindblad on the spiral structure of extragalactic nebulae is well known. The traditional studies of spectroscopic parallaxes are being continued. Solar studies at the Stockholm Observatory are under the direction of Y. Ohman, while the main observations are obtained at the Capri, Italy branch of the Observatory. Electrophotometric work on a very high technical level must also be mentioned.

During their visit to the Observatory, the participants in the Symposium heard a lecture by Ohman on astronomical applications of resonance magnetic rotation. He predicted a number of effects and suggested that the corresponding observations ought to be begun since it is hoped that these will give new information on the atmospheres of the stars and the Sun.

The Symposium called by the International Astronomical Union in Stockholm was undoubtedly a very important event in astronomy. The papers and discussions during the Symposium are of interest not only to astrophysicists, but also to physicists and the geophysicists. The excellent organization of the Symposium must be noted, and for this the participants are indebted to the organizing committee led by Prof. Alfven.

Swedish astronomers, physicists, and geophysicists who bore the main burden of the organization of the Symposium deserve the deep gratitude of all the participants.

A. Kipper

Received February 9, 1957

# OPENING OF THE BIURAKAN ASTROPHYSICAL OBSERVATORY OF THE ACADEMY OF SCIENCES OF THE ARMENIAN SSR AND THE CONFERENCE ON NONSTATIONARY STARS

The construction of the Astrophysical Observatory of the Academy of Sciences of the Armenian SSR was begun in 1946 on the southern slopes of the Aragats Mountain, at a height of about 1500 m above sea level. The location was chosen south of Biurakan (30 km northwest of Erevan, the Capital of the Republic) and hence the name of the Observatory. Simultaneously with the construction, the scientific activity of the new Observatory began to develop.

Among the buildings constructed during the last ten years is the main body of the Observatory, consisting of a conference hall, individual research rooms, laboratories and a library, a few observation towers and pavilions, a series of houses for the staff of the Observatory, a guest house for visiting scientists, the building of the instrument construction laboratory and a temporary accommodation for the radio-astrophysics laboratory. A number of observational instruments have been set up (8" and 21" Schmidt cameras, 16" anaberrational telescope, 10" spectrographic telescope, a nebular spectrograph and others). Three radio telescopes for studying cosmic radio emission on 0.5 m, 1.5 m and 4.2 m have been designed and constructed in the workshops of the Observatory. The scientific staff of the Observatory, which was very small to start with, has grown considerably.

An important event in the life of the Observatory was the discovery of stellar associations in 1947. The subsequent work of the Observatory was devoted to the study of these systems, as well as the physical processes which take place in the stars and nebulae which form them.

In recent years, studies of the discrete sources of cosmic radio emission and extragalactic nebulae have developed.

The Biurakan Astrophysical Observatory was given the status of an independent Scientific Research Institute of the Academy of Sciences, as of 1956, by a decision of the Council of Ministers of the Armenian SSR.

On the completion of the first phase of the construction, an official opening of the Observatory took place on September 19, 1956 in the conference hall of the Observatory. At the opening, among the large number of Soviet and foreign astronomers, were the representatives of the Government and Communist Party of Armenia, representatives of the Presidium of the Academy of Sciences of the USSR, members of the Presidium of the Academy of Sciences of the Armenian SSR, members of the Astronomical Council of the Academy of Sciences of the USSR, and representatives of a number of scientific research institutions and higher scientific establishments of Armenia.

Simultaneously with the opening of the Observatory, a joint meeting of the Section for physicomathematical sciences of the Academy of Sciences of the Armenian SSR and the Astronomical Council of the Academy of Sciences of the USSR took place.

The meeting was opened by the Secretary of the Section for physicomathematical sciences, Academician of the Acad. Sci. Armenian SSR, A.L. Shaginian who gave a short and interesting address. He warmly greeted the staff of the Observatory, and welcomed the guests taking part in the joint meeting on behalf of the Presidium and the Section for physicomathematical sciences of the Acad. Sci. Armenian SSR.

Warm reception was given to the speech by the chairman of the Astronomical Council, Corresponding Member Acad. Sci. USSR A.A. Mikhailov, who congratulated those taking part in the meeting on the official opening of the new scientific center of Armenia, already well known for its work.

There followed a paper by the Director of the Observatory, Academician V.A. Ambartsumian who spoke on "Possible future developments in the work of the Biurakan Astrophysical Observatory."

The following telegram, sent by Presidium of the Acad. Sci. USSR, was read at the meeting.

"The Presidium of the Academy of Sciences of the USSR greets the Academy of Sciences of the Armenian SSR, and you dear Viktor Amazaspovich, and congratulates you on the opening of the Biurakan Astrophysical Observatory, and wishes all its staff major successes to the glory of our Soviet science.

President of the Academy of Sciences of the USSR, Academician Nesmeianov,

Chief scientific Secretary of the Presidium of the Academy of Sciences of the USSR, Academician Topchiev."

Prof. J. Greenstein (Mount Wilson and Mount Palomar Observatories, USA) congratulated the staff of the Observatory and read the following letter from the President of the American Astronomical Society: -

"Mr. Chairman, Ladies and Gentlemen! In connection with the visit to Biurakan by Dr. Greenstein, I, as the President of the American Astronomical Society wish to send greetings and congratulations to our colleagues in the USSR. The opening of this new establishment of the Academy of Sciences of the Armenian SSR is a very auspicious event. It brings together eminent scientists from many countries to discuss the problem in which international activity is most worthy of note. Early observations of T. Tauri were carried out with telescopes in the USA, a considerable amount of work was done in Mexico, and very extensive observational and theoretical work was carried out by our Soviet colleagues.

This event brings pleasant memories of the hospitality which was shown to me on my visit to the USSR during the full solar eclipse in 1936. American astronomers are looking forward to the meeting of the International Astronomical Union in 1958.

Donald G. Menzel, President
American Astronomical Society"

Warm congratulations were expressed by the Director of the Tonantsintla Observatory, Prof. G. Haro (Mexico), the Director of the Abastuman Astrophysical Observatory, Academician of the Acad. Sci. Georgian SSR, E.K. Karadze, representative of Chinese Astronomers, Prof. Gun Shu-mo (Mount Purple Observatory), the Director of the Crimean Astrophysical Observatory of the A.S. USSR, Prof. A.B. Severnyi, and on behalf of the Presidium of the Supreme Soviet of the Armenian SSR, the Council of Ministers of the Armenian SSR and the Central Committee of the Communist Party of Armenia, the Director of the Department of Science and Culture of the Central Committee, R.G. Khachatrian.

In connection with the official opening of the Observatory greetings were received from a number of learned and scientific institutions of the Soviet Union and foreign countries.

The second half of the day was spent on a tour of the Observatory.

On September 20th, at 10 a.m. local time, the Conference on nonstationary stars, timed to coincide with the opening of the Observatory, began its work. The Conference was organized by the Astronomical Council of A.S. USSR and the Biurakan Astrophysical Observatory.

Over fifty scientists took part in the Conference, coming from the P.K. Shternberg State Astronomical Institute, State Astronomical Observatory of the Academy of Sciences of the USSR at Pulkovo, Astronomical Observatory of the Leningrad State University, Crimean Astrophysical Observatory, Abastuman Astrophysical Observatory, Kiev Astronomical Observatory, Astronomical Council of the Academy of Sciences of the USSR, and the Biurakan Astrophysical Observatory, as well as foreign astronomers G. Haro (Mexico), J. Greenstein (USA), E. Shatsman (France), Gun Shu-mo (CPR) G. Herbig (USA), V. Oskanyian (FPRY), N. Romen (USA) and Shen'lian-Shzhao (CPR).

The Conference was devoted to a discussion of the problem of nonstationary stars, particularly stars of T Tauri class, and the possible ways of dealing with this problem. In addition, papers on other current problems of astrophysics were given at the Conference.

The Conference was opened by Academician V.A. Ambartsumian.

Academician V.A. Ambartsumian expressed the hope that, in distinction to previous conferences devoted to the problem of nonstationary stars, during the Biurakan Conference, "emphasis will be placed on the unresolved problems and an exploration of their solution."

The first meeting of the Conference was devoted to problems relating to: stars of T Tauri class, T associations and their connection with diffuse nebulae.

In his opening remarks V.A. Ambartsumian considered in detail the following problems which, in his opinion, are of great importance to the problem of nonstationary stars.

1. Classification of T Tauri and UV Ceti stars.

2. Luminosity curves for stars of T Tauri class.

3. Periodic changes in the value of the color index for T Tauri stars.

4. T associations and their connection with diffuse nebulae.

G. Herbig (Lick Observatory) and Candidate Phys. Math. Sciences P.N. Kholopov gave an account of the principles which should lie at the basis of any classification of stars belonging to the T Tauri class. P.N. Kholopov emphasized the necessity for systematic photoelectric observations of T Tauri stars and detailed studies of T associations.

V. Oskanian, a member of staff of Belgrade Astronomical Observatory, reported results of an analysis of almost all the existing observations of UV Ceti variables. It has been established that small bursts always precede larger ones. In other words, explosions in UV Ceti in all cases have preceding small maxima on the ascending arm. In some cases they are simply double explosions.

Prof. B.A. Vorontsov-Vel'iaminov, Prof. O.A. Mel'nikov, Prof. G. Haro, V.A. Ambartsumian and others took part in discussions on the papers given at the first meeting.

On behalf of the Conference, Prof. B.V. Kukarkin suggested that Prof. G. Haro, Dr. G. Herbig and Candidate Phys. Math. Sciences P.N. Kholopov be entrusted with the preparation of a preliminary classification scheme for stars belonging to the T Tauri class.

The role of the thermal and nonthermal emission in the changes in the luminosity of stars belonging to the T Tauri class, the nature of continuous emission, and the ultraviolet excess were discussed during the second meeting of the Conference which began at two P.M. on the same day.

The opening remarks by Dr. G. Herbig were concerned with observational facts obtained at the Tonantsintla Observatory.

According to the latter speaker two kinds of continuous emission can be observed at the present time:

1. Continuous emission seen in the spectra of all stars belonging to the T Tauri class, which masks the absorption lines (discovered by A. Dzhoe).

2. Continuous emission seen only in the spectra of certain stars of the T Tauri class which have moderate and low luminosity with a maximum intensity at λ3700 A.

G. Haro and G. Herbig showed that it is impossible to explain results of observations of bright ultraviolet stars by the usual line and continuous Balmer emission. The same result was obtained by G. Herbig from three-color photoelectric observations of Walker. Attempts to explain the observed continuous emission by a combination of two stars, one hot and one cold, or by the presence of a cold star with "hot spots," have been unsuccessful.

Further accumulation and systematization of observational data is necessary in G. Herbig's opinion, if the nature of the continuous emission of the above two kinds is to be explained.

Walker's paper, which was read by Prof. J. Greenstein, was concerned with the results of three-color photoelectric observations of certain open stellar clusters. Color-luminosity diagrams for the cluster NGC6530, as well as the cluster NGC2264 which was studied earlier, have the usual form in the interval between the brigher stars and stars of type A0. However, for later stars this diagram departs from the standard main sequence and extends upwards in the form of a band, higher by 2 than the latter sequence. It is characteristic that all the stars which lie above the main sequence appear to be stars of the T Tauri class. According to Walker, the above clusters appear to be very early. There are reasons for thinking that the clusters NGC6611 and IC5146 have the same properties.

The paper by Candidate phys. math. sciences L.V. Mirzoian was concerned with properties of the emission from AG Dragonis variable which has a number of properties in common with stars of the T Tauri class. The distribution of energy in the continuous spectrum of this star and its variation with time appears to support the hypothesis of the nonthermal nature of the emission which is observed in its spectrum.

Candidate phys. math. sciences G.S. Badalian reported on his two-color photographic observations of T, UX and XZ Tauri as well as the AG Dragonis variable. For these stars the amplitude of the variation of luminosity in the photographic range is more than three times greater than the photovisual amplitude, while for purely temperature measurements this ratio should be close to 1.3.

Two papers by Prof. A.B. Severnyi, namely, "On the nonstationary origin of the continuous emission from active parts of the sun" and "The special character of the line emission from active parts of the sun" were concerned with processes observed on the sun, and the nature of the possibly allied processes which lead to the appearance of a continuous emission in the spectra of stars of the T Tauri class.

In the paper by the late Academician G.A. Shain "On the magnetic field of the galaxy," which was read by Prof. A.B. Severnyi, some new observational facts which characterize this field were reported.

At the end of the meeting Academician V.A. Ambartsumian read two papers entitled "On dense clouds of relativistic electrons" and "On the release of the energy of explosions under the photospheric layers."

The first paper was concerned with the calculations carried out by the author on the continuous emission on nonstationary stars treated as the emission from relativistic electrons in magnetic fields. In particular, a study was made of the effect of energy loss of relativistic electrons during Compton scatters on quanta emitted by the electron cloud itself.

The second paper was devoted to a study of the external manifestations of processes giving rise to the emission of discrete amounts of energy in cases where this emission takes place under the photospheric layers. It was shown that if the amounts of energy thus emitted are small, and the optical depth is large (of the order of $10^4$ or more), the variation in temperature between explosions in stars of the UV Ceti class and fast Haro variables should be insignificant.

Prof. G. Greenstein, Prof. G. Haro, Dr. G. Herbig, Cand. phys. math. sciences P.N. Kholopov and others took part in a discussion of these papers.

The evening meeting, which was devoted to the sources of luminescence of cometary nebulae, was opened by Candidate phys. math. sciences V.A. Dombrovskii who reported data indicating the major importance of polarimetric observations of nebulae to the discovery of continuous emission.

On the basis of such polarization data for a number of nebulae (Crab, M 17, IC 410 and others) V.A. Dombrovskii established the presence of emission which is characterized by nonradial polarization in some nebulae.

E.E. Khachikian gave a paper entitled "On the luminosity of the IC432 nebula." This nebula, because of its structure, is close to cometary nebulae and stands out in respect to the nonradial nature of polarization of light from it. Colorimetric observations have shown that the color of this nebula is unusually blue and this confirms the conclusion that the luminescence of the nebula is not due to the reflection of light by the central star and that it has a nonthermal nature.

During the discussion, Academician V.A. Ambartsumian showed that the nonradial polarization is characteristic of continuous emission.

Prof. G. Greenstein announced that observations of the cometary nebula NGC 2261 (near R. Unicorn) show that changes in its luminosity are very slow and the spectrum of the nebula is the same as the spectrum of the star. This leads to the conclusion that in this case reflection predominates.

In his opinion, nonradial polarization cannot be used as an argument against the reflection hypothesis if one takes into account the possibility of nonuniformities in the structure of the nebula.

Prof. D.Ia. Martynov and others took part in the discussion.

The morning session on September 21st was devoted to the problem of the origin of the bright lines in the spectra of stars of the T Tauri class.

Prof. V.V. Sobolev, in his opening remarks, considered the following three hypotheses:

1. Interaction of stars with nebulae.

2. The presence of a stellar corona, similar to the solar corona, round stars of the T Tauri class.

3. The presence of shells round hot stars, analogous to the model suggested in order to explain the spectrum of Z Andromeda.

Candidate phys. math. sciences V.G. Gorbatskii contributed a paper entitled "On certain nonstationary processes in the atmosphere of long-period variable stars" which was concerned with his studies of the following scheme for these stars. In the atmosphere of a cold star an explosion took place leading to the ionization of hydrogen atoms. The nonstationary process of hydrogen emission is considered. It is shown that,in this case, hydrogen emission may give rise to metal lines.

Prof. G. Greenstein and Candidate phys. math. sciences V.S. Safronov based their explanations of the origin of emission lines in the spectra of stars of the T Tauri class on the phenomenon of accretion, while Prof. E. Shatsman based his explanation on gravitational conduction. In both cases, the presence of bright lines is considered to be a result of interaction of stars with nebulae (first hypothesis).

In the opinion of Prof. V.V. Sobolev, the following observational facts are against this hypothesis. The rapidity of the explosions of stars of the UV Ceti class, the presence of stars with bright lines which are not surrounded by any traces of nebulae, bright lines observed in the spectra of stars of the T Tauri type originating in deeper layers than the absorption lines. Prof. A.B. Severnyi took part in the discussion.

During the following day, problems connected with the Herbig-Haro objects, the origin of their luminescence, and their connection with the T Tauri were discussed.

In his introductory talk Prof. G. Haro placed a particular emphasis on the problem of whether there are stars within these objects.

G. Haro reported a number of new and interesting facts about ultraviolet stars and galaxies.

Prof. G. Greenstein gave a paper entitled "Possible energy sources for stars of the T Tauri class." According to him, the major part of the excess radiation from stars of the T Tauri class can be explained by a contraction of a protostar to a star of the main sequence.

G. Greenstein then discussed some possible applications of nuclear physics to the problem of energy sources in stars of the T Tauri class.

Dr. G.Herbig discussed in detail the problem of the brightness of T Tauri as a function of wavelength. The absence of stars in Herbig-Haro objects in infrared photographs may be due to the fact that the intensity of these rays is not sufficient.

The next paper was by Prof. O.A. Mel'nikov who showed that it is necessary to take into account the effect of absorption bands in the infrared region of the spectra of these stars.

The meeting was then followed by an excursion to the village of Voskevaz (Golden Branch). Here, in the vineyards of the Voskevaz Kolkhoz, the guests met the staff of the Observatory and the Kolkhoz workers. The meeting took place in a simple and cordial atmosphere.

The morning meeting on September 21st (comparison of stars of the T Tauri class with objects of other types) was opened by Prof. J. Greenstein who read a paper by A. Dzhoe entitled "SS Cygni as spectroscopically double." It was shown that stars of SS Cygnus and AE Aquarius appear to be double (P = 0.d276 and 0.d701,respectively) and consist of hot B and cold (G5 and K0) components. The components of both systems are subject to fast flares which have an effect on the general brightness of these stars, particularly in the UV, and are the reason for the change in the intensity of the emission lines H and K (CaII) as well as the continuum on short wavelengths.

The paper by Prof. Shatsman, "On the vibrational stability of newly formed stars" was concerned with the possibility of explaining the reason for the explosions in stars by a disturbance of their vibrational stability. It was shown that the observed explosion may be a result of the doubleness of stars when an explosion occurs as a result of a resonance between orbital motion and one of the periods of pulsation of the star. If a star is vibrationally unstable, then its energy sources turn out to be located not very far below its surface.

A paper by I.M. Gordon was read and was concerned with his new theory of supernovae in which relativistic electrons moving in the magnetic fields of stars play a major role.

Prof. V.A. Krat, Prof. J. Greenstein, A.G. Masevich and others took part in the discussion.

The concluding session was concerned with miscellaneous papers.

Prof. Shatsman, in a paper entitled "On the cosmogonic importance of stars of the T Tauri class," considered the hypothesis in which the formation of the T Tauri occurs as a result of strong condensation of diffuse matter. Much attention was given to the elucidation of the observed angular velocities of the T Tauri (which, as was pointed out in the discussion by Prof. O.A. Mel'nikov, include effects of large scale turbulence and possibly also radial convection) and the possible role of the postulated magnetic fields in the loss of angular momentum of the stars.

Candidate phys. math. sciences B.E. Markarian contributed a paper entitled "On the interrelation of diffuse emission nebulae and early clusters." It was shown that in all cases in which in an open stellar cluster there are stars belonging to stellar subclusters O5-O8, these stars are connected with diffuse nebulae, and, conversely, if in a cluster the earliest stars belong to subclusters O9-BO, then it is not connected with the nebula. From this it is concluded that O-clusters which are connected with diffuse nebulae are the earliest clusters.

P.N. Kholopov and G. Herbig reported on the following preliminary classification scheme for stars of the T Tauri class which they had worked out in collaboration with G. Haro at the request of the Conference.

I – irregular variables.

$I_n$ – irregular variables associated with nebulae.

$I_{n\alpha}$ – irregular variables associated with nebulae and having a bright $H_\alpha$ line in their spectra.

$I_{ne}$ – irregular variables having emission spectra and associated with nebulae but not belonging to the T Tauri class in the proper sense of the word (Z CMa, R CrA, ABAur, etc.).

$I_nT$ – irregular T Tauri variables associated with nebulae.

$I_{nf}$ – exploding stars in nebulae.

$I_s$ – irregular variables of type RW Auriga in Hoffmeister's sense.

Variable stars of the UV Ceti class remain an isolated class.

Prof. B.A. Vorontsov-Vel'iaminov, in a paper entitled "Radio-galaxies and galaxies with a wide emission in the spectrum of the nucleus," reported some results of an analysis of observational data on a number of extragalactic nebulae. He concluded that the observed radial emission of some galaxies is a property due exclusively to internal physical properties of these galaxies.

In connection with this, Academician V.A. Ambartsumian pointed out that, in all the known cases, radiogalaxies have absolute magnitudes close to $20^m$, i.e., they are giants, and this supports the conclusion about internal causes of the radio-emission of these systems.

Prof. S.K. Vsekhsviatskii spoke on the possible role of cosmic vulcanism in the solar system.

Prof. J. Greenstein, Prof. A.B. Severnyi, A.G. Masevich and others took part in a discussion on the above problems.

The concluding remarks were given by Prof. B.V. Kukarkin.

He pointed out that the work of the Conference was very productive, which, to a great extent, was due to the informal and friendly atmosphere during the discussions on the various papers. He expressed the conviction that "as a result of our Conference the friendship of astronomers of all countries will be strengthened as well as the concerted effort in the solution of the most burning problem, namely, the problem of the origin and the evolution of the worlds which surround us."

Prof. B.V. Kukarkin congratulated the members of the Biurakan Observatory on the excellent organization of the Conference. He also congratulated all the participants in the Conference, both Soviet and foreign, whose activity ensured the success of the Conference.

On behalf of foreign guests, Prof. E. Shatsman expressed cordial thanks and concluded with the words "to the next meeting at Biurakan."

On the suggestion of Academician V.A. Ambartsumian, a telegram of greetings was sent to O. Struve, D. Menzel and F. Oort on behalf of the Conference.

On the evening of September 22nd an excursion to Erevan was organized.

A visit was made to the Akademicheskii Theatre and the Spendiarov Ballet where a classic of Armenian music, the opera "Arshak II" by Tigran Chykhadzhian was seen. On September 23rd an excursion was organized to Echmiadzin, Evartnots and Erevan. The guests visited the local places of interest and saw various aspects of contemporary Armenian architecture and culture. A reception was organized in the evening, in Biurakan, in honor of the guests and the Director of the Observatory.

The proceedings of the Biurakan Conference on nonstationary stars will be published in a separate book in the near future.

L.V. Mirzoian

Received January 19, 1957

# CONFERENCE ON THE PHYSICS AND THE ORIGIN OF PLANETARY NEBULAE

On the 3rd and 4th of February of this year, a Conference on the physics and the origin of planetary nebulae took place in the University of Leningrad and was organized by the Commission for Cosmogony of the Astronomical Council of the Academy of Sciences of the USSR. Among those who took part in the Conference were specialists in the studies of planetary nebulae, members of the Commission for cosmogony, and a considerable number of Leningrad astronomers. Altogether, 75 persons took part in the Conference.

V.V. Sobolev gave a review of the present state of the physics of planetary nebulae. He considered the following problems: the temperature of nuclei and optical thicknesses beyond series limits, the theory of Balmer decrement, electron temperatures and concentrations, the problem of continuous spectrum, diffusion of $L_\alpha$ radiation, and radiation pressure in nebulae.

A.Ia. Kipper and V.M. Tiit gave a paper entitled "The splitting of light quanta and the importance of this process in the physics of gaseous nebulae." Splitting of quanta and the formation of a continuous spectrum in gaseous nebulae may take place as a result of the following processes: (a) the splitting of $L_\alpha$ quanta into the quanta $\lambda 4686$ and $\lambda 1462$ by means of an atom of ionized helium; (b) two-quantum emission by a hydrogen atom in the transition $2S_{1/2} - 1S_{1/2}$; (c) the splitting of light quanta by free electrons (two-quantum scattering); (d) the splitting of $L_\alpha$ quanta in a two-quantum transition $2P_{1/2,3/2} - 1S_{1/2}$ of an atom of hydrogen. The processes (a) and (b) were considered by A.Ia. Kipper, and the process (c) is not effective in planetary nebulae. Process (d) was studied by V.M. Tiit. It was found that one two-quantum emission takes place in $10^{13}$ one-quantum events. In optically thin planetary nebulae the probability of such a two-quantum transition is small, in optically thick nebulae process (d) is still as effective as process (b), and in the region of radio frequencies, it is more effective. The theory of two-quantum transitions is applicable also in the case of ionized helium. In this case the probability of the transitions turns out to be higher by one order than in the case of hydrogen. In spite of the fact that the helium content in nebulae is only 10%, it interacts with radiation several times more effectively than hydrogen.

G.A. Gurzadian, in his paper on the dynamics of planetary nebulae, noted that bipolar nebulae are very widespread and should, evidently, be connected with the magnetic field. Since nebulae are randomly oriented relative to the galactic plane, the magnetic field of the galaxy does not play a significant role. It is possible that bipolar structure is connected with the existence of a self-magnetic field of a nebula and different rates of its diffusion down and across the field. The small speeds of expansion of nebulae indicate, according to this author, that the formation of nebulae is not an abrupt process similar to the formation of an envelope during the explosion of a new star. The rapid decrease of the luminosity of a nebula during its expansion means, according to him, that during the formation of nebula its nucleus could not be a star, since otherwise only $10^4$ years ago, when the nebula was much denser, its luminosity would be $15^m$. G.A. Gurzadian considers that a planetary nebula is the remainder of a primary material from which the central star (nucleus of the nebula) was formed. Gradual heating up of the star leads to a gradual expansion of the envelope and to its separation. The growth of planetary nebulae and their nuclei takes place over a few tens of thousands of years. According to this author, the stars of the intermediate component of the galaxy have passed through the stage of planetary nebulae during the time of their formation.

S.A. Kaplan contributed a paper entitled "On the theory of ionization waves in the envelopes of stars in connection with the problem of the origin of planetary nebulae."

Shock waves are usually accelerated in stellar envelopes and parts of envelopes break away with a speed of the order of 1,000 km/sec as is observed in novae and supernovae. The small speeds of expansion of planetary nebulae may be connected only with shock waves in which strong absorption of energy takes place. The role of such a shock wave may be played by an ionization wave, i.e., a boundary between ionized and unionized regions which moves relative to the gas. S.A. Kaplan derived an equation which makes it possible to determine the conditions under which the formation of an ionization wave and the breaking off of the envelope may take place. An actual numerical estimate, carried out by him, gives results which apparently do not contradict observational data.

S.B. Pikel'ner announced the results of work which was done in collaboration with I.S. Shklovskii and which was devoted to a study of the nature of the spherical gaseous corona of the galaxy. In this work, the authors criticize Spitzer's hypothesis about the corona of the galaxy in which the latter is considered as a hot gas (a million degrees) without appreciable relative motion, and it is concluded that the spherical subsystem of the interstellar gas consists of relatively cold hydrogen which is 20-30% ionized and moves turbulently with relative speeds of the elements of the gas reaching 50-70 km/sec. The distribution of radio emission may be used to find the intensity of the magnetic field in the upper and lower layers of the corona. The condition of equilibrium for the gas gives a concentration of $n \sim 0.01$ for large z-coordinates and $n \sim 0.06$ in the galactic plane. Difficulties which were pointed out by Spitzer and which are connected with the large dissipation of kinetic energy in ultrasonic motion may be disregarded if one assumes that the presence of a magnetic field lowers the dissipation by a factor of 20-30. In the opinion of the authors the gas motion is apparently maintained by waves emitted from the center of the galaxy in which fast motion is observed.

In the paper by I.N. Minin the major role played by radiation pressure in nebulae on the boundary of HII region was noted. If the mass of HI is of the order of 0.01-0.1 of the mass of the whole envelope, its separation becomes possible, as well as the formation of a second envelope.

I.S. Shklovskii briefly reported on his work on planetary nebulae which was published in the Astronomical Journal, 1956, No. 3. He emphasized that the absolute magnitudes of nuclei of planetary nebulae, determined from their distances taken according to his scale, turned out to be about $+10^m$. The small luminosity and high temperature of nuclei indicate that they have small dimensions and consequently a high density which turns out to be of the order of $10^8$, i.e., as in the case of the most dense white dwarfs. Over a few tens of thousands of years the nebula diffuses and leaves behind a very hot star which cools down and turns into a white dwarf. The smaller the dimensions of the nebula the larger its optical thickness for ultraviolet radiation. With a sufficient contraction an HI region should appear surrounding HII. It follows that in the past, a planetary nebula was in the form of a gigantic cold envelope through which shines HII, i.e., a cold giant.

B.A. Vorontsov-Vel'iaminov, in a paper entitled "On the distance scales of planetary nebulae," noted that in the majority of cases it is impossible to determine whether a given nebula is optically thin or optically thick. For this reason all the distance scales of planetary nebulae are subject to major systematic errors. Theoretical models of hydrogen nebulae are not a convenient basis for this purpose since real nebulae differ from these models.

P.P. Parenago, in a paper entitled "Kinematic Characteristics of Planetary Nebulae," pointed out that Kamm's function, which was set up by him for planetary nebulae with distances in accordance with those given by B.A. Vorontsov-Vel'iaminov and I.S. Shklovskii, have, in both cases, a large dispersion. It follows that a good distance scale for planetary nebulae does not as yet exist. It is possible that the scale of B.A. Vorontsov-Vel'iaminov is somewhat better.

Iu.K. Gulak reported results of observations on planetary nebulae. He concluded that layers of equal radiation can apparently be represented as figures of rotation.

N.A. Razmadze spoke on the masses of envelopes and expansion speeds of planetary nebulae. He noted that the mass of an envelope which is distributed down the major and the minor axes of a bipolar nebula is roughly the same. The difference in brightness is connected with the fact that matter is distributed over different volumes.

E.R. Mustel', V.P. Tsesevich, A.G. Masevich, the authors mentioned above, as well as other astronomers, took part in the discussion of the papers given during the Conference.

Concluding remarks were given by B.A. Vorontsov-Vel'iaminov and were concerned with the further development of studies of planetary nebulae.

V.S. Safronov

Received February 19, 1957

# A MEETING OF THE COMMISSION FOR COSMOGONY DEVOTED TO THE FUTURE DEVELOPMENT OF WORK ON COSMOLOGY

On the 30th of December, 1956, a meeting of the Commission for cosmogony of the Astronomical Council took place, and the possibility of the development of work on cosmology and its connection with extragalactic astronomy was discussed. Representatives of astronomical, physical, and philosophical institutions in Moscow and other cities took part in the work of the meeting.

In his opening remarks, Academician V.A. Ambartsumian pointed out that cosmological problems are somewhat neglected in the USSR while a considerable number of papers on the subject are appearing abroad. Theoretical papers are often unconnected with new observational data. There is no basis for doubting the reality of the expansion of the observable part of the universe. Attempts to explain the red shift by non-Doppler effects have been unsuccessful. It is necessary to construct a theory which would explain this fact on the basis of observational data of extragalactic astronomy. At present it may be considered as established that the nonuniformity in the spacial distribution of galaxies is very considerable. There are clusters of galaxies, and clusters of such clusters. Galactic clusters apparently correspond to the two forms of stellar clusters, namely, scattered and globular clusters. Whole clouds of galaxies are known. In order to explain all these observed properties it is necessary to bring in the theory of gravitation. Moreover, almost all the existing cosmological theories start with a uniform distribution of matter.

The masses of separate galaxies of the clusters, determined by using the virial theorem, in some cases turn out to be indefinitely large. It is natural to question the stability of these systems. It is possible that such clusters are in the process of disintegration, just as is the larger observed system. In that case, the calculated masses of the separate galaxies may turn out to be different. It would be desirable to bring in partial solutions of Einstein's equations in order to explain these phenomena. Not enough attention is being paid in the Soviet Union to the theory of gravitation. It is necessary to stimulate more work in extragalactic astronomy and cosmology.

A.L. Zel'manov (Shternberg Astronomical Institute [GAISh]) also remarked on the insufficient amount of work on nonrelativistic cosmology in the USSR. The most common cosmological hypotheses used abroad are those of the theory of uniform isotropic universe. Among the difficulties of such theories (both in the general theory of relativity and in Newtonian physics) are those of a fundamental nature, i.e., inherent in the theory (plurality of models and "special states") as well as those connected with the problem of correspondence with observational data (short time scale, and limited time of formation of condensations). The many attempts to remove these difficulties abroad are concerned with changes of form of physical theories, or their arbitrary generalization and even departure from physics as the basis of cosmology through the conservation of the postulate of uniformity and isotropy, and the promotion of this postulate to a "cosmological principle." Moreover, the most suitable course appears to be the rejection of this postulate in large scale phenomena, i.e., the development of the theory of nonuniform anisotropic universe based on verified physical theories and applied to a sufficiently large region, as well as taking into account local anisotropy and local nonuniformity. It is of interest to search for a rational generalization of the general theory of relativity in connection with the problems of "special states." Other important problems of cosmology are nonrelativistic removal of thermodynamic difficulties, the theory of stepped structure, the problem of spacial infinity of the universe within the general theory of relativity, and the investigation of the red shift.

In the exposition of a whole series of cosmological theses, which have an idealogical significance, it is important not to introduce simplifications and dogmatism.

A.B. Severnyi (Crimean Astrophysical Observatory) considered the problem of the origin of chemical elements, which is of major interest in cosmology. Recent analyses of the chemical composition of stars have lead to results which may change our ideas on the origin of heavy elements. A.B. Severnyi reported new results obtained at the Crimean Observatory on the relative content Th/Pb on the sun, which turns out to be a hundred times less than on the Earth.

E.M. Livshits (Institute for Physical Problems, Academy of Sciences of the USSR) pointed out that the application of the general theory of relativity to a nonuniform nonisotropic universe has definite prospects. It is possible, on the basis of very general assumptions, to obtain time dependent properties in the solution of Einstein's equations. This problem requires further investigation.

I.S. Shklovskii (GAISh) discussed the radio-astronomical studies which are of importance to cosmology (radio galaxies, studies of intergalactic hydrogen, etc.).

Ia.P. Terletskii (Department of Physics of the Moscow State University) noted that in considering cosmological problems it is desirable to introduce also thermodynamics and statistical physics.

D. Ia. Martynov (GAISh), V.L. Ginzburg (Physical Institute of the Academy of Sciences [FIAN]), A.G. Masevich (GAISh), E. Kol'man (Institute of History of Natural Sciences) pointed out the necessity of an intensification of theoretical work and the use of scientific argumentation in critical discussion of cosmological hypotheses, the absence of good reviews and papers on cosmology, and the desirability of a translation of a number of foreign monographs on these problems.

All of the speakers noted the absence of an observational basis for extragalactic studies and the necessity of obtaining such a basis. The desirability of using new methods of investigation was pointed out. It was also stressed that a close contact between physicists, astronomers, and philosophers is important to a detailed study of cosmological problems.

It was decided to call, in 1957, the sixth All-Union Conference on the problems of cosmogony which will be devoted to extragalactic astronomy and cosmology.

As a preparation to this conference it was decided to approach the Editors of Uspekhi Fiz. Nauk and "Voprosy Kosmogonii" and ask them to publish review articles on extragalactic astronomy and cosmology, and the State Technical and Theoretical Literature Press (GITTL) with a request for the publication of a number of foreign books on cosmology.

A. Masevich

Received February 23, 1957

# ACADEMY OF SCIENCES USSR PRESS

## OFFICE OF THE "AKADEMKNIGA"

Books on Sale:

Astronomical Year Book of the USSR for 1957, 36th year of publication (Institute of Theoretical Astronomy, Acad. Sci. USSR) (1954), 584 pp., price 67 rubles 80 kop., bound.

Astronomical Year Book of the USSR for 1958, 37th year of publication (Institute of Theoretical Astronomy, Acad. Sci. USSR) (1955), 584 pp., price 67 rubles 70 kop., bound.

Astronomical Year Book of the USSR for 1959, 38th year of publication (Institute of Theoretical Astronomy, Acad. Sci. USSR) (1956), 584 pp., price 67 rubles 80 kop., bound.

F.A. Bredikhin, Meteor Studies, papers and commentary by A.D. Dubiago, edited by S.V. Orlov ("Classics of Science" series) (1954), 607 pp., illustrated, price 24 rubles 20 kop., bound.

E.L. Krinov, Meteorites (Popular Science series) (1948), 334 pp., illustrated, price 1 ruble, bound.

E.L. Krinov, The Tungus Meteorite ("Progress and Problems of Contemporary Science" series) (1949), 191 pp., illustrated, price 6 rubles 80 kop.

V.Ia. Struve, Studies in Stellar Astronomy ("Classics of Science" series), trans. by Prof. M.S. Eigenson, edited by Corresponding Member of the Acad. Sci. USSR, A.A. Mikhailov (1953), 234 pp., price 10 rubles, 50 kop., bound.

Progress in the Astronomical Sciences, V. IV (1948), 287 pp., price 18 rubles 40 kop., bound.

Progress in the Astronomical Sciences, V. V (1950), 333 pp., illustrated, price 18 rubles 40 kop., bound.

Progress in the Astronomical Sciences, V. VI (1953), 322 pp., price 20 rubles 70 kop., bound.

These books may be purchased at the following "Akademkniga" shops: Moscow, 6 Gorki St.; Leningrad, 57 Liteinyi Avenue; Sverdlovsk, 71-v Belinskii St.; Kiev, 42 Lenin St.; Khar'kov, 4/6 Goriainovskii Lane; Alma-Ata, 129 Furmanov St.; Tashkent, 29 Karl Marx St.; Baku, 13 Dzhaparidze St.

Books may be sent to customers in other towns, prepaid. Orders should be sent to the Office of "Akademkniga," 8 Kuibyshev St., Moscow, or to any of the above bookshops.